Author:
Mullally, Grace

Title:
The Engineering and Evaluation of Genome Editing Tools in Mitochondria

The engineering and evaluation of genome editing tools in mitochondria

Grace Mullally

School of Biochemistry

September 2018

A dissertation submitted to the University of Bristol in accordance with the requirements for award of the degree of Doctor of Philosophy in Biochemistry in the Faculty of Life Sciences

Word count: 51539

Abstract

Mutations in mtDNA can have severe consequences for cellular energy production and result in a severe class of incurable mitochondrial diseases. There is presently a lack of tools for the efficient editing of mitochondrial genomes which hinders the study of mitochondrial biology and disease. Since their development in 2013, CRISPR genome editing tools have had huge popularity and impact on molecular genetics due to their efficiency of targeting, versatility and ease of modification. Most studies using CRISPR have targeted the nuclear genome. This thesis details the first steps in the development of a suite of tools, which we have termed MitoCRISPR, broadening the current scope of CRISPR systems by tailoring them for the manipulation of mitochondrial genomes. Although we did not complete development of a MitoCRISPR system in this thesis, the work detailed here sets out a framework for the project to move forward within.

Central to the development of a MitoCRISPR system is the targeted delivery of functional CRISPR machinery, namely a protein endonuclease and guide RNA, to the mitochondria. To this end, this thesis describes the cloning a plasmid encoding mitochondrially targeted *Spy*Cas9 and its expression in mammalian cells.

A library of modified CRISPR gRNAs were designed to incorporate RNA mitochondrial targeting aptamers. This thesis details our findings that *Spy*Cas9 gRNAs can be modified at several sites without impacting Cas9 complex formation and activity and investigates the import of gRNAs into whole cells and isolated mitochondria. Building on these findings, gRNA modifications which do impact Cas9 endonuclease activity and modified *Lb*Cas12a crRNAs are also studied.

Given that the development of tools for genome editing has real ethical implications, this thesis also details the development and findings from an art-science public engagement exercise through which we sought to open up a dialogue with the Bristol-based public and gauge the perception of genome editing tools.

Author's Declaration

I declare that the work in this dissertation was carried out in accordance with the requirements of the University's *Regulations and Code of Practice for Research Degree Programmes* and that it has not been submitted for any other academic award. Except where indicated by specific reference in the text, the work is the candidate's own work. Work done in collaboration with, or with the assistance of, others, is indicated as such. Any views expressed in the dissertation are those of the author.

Signed: Date:

Acknowledgements

To Mark and Jon - Thank you for giving me the opportunity to have been part of this fantastically interesting project over the past four years. Though I live my life on a rollercoaster (and tend to say 'yes' to too many side projects) thank you for keeping me on track. I am grateful for your teaching, guidance and care.

Holly and Zuri, I am so grateful for you coming and joining the MitoCRISPR team. I know it's not easy, but best of luck with continuing the project. You can do it!

I consider myself tremendously lucky to have been part of the fantastic community in the School of Biochemistry over the past 8 years. In particular, I will always be grateful to members of D40 and C50 past and present. To the other PhD students who laid the path before me (Gemma, Jack, Ben), to those who have shared the journey (Eudmar, Jonnie), and to those who follow just behind (Emma, Cat, Lucy), thank you for company. To those of you who have supported us and shown us the way: Kara and Virginie, Fiona, Anna, Abby, Gabo, Olly, Kel, and many more. Thank you all for your ongoing support, for always making me feel at home, and, of course, for always being ready to laugh (and cry) over a pint in the Robin.

Thanks, as always, to my family - Thank you for providing for me the tremendous privilege of education and thank you for always encouraging me to be the best I can be. Thank you for always being there, for your unwavering love and support.

Finally, to my friends, in particular to Shannon and Joe - I feel so incredibly lucky to have fallen into a network of such exciting, funny and intelligent people. Thank you for the adventures, and for making me feel the happiest and most accepted I have ever been. I couldn't have stuck at it without you.

Table of Contents

List of Tables

List of Figures

List of Abbreviations

aa	amino acid
AAV	adeno-associated viruses
AD-488	Alexa™ 488-5-UTP labelled AD RNA
ADP	adenosine diphosphate
ATP	adenosine triphosphate
βME	β-mercaptoethanol
BoBS	bunch of baby spinaches (extended fluorescent RNA structure)
bp	base pairs
BS	baby spinach fluorescent RNA structure
BSA	bovine serum albumen
CMV	cytomegalovirus
COI-III	cytochrome c oxidase subunit I - III
COX8A	cytochrome c oxidase subunit viii mitochondrial targeting sequence
CRISPR	clustered randomly interspaced short palindromic repeats
crRNA	CRISPR RNA
CsCl	caesium chloride
Cybrids	cytoplasmic hybrids
Cyt b	cytochrome b
Cyto	cytoplasmic
dNTP	deoxyribonucleotide triphosphate
ds	double stranded
DSB	double strand break
EDTA	ethylenediaminetetraacetic acid
EtOH	ethanol
FACS	fluorescence activated cell sorting
FBS	foetal bovine serum
FD	FD mitochondrial targeting hairpin
FD-488	Alexa™ 488-5-UTP labelled F1D1 RNA
FDA	US Food and Drug Administration
Fn	*Francisella novicida*
FRET	förster resonance energy transfer
G	guanine
GCDA	genomic cleavage detection assay
GM	genetic modification
GMO	genetically modified organism

gRNA	guide RNA
GWAS	genome wide association studies
h	hour(s)
H1/H2	hairpin position 1/2
HCl	hydrochloric acid
HEFA	Human Embryology and Fertility Agency
HP	hybridisation probe
HR	homologous recombination
HSP	heavy strand promoter
IF	immunofluorescence
IMM	Inner mitochondrial membrane
IMS	Inter-membrane space
IVT	*in vitro* transcription
k_a	rate of first strand cleavage (supercoiled to open circle DNA)
k_b	rate of second strand cleavage (open circle to linear DNA)
kb	kilobase
KSS	Kearns-Sayre Syndrome
Lb	*Lachnospiraceae bacterium*
LB	lysogeny broth
LBA	LB-Agar
LHON	Leber's hereditary optic neuropathy
Lin	linear DNA
LS	Leigh syndrome
LSP	light strand promoter
M	marker
MCP	MS2 bacteriophage coat protein
MELAS	mitochondrial encephalomyopathy, lactic acidosis and stroke-like episodes
MERRF	myoclonic epilepsy and ragged red fibre disease
mins	minutes
Mito	mitochondrial
MitoRE	mitochondrial targeted restriction endonuclease
MitoTALEN	mitochondrial targeted TALEN
MitoZF	mitochondrial targeted Zinc Finger
MitoZFN	mitochondrial targeted Zinc Finger nuclease
MRT	mitochondrial replacement therapy
MS2	Bacteriophage MS2
mtDNA	mitochondrial DNA

MTS	mitochondrial targeting sequence
NaCl	sodium chloride
NaOH	sodium hydroxide
NARP	neurogenic muscle weakness, ataxia, retinitis pigmentosum
ND1-5	NADH dehydrogenase subunit 1 - 5
nDNA	nuclear DNA
NLS	nuclear localisation sequence
nt	nucleotide
NTP	ribonucleotide triphosphates
Nuc	nuclear
NUC	*Spy*Cas9 nuclease lobe
OC	open Circle DNA
OCR	oxygen consumption rate
OMM	outer mitochondrial membrane
OXPHOS	oxidative phosphorylation
PAGE	polyacrylamide gel electrophoresis
PAM	protospacer adjacent motif
PEI	polyethylenimine
PEO	progressive external opthalmoplegia
PBS	phosphate buffered saline
PCR	polymerase chain reaction
PEI	polyethylenimine
PGD	pre-implant genetic diagnostics
PS	pancreas syndrome
PVP	polyvinylpyrrolidone
RB	reaction buffer
RE	restriction endonuclease
REC	*Spy*Cas9 recognition lobe
RFLP	restriction fragment length polymorphism
RNP	ribonucleoprotein
ROS	reactive oxygen species
RP	RNase P mitochondrial targeting hairpin
RPE-1	retinal pigment epithelium 1 cells
rpm	rotations per minute
RRI	responsible research and innovation
rRNA	ribosomal RNA
RT	room temperature

Sa	*Staphylococcus aureus*
SB	sample buffer
SC	supercoiled DNA
SDS	sodium dodecyl sulphate
sgRNA	single guide RNA
Spy	*Streptococcus pyogenes*
ss	single stranded
Sth	*Streptococcus thermophilus*
Su9	*Neurospora crassa* ATPase subunit 9 mitochondrial targeting sequence
TAE	Tris, acetic acid and EDTA buffer
TAV-CHYSEL	*Thosea asigna* virus self-cleaving peptide
TBE	Tris, boric acid and EDTA buffer
TE	Tris-EDTA buffer
TALEN	transcription activator-like effector nuclease
TIM	translocase of the inner mitochondrial membrane
TOM	Translocase of the outer mitochondrial membrane
tracrRNA	trans-activating CRISPR RNA
tRK1	Yeast $tRKA_{Lys}$
US	upper stem
UV	ultraviolet
VOA	valinomycin, oligomycin, antimycin A
WB	Western blot
WCE	whole cell extract
ZF	zinc finger
ZFN	zinc finger nuclease

1 Introduction

1.1 Mitochondria

All living things need energy to survive. Across all complex organisms, the molecule adenosine triphosphate (ATP) is the major source of chemical energy, enabling all metabolic processes. Eukaryotic and multicellular organisms have developed several pathways for the generation of ATP, the most significant of which are dependent on mitochondrial proteins[1]. Central to sustaining life as we know it, mitochondria are also responsible for the generation of important metabolites and play a key role in a number of intracellular pathways including Ca^{2+} homeostasis[2], autophagy[3], apoptosis and cellular ageing[4] (summarised in Figure 1-1A). Mitochondria are believed to have originated as an endosymbiotic protobacteria from the *Rickettsiales* family which was taken up into a primordial eukaryotic cell[5]. As such, they contain their own genome — mitochondrial DNA (mtDNA)[6] — distinct from nuclear DNA (nDNA), Figure 1-1B.

1.1.1 The structure of mitochondria

Distinct from their familiar oval shape described by illustrations of textbooks, mitochondria form extensive dynamic networks throughout cells[7]. The constant cycle of fusion and fission of mitochondrial structures is of key importance for mitochondrial function, and cellular health as a conseneuence[8,9]. Mitochondria are surrounded by an inner mitochondrial membrane (IMM), which is folded into cristae, and an unfolded outer mitochondrial membrane (OMM), Figure 1-1A. Together, these membranes give the organelle its characteristic structure. The two mitochondrial membranes generate four distinct mitochondrial environments: the OMM; the intermembrane space (IMS); the IMM; and the matrix, the internal environment of the organelle. The compartmentalisation of these distinct environments is central to many of the biochemical processes carried out by mitochondria. For example, the IMM incorporates macromolecular protein complexes that drive cellular ATP production through biochemical coupling in the oxidative phosphorylation pathway (OXPHOS).

The mitochondrial OMM is permeable to small molecules, whereas the inner membrane is not. This allows the establishment of a proton gradient and membrane potential which drive ATP production in OXPHOS. Small molecules which function within the matrix are transported across the IMM via channels and pores[10]. Although mitochondria contain their own genome, some 1,500 proteins (approximately 99% of mitochondrial proteins) are encoded by nDNA[11]. Since proteins are not able to pass freely across either the OMM or IMM, these proteins are trafficked across the cytoplasm and require a dedicated import pathway[12] (see section1.3.3).

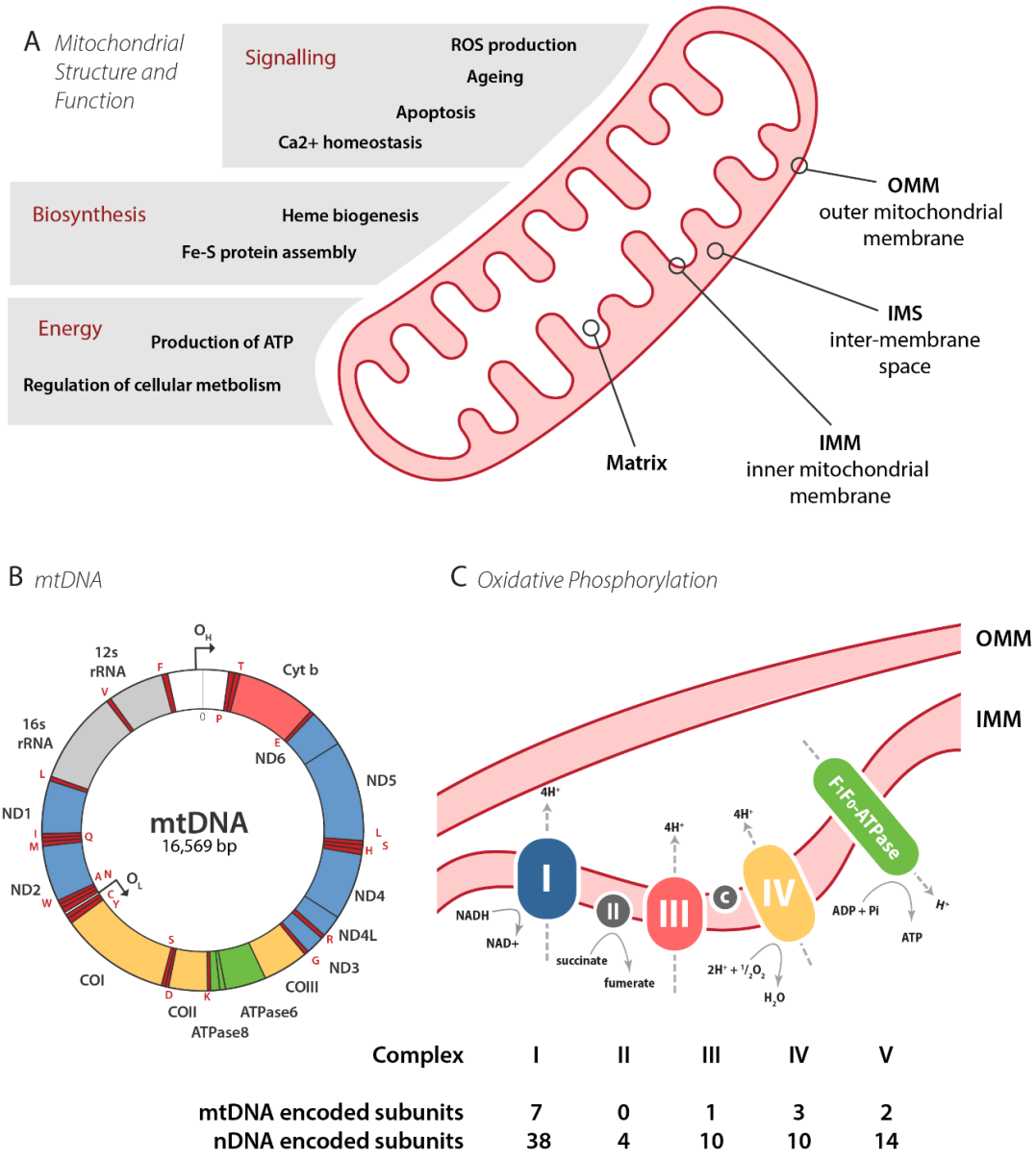

Complex	I	II	III	IV	V
mtDNA encoded subunits	7	0	1	3	2
nDNA encoded subunits	38	4	10	10	14

Figure 1-1 Mitochondrial Structure and Function A *Mitochondria are involved in a wide range of functions, ranging from cellular signalling and health through biosynthetic pathways and energy production, as summarised here. These functions are often a result of the unique mitochondrial structure: mitochondrial are surrounded by two membranes, the outer and inner mitochondrial membranes (OMM, IMM) which separates the organelle into distinctive environments, the matrix and inter-membrane space (IMS).* ***B*** *mtDNA encodes 37 genes on a double stranded, circular genome. 13 proteins, all part of the OXPHOS pathway are punctuated by 22 tRNAs (red) (made with reference to MITOMAP.org)* ***C*** *Oxidative Phosphorylation (OXPHOS) is performed by proteins in the electron transport chain (ETC) in the inner mitochondrial membrane (IMM), and most of these multi-subunit complexes is made up of proteins encoded by both the mitochondrial and nuclear genomes, as summarised in the table below.*

1.1.2 OXPHOS

Given the importance of cellular energy production through OXPHOS, mitochondrial health is central to cellular homeostasis. ATP generation is the result of electron transport between five multi-subunit protein complexes, also called the electron transport chain (ETC), Figure 1-1C. Electrons enter the ETC via NADH at complex I, and succinate at complex II, ultimately

being transported to the terminal electron acceptor, oxygen, at complex IV. Electron transport is coupled to proton pumping into the IMS, generating a proton gradient between the IMS and the matrix. The resulting proton motive force drives ATP synthesis at the F_1F_0-ATPase.

1.1.3 mtDNA

The mitochondrial genome is a high copy number closed circular molecule of double stranded DNA distinct from the nuclear genome. The size of the mtDNA molecule is highly variable between species - in humans, it takes the form of a 16,569 bp genome encoding 22 tRNAs, 2 rRNAs and 13 proteins[6], Figure 1-1B. mtDNA is present in hundreds to thousands of copies per cell[13] and packaged in nucleoids, IMM associated structures responsible for the regulation, maintenance and transcription of mtDNA. mtDNA is transcribed into a long polycistronic RNA by mitochondrial RNA polymerase from the light and heavy strand promoters (LSP, HSP) respectively[14]. Not containing introns, mtDNA also encodes a higher density of information than nDNA and genes in mtDNA are interspersed with tRNAs, so-called 'tRNA punctuation'. The transcribed polycistronic RNA is processed into mRNAs and functional RNAs before translation by the mitochondrial ribosome[15].

Mitochondria have high levels of reactive oxygen species (ROS), a by-product of OXPHOS, resulting in a much higher rate of mtDNA damage in comparison with nDNA. This high rate of sporadic mutation in mtDNA results in a state of "heteroplasmy" where not every copy of the mtDNA is identical. mtDNA repair mechanisms, though poorly understood, are recognised to be limited in comparison with nDNA repair. Mitochondria have an absence of efficient double strand break (DSB) repair, any evidence for homologous recombination (HR) being seen as controversial in the field[16]. Together, these result in a particularly high mutation rates for mtDNA. The high copy number nature of mtDNA means that damage to mtDNA often leads to clearance rather than repair[17,18]. Mitochondrial genetics impact the inheritance, genotype and presentation of mitochondrial diseases, and mtDNA and mitochondrial genetics will be detailed explicitly in the context of mitochondrial diseases in section 1.2.2.

1.2 Mitochondrial disease

Given the crucial role of mitochondria in OXPHOS function, it is not surprising that mutations in mitochondrial genes can have severe consequences for the maintenance of cellular energy levels. All 37 genes in mtDNA encode or aid biosynthesis of the proteins of the OXPHOS pathway which is complemented by nuclear encoded subunits[19] and although just 1% of the mitochondrial proteins are encoded in mtDNA, four out of the five complexes in the OXPHOS pathway contain mtDNA-encoded subunits, Figure 1-1C. Consequently, mutations in both nuclear and mitochondrial genomes can result in a severe class of incurable mitochondrial

diseases. Mitochondrial diseases have a range of clinical manifestations, broadly the result of defective OXPHOS.

1.2.1 A brief description of mitochondrial diseases

Although mitochondria were not discovered until 1890[20], the first mitochondrial disease was described almost two decades earlier in 1871 by Theodor Leber, a German ophthalmologist. Leber documented a group of young men with sudden loss of central vision, naming the condition Leber's hereditary optic neuropathy (LHON). It was not until 1972 that LHON was linked to a mitochondrial dysfunction[21]; LHON remains one of the most prevalent mitochondrial diseases worldwide today.

Table 1 Mitochondrial diseases caused by mtDNA mutations for mutations, see Figure 1-2A

Disease	Mutation	Genetics	Symptoms
MELAS Mitochondrial encephalomyopathy, lactic acidosis and stroke-like episodes	m.A3243G ($tRNA^{Leu}$)	Heteroplasmic threshold is tissue specific. In general ~60-90%	Encephalomyopathy stroke-like episodes before 40 lactic acidosis leading to migraine, recurrent vomiting and seizures dementia
LHON Leber's hereditary optic neuropathy	m.G3460A m.G11778A m.T14484C	Mutations often homoplasmic	blindness
MERRF myoclonic epilepsy and ragged red fibre disease	m.A8344G ($tRNA^{Lys}$)	Heteroplasmic; threshold: ~73%-98%	epilepsy progressive myopathy and stiffness ragged red fibres
NARP neurogenic muscle weakness, ataxia, retinitis pigmentosum	m.T8993C/G	Heteroplasmic; threshold: ~70%-90%	neurogenic muscle weakness ataxia – unsteadiness whilst moving retinitis pigmentosum - retinal degeneration
Leigh Syndrome	m.T8993C/G Also nDNA mutations in complex I, II and IV	Heteroplasmic; threshold: >90%	Psychomotor repression - mental and motor degeneration in childhood overall failure to thrive
KSS Kearns-Sayre syndrome	5kb 'common deletion'	Heteroplasmic, appears sporadically (mothers/siblings unaffected)	fatal multi-systemic disorder opthalmoplegia – weakness in muscles that move the eye retinitis pigmentosum ataxia
PEO progressive external opthalmoplegia	5kb 'common deletion'	Heteroplasmic, appears sporadically (mothers/siblings unaffected)	opthalmoplegia – weakness in muscles that move the eye difficulty swallowing limb weakness
PS Pancreas Syndrome (Pearson's marrow)	5kb 'common deletion'	Heteroplasmic, appears sporadically (mothers/siblings unaffected)	endocrine pancreas dysfunction sideroblastic anaemia – defective red blood cell production often fatal in infancy

The 1970s and 1980s saw the beginning of the study of mitochondrial medicine, aided by the sequencing of the mitochondrial genome in 1981[6]. The first link between a mitochondrial disease and mtDNA mutations were shown by Wallace in 1988[22] and there are now over 200 reported pathogenic mutations in mtDNA registered in the online archive Clinvar[23]. The most recent study from the North of England calculated that 1 in 4,300 adults in the studied area suffer from a mitochondrial disease caused by either a nuclear (2.9 in 100,000) or mtDNA (1 in 5,000) mutation[24]. 1 in 200 people are estimated to be carriers of mitochondrial disease-causing mutations. Table 1 summarises some of the most common mitochondrial disease-causing mutations, including their associated genotype and clinical presentation.

There is an apparent disconnect between the prevalence and notoriety of mitochondrial diseases which might be explained by their varied clinical presentation[25]. Where some pathogenic mutations only impact one tissue or organ (e.g. LHON), others are progressive multi-systemic diseases resulting in muscle weakness (myopathy), impacting the brain (encephalopathy) and heart muscle (cardiomyopathy), and resulting in major disability and often premature death. Individuals with the same genotype will often present differently clinically, meaning this class of diseases perhaps do not appear to sit naturally together. Although the onset of some mitochondrial diseases is in adulthood, most mitochondrial diseases emerge clinically at younger than 18 months and the majority before 18 years of age, meaning these rare diseases are often also diseases of childhood.

1.2.2 mtDNA and disease

Inherited disease-causing mtDNA mutations have been shown to be either homoplasmic, where near to 100% of mtDNA copies carry the mutation, or heteroplasmic, where the mutation is carried by a subset of the total mtDNA. Additionally, mutations can affect single nucleotides as with the NARP and Leigh causing m.T8993C/G mutation, and large deletions, such as the 5 kb KSS, PEO and PS causing 'common deletion', Figure 1-2A. The percentage of total mtDNA copies that carry a certain mutation confers the functional penetration, the severity of phenotype experienced by mitochondrial disease sufferers, in a phenomenon known as the threshold effect, Figure 1-2B[26,27]. In general, mtDNA mutation load above ~70% is required to present a severe phenotype, though this threshold is disease specific. For the m.T8993TG mutation in the ATP Synthase gene *ATP6*, a mutation load of less than 70% is asymptomatic; 70 – 90% mutation results in neuropathy, ataxia and retinitis pigmentosum (commonly known as NARP syndrome); and more than 90% results in Leigh syndrome (see Table 1 for more examples). In general, homoplasmic mtDNA mutations have only mild biochemical impacts and tissue specific presentations, as is the case with LHON.

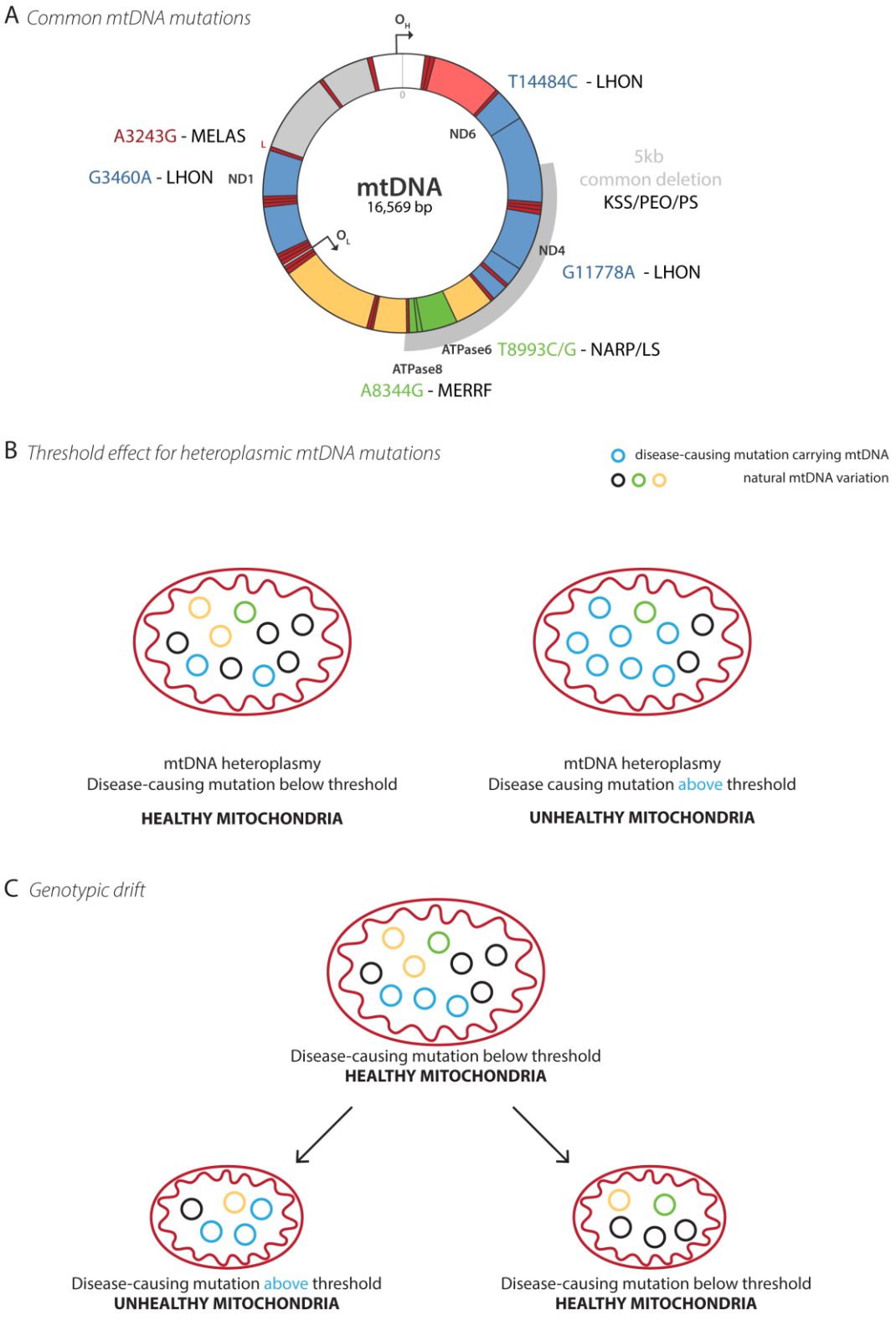

Figure 1-2 mtDNA and disease A *A map of mtDNA detailing the most common disease-causing mutations, mentioned in Table 1 and the diseases they cause* ***B*** *A heteroplasmic distribution of mtDNA can still contain some disease-causing mutation encoding copies (blue) and result in healthy mitochondrial activity, left. Mitochondrial diseases display a disease-specific thresholding effect whereby only mutations above a certain threshold impact mitochondrial function, right.* ***C*** *Genotypic drift, that is to say a change in the mtDNA mutation load, is evident through individuals lives and bodies due to random mtDNA segregation at mitosis. The new cell will replicate the sub-set of mtDNA copies it receives, sometimes resulting in a mutation load above a disease-causing threshold.*

A certain amount of genotypic drift means that the thresholding effect is also clear within individuals throughout their body, or indeed during an individual's lifespan[28,29]. During mitosis, mitochondria and mtDNA segregate randomly, resulting in an asymmetrical distribution of mutated mtDNA copies between daughter cells, Figure 1-2C. Some mtDNA mutations also show phenotypic tissue specificity. For example, mutations in $tRNA_{Ile}$ cause deafness but have no apparent effects elsewhere[30].

mtDNA is maternally inherited. Paternal mtDNA is ubiquitin labelled and degraded in the early stages of embryogenesis. As such, only mothers with mutations in mtDNA can pass on mitochondrial diseases, whereas disease-causing mutations in nDNA can be inherited from either parent. The heteroplasmic mix of mtDNA in the oocyte results in stochastic inheritance where mtDNA is randomly distributed in the ova of mitochondrial disease sufferers, meaning that offspring inherit only a random sample of maternal mtDNA. In this phenomenon, known as the genetic bottleneck, this small sample of mtDNA is then rapidly replicated, and results in vast phenotypic differences between generations due to the variable load of mutated mtDNA and the phenotypic thresholding effect[31,32].

Although complex in isolation, these factors intersect to give discrepancies in the clinical and biochemical presentation of mitochondrial diseases. This makes their diagnosis, and therefore treatment, very challenging.

1.2.3 The complexities of treating mitochondrial diseases

The complex genetics of mitochondrial diseases are just one of the many factors contributing to the barriers to the development of effective treatments[25]. A lack of understanding and expertise by medical professionals, alongside no standardised regime for diagnosis can often leave sufferers undiagnosed[33]. This is compounded by the biochemical complexity of the diseases – often patients with the same mutations will respond differently to biochemical analyses[34]. Though developments in high-throughput -omics and bioinformatic technologies are presently aiding the more comprehensive characterisation of mitochondrial pathways, remaining gaps in our understanding of mitochondrial biology also impact medicine and the identification of targets for the development of disease treatments[35].

Randomised double-blind clinical trials form a core component of many drug development pipelines. However, as with many rare diseases, traditional trial design often isn't appropriate for mitochondrial disease treatments. Recruiting for trials is complicated by the lack of large group numbers - it is often impossible to find multiple patients with same genetic defect, mtDNA load and functional penetration. Assessment of drug efficacy is also impacted by a lack of robust biomarkers, also impacting diagnosis and monitoring of disease progression ([36] and personal communication, Mitochondrial medicine conference, 2018).

A number of stories relating to mitochondrial diseases have been covered in the mainstream media in recent years, mostly due to difficulties and controversies surrounding treatment options. A lot of media attention was given to one recent example in 2017 culminating in a High Court legal case between Great Ormond Street Hospital and the family of a mitochondrial disease sufferer[37]. Charlie Gard was an infant who had mtDNA depletion syndrome resulting from mutations in a gene (RRM2B) of which there had only been 15 recorded previous cases. This story brings together several of the difficulties surrounding the treatment of mitochondrial diseases. Due to the rare nature of his condition, there have been no treatments developed for the mitochondrial disease which Charlie Gard suffered. The only potential option, an experimental treatment, was unfortunately offered too late at which point doctors refused treatment in the best interests of the infant. With serious and rare diseases such as these, there not only needs to be continued study of basic mitochondrial biology and development of treatments, but also communication and connection between individuals in the mitochondrial disease field. It is only with a consensus on the importance of idea and knowledge sharing between clinicians and researchers that we will enable better understanding of diseases and treatment regimens to positively impact the lives of mitochondrial disease sufferers.

1.2.4 Available and emerging treatments for mitochondrial diseases

At present, mitochondrial diseases are incurable. Treatment largely focusses on individually tailored symptom management through exercise and supplementing diet with vitamins, enzymes and antioxidants[38,39]. For example, the MELAS m.A3243G mutation results in a dysfunction in the glutamate pathway. Switching to a ketogenic (high fat, low carbohydrate) diet in patients can have a significant impact on motor function[40]. However, across mitochondrial diseases there is much contradiction in the literature and it is difficult to predict the success of dietary and exercise-based interventions[41].

Throughout the timeline of this project, clinical trials have been ongoing for several drugs to improve cellular energy function. NeuroVive Pharmaceuticals currently have an NAD+ modulator (KL1333) in phase 1 trials[i]. The same company also has several drugs in pre-clinical trials. Several important technological advances have also been made regarding mitochondrial disease related vision loss, such as with LHON. GenSight Biologics have successfully treated the eyes of LHON model mice with adenoviral vector injection, expressing a mitochondrial targeted wildtype ND4 to recover lost function. They are currently

[i] Clinicaltrials.gov identifier: NCT03056209

undergoing clinical trials in humans[ii]. In 2018 there was also a successful trial to treat damaged retina in humans with age-related macular degeneration with engineered stem cells[42], a technology which could be adapted for LHON patients. However, it remains to be seen whether tools such as these could be applied to other areas of the body; these treatments both benefit from the unique accessibility of the eye, and its immune privileged status - the eye does not have the same system for inflammation as the rest of the body[43].

1.2.5 Pre-implant genetic diagnostics and mitochondrial replacement therapies

Given the lack of successful treatments for mitochondrial diseases, pre-implant genetic diagnostics (PGD) are relied upon by mtDNA mutation carriers who wish to have a child. PGD minimises the risk of passing on pathogenic mtDNA mutations by screening *in vitro* fertilised oocytes. However, there are several shortcomings with this process, including a number of ethical concerns. Given the random segregation of mtDNA in mitosis, the mtDNA of the tested blastomere might not be representative of the embryo as a whole. Moreover, given the possibility for heteroplasmy shifts, it is complex to decide the mutation load cut-off for an acceptable embryo. The conundrum behind both of these factors can be summarised to questioning whether, when there is still a risk of serious harm to the future child, is it ethical to still offer assisted reproductive therapies to a mitochondrial disease carrier wishing to conceive[44]? These concerns highlight the importance of informed consent for mitochondrial disease sufferers and proper genetic counselling[45]. Besides these shortcomings, PGD is very useful for some. However, where a mtDNA mutation is homoplasmic, or where after several rounds tested embryos are all unacceptable for implantation, PGD is unsuitable. In these cases, some individuals opt for oocyte donation. Unfortunately, this can often require long wait times for suitable oocyte donors, and some do not see this as an acceptable alternative.

In 2017, the UK Human Embryology and Fertility Agency (HEFA) approved mitochondrial replacement therapy (MRT) by nuclear transfer for mothers carrying mtDNA mutations, making the UK the first country to approve the technique[46]. This development was widely covered in the press at the time, referred to as “three parent families”. Ethical concerns from families, experts and the public included conversations on whether this would make it more acceptable to genetically engineer offspring based on non-medical grounds, raising the importance of involvement of the public in ethical debate surrounding genome engineering. Despite, or perhaps because of this debate, the technique seemed to be widely accepted by the public[47,48].

[ii] Clinicaltrials.gov identifier: NCT03293524

There are several methods for MRT, with pronuclear transfer and maternal spindle transfer being the most popular. MRT was first developed in the 90s as an infertility treatment after IVF clinics found that using a mitochondrial donor improved success rates[49]. The technique was stopped following a US Food and Drug Administration (FDA) request for further investigations into the technique, which was never completed. Although mitochondrial replacement therapy is now UK HEFA approved, it will be important to monitor these individuals' quality of life. In particular, there is an unknown impact on mitochondrial-nuclear crosstalk[50] and research in mice has highlighted a potential for corrected mtDNA heteroplasmy to shift back to mutant genotype[51].

PGD and MRT offer some hope for carriers of mitochondrial diseases who wish to have unaffected children. However, it is important to remember that these fertility techniques are still not suitable for all: some individuals might decline on ethical grounds[52,53], and they are no use for individuals already suffering from mitochondrial disease in somatic cells.

1.3 Tools for the manipulation of mtDNA

1.3.1 Motivation

Tools for the manipulation of nuclear DNA (nDNA) have expanded our understanding of replication, transcription and gene expression in health and disease. Given the unique structure and organisation of mtDNA, and its role in mitochondrial disease (as summarised above), the development of mitochondrial equivalents of nuclear molecular genetics techniques remains an important, unmet challenge. Furthermore, expanding understanding of mitochondria and mtDNA could have therapeutic potential with a view to meet the challenges highlighted in the previous section. To this end, a growing body of work has successfully developed mtDNA targeting nucleases, including mitochondrial restriction endonucleases (MitoREs), Zinc Finger Nucleases (MitoZFNs) and TALENs. Additionally, several more controversial studies have also focussed on the mitochondrial targeting of oligonucleotides. However, development of tools for the interrogation of mitochondrial genomes is not trivial, and it is still not possible to easily manipulate mtDNA.

The main barriers to developing mtDNA-targeted tools are a consequence of mitochondrial structure: tools must be correctly trafficked within the cell and cross the OMM and IMM into the dynamic mitochondria. This is particularly difficult for large complexes. Proteins can usually be quite easily directed to the mitochondria through the addition of a mitochondrial targeting peptide sequence (MTS), however equivalents for polynucleotides remain unclear. Regardless of these challenges, an efficient and versatile method for manipulation of mitochondrial genomes would have a significant impact on our understanding of

mitochondrial biology. Moreover, there is potential for these techniques to be used as therapies for mitochondrial diseases. One could imagine the potential for an alternative to the MRT IVT techniques, or a gene therapy which could be used in the somatic cells of an individual to ameliorate symptoms in a tissue-specific manner and not be passed on to future generations.

1.3.2 Heteroplasmy purification

Heteroplasmy purification provides the clearest illustration of the therapeutic potential for mtDNA targeting tools. Due to the phenotypic threshold effect, a small change in mutant mtDNA load can result in a great change in the clinical presentation of a mitochondrial disease. Indeed, much of the work in this field has focussed on developing tools which selectively degrade sub-populations of mtDNA on the basis of sequence towards heteroplasmy purification, Figure 1-3. A cell heteroplasmic for a mtDNA mutation has a balance of mutated and wild-type mtDNA molecules. When the number of mutated mtDNA molecules is above a certain mutation-specific threshold, mitochondrial function is compromised. mtDNA editing techniques selectively cleave mutated mtDNA copies, which are degraded by the mitochondria, rather than being repaired[17,18]. The remaining wild type mtDNA is replicated to re-establish mtDNA copy number. This results in a heteroplasmy shift towards a 'healthier' mitochondria. A complete removal of mutated mtDNA results in mtDNA homoplasmy.

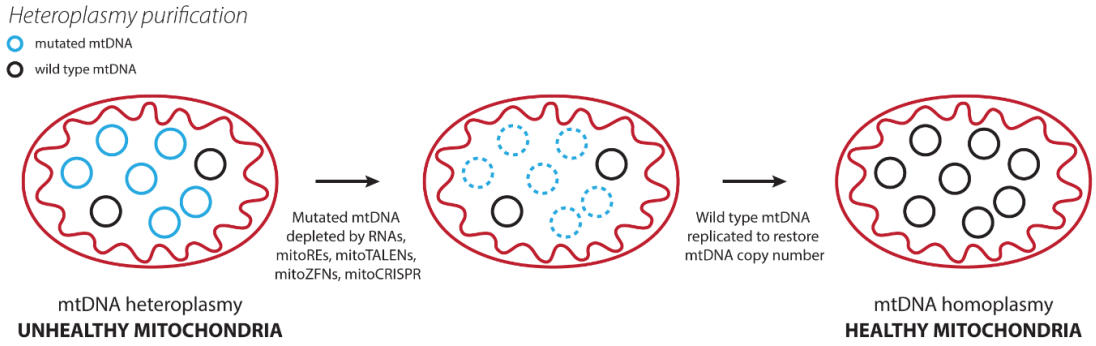

Figure 1-3 Heteroplasmy purification *involves the selective degradation of mutated (here blue) copies of mtDNA based on their sequence. This can be achieved via anti-sense RNAs, mitochondrial-targeted restriction endonucleases (REs), TALENs, zinc finger nucleases (ZFNs) or, theoretically, the CRISPR machinery. Following degradation of mutant mtDNA copies, the remaining 'healthy' (here black) mtDNA population is replicated to restore mtDNA copy number, resulting in a 'healthy' mitochondrion.*

Heteroplasmy purification has been successfully utilised in cells grown in culture and a number of model organisms with endonucleases expressed and targeted to mutant mtDNA. These include MitoREs and programmable nucleases including ZFNs and TALENs, which will be covered in more detail in sections 1.3.5 and 1.3.6.

1.3.3 Mitochondrial protein import is critical for tool use

Developing strategies for the specific targeting of endonucleases to the mitochondria requires an appreciation of natural mitochondrial protein import pathways. Nuclear encoded mitochondrial preproteins are translated in the cytosol, containing a mitochondrial targeting sequence (MTS) which directs protein import into the appropriate mitochondrial compartment: namely the OMM, IMM, IMS, or the matrix. Most matrix targeted proteins contain a cleavable n-terminal MTS, often in the form of an amphipathic α-helical leader peptide, approximately 15-50 amino acids in length[54] and recognised by proteins throughout the TOM/TIM pathway[55]. Termed the 'presequence import pathway', matrix targeted protein import is considered the classical import pathway. Preproteins in the cytosol are imported across the OMM by a translocase of the outer mitochondrial membrane (TOM) complex which delivers proteins into the IMS. A translocase of the inner mitochondrial membrane (TIM) complex delivers them into the matrix where the MTS leader peptide is cleaved off by the mitochondrial processing peptidase (MPP)[56]. Additional pathways which target proteins to other compartments of the mitochondria rely on internal MTSs. As they are not directly relevant here, these pathways will not be covered in this thesis; see Wiedemann & Pfanner for a recent review[57].

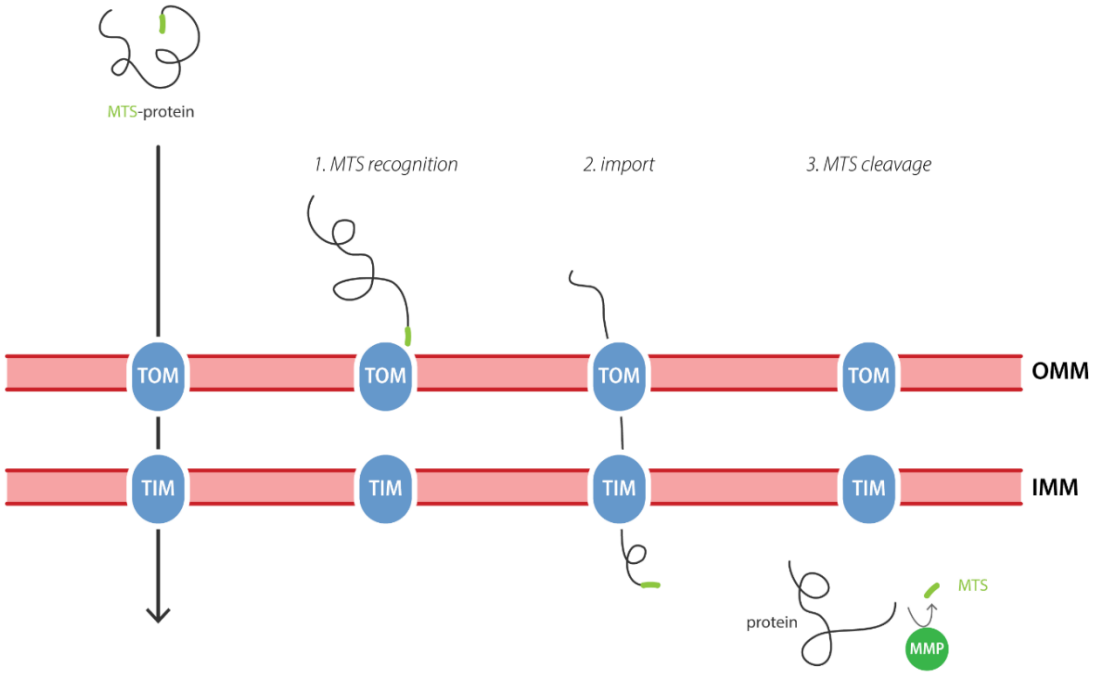

Figure 1-4 The presequence import pathway *directs proteins with an MTS from the cytosol into the mitochondrial matrix. The schematic above shows import of an unfolded protein across the OMM and IMM following recognition of an N-terminal peptide MTS sequence (light green) by components of the TOM complex (1). Following translocation through TOM and TIM (2), the N-terminal MTS is cleaved by the mitochondrial processing peptidase (MPP, dark green) in the mitochondrial matrix (3).*

1.3.4 Targeted mitochondrial protein import

Mitochondrial protein import pathways are sufficiently understood to be harnessed for directed import of non-native proteins[58]. To this end, a naturally occurring MTS leader peptide sequence is cloned upstream of the protein of interest so that the MTS is expressed in-frame with the N-terminus of the protein of interest. The MTS from cytochrome c oxidase subunit viii (COX8A) is one of the most widely used in commercially available mitochondria-targeting constructs and comprises a 29-residue helix. The 69-residue mitochondrial targeting sequence from *Neurospora crassa* ATPase subunit 9 has also been characterised[59] and used to target proteins of interest to mitochondria[60]. Some MTSs display unique features, such as controlled cellular localisation. The mammalian ATG4D contains a cryptic 42-residue MTS, downstream of a caspase cleavage site. Upon cleavage by caspase, such as during cell stress, the cryptic MTS is revealed, and ATG4D localisation shifts from cytosolic to mitochondrial[61].

The relative simplicity of MTS addition has meant that targeting proteins to mitochondria in this way has become widely used since it was first shown in 1988[62]. In the first example of allotopic rescue of a disease model, the low ATPase activity of *S.cereviciae* carrying a mutation in the ATP8 gene was rescued by expressing a functioning subunit appended to an MTS. Allotopic rescue of mutated OXPHOS proteins has also been shown in human cells. Targeting a functional ATP6 gene to mitochondria NARP cybrids carrying the m.T8993C/G mutation) successfully compliments complex V and rescues ATP synthesis and cell growth[63]. It is this same method which is being used to rescue defective ND6 function in LHON patients, as mentioned in section 1.2.4. MitoREs and programmable nucleases including ZFNs and TALENs, have also been targeted to the mitochondria, a brief review of which will be given in sections 1.3.5 and 1.3.6.

1.3.5 Mitochondrial type II restriction endonucleases

Type II Restriction Endonucleases (REs) have been widely used in molecular genetics since the 1970s to generate targeted DSBs in DNA[64]. Originally found in bacteria, REs defend against invading pathogenic DNA by cleaving upon recognition of a restriction site, a DNA sequence usually 4-8 nts in length[65]. There have been many successful attempts at targeting type II REs to mitochondria for heteroplasmy purification. The first demonstrations of this in cultured cells were the transient expression of PstI[66] and SmaI[67] in disease model cybrid cell lines, published in 2001 and 2002 respectively. Cybrids (cytoplasmic hybrids) are cell lines which model mitochondrial diseases by fusing the patient mitochondria with immortalised cell lines. In both cases, a shift in heteroplasmy was observed, and the wild-type mtDNA population expanded.

Mitochondria-specific delivery of REs in animal models was first shown in 2002; EcoRI was *in vivo* electroporated into hamster skeletal muscle, showing a decrease in cytochrome c oxidase activity and no measurable off target impact in nuclei[67]. Heteroplasmy purification was also shown with recombinant viral transfection of ApaLI in heteroplasmic NZB/BALB mice muscle and brain tissues[68], later targeting liver and heart[69]. Germline specific heteroplasmy purification using MitoREs has even shown the ability to prevent transmission of mtDNA mutations to offspring in NZB/BALB mice[70].

Although delivery mechanism into cells and living organisms differed in the publications highlighted above, in each case mitochondrial targeting was achieved by cloning the RE protein coding sequence downstream from the COX8A MTS. Though MitoREs can efficiently target mtDNA and be used for heteroplasmy purification, naturally occurring target sites match few clinically occurring pathogenic mtDNA mutations, and even fewer without off-target specificity. Indeed, of the over 200 known mtDNA mutations, only the NARP/Leigh causing m.T8993C/G has been shown to be targeted by naturally occurring REs[70].

1.3.6 Mitochondrially targeted engineered nucleases (ZFNs, TALENs)

Although naturally occurring REs have a broad range of target sequences, their short sequence specificities often occur several times in a genome. Moreover, it is extremely difficult to re-engineer proteins, such as REs, with no clear structure-sequence determinants[71].

Engineered nucleases fuse a programmable DNA recognition domain to a nuclease domain, providing more sequence specificity and fewer off-target effects. As well as being widely influential in molecular genetics, engineered nucleases can be used to expand the available endonucleases matching pathogenic mtDNA mutations as they can be engineered to target almost any sequence. Programmable DNA recognition domains including zinc finger and TAL-like effector domains have both been used to target mtDNA, as summarised below:

1.3.6.1 Mitochondrial Zinc Finger Nucleases

Zinc finger nucleases (ZFNs) are chimeric proteins containing a modular zinc finger DNA recognition domain and an endonuclease domain. Zinc finger motifs are naturally occurring Cys_2His_2 DNA interacting domains found in many transcription factors. Each designed to target a 3nt codon, a string of ZFs can be cloned together to target a DNA sequence, often about 20 base pairs long. DSB formation is usually through the dimeric RE FokI, achieved by tethering FokI monomers to ZFNs targeting adjacent sequences on complimentary DNA strands[72,73].

MitoZFs have been designed to target both large scale deletions and single nucleotide mutations in mtDNA[74], in addition to being used to bring alternative functionalities to mtDNA such as sequence specific methylation through fusion of methyltransferases to MitoZFs[75]. Fusion of MitoZFs targeting adjacent sequences to the dimerising endonuclease FokI has shown heterodimeric MitoZFNs to be able to recognise 1nt change in a 12nt sequence[76].

In cybrid cells and animal models, MitoZFNs can be designed and used for heteroplasmy purification and a rescue of disease phenotype. MitoZFNs designed to target mT89993G and the mtDNA common deletion showed a shift from mutant to wild-type mtDNA, and a rescue of oxygen consumption rate and functioning respiratory complex subunits[77].

1.3.6.2 Mitochondrial TAL-like effector nucleases

TAL-like effector nucleases (TALENs) are engineered endonucleases which target specific sequences on DNA by utilising the 34 amino acid repeat-containing TALE domains from the agrobacterium *Xanthomonas*[78]. Each TALE domain recognises a single nucleotide, and sequences of interest are targeted by 'building' TALE proteins. As with ZFNs, TALENs are often heterodimeric, utilising the split FokI for endonuclease activity. MitoTALENs have been developed which localise to the mitochondria and induce DSBs in mtDNA in a sequence specific manner, as shown in patient derived cybrid cell lines containing the common deletion[79] and the m.T8993C/G point mutation[80]. In each case, eliminating mutated mtDNA copies rescued the oxygen consumption rate of the patient derived cells, a result of heteroplasmic purification. As with MitoREs, MitoTALENs have also been used to prevent germline transmission by clearing mutated mtDNA in mouse oocytes[70].

1.4 The case for a MitoCRISPR system

Although MitoZFNs and MitoTALENs offer a much wider range of sequence specificity than MitoREs, there are still several shortcomings which hinder their application. Firstly, although there have been several advances in the cloning ZFN and TALEN libraries in recent years, engineering and verifying engineered nucleases can still be time consuming. Secondly, ZFN and TALENs have some inherent limitations which impact the breadth of sequence which can be targeted: TALENs have a requirement for a thiamine at the start of a sequence, and ZF modules do not exist for every combination of 3 nucleotides. There are also several issues relating to the cellular delivery and mitochondrial targeting of engineered nucleases. It has been shown that large protein complexes are inherently challenging to import into the mitochondria[81] and indeed the DNA coding sequence for TALEN is likely to exceed the AAV size limit of 5 kbp, making viral delivery to cells complex if not impossible[80]. Finally, ZFs are

trafficked to the nucleus due to internal nuclear targeting sequences. It is important that a mtDNA targeting tool avoid off-target activity on nDNA. As such, nuclear export sequences such as the murine minute virus NS2 sequence in addition to mitochondrial targeting sequences can be included but must be considered to add an extra layer of complexity.

Although some good progress has been made with regards to mitochondrial targeted endonucleases, the tools available for the manipulation of mitochondrial genomes are still meagre in comparison to those available for nuclear DNA. This project aims to fill the gap in the currently available technologies for the study of mtDNA by working towards making the varied toolbox of CRISPR methods available for mitochondrial genetics.

The following section firstly contextualises the fast-moving field of CRISPR research before giving a brief overview of the mechanism of some of the most commonly used CRISPR systems, highlighting several applications which might be made available for the manipulation of mtDNA.

1.4.1 "A new era of biological understanding and control"[82]

Following the first published reports showing their potential in 2013, CRISPR systems have quickly revolutionised molecular genetics by providing a quick and convenient method for efficiently targeting proteins to almost any short DNA sequence. CRISPR has proven an incredibly adaptable and versatile tool, hurrying in a so-called 'new era of biological understanding and control' which has quickly offered a whole new toolbox for manipulation of DNA[82].

With applications from basic science to the clinic, the impact of CRISPR has been such that some scientists have, somewhat esoterically, begun calling molecular genetic techniques pre-2013 as 'BC' (to mean 'before CRISPR'). It would be foolish to suggest that now in the CRISPR era there is no place for 'traditional' techniques, but the advantages of CRISPR over other genome editing techniques – namely high accuracy, efficiency and flexibility – has led to a surge in its implementation, giving an unparalleled level of control over nucleic acids with implications in the understanding of: genome editing and regulation, modification of genomes, control of living systems and much more. CRISPR tools are fast becoming standard laboratory techniques and a huge amount of research funding and a corresponding surge in literature has been published on the topic. In 2007, 12 papers were published that tagged 'CRISPR' in pubmed. This rose to 283 papers in 2013, and an astonishing 3012 in 2017.

Although the term CRISPR is now synonymous with its applications in genome engineering, in their natural form, the clustered regularly interspaced short palindromic repeats (CRISPR)

system is a bacterial and archaeal acquired immune system that works by specifically cleaving pathogenic DNA such as that from invading viruses and plasmids.

1.4.2 CRISPR as adaptive immunity

First identified in 1987 by their characteristic short repetitive DNA sequences interspersed with random sequences at regular intervals[83], the biological significance of CRISPR arrays was unknown until the mid-to-late 2000s. It was then that they were recognised to be part of an almost ubiquitous acquired immune response found in 40% of all bacterial species and 90% of archaeal species in one iteration or another[84]. The random sequences in those first observations are now known to be 'spacers' – sequences acquired from invading pathogenic DNA. Transcription and processing of the CRISPR array generate CRISPR guide RNAs (gRNAs) which target effector nucleases to form a DNA/RNA hybrid (R-loop) at the target sequence, displacing the non-complimentary DNA strand and cleaving the two strands of DNA, Figure 1-5. Protospacer adjacent motifs (PAMs) in invading DNA are recognised by the CRISPR nuclease and prevent the cleavage of self-DNA.

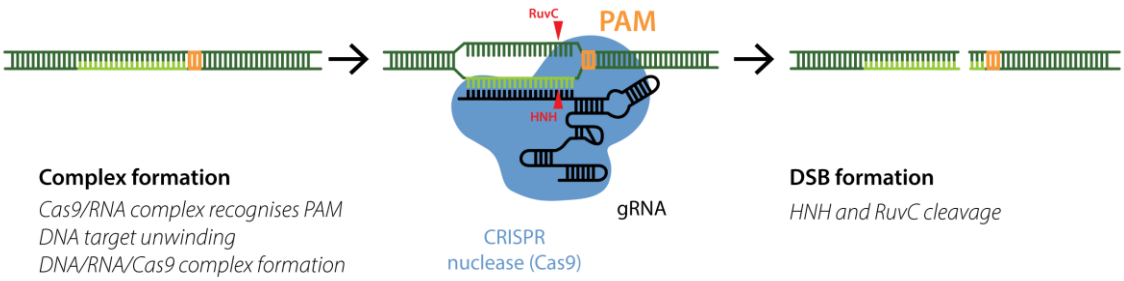

Figure 1-5 CRISPR DSB formation *CRISPR ribonucleoprotein (RNP) complex formation on a dsDNA target requires recognition of a short protospacer adjacent motif (PAM, orange) followed by target sequence (light green) unwinding and CRISPR gRNA binding to form an R-loop. In the type IIA Spy Cas9 system, two nuclease domains, HNH and Ruv C cleave (red arrows) the backbone of the target and non-target strand, respectively, forming a blunt DSB.*

The study of CRISPR biology has been extensive over the past few years, revealing a growing family of proteins. Due to their rapidly changing nature and fast evolution (through its function, the CRISPR array is always acquiring new DNA sequences), CRISPR-*cas* genomic loci show a great diversity in sequence which has been challenging to classify. Nevertheless, a classification of CRISPR systems has emerged into 2 classes, 6 types and up to 33 sub-classes [85,86] mainly on a basis of the phylogeny of *cas* genes but also the crRNA composition. Although many CRISPR family proteins are being used for a wide range of applications in molecular biology, the type IIA and VA are most common, and the main features of both are summarised in the following sections. Interestingly, the effector proteins of both type IIA and VA show functional similarity, both being roughly similar in size and jaw-like conformation containing a RuvC nuclease domain. Intriguingly, this functional similarity comes without a corresponding match at a sequence or structural level [87,88].

1.4.3 Type IIA CRISPR systems

There are several naturally occurring type II CRISPR systems, separated into 3 sub-classes. It is the type IIA subclass, in particular those from *Streptococcus thermophilus (Sth)* and *Streptococcus pyogenes* (*Spy*) which have been the most widely used for genome engineering. The type IIA nuclease is Cas9, comprising two nuclease domains, the RuvC-like and HNH domains, that generate blunt ended DNA double strand breaks, targeting the displaced and target strand respectively, Figure 1-5.

In naturally occurring CRISPR systems, Cas9 is guided by two RNA elements; the CRISPR RNA (crRNA), which directs Cas9 sequence specificity, and the trans-activating CRISPR RNA (tracrRNA), which mediates RNA/Cas9 contacts. However, these RNA components can be replaced by a single integrated synthetic alternative, the guide RNA (gRNA), and these integrated gRNAs have been widely adopted when using CRISPR for molecular genetics. The gRNA targets a 19-22 nt sequence and *Spy*Cas9 has a 5′-NGG-3′ PAM requirement [89,90]. Mismatches throughout target sequence impact specificity, and are not tolerated in the 8-12 nt PAM-proximal seed region, due to mechanism of duplex unwinding and RNA-DNA duplex formation [91,92].

The crystal structure of *Spy*Cas9 in complex with gRNA and target DNA has been solved[93], showing much of the gRNA to have extensive contacts with the Cas9 internal surface. It can be presumed that these interactions between the gRNA and Cas9 are crucial for optimal complex formation, and as a result optimal complex formation on DNA and positioning of the endonuclease domains and activity. However, the crystal structure also reveals some regions of the gRNA which are positioned externally from the Cas9 protein, which might be amenable to modification.

1.4.4 Type VA CRISPR systems

Cas12a, also referred to as Cpf1, is a type VA CRISPR endonuclease which naturally produces staggered nicks on DNA. There are several naturally occurring Cas12a systems from different species, of which the *Lachnospiraceae bacterium (Lb)* Cas12a and *Francisella novicida (Fn)* Cas12a have been shown to be suitable for mammalian cell genome engineering[94]. Containing a single RuvC endonuclease domain, Cas12a cleaves the two DNA strands in turn, resulting in a DNA DSB with a 5′ 3 nt overhang. Cas12a has a much smaller RNA than the type IIA *Spy* cr:tracrRNA. The Cas12a crRNA is naturally one-component, comparable to the designed gRNA. Cas12a also utilises a hairpin to mediate interactions between the endonuclease domain containing protein and the RNA but lies in the opposite direction to the Cas9 gRNA with the hairpin at the 5′ end of the protospacer sequence, Figure 1-6 bottom. *Lb*Cas12a has a 5′-TTN PAM requirement. A number of studies have solved the structure of

Cas12a[95–97] which can inform potential structural modifications to the ribonucleoprotein complex. Figure 1-6 gives a comparison of the major features of the type IIA and VA systems.

Class	Class 2	Class 2
Type-subtype	Type II-A	Type V-A
Effector nuclease	Cas9	Cas12a (Cpf1)
Nuclease domains	RuvC, HNH	RuvC, pre-crRNA processing
Target (length)	dsDNA (19-22 nt)	dsDNA (20 nt)
Pam specificity	5' NGG to the 3' end	5' TTTN to 5' end
Cut structure	Blunt ended DSB	3 nt 5' staggered overhang
crRNA structure	crRNA/tracrRNA (42/84 nt)	Single crRNA (50 nt)
	sgRNA 100 nt	
RNA processing	Endogenous RNase III	Cas12a

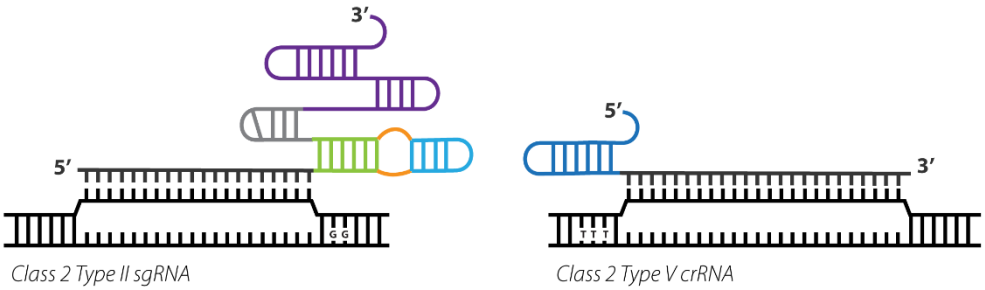

Figure 1-6 Comparing type IIA and VA CRISPR systems *Top: Table comparing major characteristcs of type IIA and VA CRISPR systems Bottom: Schematic comparing RNA structures between type IIA and VA CRISPR systems. The main differences between the sgRNAs concern the structural component which mediates interactions between the sgRNA and nuclease. The type II sgRNA has a much larger structural component than type V, which is found 3′ of the spacer in contract to the type V sgRNA which is 5′ of the spacer.*

1.4.5 CRISPR tools

Genome editing using restriction enzymes, ZFNs, and TALENs has largely focused on the introduction of one or more DSBs to be repaired by the cell's own repair mechanisms. Similarly, efficient generation of sequence-specific DSBs was perhaps the biggest initial revelation of CRISPR, widely becoming a standardised technique for creating knockout and mutant cell lines and model organisms. To this end, there was an initial boom of studies before the end of 2013, demonstrating CRISPR in: bacteria[98]; mammalian and patient-derived cells [99–101]; zebrafish[102], mice[103,104] and other model organisms. Several significant CRISPR studies also achieved increased on-target and reduced off-target DSB formation: for example, staggered nicks on DNA double the recognition domain and increase sequence specificity[105].

Without a template, DNA DSBs result in indels and mutations from non-homologous end joining (NHEJ) mediated repair. Much of the nuclear-targeted CRISPR toolbox has focussed on preferentially directing repair from a template via the homologous recombination (HR) pathway[106]. However, it is important for MitoCRISPR that we remember the distinct context of mtDNA. As highlighted in section 1.1.3, DNA repair mechanisms are not well understood

in mitochondria, and likely to be only a subset of those available for nuclear DNA maintenance.

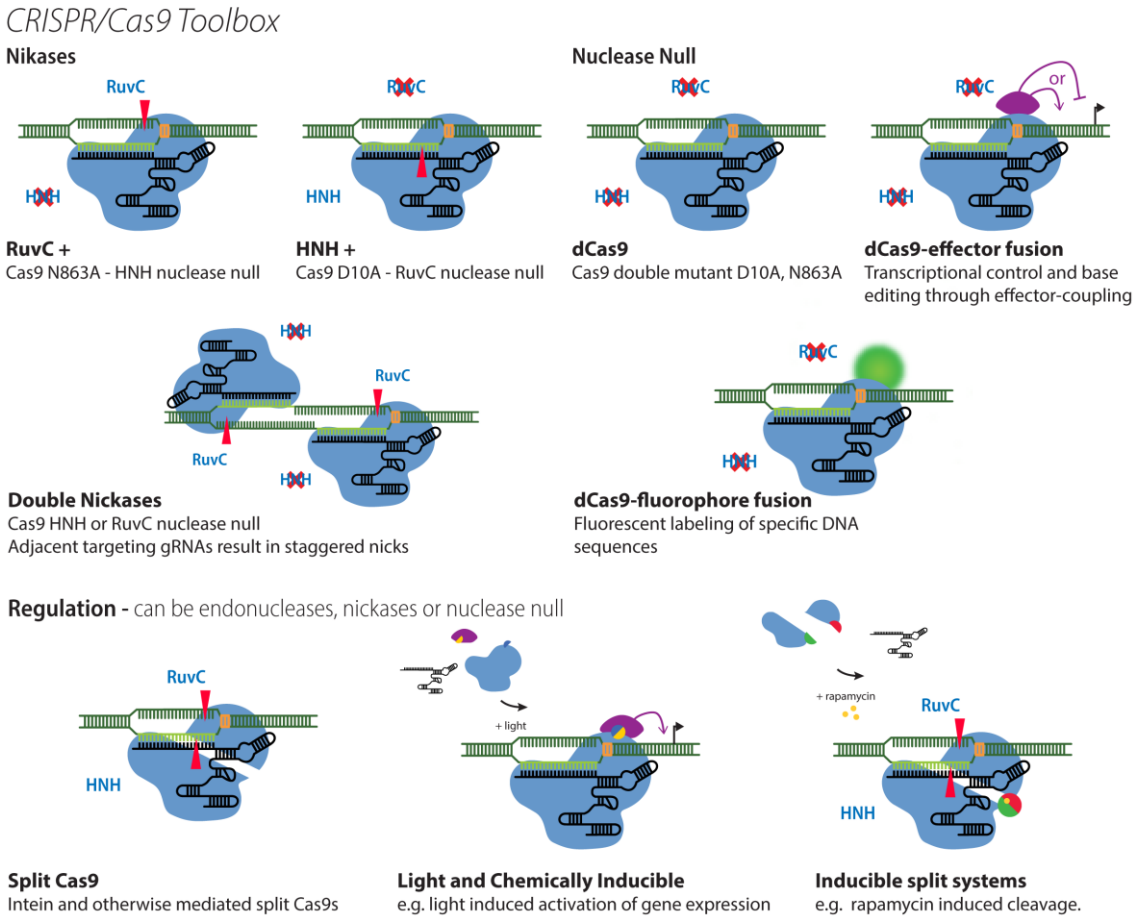

Figure 1-7 CRISPR toolbox *includes:* ***Nikases****, where either one of the two endonuclease domains (RuvC, HNH) has been inactivated to form a single stranded break on DNA. These can be used separately or to introduce staggered nicks and broaden the specificity region;* ***dCas9*** *where both RuvC and HNH endonuclease domains have been inactivated. These can be used to target functionalities to a DNA locus of interest including transcriptional control and fluorescent proteins;* ***Regulation*** *of CRISPR RNP formation, or RNP interaction with effectors, is also achieved through light and chemically induced complex formation.*

Although there may be potential for supplying a minimal HR cassette to the mitochondria, the potential for HR-repair is complicated by the absence of techniques to supply the DNA template. The applications of CRISPR systems have quickly expanded much beyond that of targeted DSB formation including break-less editing[107], transcriptional regulation[108], cellular imaging[109,110], genome wide association studies (GWAS)[111], building genetic circuits[112], and much more.

The HNH and RuvC nuclease domains can each be catalytically inactivated by point mutations. All three of the mutants — the double nuclease-null (dCas9) and the two nuclease-null (D10A targeting RuvC and H840A, HNH) – localise to DNA with high sequence specificity. Furthermore, CRISPR complex formation has been tightly and spatial-temporally controlled

through split Cas9s, brought together by inteins[113,114] or light and chemically inducible complex formation[115–117].

The enormous versatility of CRISPR systems has largely been thanks to the introduction of functional protein domains as fusion proteins. Several publications over the past few years have also proven that accessorising the gRNA structure to be a powerful tool, bringing in additional functionalities such as fluorescence and protein-interactions. This can be achieved for example through introducing protein interaction RNA sequences into the gRNA, such as bacteriophage MS2 hairpins which tightly bind MCP domains (MS2 bacteriophage coat protein domains), or S1m, an RNA structure which mimics biotin[118,119]. A unique function of the CRISPR system beyond protein-only DNA-targeting systems is the ability to bring together all three of the naturally encoded polymers (protein, RNA and DNA) into one ribonucleoprotein (RNP) complex. Based upon this, and the incredible versatility of the RNP, CRISPR has provided a fantastic platform on which to build an extensive toolbox for the interrogation of not just nDNA, but many other cellular processes.

Although tools for the efficient and accurate generation of DSBs in mtDNA are useful, such as in heteroplasmy purification, and deepening understanding of mtDNA repair mechanisms, the expanded CRISPR toolbox offers even more novel functionalities for the understanding of mtDNA. dCas9 provides a protein chassis through which other effector proteins might be brought into proximity with a locus of interest; an excellent resource for understanding mtDNA-protein interactions. Tethering transcriptional enhancers and repressors to dCas9 for CRISPRa (activation) CRISPRi (inhibition) has been used for the understanding of gene function and might be interesting in a mtDNA context. Additionally, control and rearrangement of chromatin have also been studied using these tools. Although mtDNA packaging is distinct from the processes involved in nDNA packaging, a similar tool could be used to understand the structure of the mitochondrial nucleoid. Not all mutagenesis of DNA requires the formation of DSB. Tethering an adenosine deaminase to dCas9 results in an AT pair adjacent to a targeted site being mutated to a GC pair[107]. Given the limited complement of DNA repair proteins in the mitochondria, delivery of base editing machinery might be a possibility for targeted mtDNA mutagenesis. Finally, dCas9-GFP fusions have allowed the imaging of DNA loci[110], and might be attractive as a tool for imaging specific mtDNA copies, potentially broadening understanding of the inheritance of mutated mtDNA (e.g. mtDNA segregation at mitosis, and the mitochondrial genetic bottleneck, see Section 1.2.2).

1.5 Steps necessary to develop a MitoCRISPR system

The overall ambition of the MitoCRISPR project is to design and evaluate a set of CRISPR tools to enable the manipulation of mitochondrial genomes. The development of this system will require the realisation of the following milestones, as summarised in Figure 1-8.

1. Mitochondrial targeting of a CRISPR protein
2. Mitochondrial targeting of a CRISPR guide RNA
3. Proof of ribonucleoprotein complex assembly within mitochondria, and on mtDNA
4. Proof of ribonucleoprotein complex activity on mtDNA *in situ*.

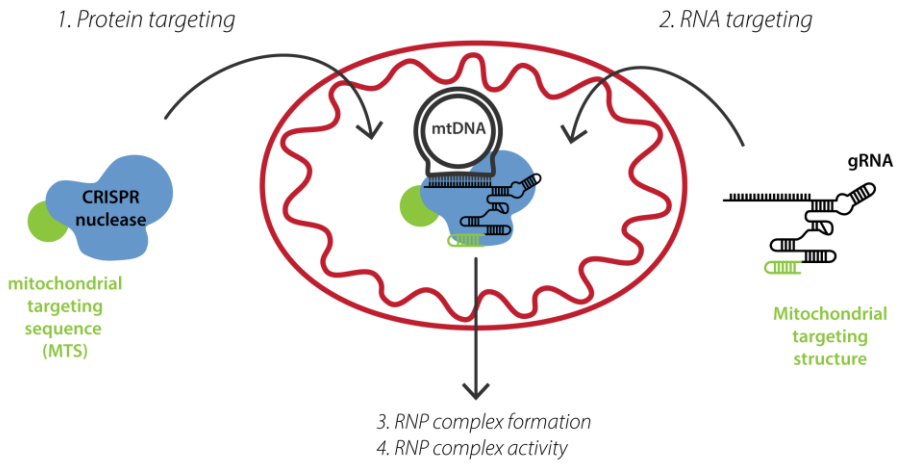

Figure 1-8 MitoCRISPR project summary *The four main steps required for the development of a MitoCRISPR system include* ***1*** *the targeted delivery of a CRISPR nuclease to the mitochondria by fusion to a peptide mitochondrial targeting sequence (MTS),* ***2*** *the targeted delivery of a CRISPR guide RNA (gRNA) to the mitochondria through fusion to a mitochondrial targeting structure (here, RNA),* ***3*** *the formation of a functional CRISPR ribonucleoprotein complex (RNP) inside the mitochondrial matrix on mtDNA, and* ***4*** *functional activity of the CRISPR RNP (this could be through cleavage activity, or another accessorised functionality).*

1.5.1 Mitochondrial targeting of CRISPR proteins

The first aim of the MitoCRISPR project is the mitochondrial targeting of a CRISPR endonuclease protein. It is important that this is achieved without compromising mitochondrial viability, such as by causing fragmentation, or disturbances to mitophagy and OXPHOS. When this project was started, the most studied CRISPR endonuclease, particularly in the development of novel molecular genetics tools, was the *Spy*Cas9. On the basis of extensive work targeting other proteins to the mitochondria through the addition of an MTS, initial work focussed on the modification of this protein for mitochondrial import, as detailed in Chapter 3.

There are several ways in which a CRISPR protein might be delivered into the cell for subsequent trafficking to and import into the mitochondria, which can be broadly envisaged through the central dogma as being at the level of DNA, mRNA, or protein. Accordingly: DNA can be either stably expressed by incorporation into the genome, or transiently transfected

and expressed from a plasmid; the mRNA encoding the protein might be transiently transfected into the cell; the protein itself can be transiently transfected into the cell as a ribonucleoprotein (RNP) particle. Furthermore, reagents appropriate to each of these levels can be delivered into cells via a plethora of different methods, including (though not limited to) a range of commercially available lipid-based transfection techniques, electroporation, viral delivery mechanisms.

1.5.2 Mitochondrial targeting of CRISPR RNAs

The development of a CRISPR system for use on mitochondrial DNA requires the mitochondrial targeting of the gRNA. There are several ways through which this might be achieved, either harnessing natural mitochondrial RNA import machineries (reviewed below), or through non-natural means. The ability to modify the gRNA extensively has been shown, but little work had been done on the impact of modifications on complex formation and cleavage activity, which we aimed to interrogate through ensemble and single molecule biochemical techniques in Chapters 4 and 5.

1.5.2.1 Overview: 'natural' mitochondrial RNA import

Section 1.3.4 described how the mitochondrial protein import pathway is sufficiently well understood to allow targeting of proteins of interest. In contrast, pathways for mitochondrial RNA import are poorly understood. Whilst multiple research groups have claimed to achieve mitochondrial targeting of RNAs[120–123], there is not the same consensus of understanding as with protein import, and the existence of a dedicated pathway for mitochondrial import of RNAs is controversial [124,125].

Whilst mitochondria contain a fully functional machinery for gene expression there is an incompatibility between mitochondrial and nuclear mRNA codon usage[126]. It is unlikely therefore that any imported mRNA would be translated inside the mitochondria. However, a number of functional non-coding RNAs (ncRNAs) are believed to be imported into the mitochondria, including tRNAs, the 5S RNA, MRP RNA, RNaseP RNA and mitochondrial micro RNAs (mitomiRs). Although whole transcriptome analyses of mitochondria and mitoplasts have confirmed the presence of these RNAs[127,128], the mechanisms of import and impacts of these ncRNAs are still poorly understood[124,129,130].

1.5.2.1.1 Yeast $tRNA_{Lys}$ (tRK1)

tRNA import illustrates the variability of naturally occurring RNA import between species. Mammalian mtDNA encodes all 22 mitochondrial tRNAs[6]; Yeast (*S.cerevisiae*) have one nuclear encoded tRNA, the $tRNA_{Lys}$ (tRK1)[131]; trypanosomes encode all their tRNAs on nDNA[132]. The nuclear encoded tRK1 is distributed unequally between the cytosol (97-98%)

and mitochondria (2-3%) in yeast[133]. Although the exact mechanism of tRK1 import into mitochondria is unknown, candidate protein import factors have been implicated. Enolase (ENO2P) binds tRK1, in doing so changing its stem loop structure, and delivers it to the OMM[134]. At the OMM, tRK1 binds pre-LysRS (the pre-curser of the mitochondrial lysyl-tRNA) which aids transport of tRK1 into the mitochondria[135]. The TIM/TOM complex is believed to be involved as an intact protein import machinery is required for tRK1 import[136].

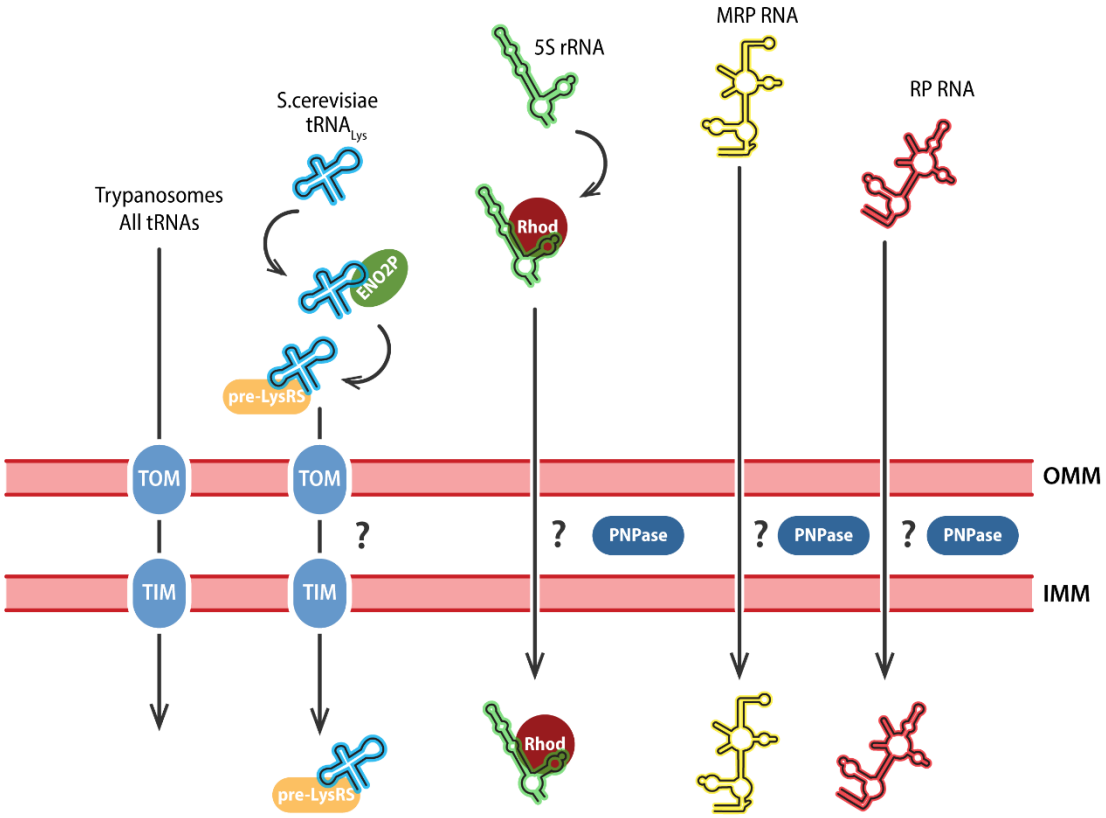

Figure 1-9 Natural RNA import mechanisms *Trypanosomes import all their tRNAs through TOM/TIM, whereas S.cerevisiae import just one, $tRNA_{Lys}$. $tRNA_{Lys}$ import involves the protein factors enolase (ENO2P) and the pre-curser of the mitochondrial lysyl-tRNA (pre-LysRS), and a functional protein import machinery. Mammalian import of 5S ribosomal RNA (rRNA), mitochondrial RNase P RNA (MRP) and RNase P RNA (RP) occur through unknown mechanisms, though some proteins have been implicated. These include Rhodanese (Rhod) in the case of the 5S ribosomal RNA (rRNA), and a potential role for PNPase in 5S, MRP and RP RNA import.*

1.5.2.1.2 5S RNA

Although containing the sequences for two rRNAs, the 16S and 12S subunits of the mitoribosome, mtDNA does not contain the coding sequence for a 5S rRNA. The mitoribosome is poorly conserved between species[137], and there is conflicting evidence over whether the a 5S rRNA is required for mammalian mitoribosome function. Some groups have suggested that the nuclear encoded 5S rRNA is imported into mitochondria, reporting interactions between 5S and the mitoribosome large subunit (LSU) and impacts on translation efficiency[138–140]. Contrastingly, cryo-EM structures have been solved of the mitoribosome without 5S rRNA[141]. In these structures, the LSU instead has mt-$tRNA^{Phe/Val}$

occupying the 5S location. The 5S rRNA contains key structural motifs (helix I, helix IV loop D) which are believed to direct its localisation to the mitochondria through interactions with the mitochondrial protein rhodanese, Figure 1-9[138]. Down regulation of rhodanese decreases mitochondrial localisation of 5S RNA and impacts translation by the mitoribosome[139]. Additionally, import of 5S rRNA into isolated mammalian mitochondria requires ATP and membrane potential[142].

1.5.2.1.3 RNaseP RNA

Mammalian mtDNA is transcribed as a polycistronic RNA, with genes punctuated by tRNAs. tRNAs are processed by mitochondrial RNase P (MRP) which cleaves the 5′ tRNA leader sequence[143]. The nuclear equivalent of RNase P functions as an RNP with several protein subunits and an RNA subunit, the H1 RNA[144]. As with the mitoribosome 5S component, there are conflicting studies as to whether mitochondrial RNaseP requires an RNA component[145] or whether it is exclusively proteinaceous[146]. Despite this disagreement, there is compelling evidence that a stem loop structure from nRNaseP can direct import into the mitochondria regardless of whether it is required for mitochondrial RNaseP function[147].

1.5.2.1.4 RNase MRP RNA

RNase MRP is mitochondrial RNA processing endoribonuclease, comprised of an RNA component, and several protein subunits, some shared with mitochondrial RNase P. RNase MRP has several nuclear functions including 5.8S rRNA processing and a role in yeast cell division. It was thought that primer processing by RNase MRP was necessary for initiation of mtDNA transcription[148,149]. However, further research has shown that other methods of mitochondrial transcription initiation are probably more likely, such as through G-quadruplex based priming[150]. Nevertheless, there is evidence of the RNase MRP 267nt lncRNA in the mitochondrial matrix. Although it remains unclear how the MRP RNA passes across the OMM and IMM, it contains a stem-loop structure which is recognised by PNPase[151]. PNPase is a homotrimeric 5′-3′ exoribonuclease, part of the mitochondrial RNA degradosome in the matrix. PNPase is also found in IMS and proposed to aid mitochondrial import of the 5S RNA, H1/MRP RNA/micro RNAs[151,152] though the mechanism of this is unknown and more work is needed to confirm whether this is a genuine second role.

1.5.2.2 Synthetic methods for targeted mitochondrial RNA import

Despite the conflicting evidence on the existence and mechanisms of mammalian RNA import, several studies have aimed to minimise the sequences of the reported nuclear encoded mitochondrial RNAs reviewed above with the aim of determining the minimal structural or functional motif(s) which direct their import[122], Figure 1-10. It is worth noting that although all the RNAs mentioned in the previous section have publications to this end,

the work is rarely validated by independent study from other research groups, if at all. A brief summary is given below:

1.5.2.2.1 Yeast $tRNA_{Lys}$ and F1D1

The yeast $tRNA_{Lys}$ (tRK1) has been shown to be imported into isolated mammalian mitochondria[153] and whole cells via binding of the pre-curser of the mammalian lysyl-tRNA synthetase, preKARS2[154]. tRK1 derived structures, screened for their ability to direct RNA import, have been shown to target RNAs to the mitochondria much more efficiently than the natural tRK1 structure[122,123,142]. Interestingly, many of these RNAs lose their ability to adopt a classical tRNA structure as they require the unfolding and re-folding of the tRK1 hairpins. The F1D1 RNA, Figure 1-10, derived from tRK1, is the structure found to have the highest import efficiency. Delivery of RNAs to mitochondria of a KSS cybrid cell line with F1D1 RNA has shown potential therapeutic potential; RNAs complimentary to mutated mtDNA specifically impacts mtDNA replication, resulting in a heteroplasmy purification effect[155]. A related control sequence, the AD RNA, does not have the same effect.

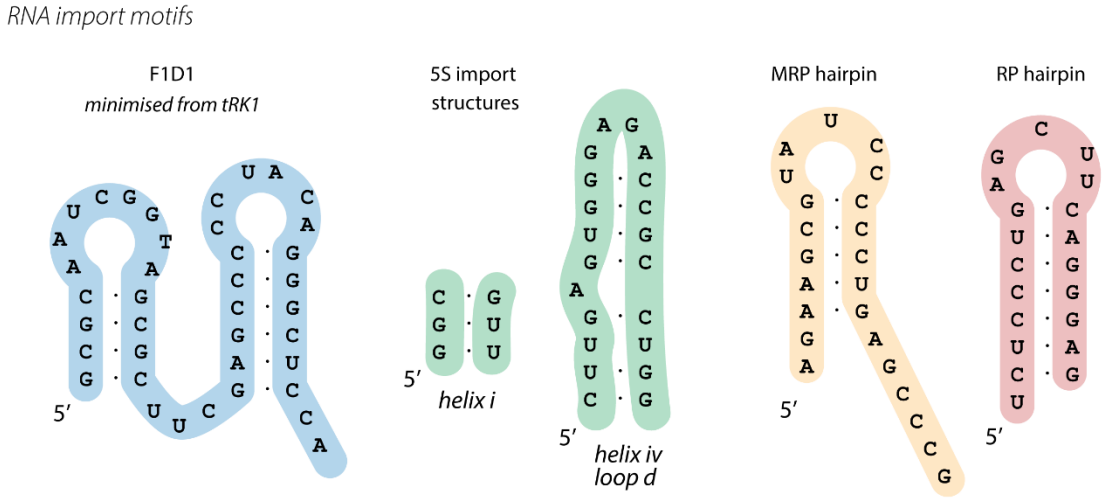

Figure 1-10 Minimised RNA import motifs *have been identified for tRK1, 5S rRNA, MRP RNA and RP RNA, the sequences of which are given here. Each of these motifs has been shown to be capable of directing RNA sequences of interest into the mitochondria.*

1.5.2.2.2 5S RNA

As with tRK1, understanding the potential natural import of 5S RNA has aided the use of 5S RNA structures to recombinantly target RNAs to the mitochondria[142]. The 5S helix IV loop D and helix I, Figure 1-10, are required for import, and other structural components can be deleted without negatively impacting import[138], instead being replaced by an RNA sequence of interest. As with tRK1 structures, 5S RNA structures have been shown to target desired RNA sequences to KSS cybrid cells and decrease heteroplasmy[155]. It is these structures which have been used by Loutre *et al* in their recent publication targeting gRNAs to the mitochondria[156].

1.5.2.2.3 RP and MRP hairpins

Truncating RNase RP and MRP RNAs has allowed identification of similar approximately 20 nt RNA hairpins in both RP and MRP RNA which direct mitochondrial import, Figure 1-10. Attaching these hairpins into non-imported RNAs can also target RNAs for import, as shown with GAPDH[152]. Wang *et al* showed that the presence of PNPase aids MRP/RP-directed delivery of RNAs into yeast and mammalian mitochondrial matrix where they can ameliorate a disease phenotype. Delivering RP-tRNA$_{AAA}^{Lys}$ and RP-tRNA$_{UUR}^{Leu}$ to MERRF and MELAS cell lines respectively partially rescues their respective translation defects[157].

1.5.3 RNP complex assembly and action on mtDNA

Once both CRISPR nucleases and RNAs have been selectively targeted to the mitochondria, it will be necessary to prove their colocalisation and ability to fold into a functional complex. Immunofluorescence could form the basis for this, though sensitive reporters, such as FRET mutants which demonstrate gRNA/CRISPR endonuclease complex formation, would be a valuable addition. The proof-of-principle experiment for MitoCRISPR will be to produce a heteroplasmy purification in a mitochondrial disease cybrid cell model - as has been achieved with MitoTALENs and MitoZFNs.

1.6 Published attempts to develop a MitoCRISPR system

When the MitoCRISPR project was started at the beginning of this PhD in 2014, there were no published attempts at developing a MitoCRISPR system, though the potential impact of such a system had been alluded to in a number of publications[80,158,159]. As our work and ideas have developed in Bristol, so they have for research groups elsewhere, and there have been several reviews and research papers demonstrating opinions and work towards the same objective in the intervening years.

The first published attempt at developing a CRISPR machinery for mtDNA was in 2014. In "Efficient Mitochondrial Genome Editing by CRISPR/Cas9", Jo *et al* detail their work towards editing mtDNA with a standard nuclear targeted CRISPR/Cas9 system[160]. In contrast with our expectations that delivery of Cas9 to the mitochondria would require an MTS, the paper showed nuclear-targeted Cas9 functioning in the mitochondria. The gRNAs also did not appear to require modification for mitochondrial activity. As yet, there have not been any published applications of the tool as developed by Jo *et al*, and our own attempt to reproduce this data was not successful, as summarised in Appendix A3-III.

The second published attempt at a mitochondrial CRISPR system was published in a Russian language journal, гены & клетки (Genes & Cells). The paper does not have an English

translation beyond the abstract and consequently does not appear in PubMed. In Импорт нуклеазы Cas9 в митохондри (Import of Cas9 nuclease in mitochondria), Orishchenko *et al* targeted FLAG-Cas9 to the mitochondria of viral-producing cells (Phoenix cell line) by appending a COX8A MTS. The paper shows a confocal image of a cell where anti-FLAG colocalises with very fragmented mitochondria as stained with MitoTracker. The paper did not describe any experiments to address mitochondrial gRNA localisation. As with the Jo *et al* paper, there have not yet been any subsequent papers published which repeat this work.

A third publication of interest was published in 2017, a review which outlines the potential difficulties which would need to be overcome to develop a MitoCRISPR system, with the daunting title that "Mitochondrial Genome Engineering: The Revolution May Not Be CRISPR-ized"[125]. This article highlights the complexity of the task at hand, focussing on challenges of efficient gRNA import. The article provides a thorough review of work to date targeting RNAs to the mitochondria, particularly bringing to light controversies surrounding natural RNA import mechanisms and suggesting the need for potentially more sophisticated and inventive methods for achieving this.

A fourth paper, "Can Mitochondrial DNA be CRISPRzed: *Pro* and *contra"* has been published during the writing of this thesis in 2018[156]. The research comes from the Entelis lab who have previously published a large body of work on RNA mitochondrial import. Consequently, this was the first publication which attempts to add mitochondrial-targeting structures to the gRNA structure. In the paper, Loutre *et al* achieve a decrease in mtDNA copy number with a mitochondrial targeted CRISPR system comprised of a COX8A-Cas9 and gRNAs modified to contain the targeting sequences from 5S RNAs (section 1.5.2.2.2). Two gRNAs were required to produce a reduction of mtDNA copy number; a single target gRNAs had no significant influence on mtDNA content. The work was carried out in a heteroplasmic cell line, but the authors did not observe a shift in heteroplasmy.

1.7 Objectives

On commencing the MitoCRISPR project, the objectives of this PhD project encompassed all the milestones detailed in section 1.5 towards the overall aim of developing a MitoCRISPR system. However, it soon became apparent that that body of work required of this project was far too ambitious for one student in four years, and the scope of the PhD was readdressed. Although the work done in the earlier years of the project also included mitochondrial targeting of the Cas9 protein as the project progressed, the focus has very much become the design and modification of gRNAs for MitoCRISPR. Subsequently, two postdoctoral researchers, Zuriñe Anton and Holly Ford, have joined the project. The modified objectives of this PhD are as follows:

1. Modifying Cas9 for MitoCRISPR – Chapter 3
2. Modifying Cas9 gRNAs for MitoCRISPR – Chapters 4 and 5
3. Assessing gRNA mitochondrial import – Chapter 6

Given that there are clear and real ethical issues regarding gene editing, with the MRT legislation already paving the way for mtDNA manipulation in patients, there is a need to engage the public in an ethical discussion surrounding the development and application of these tools. The additional Chapter 7 details a public engagement project undertaken to start a dialogue surrounding genome editing with the public in Bristol.

2 Materials and Methods

2.1 Chemicals, Reagents and Solutions

2.1.1 Table of Chemicals and Reagents

Table 2 Chemicals and Reagents

Reagent	Supplier
50 bp DNA ladder	ThermoFisher Scientific
Acetic acid (glacial)	Fisher
Acetone	Fisher
Acrylamide Bis-Acrylamide 30% stock solution	Severn Biotech
Acrylamide Bis-Acrylamide 40% stock solution	Severn Biotech
Ammonium persulphate (APS)	BDH VWR
ATP	Sigma
Agarose (molecular biology grade)	Helena Bioscience
β-mercaptoethanol (98%)	Sigma
Boric acid	Fisher
Bovine Serum Albumen (BSA)	Sigma
Bromophenol blue	Sigma
Caesium chloride	Fisher
cOmplete ULTRA protease inhibitor tablets, EDTA-free	Roche
DEPC treated H_2O	Invitrogen
Digitonin	Santa Cruz Biotechnology
DTT	ThermoFisher Scientific
dNTPs	Roche
EDTA	Fisher
Ethanol	Sigma
Ethidium bromide	Sigma
Ficoll 400	Sigma
Formamide, deionised	BDH VWR
Gene Ruler 1 kb DNA Ladder	ThermoFisher Scientific
D - (+) - Glucose	Sigma
Glycerol	Fisher
Glycogen	New England Biolabs
HEPES	Apollo Scientific
Hydrochloric acid (HCl)	Fisher
Hionic-Fluor Scintillation Cocktail	Perkin Elmer
Imidazole	Fisher
InstantBlue™ Protein Stain	Expedeon
Instant dried skimmed milk	The cooperative

Table 2 Chemicals and Reagents ctd.

Reagent	Supplier
IPTG	Fisher
LB and LBA capsules	MP Biomedicals
Magnesium chloride hexahydrate	Alfa Aesar
MOPS	Sigma
NADH	PauReac AppliChem
NTPs	New England Biolabs
Polyethylenimine (PEI)	Sigma
Phosphate Buffered Saline (PBS)	Sigma
PMSF	Sigma
Polyvinylpyrolidone (PVP)	Sigma
Potassium Chloride (KCl)	Chem Cruz
Propan-2-ol	Fisher
Sodium Dodecyl Sulphate (SDS)	Fisher
Sodium Acetate	Sigma
Sodium Perchlorate	Fisher
Sodium Chloride (NaCl)	Fisher
Sodium Hydroxide (NaOH)	Fisher
Sucrose	BDH VWR
SYBR-Gold	Invitrogen
TEMED	BioRad
Tris base (Trizma)	Sigma
Triton-X100	Sigma
TriZOL	Invitrogen
0.05 % Trypsin-EDTA (1X)	Gibco
Tween-20	Sigma
Urea	Fisher
Xylene cyanol	BioRad

2.1.2 Enzymes

Table 3 Enzymes

Enzyme	Supplier	Catalogue No
Antarctic Phosphatase	New England Biolabs	M0289
RQ1 RNase-free DNase I	Promega	M6101
HiScribe™ T7 High Yield RNA polymerase	New England Biolabs	E2040
Phusion High-Fidelity DNA Polymerase	Thermo Scientific	F530L
Proteinase K (PK)	New England Biolabs	P8107

Table 3 Enzymes ctd.

Enzyme	Supplier	Catalogue No
Restriction Endonucleases (various)	New England Biolabs	various
RNase A	Thermo Scientific	EN0531
SUPERase In™ RNase Inhibitor (20 U/µl)	Invitrogen	AM2694
T4 DNA ligase	New England Biolabs	M0202
T4 polynucleotide kinase (PNK)	New England Biolabs	M0201

2.1.3 Buffers

Table 4 Buffers

Name	Composition
10 % (w/v) APS	10% (w/v) APS in ddH_2O, filter sterilise and store aliquots at –20 °C
0.2 M ATP	0.2 M ATP in ddH_2O, prepare fresh
Blocking Solution (Western)	5% (w/v) milk powder in PBS, store at 4°C
0.1 M $CaCl_2$	0.1 M $CaCl_2$ in ddH_2O, autoclaved
20% Casamino acids	Prepared by media kitchen
CsCl saturated TE isopropanol	An excess of CsCl in equal volumes TE (50 mM Tris pH 8.0: 50 mM EDTA pH8.0 in ddH_2O) and Isopropanol
100 X Denhardt's Solution	2% (w/v) BSA, 2% (w/v) Ficoll 400, 2% (w/v) polyvinylpyrolidone in ddH_2O and filter sterilise. Aliquot and store at -20 °C.
Digitonin solution	Prepare to 1 mg/ml in ddH_2O, preheat to 90 °C for 1 minute
1 M DTT	1 M DTT in 0.01 M sodium acetate pH 5.2, prepare fresh or store aliquots at – 20 °C
DTT buffer	100 mM Tris-SO_4 pH 9.4, 10 mM DTT in ddH_2O
0.5 M EDTA pH 8.0	0.5 M in ddH_2O, pH with NaOH and autoclave
Gel Filtration buffer	20 mM Tris pH 7.5, 200 mM KCl, 1 mM TCEP, 10% glycerol
Gel Fixing Solution	10% (v/v) MetOH, 10% (v/v) Acetic Acid in ddH_2O
20 mg/ml Glycogen	Prepare to 20 mg/ml in DEPC H_2O and filter sterilise
HisElution	50 mM Tris pH 9.0, 500 mM NaCl, 1 mM β-mercaptoethanol, 500 mM imidazole pH 8.0 in ddH_2O
HisWash 1	50 mM Tris pH 9.0, 500 mM NaCl, 1 mM β-mercaptoethanol, 30 mM imidazole pH 8.0 in ddH_2O
HisWash 2	50 mM Tris pH 9.0, 200 mM NaCl, 1 mM β-mercaptoethanol in ddH_2O
Homogenisation buffer	0.6 M sorbitol, 10 mM Tris-HCl pH 7.4, 0.5% BSA, 1 mM PMSF (from frozen stock, added just before use).

Table 4 Buffers ctd.

Name	Composition
Hybridisation solution	Prehybridisation solution containing 2 ng/ml 5′ -^{32}P -labelled oligonucleotide probe
1 M Imidazole pH 8.0	1 M Imidazole in ddH_2O – adjust to pH 8.0 with NaOH and autoclave
1 M IPTG	1 M IPTG in ddH_2O – filter sterilise and store aliquots at – 20 °C
3 M KCl	3 M KCl in ddH_2O – autoclave
0.2 M NADH	0.2 M NADH in ddH_2O – prepare fresh
5 M NaCl	5 M NaCl in ddH_2O – autoclave
Mitochondrial Isolation Buffer (mammalian)	0.44 M Sorbitol, 40 mM EDTA, 10 mM HEPES-NaOH pH6.7, 0 %, 0.01 % or 0.1 % (w/v) SDS
Mowiol	2.4 g mowiol, 6g glycerol, 12mL 0.2M Tris, pH 8.5, supplemented with 25mg/mL DABCO
PBS	137 mM NaCl, 2.7 mM KCl, 10 mM Na_2HPO_4, 2 mM KH_2PO_4 in ddH_2O
Prehybridisation solution	6 X SSC, 0.1 % (w/v) SDS, 10 X Denhardt's solution in ddH_2O
RIPA buffer	150 mM NaCl, 10 mM Tris, pH 7.2, 0.1 % SDS, 1.0 % Triton X-100, 1 % Deoxycholate, 5 mM EDTA in ddH_2O
5 X RNA aptamer buffer	0.15 M KCl, 40 mM HEPES (pH 7.5), 0.1 mM $MgCl_2$
10 X RB (Reaction buffer)	100 mM Tris pH 7.5, 1 M NaCl, 100 mM $MgCl_2$, 1 mM DTT, 0.05 mg/ml BSA in ddH_2O, filter sterilised, aliquoted and stored at -80 °C
2 X RNA loading dye	95 % deionised formamide, 0.025 % (w/v) bromophenol blue, 0.025 % (w/v) xylene cyanol, 5 mM EDTA pH 8.0, 0.025 % (w/v) SDS in ddH_2O
RNA resuspension buffer	10mM Tris pH7.5, 100mM NaCl, 1mM EDTA
10 X SB (Sample buffer)	100 mM Tris pH 7.5, 1 M NaCl, 10 mM EDTA, 1 mM DTT, 0.05 mg/ml BSA in ddH_2O, filter sterilised, aliquoted and stored at -80 °C
2 X SDS-PAGE loading dye	100 mM Tris-Cl pH 6.8, 4 % (w/v) SDS, 0.2 % (w/v) bromophenol blue, 20 % (w/v) glycerol – filter sterilise and store at room temperature. Add 200 mM β-mercaptoethanol immediately before use
Seahorse Assay Buffer	70 mM sucrose, 220 mM mannitol, 10mM KH_2PO_4, 5mM $MgCl_2$, 2mM HEPES, 1mM EGTA and 0.2% (w/v) BSA, pH 7.2 in ddH_2O
SM buffer	250 mM sucrose, 10 mM MOPS-KOH pH 7.2, store at -20°C
Solution I	25% (w/v) sucrose, 50 mM Tris pH 8.0
Solution II	10 mg/ml lysosyme, 250 mM Tris pH 8.0

Table 4 Buffers ctd.

Name	Composition
Solution III	200 mM EDTA pH8.0
Solution IV	2% (w/v) Triton X100, 50 mM Tris pH 8.0, 50 mM EDTA pH8.0
Sonication buffer	50 mM Tris pH 8.0, 500 mM NaCl, 1 mM β-mercaptoethanol, 5 mM $MgCl_2$, 0.5 mM EDTA, cOmplete ULTRA protease inhibitor.
1 M Sorbitol	1 M Sorbitol in in ddH_2O – filter sterilise or autoclave
20 X SSC	3 M NaCl, 0.3 M Sodium citrate, 1 mM EDTA in ddH_2O
DNA loading buffer (3 X STE)	0.05 M Tris-HCl ph 8.0, 0.05 M EDTA, 20 % (w/v) sucrose
DNA loading buffer (3 X STEB)	0.05 M Tris-HCl ph 8.0, 0.05 M EDTA, 20 % (w/v) sucrose, 0.0125 % (w/v) bromophenol blue, 0.0125 % (w/v) xylene cyanol
1M Sucrose	1 M Sucrose in ddH_2O – autoclave before use
1/1,000 SYBR Gold staining solution	1 µl SYBR Gold in 1 ml 1 X TBE
50 X TAE	2 M Tris-acetate, 50 mM EDTA 242 g Tris base, 57.1 ml glacial acetic acid, 100 ml 0.5 M EDTA pH 8.0
1 X TBE/0.5 X TBE	Dilute 5 X TBE 1/5 or 1/10 respectively in ddH_2O
5 X TBE	450 mM Tris-borate, 10 mM EDTA 54 g Tris base, 27.5 g boric acid, 20 ml 0.5 M EDTA pH8.0 in ddH_2O
TE (50:50)	50 mM Tris pH 8.0: 50 mM EDTA pH8.0 in ddH_2O
TE CsCl 1.085 g/ml	108.5 g CsCl dissolved in 100 ml TE (50:50) - 1 ml weighs ~ 1.63 g
TE CsCl 1 g/ml	100 g CsCl dissolved in 100 ml TE (50:50) – 1 ml weighs ~ 1.58 g
1 M Tris pH 7.5	1 M Tris in ddH_2O – adjust to pH 7.5 with HCl and autoclave
1 M Tris pH 8.0	1 M Tris in ddH_2O – adjust to pH 8.0 with HCl and autoclave
1 M $MgCl_2$	1 M $MgCl_2$ in ddH_2O – autoclave before use
1 M $MgSO_4$	1 M $MgSO_4$ in ddH_2O – autoclave before use
VOA mix (death cocktail)	1 mM valinomycin, 10 mM oligomycin, 8 mM antimycin A
Yeast RNA import buffer	50 mM sucrose, 80 mM KCl, 5 mM $MgCl_2$, 10 mM KH_2PO_4/K_2HPO_4 pH 7.2, 10 mM MOPS, in ddH_2O
Yeast RNA import mix	100 µl yeast RNA import buffer with 2 mM ATP, 2 mM NADH.
Zymolase buffer	1.2 M sorbitol, 20 mM KPi pH 7.4 in ddH_2O

2.2 General microbiology techniques

2.2.1 *Escherichia coli* (*E.coli*) strains

Table 5 E coli strains

Cell line	Supplier	Genotype	Use
One Shot™ TOP10 Chemically competent *E.coli*	Invitrogen	*F- mcrA Δ(mrr-hsdRMS-mcrBC) Φ80lacZΔM15 Δ lacX74 recA1 araD139 Δ(araleu)7697 galU galK rpsL (StrR) endA1 nupG*	Plasmid preparation
HB101	Promega	F–, *thi*-1, *hsd*S20 (r_B^-, m_B^-), *sup*E44, *rec*A13, *ara*-14, *leu*B6, *pro*A2, *lac*Y1, *gal*K2, *rps*L20 (str^r), *xyl*-5, *mtl*-1	^{3}H CsCl Maxipreps
Rosetta 2 (DE3)	Novagen	F^- *ompT hsdS*$_B$(r_B^- m_B^-) *gal dcm* (DE3) pRARE2 (Cam^R)	Protein expression

2.2.2 Yeast strains

Table 6 Yeast strains

Cell line	Source	Genotype	Use
YPH499	Collinson lab (University of Bristol)	*MATa ura3-52 lys2-801_amber ade2-101_ochre trp1-Δ63 his3-Δ200 leu2-Δ1*	Preparation of mitochondria

2.2.3 Media

All media was prepared with ddH_2O and autoclaved at 121 °C for 15 minutes at 15 psi.

Table 7 Media

Media	Composition	Use
20% Casamino acids	Prepared by media kitchen	CsCl plasmid preparation
Luria-Bertani (LB)	Capsules dissolved in ddH_2O	Liquid *E.coli* culture
LB-Agar (LBA)	Capsules dissolved in ddH_2O	*E.coli* culture on plates
5 X M9 Salts	33.9 g/L Na_2HPO_4, 15 g/L KH_2PO_4, 5 g/L NH_4Cl, 2.5 g/L NaCl	CsCl plasmid preparation
SOC	0.5 % (w/v) yeast extract, 2% (w/v) tryptone, 10 mM NaCl, 2.5 mM KCl, 10 mM $MgCl_2$, 10 mM $MgSO_4$, 20 mM Glucose	Heat-shock transformation recovery
YPG	1% (w/v) yeast extract, 2% (w/v) peptone, 3% (w/v) glycerol in ddH_2O, adjusted to pH 5.2 with NaOH	Yeast growth

2.2.4 Antibiotics

Table 8 Antibiotics

Antibiotic	Stock concentration	Used at Concentration	Supplier
Ampicillin	100 mg/ml in ddH_2O	100 µg/ml	Sigma
Kanamycin	50 mg/ml in ddH_2O	50 µg/ml	Sigma
Chloramphenicol	34 mg/ml in 100% EtOH	0.2 mg/ml	Sigma

2.2.5 Transformation techniques

Transformation of commercial competent *E.coli* cell lines was performed by heat shock according to the protocols supplied by the manufacturer. Transformed cells were grown for 16 hours at 37 °C on LBA plates supplemented with an appropriate antibiotic, Table 8.

2.3 General DNA techniques

2.3.1 Plasmid DNA handling and purification

Plasmid DNA purification was performed with either GeneJET plasmid Miniprep Kit (Thermo Scientific) or Plasmid Mini-, Midi- or Maxiprep kits (Qiagen), according to the manufacturer's instructions. Plasmids were either eluted in ddH_2O or the supplied TE buffer and stored at -20 °C. DNA concentrations were calculated using a DeNovix DS-11 spectrophotometer to measure absorbance at 260 nm. The $A_{260/280nm}$ ratio was used as an indication of purity. DNA sequencing was performed by DNA Sequencing & Services (MRC I PPU, School of Life Sciences, University of Dundee, Scotland, www.dnaseq.co.uk) using Applied Biosystems Big-Dye Ver 3.1 chemistry on an Applied Biosystems model 3730 automated capillary DNA sequencer.

2.3.1.1 Plasmids

Table 9 Plasmids

Chapter 3: Mito-Cas9 and associated plasmids		
Name	**Use**	**Source**
pD1301-AD	Cloning Cas9 and gRNA plasmids, below	DNA2.0
pD1301i	Expression of NLS-Cas9 and gRNA cassette	this thesis
pD1301iABC	Expression of MTS-Cas9	this thesis
pD1301iE	Expression of NLS-Cas9-GFP and gRNA cassette	this thesis
pD1301iABCE	Expression of MTS-Cas9-GFP	this thesis
pDsRed-Mito	Expression of MTS-RFP	Lane lab
pEGFP-N1	Expression of EGFP	Clontech
pMTS-EGFP	Expression of MTS-EGFP	this thesis
pEX-A2-MTS and Spinach	COX8A MTS sequence	Eurofins *Sequence in A2*
phCas9$_{D10A}$	Expression of NLS-Cas9$_{D10A}$ and gRNA cassette	Addgene #41816[118]
phCas9$_{WT}$	Expression of NLS-Cas9 and gRNA cassette	Addgene #41815[118]
Chapter 4: Modified gRNAs		
Name	**Use**	**Source**
pD1301i-SP1	Unmodified gRNA template generation	this thesis
pEX-A2-g#GM SP1gRNA 5′ Baby Spinach	5′ Baby Spinach (fluorescent RNA structure) gRNA template generation	Eurofins *Sequence in A2*
pEX-A2-g#GM SP1gRNA 3′ Baby Spinach	3′ Baby Spinach (fluorescent RNA structure) gRNA template generation	Eurofins *Sequence in A2*
pEX-A2-g#GM SP1gRNA 5′ RP	5′ RP-gRNA template generation	Eurofins *Sequence in A2*
pEX-A2-g#GM SP1gRNA 3′ RP	3′ RP-gRNA template generation	Eurofins *Sequence in A2*
pEX-A2-g#GM SP1gRNA US RP	RP US gRNA template generation	Eurofins *Sequence in A2*
pEX-A2-g#GM SP1gRNA H RP_1	RP H1 gRNA template generation	Eurofins *Sequence in A2*

Table 9 Plasmids ctd

Chapter 4: Modified gRNAs *ctd*		
Name	**Use**	**Source**
pEX-A2-g#GM SP1gRNA H RP_2	RP H2 gRNA template generation	Eurofins *Sequence in A2*
pEX 5′ RP U	5′ RP-U gRNA template generation	this thesis
pEX 5′ RP 2U	5′ RP-2U gRNA template generation	this thesis
pEX 5′ RP 4U	5′ RP-4U gRNA template generation	this thesis
pEX 5′ RP 8U	5′ RP-8U gRNA template generation	this thesis
pEX-A2-BoBS & tRNA(K)	BoBs and tRK1 templates for HiFi	Eurofins *Sequence in A2*
pEX US tRK1	US tRK1 gRNA template generation	this thesis
pEX US BS	US Baby Spinach gRNA template generation	this thesis
pEX US BoBS	US BoBS gRNA template generation	this thesis
pSUMOCas9$_{hinge}$	Expression of Cas9$_{hinge}$	Szczelkun lab
pSUMOdCas9$_{HNH}$	Expression of dCas9$_{HNH}$	Szczelkun lab
pSP1	Plasmid cleavage assays substrate plasmid	Siksnys lab[92]
pUC19	Negative control, plasmid cleavage assays	

2.3.2 DNA electrophoresis

2.3.2.1 Agarose gel electrophoresis

Agarose gel electrophoresis was performed in a horizontal transfer system (Flowgen Biosciences). Agarose gels were prepared by dissolving 1 – 3% (w/v) Agarose in *1X TAE* and heating in a microwave oven. Once cooled, the gel mix was supplemented with Ethidium bromide to 0.05 % (w/v) and set in gel trays with an appropriate comb. Once set, gels were placed in a tank containing *1X TAE* with Ethidium bromide to 0.05 % (w/v). DNA samples were prepared by adding 1/3 volume *3X STEB*, heated to 80 °C for 10 minutes and loaded onto the gel and run at 25 – 120 V until DNA bands were appropriately separated. Gels were imaged using the GelDoc™ XR+ system (BioRad).

2.3.2.1.1 DNA isolation from Agarose gels

DNA fragments separated by agarose gel electrophoresis were extracted from gel slices with the QIAEX-II Gel Extraction Kit (Qiagen), following the manufacturer's instructions.

2.3.2.2 TBE-PAGE

TBE-PAGE was performed in the Mini-PROTEAN 3 vertical transfer system (BioRad). TBE gel mix (1X TBE, 8/10 % (v/v) acrylamide (from 40% Acrylamide/Bis-acrylamide (19:1)) was prepared and passed through a 0.45 µm nitrocellulose filter prior to the addition of 0.05% (w/v) APS and 0.05% (v/v) TEMED. Gels were set at room temperature in the Mini-PROTEAN 3 apparatus, as per the manufacturer's instructions. Once set, gels were placed in a tank containing 1X TBE. DNA samples were prepared by adding 1/3 volume 3X STEB, loaded into

the gel and run at 180 V until DNA bands were appropriately separated. Gels were soaked in a 1X TBE solution containing 0.05 % (v/v) Ethidium bromide for 15 minutes and imaged using the GelDoc™ XR+ system (BioRad).

2.3.2.2.1 DNA isolation from TBE-PAGE gels

DNA was isolated from TBE-PAGE gel by electroelution. Once separated by TBE-PAGE, gels were soaked in a 1X TBE solution containing 0.05 % (v/v) Ethidium bromide for 15 minutes and viewed on the DarkReader transilluminator (Clare Chemical Research). The band of interest was cut out of the gel and sealed into a length of pre-soaked snakeskin dialysis tubing containing 250 µl 0.1 X TBE. The tubing was placed into a gel tank in 0.1 X TBE and run at 30mA for 30 minutes.

2.3.3 Molecular Biology and Cloning

All restriction enzymes (New England Biolabs) were used according to the manufacturer's instructions. DNA ligation with T4 DNA Ligase (Roche) was performed according to the manufacturer's instructions at 16 °C for 16 hours.

2.3.3.1 Polymerase Chain Reaction (PCR)

PCR was performed with Phusion high-fidelity DNA polymerase according to the manufacturer's instructions. Amplified DNA was purified with QIAquick PCR purification kit (Qiagen).

2.3.4 Oligonucleotides and Synthetic genes

All oligonucleotides and synthetic genes were purchased from MWG Eurofins.

Oligonucleotides for cloning and sequencing pD1301 (Chapter 3 - MTS-Cas9 expression)

Table 10 Oligonucleotides 1

Primer/Oligo	Sequence (5′-3′)	Application
oli#GM_SeqF1	AGTACAAAATACGTGACGTAGAAAG (25)	Sequencing primer
oli#GM_SeqF2	ATAGGGACTTTCCATTGACG (20)	Sequencing primer
oli#GM_SeqF3	AGAGACCACACCCAAGCTGG (20)	Sequencing primer
oli#GM_SeqF4	ACCTGAACCCCGACAACAGCG (21)	Sequencing primer
oli#GM_SeqF5	AGCCAGGAAGAGTTCTACAAG (21)	Sequencing primer
oli#GM_SeqF6	ACCAACCGGAAAGTGACCGT (20)	Sequencing primer
oli#GM_SeqF7	AGTGATGGGCCGGCACAAGC (20)	Sequencing primer
oli#GM_SeqF8	ACTCCCGGATGAACACTAAG (20)	Sequencing primer
oli#GM_SeqF9	AGTACGGCGGCTTCGACAGC (20)	Sequencing primer
oli#GM_SeqF10	ACGCCACCCTGATCCACCAG (20)	Sequencing primer
oli#GM_SeqF11	AGGACGGGCATATTCTTCGGAAG (23)	Sequencing primer

Table 10 ctd.

Primer/Oligo	Sequence (5′-3′)	Application
oli#GMpD1303_Af	P-GGCACATCTGAGGGCAGGGGAAG (23)	3′ NLS removal primer F
oli#GMpD1303_Ar	P-GTCGCCTCCCAGCTGAGACAGG (22)	3′ NLS removal primer R
oli#GMpD1303Ar2	P-GTCGCCTCCCAGCTGAGACAGGT (23)	3′ NLS removal R + 3′ T
oli#GMpD1301iT	CCGTGAAGAGCGCTCTTCA (19)	2x SapI sites F
oli#GMpD1301iB	AACTGAAGAGCGCTCTTCA (19)	2x SapI sites R
oli#GMpD1301iTs	CCGTGAAGAGCAGAGTGGCTCTTCA (25)	SapI sites + 6bp stuffer
oli#GMpD1301iBs	AACTGAAGAGCCACTCTGCTCTTCA (25)	SapI sites + 6bp stuffer
oli#GMpD1303_Cf	CGTCAGTCGCAGATCGCGTCAGTCGCAGATCGT GATCGTCGACGATACGATCGCTGAC (78)	5′ NLS removal and MTS insertion (3′ end) F
oli#GMpD1303_Cr	P-CCGGGCCGAGCCTGTCAAGCCCCGCAGCAG CAGCAGCGGCGTCAGGACGGACATGGTGGCGGC CAGTTG (67)	5′ NLS removal and MTS insertion (5′ end) R
oli#GMpD1301CFt	P-GACAAGAAGTACAGCATCGGCCTGGAC (27)	Primer C F truncated
oli#GMpD1301CRt	CATGGTGGCGGCCAGCTTG (19)	Primer C R truncated
oli#GM NestRev 3	CGCCGGGCCGAGCCTGTCAAGCCCCGCAGCAGC AG (35)	Nested PCR MTS insertion
oli#GM NestFow 3	GCTCCCAGTGCCGCGCGCCAAGATCCATTCGTT G (34)	Nested PCR MTS insertion
oli#GM NestRev 1	TCAGGACGGACATGGTGGCGGCCAGCTTG (29)	Nested PCR MTS insertion
oli#GM NestRev 2	GCAGCAGCAGCGGCGTCAGGACGGACATG (29)	Nested PCR MTS insertion
oli#GM NestFow 1	TCCACCGGTCGACAAGAAGTACAGCATCG (29)	Nested PCR MTS insertion
oli#GM NestFow 2	TCCATTCGTTGGGGGATCCACCGGTCGAC (29)	Nested PCR MTS insertion

Oligonucleotides for generating gRNA library: 5′ insertions with inverse PCR (Chapter 4)

Table 11 Oligonucleotides 2

Primer/Oligo	Sequence (5′-3′)	Application
oli#GM PS1 fow	CGCTAAAGAGGAAGAGGACAG (21)	Forward primer
oli#GM 5′ RP U rev	ACTCCCTGAAGCTCAGGG (18)	U insertion
oli#GM 5′ RP 2U rev	AACTCCCTGAAGCTCAGGG (19)	2U insertion
oli#GM 5′ RP 4U rev	AAAACTCCCTGAAGCTCAGGG (21)	4U insertion
oli#GM 5′ RP 8U rev	AAAAAAAACTCCCTGAAGCTCAGGG (25)	8U insertion
oli#GM MRP fow	CCCGCTGAGCCCGCGCTAAAGAGGAAGAGG (30)	MRP insertion Forward
oli#GM MRP rev	ATACGCTTCTTGTTTCGTCCTTTCCACAAG (30)	MRP insertion Reverse

Oligonucleotides for generating gRNA library: Upper Stem insertions with HiFi (Chapter 4)

Table 12 Oligonucleotides 3

Primer/Oligo	Sequence (5′-3′)	Application
oli#GM USBS iFP1	TTTAGAGCTAGGTGAAGGACGGGTCCAGTAG (31)	US BS insertion
oli#GM USBS iRP1	TAACTTGCTAGGAGCTCACACTCTACTCAAC (31)	US BS insertion
oli#GM USBS vFP2	TGTGAGCTCCTAGCAAGTTAAAATAAGGC (29)	US BS insertion
oli#GM USBS vFP2	GTCCTTCACCTAGCTCTAAAACTGTCCTCT (30)	US BS insertion
oli#GM BoBS FP1 oli#GM BoBS RP1	TTTAGAGCTAAAGGACGGGTCCGGACGCAA (30) TAACTTGCTACTCACACTCTACTCAACGGA (30)	US BoBS insertion US BoBS insertion
oli#GM BoBS FP2	AGAGTGTGAGTAGCAAGTTAAAATAAGGCT (30)	US BoBS insertion
oli#GM BoBS RP2	ACCCGTCCTTTAGCTCTAAAACTGTCCTCT (30)	US BoBS insertion
oli#GM tRK1 FP1	TTTAGAGCTAgaGCCTTGTTGGCGCAATCG (30)	US tRK1 insertion
oli#GM tRK1 RP1	TAACTTGCTAGAGCCCTGTAGGGGGCTCGAA (31)	US tRK1 insertion
oli#GM tRK1 FP2	TACAGGGCTCTAGCAAGTTAAAATAAGGC (29)	US tRK1 insertion
oli#GM tRK1 RP2	AACAAGGCtcTAGCTCTAAAACTGTCCTCT (30)	US tRK1 insertion

Oligonucleotides for generating gRNA IVT template by PCR (Chapter 4 and 6)

Table 13 Oligonucleotides 4

Primer/Oligo	Sequence (5′-3′)	Application
oli#GM SP1 T7 (G)	GACACTAATACGACTCACTATAGCGCT AAAGAGGAAGAGG (40)	T7 introduction, unmodified 5′
oli#GM SP1 T7 (GG)	GACACTAATACGACTCACTATAGGCGC TAAAGAGGAAGAGG (41)	T7 introduction, 5′ GG
oli#GM SP1 T7 (GGG)	GACACTAATACGACTCACTATAGGGCG CTAAAGAGGAAGAGG (42)	T7 introduction, 5′ GGG
oli#GM SP1 T7rev	AAAAGCACCGACTCGGTGCC (20)	Reverse primer, unmodified 3′
oli#GM RP T7 (G)	gacacTAATACGACTCACTATAGTCTCCC TGAGCTTCAGG (40)	T7 introduction, RP 5′
oli#GM 5′ BS T7 (G)	gacacTAATACGACTCACT ATAGGGTGAAGGACGGG TCCAG (41)	T7 introduction, BS 5′
oli#GM 3′ RP T7 R	AAAACTCCCTGAAGCTCAGG (20)	Reverse primer, RP 3′
oli#GM 3′ BS T7 R	AAAAGGAGCTCACACTCTAC (20)	Reverse primer, BS 3′
oli#GM5′ MRPT7fow	gacacTAATACGACTCACTATAGAGAAGC GTATCCCGCTGAGC (43)	T7 introduction, MRP 5′
Oli#GM5′ FDT7fow	gacacTAATACGACTCACTATAGGCGCAA TCGGTAGCGCTTCG (43)	T7 introduction, FD 5′

Oligonucleotides for generating Baby Spinach (fluorescent RNA) IVT template by PCR (Chapter 4)

Table 14 Oligonucleotides 5

Primer/Oligo	Sequence (5′-3′)
oli#GM T7Spin2 Fow	taatacgactcactataggGATGTAACTGAATGAAATGGTGAAGGACG (48)
oli#GM Spin2 Rev	GATGTAACTAGTTACGGAGCTCACACTC (28)

Oligonucleotides for generating gRNA template by annealing (Chapter 5)

Table 15 Oligonucleotides 6

Primer/Oligo	Sequence (5′-3′)	Application
oli#GM LbCas12a crRNA T7 top	GAAATTAATACGACTCACTATAGGG (25)	LbCas12a crRNA IVT template
oli#GM LbCas12a unmod bottom	AGCTCGAATTGAAATTCTAAACGCATCTAC ACTTAGTAGAAATTCCCTATAGTGAGTCGT ATTAATTTC (69)	LbCas12a crRNA IVT template
oli#GM LbCas12a 5′ U bottom	AGCTCGAATTGAAATTCTAAACGCATCTAC ACTTAGTAGAAATTAAAACCCTATAGTGAG TCGTATTAATTTC (73)	LbCas12a crRNA 5′ U IVT template
oli#GM LbCas12a 3′ U bottom	AAAAAGCTCGAATTGAAATTCTAAACGCAT CTACACTTAGTAGAAATTCCCTATAGTGAG TCGTATTAATTTC (73)	LbCas12a crRNA 3′ U IVT template
oli#GM LbCas12a 5′ RP bottom	AGCTCGAATTGAAATTCTAAACGCATCTAC ACTTAGTAGAAATTAAACTCCCTGAAGCTC AGGGAGACCCTATAGTGAGTCGTATTAATT TC (92)	LbCas12a crRNA 5′ RP IVT template

Oligonucleotides for AD and FD RNA IVT template PCR (Chapter 6)

Table 16 Oligonucleotides 7

Primer/Oligo	Sequence (5′-3′)
oli#GM T7 AD T	TAATACGACTCACTATAGGGCCTTGTTGGCGCAATCGGTAGCGCAAATACA GGGCTCCA (59)
oli#GM AD T7 B	TGGAGCCCTGTATTTGCGCTACCGATTGCGCCAACAAGGCCCTATAGTGAG TCGTATTA (59)
oli#GM T7 F1D1 T	TAATACGACTCACTATAGGGCGCAATCGGTAGCGCTTCGAGCCCCCTACAG GGCTCCA (58)
oli#GM T7 F1D1 B	TGGAGCCCTGTAGGGGGCTCGAAGCGCTACCGATTGCGCCCTATAGTGAGT CGTATTA (58)
oli#GM T7 FD fow	GACACTAATACGACTCACTATAGG (24)
oli#GM T7 FD rev	AAAATGGAGCCCTGTA (16)

Oligonucleotides for Northern Blotting probes (Chapter 6)

Table 17 Oligonucleotides 8

Primer/Oligo	Sequence (5′-3′)
cyto $tRNA^{Lys}_{UUU}$ hybridisation probe	ACTTGAACCCTGGACC (16)
Mito $tRNA^{Leu}$ hybridisation probe	GAACCTCTGACTCTAAAG (18)
mito $tRNA^{Thr}$ hybridisation probe	TCTCCGGTTTACAAGAC (17)
tRK1 hybridisation probe	TGGAGCCCTGTAGGGG (16)
gRNA hybridisation probe	GCACCGACTCGGTGCCACTT (20)

Oligonucleotides for $dCas9_{HNH}$ FRET assay (Chapter 4)

Table 18 oligonucleotides 9

Primer/Oligo	Sequence (5′-3′)	Application
oli#GM pSP1 55bp TOP	GAATTGAAATTCTAAACGCTAAAGAGGAAGAG GACATGGTGAATTCGTAATCATG (55)	55 bp dsDNA template for FRET assay
oli#GM pSP1 55bp BOTTOM	CATGATTACGAATTCACCATGTCCTCTTCCTCT TTAGCGTTTAGAATTTCAATTC (55)	55 bp dsDNA template for FRET assay

2.3.4.1 Oligonucleotide annealing

Desired oligonucleotides were mixed in equimolar ratios in 150 mM NaCl and heated to 90 °C for 10 minutes. The mix was then allowed to cool to room temperature slowly overnight.

2.4 General RNA techniques

2.4.1 RNA handling

RNA is readily degraded by environmental RNases, such as those found on the skin. The following precautions were taken when working with RNA containing samples: Gloves were regularly changed; all tubes and tips were certified RNase-free (Ambion, Gilson); the bench and pipettes were regularly cleaned with RNaseZap™ (Invitrogen); DEPC-treated water (Invitrogen) was used in reaction buffers and experimental set-up.

2.4.2 *in vitro* transcription (IVT)

Except in the case of G/GG/GGG gRNAs (Chapter 5) IVT was performed with HiScribe™ T7 High Yield RNA synthesis kit (New England BioLabs) as per the manufacturer's instructions. gRNAs were purified by either phenol chloroform extraction or with RNA Clean and Concentrator™ Columns (Zymo Research) and eluted in DEPC treated H_2O. gRNA concentration was calculated by taking A_{260} with a DeNovix DS-11 spectrophotometer. gRNA size and integrity was monitored by separation with urea-polyacrylamide gel electrophoresis (urea-PAGE) with 10% (w/v) acrylamide.

EnGen IVT (NEB) IVT by EnGen kit (gRNAs with 5′ guanines) was performed as per the manufacturer's instructions. gRNAs were purified as above.

2.4.2.1 gRNA template design

Templates for gRNA library IVT double stranded DNA templates amplified by PCR from the relevant plasmid (see Table 9). These incorporations were made to plasmid DNA templates through a number of standard cloning methods and synthesised by *in vitro* transcription to give the modified gRNA library, Appendix A4. Primers were designed for gRNA IVT that amplified the gRNA spacer and structural component from pD1301 and introduced the T7 promoter upstream of the gRNA sequence, Table 13.

2.4.2.2 *in vitro* transcription of ^{33}P-UTP labelled RNA

In vitro transcription was performed using the T7 HiScribe High Yield RNA synthesis kit. The reaction was prepared to a final volume of 20 µl, containing a final concentration of 1X reaction buffer, 1 mM ATP, GTP and CTP. UTP was added to a final concentration of 4 µM with 0.25 µM α^{33}P UTP, 0.5 MBq/reaction (Hartman Analytic, SRF 210). To this, 0.25 µg template DNA and 1 µl T7 RNA pol mix was added. The assembly was incubated at 37 °C for 10 minutes, treated with DNase and purified with MicroBioSpin (BioRad) columns.

2.4.3 Purification and analysis of RNA

RNAs were purified with RNA Clean and Concentrator–5 columns (Zymo Research), eluted in DEPC-treated ddH_2O and stored at -80 °C. RNA concentrations were calculated using a DeNovix DS-11 spectrophotometer to measure absorbance at 260 nm. The $A_{260/280nm}$ ratio was used as an indication of purity.

2.4.4 Denaturing urea-PAGE

RNA was separated on a denaturing urea-PAGE gel containing 10% (w/v) acrylamide, 1X TBE and 50% (w/v) urea. Gel mix was prepared, filter sterilised with a 0.2 µm nitrocellulose membrane and stored at 4 °C for up to 2 weeks. Gels were set using the BioRad Mini-PROTEAN 3 system and pre-run in 1 X TBE at 200 V for 45 minutes prior to loading samples. RNA samples were heated to 90 °C with 1X *RNA Loading Dye* for 10 minutes and migrated in 1 X TBE at 200 V. Gels were stained with 1 ml 1/1,000 SYBR Gold Nucleic Acid Gel Stain (ThermoFisher Scientific) and imaged with the GelDoc™ XR+ system (BioRad).

2.5 General Protein techniques

2.5.1 Polyacrylamide gel electrophoresis (PAGE)

SDS-PAGE for Western blotting SDS polyacrylamide gels were made and run using the MiniPROTEAN 3 system (BioRad). Resolving gels for protein separation were prepared from 30% (w/v) Acrylamide/Bis-acrylamide (37:1) stock at a percentage tailored to the size of protein of interest (30-95 kDa, 8%; 20–80 kDa, 10%; 10-60 kDa, 12%). Stacking gel was consistently 4% (w/v) acrylamide. Samples were boiled at 98 °C for 5 minutes with 3X sample buffer prior to loading. Gels were run at 100 V until all samples had migrated through the stacking gel, and then at 180 V through resolving gel.

SDS-PAGE for protein purification For protein purification, Mini-PROTEAN TGX™ Precast gels were used for protein separation. Proteins were stained with InstantBlue™ Protein stain (Expedeon) and imaged with the GelDoc™ XR+ system (BioRad).

2.5.2 Western blotting

Proteins separated by SDS-PAGE were transferred to nitrocellulose membrane using the Trans-Blot® Turbo™ Blotting System (Bio Rad) as per the manufacturer's instructions. Following transfer, the nitrocellulose membrane was stained with ponceau for 5 minutes to reveal protein distribution.

Nitrocellulose membrane was incubated in blocking solution for 1 hour prior to incubation with primary antibody, prepared to the required concentration in blocking solution. Primary antibody incubation was for 45 minutes at room temperature or overnight at 4°C. Membranes were washed three times in 1X TBS-T (Tris Buffered Saline with 0.1% (v/v) Triton X100) prior to incubation with secondary antibody prepared to the correct dilution in blocking solution for 45 minutes at room temperature. Membranes were washed a further three times with TBS-T. Membranes were incubated for 3 minutes with freshly prepared EZ-ECL Enhanced Chemiluminescence detection substrate (Biological Industries). For detection of chemiluminescence, membranes were exposed to Hyperfilm (GE Healthcare) in a dark room for an appropriate period given the signal strength. Film was developed with a Curix 60 film developer (AGFA).

2.6 General Mammalian Cell Culture Techniques

2.6.1 Cell lines

Table 19 Mammalian Cell Lines

Cell line	Description	Source
RPE-1	hTERT-immortalised Human Retinal Pigment Epithelial cells	Lane lab
HeLa	Human cervix epithelioid carcinoma	Lane lab
94αT4 MELAS Cybrids	Cytoplasmic hybrid cells carrying m.A3243G mtDNA mutation	Dr José Sanchez-Alcázar, Seville[161]
wild type ACH Cybrids	Cytoplasmic hybrid cells not carrying m.A3243G mtDNA mutation	Dr José Sanchez-Alcázar, Seville

Unless otherwise stated, cultured in *Standard Cell Culture Media* in 10cm culture dishes at 37°C and 5% CO_2.

2.6.2 Media

Table 20 Media

Media	Components	Use
Standard Cell Culture Media	Dulbecco's Modified Eagle's Medium – high glucose (DMEM, Sigma) with 10% (v/v) FBS	Culturing HeLa and RPE-1 cells
Cybrid media	DMEM 4.5 g/L glucose, 10% (v/v) FBS 100 µg/ml sodium pyruvate 50 µg/ml uridine	Culturing MELAS and WT cybrid cell lines
Reduced Serum medium	OptiMEM (Gibco)	Transfecting HeLa and RPE-1
Freezing media	50% Standard Cell Culture Medium 40% (v/v) FBS 10% (v/v) DMSO	Freezing cell stocks

2.6.3 Transient transfection

2.6.3.1 Lipofectamine 2000

Transient transfection was performed with Lipofectamine®2000 (Invitrogen) as per manufacturer's instructions: Cells were grown to 70-80% confluency before transfection.

2.6.3.2 Polyethylenimine (PEI)

PEI working solution of 1 mg/ml PEI in ddH_2O was prepared by dissolving PEI overnight at room temperature, adjusting to pH 7.5 and sterilising through 0.2 µm nitrocellulose filter. For a 6-well dish, 20 pmoles RNA was added to 100 µl OptiMEM. 12 µl PEI working solution was added, tube pulse vortexed (15 x 1 second bursts) and incubated at room temperature for 10 minutes. 0.6 ml full media was added to PEI-RNA mix, mixed thoroughly and added to 70-80% confluent cells and returned to 37 °C incubator. After 2-3 hours, 1ml media was added to each well.

2.6.4 Immunofluorescence

Cells were grown on glass coverslips (13mm, thickness 1, VWR) and fixed and permeabilised with either Methanol or Formaldehyde fixation followed by permeabilization with Triton.

Methanol fixation: Coverslips were washed three times with PBS, then incubated in -20 °C methanol for 4 minutes before a further three washes with PBS.

Formaldehyde Fixation: Coverslips were washed three times with PBS and incubated in 3.7% formaldehyde in PBS for 10 minutes. Coverslips were washed three times in PBS and permeabilised by incubation with 0.1% (v/v) Triton X100 in PBS for 5 minutes. Following three further PBS washes (once with a drop of 1 M glycine to block non-specific binding of antibodies to unreacted aldehyde groups), coverslips were incubated with primary antibody diluted in PBS for 30 minutes (see Table 21 for a complete list of primary antibodies). Coverslips were then washed three times in PBS before incubation with secondary antibody diluted in PBS for 30 minutes followed by a further three washes with PBS. Nuclei were stained with DAPI (4′, 6-diamino-2-phenylindole) by incubation in 0.1 µg.ml^{-1} for 5 minutes. Coverslips were then washed with PBS and ddH_2O prior to mounting on slides with Mowiol.

2.6.5 Fluorescence Imaging

Widefield microscopy was performed using an Olympus IX-71 inverted microscope.

2.6.6 Antibodies

The primary antibodies used are detailed in the table below:

Table 21 Antibodies

Antibody	Supplier	Cat. No.	Type	Dilution
Anti-Cas9	Abcam	Ab204448	Rabbit polyclonal	WB: 1:5000 IF: 1:1000
Anti-GFP	Covance	MMS-118R	Mouse monoclonal	WB 1:2000
Anti-Hsp60	Sigma	H4149	Mouse monoclonal	WB: 1:3000 IF: 1:1000

Table 21 ctd.

Antibody	Supplier	Cat. No.	Type	Dilution
Anti-Lamin B1	Santa Cruz	SC-216	Goat polyclonal	WB: 1:2500
Anti-LC3B	Sigma	L8918	Rabbit Polyclonal	IF: 1:400
Anti-Tubulin B-512	Sigma	T5168	Mouse monoclonal	WB: 1:2500

HRP-conjugated secondary antibodies (Jackson Immunoresearch Laboratories) used for western blotting were diluted to 1:20,000 in blocking solution. Alexa Fluor™ 594 conjugated secondary antibodies (Molecular Probes, Life Technologies) used for immunofluorescence were diluted to 1:100 in PBS.

2.6.7 Cell lysis and protein quantification for Western blotting

Cell culture medium was aspirated, and cells were washed twice with ice-cold PBS. Cells were incubated in Lysis Buffer (RIPA buffer + 1% (v/v) NP40, 1 mM PMSF and 1 µM protease inhibitors) - 150µl for a 12-well dish and 300µl for a 6-well dish. Cells were scraped from the culture dish and transferred to a 1.5ml Eppendorf and incubated on ice for 15 minutes with occasional disruption. Cells were spun at 20,000 x *g* for 5 minutes, 4°C and lysates stored at -20°C until required. Protein concentration was quantified using the Pierce™ BCA Protein Assay Kit (Life Technologies) as per the manufacturer's instructions.

2.7 Techniques to study *Spy*Cas9 domain motions[162,163]

2.7.1 Purification of $Cas9_{hinge}$ and $dCas9_{HNH}$

Unless stated otherwise, all columns were run on an AKTA Prime Plus Liquid Chromatography System (GE Healthcare) at 4 °C.

2.7.1.1 Bacterial growth of $Cas9_{hinge}$ and $dCas9_{HNH}$

BL21 Rosetta 2 (DE3) cells were transformed with pSUMOCas9$_{hinge}$ and pSUMOdCas9$_{HNH}$ and grown overnight on LBA with appropriate antibiotic. 500 ml LB was inoculated with a single colony and cells were grown at 37 °C in a 2.5 L flask at 250 rpm for 16 hours. Once grown, bacteria were pelleted by centrifugation for 20 mins at 4,000 x *g*, 4 °C, and supernatant discarded. Pellets could be frozen in liquid nitrogen and stored at -20 °C at this point.

2.7.1.2 $Cas9_{hinge}$ and $dCas9_{HNH}$ purification

Sonication buffer, HisWash 1, HisElution and HisWash 2 buffers were prepared in advance, filtered through a 0.2 µm nitrocellulose filter and chilled to 4 °C. β-mercaptoethanol and protease inhibitors were omitted and added immediately before use. The bacterial pellet was resuspended in 25 ml sonication buffer and lysed by sonication 2 x 2 minutes (10 seconds on/off) at 75% of maximum with a standard sonication tip. Total lysate was cleared by ultracentrifugation for 40 minutes at 37,000 x *g*, 4 °C and supernatant was dialysed at 4 °C against 1L HisWash1 in Snakeskin™ 10,000 MWCO Dialysis tubing (Thermo Scientific). Sample was filtered through a 0.45 µm nitrocellulose filter and loaded onto a 5 ml HisWash1-equilibrated HisTrap HP column (GE Healthcare. 2 ml fractions were collected through a linear gradient over 100ml up to 100% HisElution. Both Cas9$_{hinge}$ and dCas9$_{HNH}$ were eluted in the range of 120 - 170 mM imidazole (roughly 20 – 30 % HisElution). Pooled fractions were dialysed at 4 °C against HisWash2 and total protein concentration estimated using a DeNovix DS-11 spectrophotometer to measure absorbance at 260 nm. The His tag-SUMO was cleaved overnight with SUMO protease (2 µl SUMO protease was added per mg Cas9 protein) in Snakeskin dialysis tubing, dialysed against 2L HisWash2 at 4 °C. The next morning, an appropriate amount of NaCl and imidazole were added to give a final concentration of 30 mM imidazole, and the cleaved sample was loaded onto a HisWash2 equilibrated 5 ml HisTrap HP column (GE Healthcare). Cas9 containing flow-through was collected as 2 ml fractions, and bound tag and SUMO protease eluted with HisElution. Cas9 containing fractions were concentrated and buffer exchanged into GelFiltration buffer with Amicon Ultra-15 50 kDa cut-off centrifugal filter units (Millipore). Protein was frozen with liquid nitrogen and stored at -80°C. See Appendix A4 for column traces and summary gels.

2.7.1.3 Labelling $Cas9_{hinge}$ and $dCas9_{HNH}$ with Cy3 and Cy3/5

$Cas9_{hinge}$ and $dCas9_{HNH}$ were either single labelled with Cy3 only or double labelled with Cy3 and Cy5 maleimide monoreactive dyes (Amersham, GE Healthcare). 10 µM Cas9 was labelled with 25 µl dye in GelFiltration buffer in a dark tube following the manufacturer's instructions. Proteins were incubated for 2 hours at room temperature, and overnight at 4 °C. Labelling reaction was quenched with 10 mM DTT and free dye was separated by size exclusion chromatography on a HiLoad Superdex 200 16/60 column (GE Healthcare). Collected 2ml fractions were pooled and concentrated with Amicon Ultra-15 50 kDa cut-off centrifugal filter units (Millipore), frozen with liquid nitrogen and stored at -80°C. See Appendix A4 for column traces and summary gels. To assess labelling efficiency, proteins were diluted and scanned in a quartz cuvette (Sigma C2043) with a Cary 60 UV-Vis spectrophotometer (Agilent). Extinction coefficients for Cas9, Cy3 and Cy5, the absorbance at 280 nm (protein), 552 nm (Cy3) and 650 nm (Cy5) were used to calculate the protein concentration and labelling efficiency using the following equations:

$$[Cas9] = \frac{A_{280} - (A_{280}^{Cy3} + A_{280}^{Cy5})}{\varepsilon_{Cas9}}$$

$$[Cy3] = \frac{A_{552} - (A_{552}^{Cy5})}{\varepsilon_{Cy3}}$$

$$[Cy5] = \frac{A_{650} - (A_{650}^{Cy3})}{\varepsilon_{Cy5}}$$

2.7.2 FRET measurements

100 nM RNA was assembled with 50 nM $Cas9_{hinge}$ labelled with Cy3 or Cy3/Cy5 in FRET buffer on ice. Following a 10 min incubation at room temperature, tubes were spun (5 minutes, benchtop microfuge). Measurements were collected with a FluoroLog Spectrophotometer (Horiba) at room temperature in a 130 µl Quartz cuvette (Hellma); 5 mm slit widths, 1s integration time. For each RNA, the sample was excited at 530 nm and 630 nm and spectra collected from 550 – 800 nm and 650 – 800 nm respectively. $Ratio_A$, calculated as explained in section 4.3 was calculated as a proxy measure for FRET.

2.8 Techniques to study CRISPR endonuclease activity

2.8.1 CsCl maxi prep and ^{3}H labelling

HB101 cells were transformed with pSP1 or pUC19 and selected on LBA plates with ampicillin. One colony was grown overnight in LB with ampicillin. 4 ml overnight culture was inoculated into 500 ml M9 minimal medium with 2 mM $MgSO_4$, 0.2 % (w/v) glucose, 0.005 % (w/v) $CaCl_2$, 0.2 % (w/v) casamino acids, 2 µg/ml thiamine, 100 µg/ml ampicillin and incubated at 37°C until A_{260} = 0.8. chloramphenicol was added (final concentration 0.2 mg/ml) to inhibit further protein synthesis, and cells were labelled by addition of 18.5 MBq tritiated thymine ^{3}H before incubation overnight at 37°C. Cells were chilled and pelleted at 2,000 x g for 25 mins at 4°C. Pellets were resuspended in 6.25ml *solution I* and lysed by addition of 1ml *solution II* and incubated at room temperature for 30 minutes. 3ml ice cold *solution III* was added, and samples incubated on ice for 5 minutes prior to addition of *solution IV* and incubation on ice for 30 minutes with occasional mixing. Samples were pelleted by ultra-centrifugation at 140,000 x *g* for 37 minutes at 4°C. The DNA-containing supernatant was purified by phenol chloroform extraction and isopropanol precipitation. DNA was resuspended in *TE* and then separated by caesium chloride gradient at 31,0000 x *g* for 5 hours.

2.8.2 gRNA/Cas9 Cleavage Assays

2.8.2.1 CRISPR (gRNA/Cas9, crRNA/Cas12a) complex assembly

Unless stated otherwise, 50 nM *Streptococcus pyogenes* Cas9 or 250 nM *Lachnospiraceae bacterium* Cas12a protein was mixed with 50 nM gRNA or 250 nM crRNA in SB and incubated at 37 °C for 1 hour. This assembled CRISPR complex can be stored for up to 24 hours at 4°C.

2.8.2.2 CRISPR (gRNA/Cas9, crRNA/Cas12a) complex plasmid cleavage assays

For each cleavage reaction, 3 mM plasmid substrate (pSP1 or pUC19) was assembled in RB buffer at 37 ºC and preheated for 5 minutes. The reaction was started by addition of 10/50 nM assembled Cas9/Cas12a CRISPR complex which was incubated for the time period specified. The reaction was quenched by adding 80 ºC 3X STEB and incubating at 80 ºC for 5 minutes. Samples were separated by agarose gel electrophoresis on a 1.5 % (w/v) agarose gel stained with ethidium bromide at 20 V overnight (16 hours) and visualised by UV irradiation.

2.8.3 Liquid Scintillation Counting

Agarose gel bands containing supercoiled, linear and open circle DNA were excised from the agarose gel and placed into scintillation vials, including blank gel segments at corresponding heights for calibration. 0.5 ml sodium perchlorate was added to each gel slice, and tubes were incubated at 67°C for 2 hours to melt the agarose. The vials were cooled to room temperature and 10 ml Hionic-Fluor Scintillation Cocktail (Perkin Elmer) was added to each vial and shaken thoroughly. Each vial was counted in a Tri-Carb Trio 3100TR Liquid Scintillation Counter for 10 minutes.

Scintillant optimisation: the above protocol was developed when Perkin Elmer Emulsifying Scintillator plus scintillation cocktail, as previously used by this lab, was discontinued. The previous protocol called for 5ml H_2O to be added with the scintillation cocktail, however this yielded a biphasic mixture with a range of tested reagents (Ultra Gold XR; Ultra Gold LLT; InstaGel Plus; Hionic-Fluor). Following decreasing the volume of H_2O, the scintillation cocktails were checked for a linear increase in counts with increasing DNA and the Hionic-Fluor Scintillation Cocktail was found to perform the best.

2.8.4 Berkeley Madonna

The Berkeley Madonna 8.0.2 (R. Macey, G. Oster, T. Zahley) software package was used for curve-fitting cleavage assays using the following model:

```
STARTTIME = 0
STOPTIME = 300

DT = 0.02

d/dt (CCC) = -ka*CCC - kini*CCC
d/dt (ucCCC) = kini*CCC
d/dt (OC) = ka*CCC - kb*OC - kini2*OC
d/dt (ucOC) = kini2*OC
d/dt (LIN) = kbOC

Tot CCC = CCC + ucCCC
Tot OC = OC + ucOC

Init CCC = 95
init LIN = 1
init OC = 5
init ucCCC = 0
init ucOC = 0

ka = 0.10
kb = 0.10
kini = 0.02
kini2 = 0.02
```

uncut OC/CCC allows for reaction not going to completion.

these values changed to actual percentage amounts DNA/time for each run

these values allowed to be fit by software

2.9 Techniques to study R-loop formation

2.9.1 Magnetic Tweezers

Experiments undertaken and analysed by Mark Szczelkun using pSP1 following the protocols in Szczelkun *et al*[92].

2.10 Techniques to study RNA in isolated mitochondria

2.10.1 Isolation of mammalian mitochondria

RPE-1 cells were seeded to be 90% confluent on the day of the mitochondrial isolation. Media was aspirated, cells washed two times with *PBS* and cells removed from the culture dish by addition of 2 ml trypsin. Once dissociated, cells were transferred into a 14 ml falcon tube and centrifuged at 600 x *g* at 4 °C for 10 min. The cell pellet was resuspended in 1.5 ml ice-cold *Mitochondrial isolation Buffer*. Cells were homogenized using the Cell "cracker" Homogeniser (HMG Precision Engineering) with a 10 µm spacing ball bearing. Optimal cell cracking results in completely disrupted plasma membranes but intact nuclei, which was monitored by observing the integrity of a few µl of cells on a light microscope following successive passages through the homogeniser. RPE-1 cells required passing through the homogeniser 14 times on average. The homogenate was centrifuged at 600 x *g* for 10 minutes at 4 °C to pellet nuclei. Mitochondria containing supernatant was collected into a new tube and centrifuged at 7,000 x *g* for 10 min at 4 °C to pellet mitochondria. Supernatant was discarded, and pellet was washed with isolation buffer. Mitochondrial protein was assessed with the Pierce assay as stated above. Three dishes of RPE-1 cells at 90% confluency produced approximately 60 µg mitochondrial protein.

2.10.2 Isolation of yeast mitochondria

Yeast (YPH499) was grown in 400ml YPG with Pen/Strep at 24°C, 150 rpm for ~ 48-72 hours. When OD_{600} = 7.5, cells were subcultured into 2 X 1 L YPG pH 5.2 supplemented with Pen/Strep to OD_{600} = 0.5, then grown overnight at 19°C, 120 rpm. When OD_{600} = 1.2-1.8, cells were pelleted (4,000 x *g*, 10 min, RT), supernatant discarded and pellets re-suspended in dH_20. Cells were pelleted again (1670 x *g*, 5 min, RT) and supernatant discarded. Pelleted cells were resuspended in DTT buffer (100 mM Tris-SO_4 pH 9.4, 10 mM DTT; 2 ml/g pellet) and suspension incubated (100 rpm, 15 min, 30°C) before centrifugation (1670 x *g*, 5 min, RT). Supernatant was discarded, and pellet washed with 150 ml zymolyase buffer (1.2 M sorbitol, 10 mM KPi pH7.4) and pelleted again (1670 x *g*, 5 min, RT). Pellet was resuspended in zymolyase buffer (6.5 ml/g pellet) and zymolyase added (4.5 mg/g pellet). Suspension was incubated (100 rpm, 30 min, 30°C), and cells pelleted by centrifugation (1670 x *g*, 5 min, RT). Pellet was washed with 150 ml zymolyase buffer as before. Cell pellet was resuspended

in homogenisation buffer (6.5 ml/1 g; 0.6 M sorbitol, 10 mM Tris-HCl pH 7.4, 0.5% (w/v) BSA, 1mM PMSF, added just prior to use) and homogenised with a glass potter (1,000 rpm, 15 strokes). Homogenate was pelleted by centrifugation (1480xg, 5 min, 4°C). Supernatant was transferred to a fresh tube, and remaining pellet re-suspended in homogenisation buffer, homogenised and centrifuged as before. Supernatants were centrifuged (17,370 x *g*, 15 min, 4°C) and supernatants discarded. Pellets were combined and re-suspended in 1 ml ice cold SM buffer Resuspended mitochondria were washed with 15 ml SM and centrifuged (1480 x *g*, 5 min, 4°C), supernatant was transferred to a new tube and mitochondria pelleted (17,370 x *g*, 15 min, 4°C). Pellet was re-suspended in ice cold SM and diluted to 10 mg/ml following quantification by BSA assay. 1 mg aliquots were snap frozen and stored at -80°C.

2.10.3 Assessing mitochondrial respiration

Oroboros Oxygraph O_2 electrode (Oroboros Instruments)

Isolated mitochondria were resuspended in a minimal volume respiration buffer (75 mM sucrose, 50 mM KCl, 5 mM KH_2PO_4, 3mM $MgCl_2$, 0.5mM EDTA, 30 mM Tris) and loaded into the oxygen electrode chamber containing respiration buffer. Respiration chain substrates, such as 2 mM Glutamate, 5mM Malate, 1.5mM ADP, and inhibitors such as 10 µM cytochrome *c*, 10 µM rotenone, 10 µM Antimycin A and FCCP were added directly to the chamber using Hamilton syringes.

XF^{e}96 Extracellular Flux Analyser (Seahorse Bioscientific)

Mitochondria were diluted in cold Seahorse Assay Buffer to 15 µg protein in 25 µL buffer and pipetted into a chilled 96 well cell culture microplate, suitable for the machine. The microplate was transferred to a centrifuge equipped with a swinging bucket microplate adaptor (Jouan C3i), and spun at 2,000 x *g* for 20 minutes at 4°C. After centrifugation, 155 µL 1X Assay Buffer (37°) was added to each well. The mitochondria were viewed under a microscope to ensure consistent adherence to the well and the plate was then transferred to the XF^{e}96 Analyser.

Import of protein into isolated yeast mitochondria

Experiment performed by Dr Holly Ford. Isolated yeast mitochondria were thawed on ice and diluted in ice cold *Yeast Import Buffer* with 2 mM ATP and 2 mM NADH added just before use. 100 µg mitochondria were diluted into 100 µl import buffer per condition. The mitochondrial suspension was preheated to 25°C in a thermo-mixer with gentle shaking and import started by addition of cytochrome b2 Δ43-65 Δ159-591-mouse DHFR-myc-his-cys protein, gentle vortex and incubation at 25°C. Import was stopped after 5 minutes with 1 µl *VOA mix*. "- import" condition was treated with *VOA mix* before addition of protein. Each

condition was split int two tubes and treated with proteinase K to digest unimported protein, washed twice with 250 µl *Yeast Import Buffer* and run on a SDS-PAGE gel.

2.10.4 Import of radiolabelled RNA into isolated yeast mitochondria

Isolated yeast mitochondria were thawed on ice and diluted in ice cold *Yeast Import Buffer* with 2 mM ATP and 2 mM NADH added just before use. 100 µg mitochondria were diluted into 100 µl import buffer per condition. The mitochondrial suspension was preheated to 25°C in a thermo-mixer with gentle shaking and import started by addition of ^{33}P-labelled RNA, gentle vortex and incubation at 25°C. Import was stopped after 5 minutes with 1 µl *VOA mix*. The sample was split into two Eppendorf tubes (50 µl each) and one tube incubated with 5 µg RNase A for 15 min at 25°C. RNase was stopped with 1.5 µl RNase inhibitor and incubated for 10 min at 25 °C, then washed twice with 250 µl *Yeast Import Buffer* with 1 µl RNase inhibitor (centrifugation at 17,000 x *g*, 10 mins). Washed pellets were then either run on a denaturing urea-PAGE gel directly, or RNA extracted with TRIzol reagent.

For TRIzol extraction of RNA: each pellet was resuspended in 250 µl TRIzol reagent and tubes were incubated at RT for 5 mins, 50 µl chloroform was added and tubes incubated for a further 5 mins at RT. Tubes were spun for 15 minutes at 12,000 x *g*, 4 °C. The upper aqueous phase was transferred to a new tube with 125 µl isopropanol with 0.05 µg/µl glycogen and incubated for 10 minutes at RT. Precipitated RNA was pelleted by centrifugation at 12,000 x *g* for 10 mins, 4°C. Pelleted RNA was washed twice with 250 µl 75% (v/v) EtOH (spins at 7,500 x *g*, 5mins, 4°C), air dried and resuspended in 10 µl *2X formamide RNA loading buffer*.
For direct separation by denaturing-PAGE electrophoresis: Pellets were resuspended in 5 µl *Yeast Import buffer* and 5 µl *2X formamide RNA loading buffer.*

Gel running and processing (for both): RNA in *formamide RNA loading buffer* was heated to 100°C for 10 mins before separation by denaturing urea-PAGE (see section 2.4.4). Once run, gel was fixed in *Gel Fixing Solution* for 1 hour, then 30 minutes *Gel Fixing Solution* with 5% (v/v) glycerol. The gel was dried with a pre-programmed schedule (up to 80°C, over 2h) on a BioRad model 583 gel dryer, and then exposed on a phosphorimager screen (Fujifilm). Phosphor screen was imaged with a Typhoon-Trio scanner (GE Healthcare).

2.11 Techniques to study RNA from whole cells

2.11.1 Northern blotting

2.11.1.1 Cellular fractionation and isolation of RNA for Northern blotting

HeLa cells were seeded to be 90% confluent on the day of the fractionation. Media was aspirated, and cells were washed two times with PBS. Cells were detached with trypsin and transferred into a 14 ml falcon tube and centrifuged at 600 x *g* at 4 °C for 10 min. The cell pellet was resuspended in 1 ml ice-cold isolation buffer (0.44 M sorbitol, 40 mM EDTA, 10 mM HEPES-NaOH (pH 6.7), 0.1 % (w/v) SDS). Cells were homogenized using the Cell "cracker" Homogeniser (HMG Precision Engineering) with an 8 µm spacing ball bearing, according to the manufacturer's instructions. Perfect cell cracking results in completely disrupted plasma membranes but intact nuclei, which was achieved with HeLa cells by passing ten times. 100 µl of the whole cell extract was kept for later RNA extraction. The remaining homogenate was centrifuged at 1,500 x *g* for 5 minutes at 4°C to pellet nuclei. Mitochondria containing supernatant was collected and centrifuged at 15,000 x *g* for 20 min at 4°C to pellet mitochondria. The supernatant, cytosolic fraction was kept on ice and the pellet was washed with isolation buffer and resuspended in 300 µl isolation buffer prior to disruption of the outer mitochondrial membrane with 60 ng/µl digitonin for 7 minutes at room temperature. Digitonin was diluted by a wash with 700 µl isolation buffer, and after a final wash the mitochondrial pellet, nuclear pellet, cytoplasmic fraction and whole cell sample were resuspended in 500 µl TRIzol and stored at -80 °C prior to RNA extraction as per the manufacturer's instructions.

2.11.1.2 Northern blotting

Urea-PAGE gels containing separated RNAs were electro-transferred to Hybond XL nylon membrane (GE Healthcare) at 12 V over 12 hours in 0.5X TBE for Northern hybridisation [123]. RNAs were fixed onto nylon membrane by UV irradiation at 1,500 x 100 µJ/cm^2. Membranes were prehybridised in 6 X SSC, 0.1 % (w/v) SDS, 10X Denhardt's solution for 1h at 65 °C. 20 X SSC – 3 M NaCl, 0.3 M sodium citrate, 1mM EDTA; 100X Denhardt's - 2 % (w/v) BSA, 2 % (w/v) Ficoll 400, 2 % (w/v) polyvinylpyrolidone. Hybridisation of 8 x 7cm membranes in 50ml falcons used 2.9 ml prehybridisation solution. Membranes were then hybridised in one volume prehybridisation solution containing one volume ($[probe]_f$: 2ng/ml) 5'- ^{32}P-labelled oligonucleotide probe by incubation overnight at T_m - 5°C. Probes, Table 17, of known cytoplasmic and mitochondrial RNAs were used as positive controls for cellular compartments, and designed hybridisation probes against gRNAs and mitochondrial targeted RNA aptamers determined transfected RNA cellular localisation. Following

hybridisation, membranes were washed 3 times for 10 mins in 2X SSC and 0.1% (w/v) SDS at room temperature and exposed on a phosphorimager screen which was imaged with a Typhoon-Trio scanner (GE Healthcare).

Labelling hybridisation probes: dephosphorylated DNA oligonucleotides were labelled with bacteriophage T4 polynucleotide kinase by incubation for 1 hour at 37°C with a 5-times molar excess of 10 mCi/ml γ-^{32}P ATP (Hartman Analytic, SRP 301) as per the manufacturers' instructions. The reaction was terminated by addition of EDTA (final concentration 20 mM), and probes were purified from unincorporated nucleotide with BioRad Micro Bio Spin P-6 columns.

HeLa transfection for AD/FD time course (Figure 6-3) In a 6-well dish, 70-80% confluent HeLa cells were transfected with 20 pmoles RNA using Lipofectamine. Cells were harvested at the indicated timepoint, whole-cell RNA extracted, separated by urea-PAGE and Northern Blotted with tRK1 as above.

HeLa transfection for northern blotting AD/FD: A 10 cm dish of 70-80% confluent HeLa cells were transfected with 80 pmoles AD and FD RNA using Lipofectamine. Cells were harvested, fractionated and northern blotted as above.

HeLa transfection for northern blotting gRNA±RP/FD: A 10 cm dish of 70-80% confluent HeLa cells transfected with 300 pmoles gRNA, gRNA 5' RP and gRNA 5' FD using Lipofectamine. Cells were harvested and fractionated and northern blotted as above.

2.11.2 Cellular distribution of fluorophore-labelled RNAs

In a 6-well dish, RPE-1 cells were grown on glass coverslips. When 70-80% confluent, cells were transfected with 20 pmoles Alexa™ 488-labelled RNA by PEI transfection as described above.

2.11.3 Baby Spinach fluorescent RNA characterisation

Fluorescence measurements were performed with a Varian Cary Eclipse fluorescence spectrophotometer in a Hellma Quartz cuvette (105253-QS); excitation wavelength 460 nm, emission wavelength 475-650 nm, slit widths 50 nm.

For RNA-only measurements 1 µM RNA was assembled in 1X RNA aptamer buffer on ice, with or without 20 µM DFHBI-1T (Lucerna) as described by the manufacturer.

For Cas9/gRNA complexes 1 µM RNA was assembled on ice with 1 µM Cas9 in in 1X RNA aptamer buffer, with or without 20 µM DFHBI-1T. Complexes were either incubated at 37 °C for an hour before addition of DFHBI-1T and fluorescence measurement or measured immediately.

2.12CRISPR kits

2.12.1 GeneArt™ gRNA Synthesis and Precision™ Cas9 nuclease transfection

gRNAs were synthesised using the GeneArt™ Precision gRNA synthesis kit (Invitrogen) as per the manufacturer's instructions and purified with GeneJET™ RNA purification micro columns (Thermo). HeLa cells were seeded 24 hours prior to transfection in a 24-well plate format at 0.05 x 10^6 cells per well. The GeneArt™ Platinum™ *Spy*Cas9 nuclease and *in vitro* transcribed gRNAs were transfected with Lipofectamine™ CRISPRMAX™ (Thermo) as per the manufacturer's instructions (500 ng Cas9 nuclease and 125 ng gRNA per well).

Table 22 GCDA gRNA target sequences

gRNA target	DNA target sequence (protospacer) (5′-3′)
HPRT	GCATTTCTCAGTCCTAAACA
COX1	TATTCGAGCCGAGCTGGGCC
COX2	TTCATGATCACGCCCTCATA
COX3	TAACGCTCCTCATACTAGGC

2.12.2 CRISPR GeneArt™ Genomic Cleavage Detection Assay (Life Technologies)

The GCDA assay provides a quick readout of efficiency of DSB formation by CRISPR at the desired site. The kit was used as per the manufacturer's instructions. DNA is extracted from cells which have been transfected with CRISPR components and a PCR is performed to selectively amplify a loci of interest which contains the site targeted for DSB formation, Table 23. The PCR products are melted and reannealed. If CRISPR has been effective, the target site will be highly variable between PCR amplicons, resulting in mismatches when PCR amplicons are reannealed. These mismatches are selectively cleaved by a T7 endonuclease detection enzyme to give two smaller DNA strands.

Table 23 GCDA PCR primers

gRNA target	Forward primer sequence (5′-3′)	Reverse primer sequence (5′-3′)
HPRT	AGCAGCTGTTCTGAGTACTTGC (22)	GGTATCTCCATAAGACAGAATGC (23)
COX1	GAAAATCACCTCGGAGCTGG (20)	TTTGGTATTGGGTTATGGCAGG (22)
COX2	CGAACCCCCCAAAGCTGG (18)	CAGCTCATGAGTGCAAGACGTC (22)
COX3	CGCCTTAATCCAAGCCTACG (20)	CTCTGAGGCTTGTAGGAGGGT (21)

3 Modifying *Spy*Cas9 for MitoCRISPR

3.1 Mammalian cell expression systems for Cas9

At the time of writing this thesis in 2018, the range of commercially available plasmids, kits and reagents to facilitate CRISPR workflows is extensive: Addgene has over 6,300 CRISPR plasmids contributed by over 330 labs worldwide[164], and most laboratory suppliers have their own flavour of CRISPR kits available. The story was quite different when we began this project in 2014. Although there had already been an outpouring of CRISPR products, the number of available CRISPR plasmids was only a fraction of those available today; these first CRISPR kits were only in their first iterations and required much troubleshooting.

Chapter 3 describes the use of a commercial plasmid expression system to target *Spy*Cas9 to mammalian mitochondria using the cytochrome *c* oxidase subunit viii (COX8A) MTS introduced in section 1.3.4. The results are inconclusive, since the efficiency of transformation of *Spy*Cas9 was poor. Subsequent work from the MitoCRIPSR research group is described that confirms these early observations and shows that other CRISPR-Cas enzymes (in particular *Lb*Cas12a) with alternative MTSs can be efficiently transfected into cells and targeted to mitochondria.

3.1.1 DNA transfection

Advancements in mammalian culture transfection techniques have played an important role in driving advancements in genome editing. The efficiency with which CRISPR nucleases and gRNAs can be expressed within a cell line or model organism is pivotal to CRISPR efficacy, and remains one of the key challenges to implementation[165]. Although plasmid transfection techniques were initially commonplace, the field is now increasingly moving towards mRNA or ribonucleoprotein (RNP) complex transfection-based approaches, both of which have several advantages including shorter workflows and, dependent on application, greater efficiency of CRISPR action[166].

An overview of the main techniques for the delivery of CRISPR machinery to mammalian cells is given in the following sections, with a focus on whether each method would be appropriate for developing a MitoCRISPR system. This is summarised in Figure 3-1.

3.1.1.1 Mammalian expression vectors

Mammalian expression vectors were the first available method of CRISPR delivery. An extensive range of plasmids are available which are: tailored to cell types and applications; have varying strengths of inducible and constitutively active promoters (Tet-ON[iii] and CMV[iv]

[iii] Addgene plasmid #50661[221]

[iv] Addgene plasmid #69988[94]

or CBh[v] are respective examples); incorporate a wide range of reporter genes and selectable markers such as GFP expression or drug resistance; express CRISPR nucleases and gRNAs from separate vectors, or a single combined vector. Moreover, delivery systems such as lipid-based transfection and electroporation have been widely optimised for delivery of CRISPR components for standard applications[167]. As the doubling time of many culture cell lines is approximately 24 hours, transient transfection is often sufficient when CRISPR is being used for genome editing, such as for the generation of knock-out and disease model cell lines[168], but mammalian expression vectors have also been used for generating cell lines stably expressing CRISPR components.

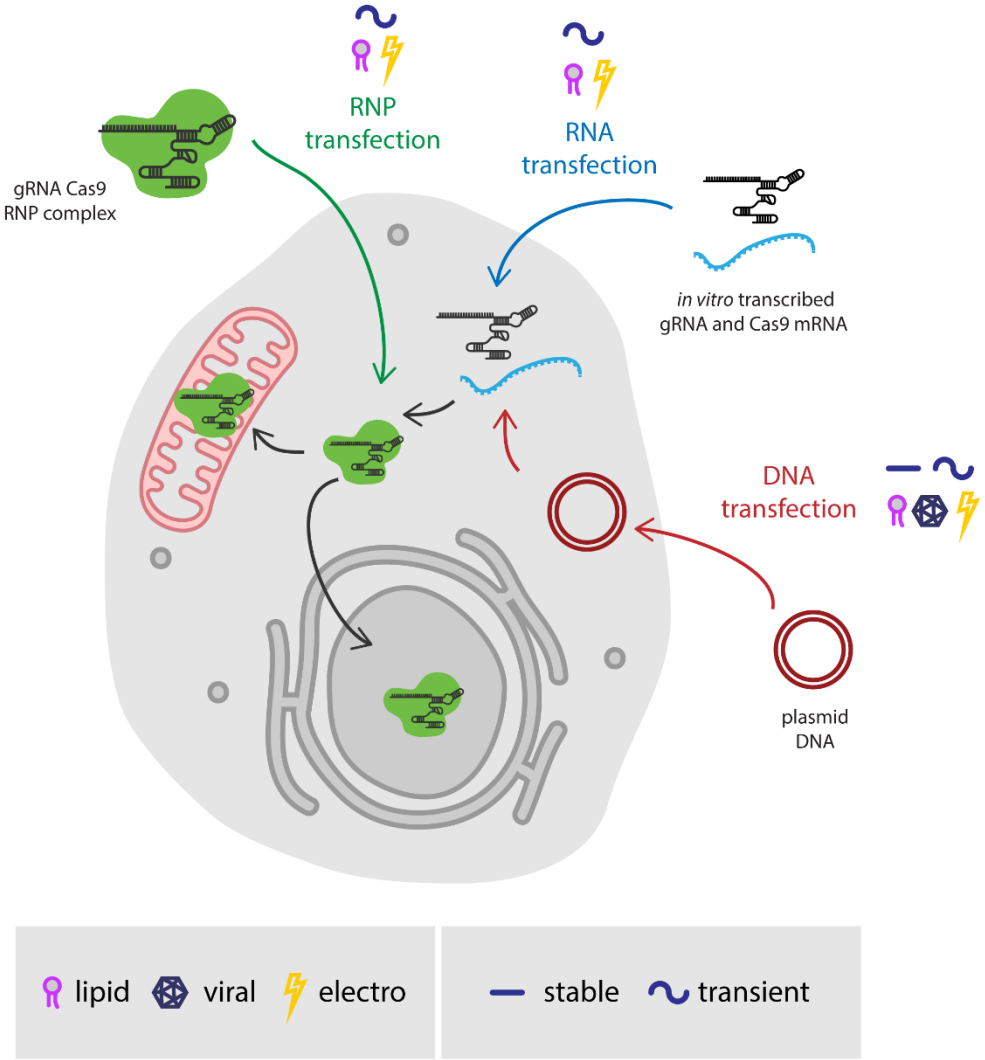

Figure 3-1 Available technologies for delivering CRISPR machinery to mammalian cells *include DNA transfection (red), RNA transfection (blue), and transfection of pre-formed ribonucleoproteins (RNPs, green). DNA encoding CRISPR components can be expressed stably or transiently, whereas RNA and RNP methods are only expressed transiently. Each route has several potential mechanisms of delivery which could theoretically be harnessed for delivery of a nuclear or mitochondrial targeted CRISPR system.*

[v] Addgene plasmid #48138[222]

3.1.1.2 Viral expression vectors

All four major viral delivery systems (retroviruses, lentiviruses, adenoviruses and adeno-associated viruses (AAVs)) have now been used to target DNA encoding CRISPR machinery to mammalian cells. Each have their own advantages and limitations, making them appropriate in different circumstances, as reviewed by Schmidt and Grimm[169].

Of particular concern at the beginning this project was the safety of using a viral delivery system for CRISPR tools, particularly given that - at that time - very few people at the University of Bristol were using CRISPR. AAVs are the only viral vector which do not contain any viral genes. Being derived from apathogenic viruses, AAVs have the lowest level of safety concern of all viral vectors as they are also incapable of replication. However, the AAV is likely not suitable for transfection of a MitoCas9. The vector has a size limit of 4.9 kbp, only just above that of the 4.2 kbp Cas9 coding sequence; once mitochondrial targeting sequences have been included, there would be limited space for necessary promoters and polyadenylation sequences, let alone the gRNA expression that would be required for full MitoCRISPR.

Although there are several attenuated strains (which, like the AAVs do not contain viral genes) lenti-, retro-, and adenoviral vectors are all derived from pathogenic viruses. This makes safety concerns surrounding their handing, such as the accidental generation of a replication-competent virus, more significant than AAVs. In the intervening years, using viral for CRISPR expression has become more commonplace, and their use is mentioned in the context of this project in section 3.4.

3.1.2 Ribonucleoprotein (RNP) complex transfection

Given that the focus of many CRISPR tools is genome editing, CRISPR machinery is only required in the target cell for a short period of activity. The persistence of Cas9 and gRNA in a cell for an extended period would potentially result in off-target activity; any way of expressing a CRISPR nuclease and gRNA in a cell for a limited time only will be advantageous in these cases. One way of doing this is to pre-form an RNP between the CRISPR nuclease and gRNA which is directly transfected into the cells. RNP transfection has been widely reported to be highly effective[170,171]. This approach also allows the incorporation of synthetic crRNA/tracrRNA or sgRNA, allowing modification of the RNA, which can increase efficacy in human cells, including fully chemically modified RNAs (without any 2'-OH groups)[172,173] or the doping of deoxyribose nucleotides at specific positions to reduce synthesis costs[174].

Many companies now sell kits to facilitate RNP transfection into mammalian cells in culture and model organisms. The eventual dilution/degradation of the CRISPR-Cas system allows the edited cell lines or organisms to no longer contain the CRISPR machinery, which could be potentially useful if MitoCRISPR were to move to the clinic and be used in embryos. However,

it remains to be seen how a folded RNP would be delivered to the mitochondrial matrix; the RNP would either need to be completely unfolded to pass through TOM/TIM or enter the mitochondria independently.

In the early stages of this project use of one of these kits, the GeneArt Genomic Cleavage Detection Assay (Invitrogen), was attempted. However, following limited success at optimising the kit this method was not pursued. The results of this are overviewed in Appendix A3-III.

3.1.3 Cas9 mRNA and gRNA transfection

A second method for transient CRISPR activity in cells is to *in vitro* transcribe the Cas9 gene and gRNA and transfect the mRNA and gRNA molecules into the cell[175]. The mRNA is then translated by the cells own machinery. Given that the mRNA and gRNA will not be replicated by the cell, they are instead degraded over time. Since proteins are translocated across the OMM and IMM unfolded, and there is a requirement for chaperones to aid the process of mitochondrial import, transfecting an mRNA to be transcribed in the cytosol shows potential for a MitoCRISPR system, but due to time constraints was not explored here.

3.2 Plasmids for mammalian cell expression of Cas9

The first approach which was taken for mammalian cell expression of Cas9 in this project was a plasmid DNA transient transfection technique. This decision was based partially on our concerns about the safety of a viral transfection technique, and on the higher level of expertise and understanding in our lab surrounding plasmid-based techniques for mammalian cell transfection over RNA or RNP-based methods. The goal was to clone a plasmid encoding *Spy*Cas9 with an N-terminal COX8A MTS and express it in mammalian cell culture.

3.2.1 pD1301 plasmid series

Standard cloning techniques, as described in section 2.3.3, were used to edit a commercially available plasmid, pD1301-AD (Formerly DNA 2.0, now ATUM), Figure 3-2, to develop a library of plasmids for mammalian cell expression of nuclear and mitochondrial Cas9 and gRNAs. For final plasmid series, see Figure 3-5.

pD1301 encodes the sequence for human codon optimised *Spy*Cas9, flanked by two nuclear localisation sequences (NLS) and followed by DasherGFP, all under the control of the constitutive mammalian cytomegalovirus (CMV) promoter. DasherGFP is a synthetic non-*Aequorea* fluorescent protein, developed by DNA2.0 ($\lambda_{excitation}$ = 505 nm; $\lambda_{emission}$ = 525 nm). Coding sequences for Cas9 and DasherGFP are separated by a self-cleaving peptide, the cis-acting hydroxylase element from the *Thosea asigna* virus (TAV CHYSEL)[176]. This allows for the

equal co-expression of both proteins, which are separated as the translating ribosome 'skips' at the C-terminus of the 18-residue CHYSEL sequence. pD1301 also encodes the gRNA scaffold under the control of a U6 promoter. gRNA spacer sequences can be added by circularising the plasmid and inserting a dsDNA with complimentary ends.

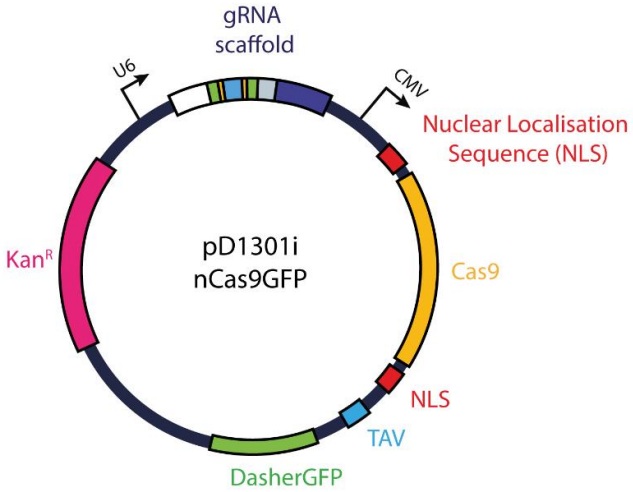

Figure 3-2 pD1301i (DNA2.0)*plasmid map. pD1301i encodes mammalian codon-optimised Cas9 flanked by two nuclear localisation sequences (NLSs) and DasherGFP under the control of the cytomegalovirus (CMV) promoter. Cas9 and GFP are separated by the Thosea asigna virus self-cleaving element (TAV). The plasmid also encodes the gRNA scaffold sequence under the control of the U6 promoter and Kanamycin resistance (Kan^R).*

Although there were several other CRISPR plasmids available at the time, pD1301 was chosen as it contains both the gRNA scaffold and Cas9 coding sequence in one plasmid. The CMV promoter is familiar to the lab and should give reliable expression in the cell types to be used (HeLa, RPE-1). Additionally, pD1301 is classed by DNA2.0 as "IP-free", meaning it has few intellectual property limitations, something we considered to be advantageous regarding a potential future where we wished to patent a MitoCRISPR system. The following section, outlined in Figure 3-3, describes the cloning of a series of plasmids, based on pD1031, for mammalian cell expression of Cas9. Briefly, this included: replacing two NLSs with the COX8A MTS; removal of the gRNA region; removal of the TAV CHYSEL to give a Cas9-GFP fusion protein.

pD1301 was delivered in a linear form, cut by DNA2.0 directly adjacent to the gRNA scaffold in preparation for use with the company's CRISPR *ELECTRA* cloning system[vi]. The *ELECTRA* system uses proprietary reagents to insert a 20 nt protospacer sequence and ligate the plasmid in one step. Following communication with DNA2.0, during which they were not willing to disclose the nature of the ends of the DNA fragment, a recircularisation method was developed as detailed in Figure 3-4 and Appendix A3: Primers were designed to amplify

[vi] https://www.atum.bio/products/expression-vectors/electra-system

the linearised pD1301 plasmid by inverse PCR and introduce *SapI* restriction sites. The blunt-end PCR was then ligated to form an intact plasmid, pD1301.

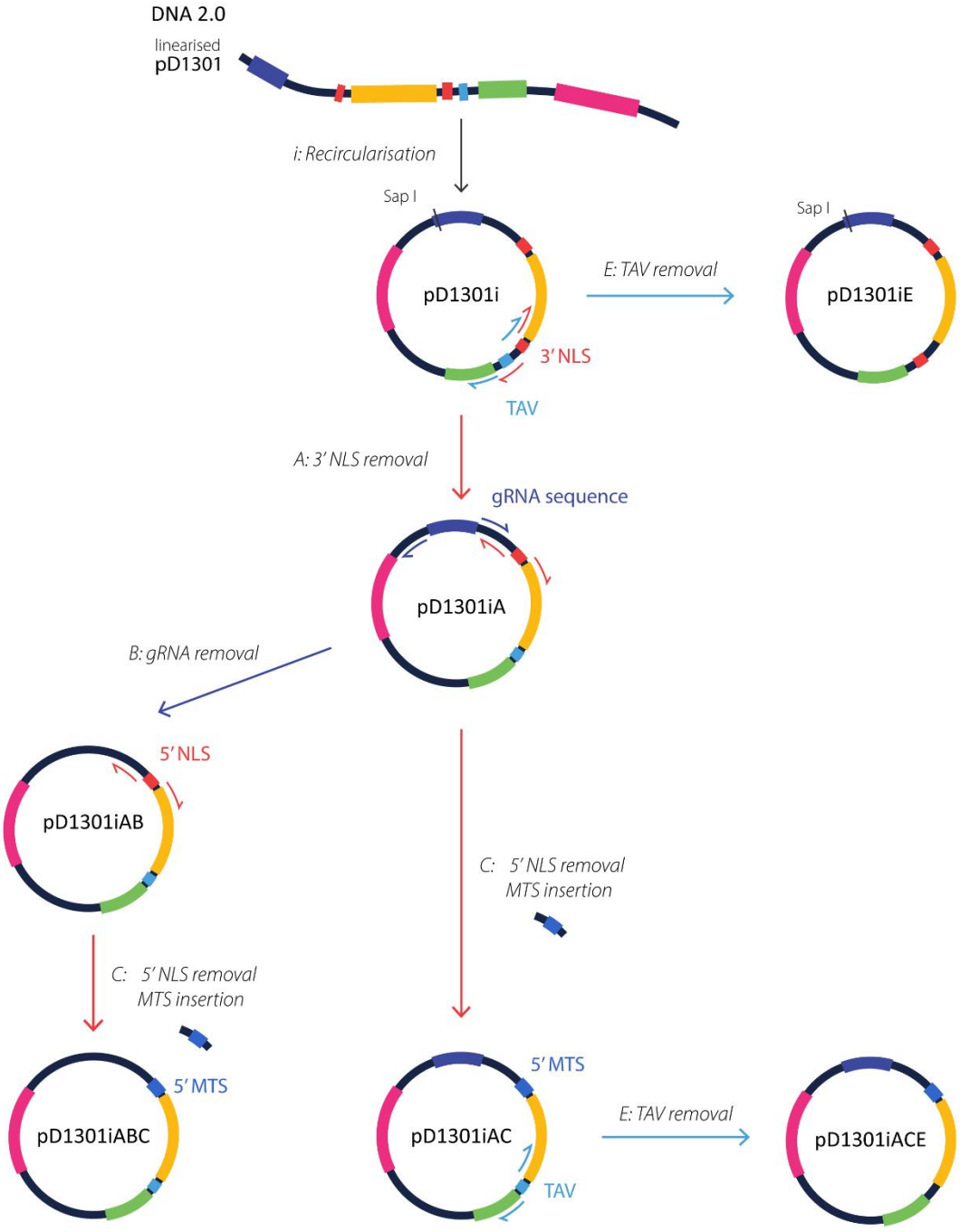

Figure 3-3 pD1301 cloning scheme *is described above, including* ***i*** *plasmid recircularisation (expanded upon in Figure 3-4)* ***A*** *removal of 3′ nuclear localisation sequence (NLS),* ***B*** *gRNA sequence removal,* ***C*** *5′ NLS removal and replacement with a mitochondrial targeting sequence (MTS) and* ***E*** *Thosea asigna virus self-cleaving element (TAV) removal. In each step where inverse PCR was used, the coloured arrows indicate the sites of primers designed to carry out each step. See Appendix A3 for gel scans of each step.*

SapI is a type IIS restriction enzyme which produces a staggered cut downstream of its recognition sequence, 5′-GCTCTTC-3′. The choice of a type IIS enzyme facilitates 'scarless' insertion of spacer sequences; cutting with *SapI* will remove the fragment of the plasmid containing its own recognition sites. A 20 nt DNA fragment with corresponding overhanging ends can then be inserted into the protospacer region of the gRNA scaffold, Figure 3-4.

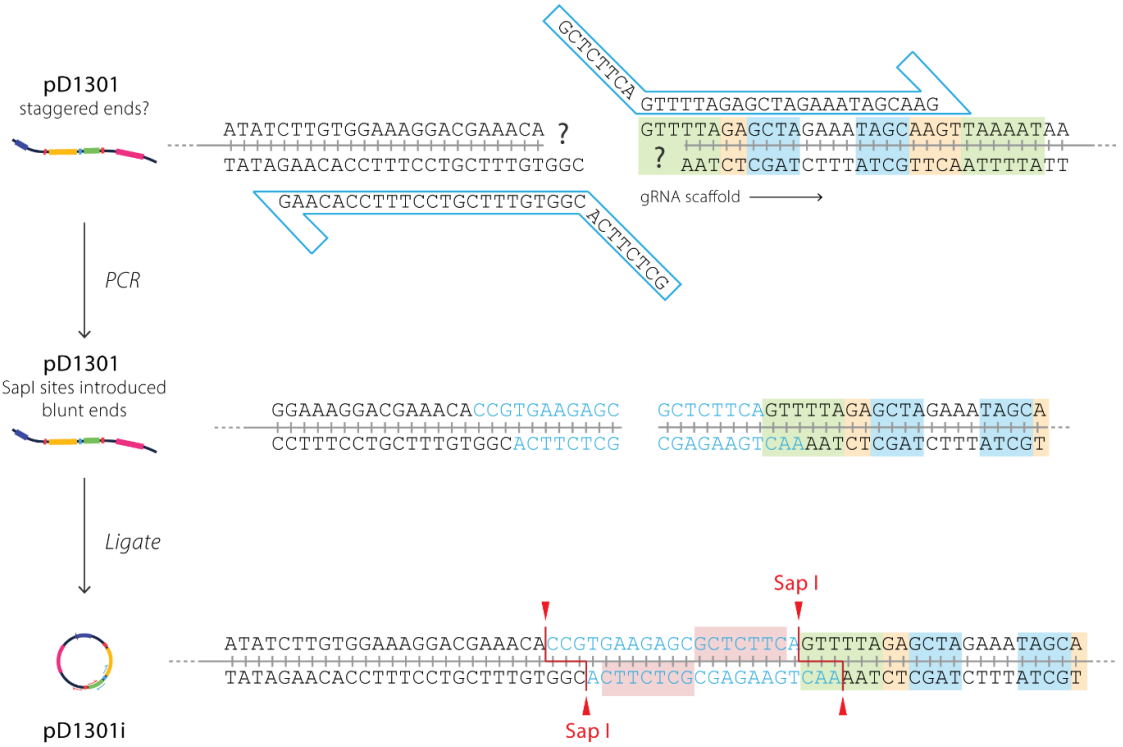

Figure 3-4 pD1301 Recircularisation *was carried out by inverse PCR, followed by blunt-end ligation. Primers were designed to introduce the recognition sites for SapI, a type IIS restriction enzyme (blue), thereby constructing a system to easily interchange protospacers in the gRNA scaffold.*

The 3′ NLS was removed by inverse PCR and the resulting plasmid, pD1301iA (9010 bp), was verified by sequencing and restriction digest, Appendix A3-I.

Proteins must be unfolded prior to mitochondrial import via TOM/TIM. It was a consideration that the expression of gRNA in the cell might result in RNP formation, holding Cas9 in a folded state which hindered mitochondrial import. For this reason, an inverse PCR method was used to remove the gRNA region from pD1301iA – the U6 promoter and the gRNA scaffold coding sequence. The resulting plasmid, pD1301iAB (8570 bp), was verified by sequencing and restriction digest, Appendix A3-I.

Initially, an inverse PCR method (as above) was attempted for removal of the NLS upstream of the Cas9 coding sequence, Appendix A3-II. Primers were designed with 50/46 nt overhangs which together would introduce the 96 bp MTS. However, although the primers were checked for hairpin and primer-dimer formation (OligoCalc[177]), the PCR was

unsuccessful, likely because the overhangs were too long. Secondly, a nested PCR method was attempted with a series of three sets of primers, successively longer in length, to construct the MTS sequence. However, PCR beyond the first round was also unsuccessful.

For the successful cloning, a plasmid was synthesised (pEX-MTS, Eurofins) which contained the COX8A MTS insert, flanked by a 5′ *Pci*I site and a 3′ *Age*I site. pD1301iAB was amplified by inverse PCR to remove the 5′NLS sequence with primers which incorporated a naturally occurring 3′ *Nco*I site (which produces ends compatible with *Pci*I) and a 5′ *Age*I site. The fragments were ligated together to form pD1301iABC, which was sequence verified by restriction digest and full plasmid sequencing. The same process was repeated with pD1301iA to produce pD1301iAC.

An inverse PCR method was also used to remove the TAV ribosomal stalling sequence from pD1301iABC and pD1301i to give pD1301iABCE and pD1301iE, constructs for the expression of mitochondrial and nuclear targeted Cas9-GFP fusion proteins, which were used by Zuriñe Anton, section 3.4.

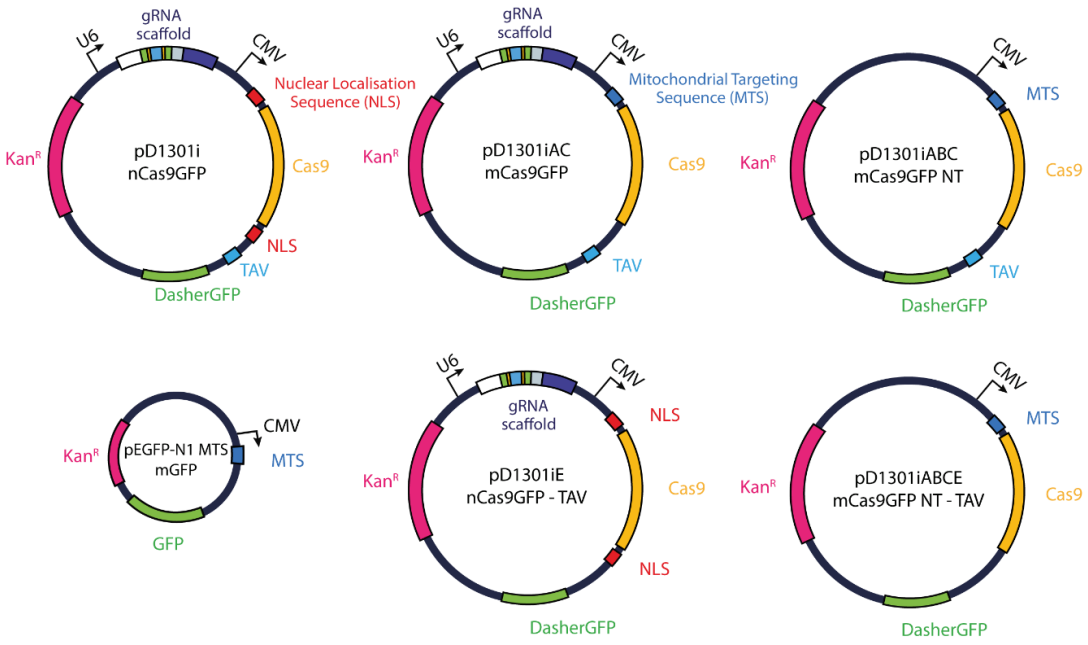

Figure 3-5 pD1301 plasmid series *pD1301i forms the basis of this plasmid series which includes plasmids expressing nuclear targeted SpyCas9 (pD1301i, pD1301iE), mitochondrial targeted Cas9 (pD1301iAC, pD1301iABC and pD1301iABCE), and mitochondrial targeted GFP (pEGFP-N1 MTS), all under the control of the cytomegalovirus (CMV) promoter. pD1301i, pD1301iAC and pD1301iABC contain the Thosea asigna virus self-cleaving element (TAV) between Cas9 and GFP, meaning the two proteins are transcribed separately. In contrast, pD1301iE and pD1301iABCE have had their TAV sequence removed so that they express a Cas9-GFP fusion protein. pD1301i, pD1301iAC and pD1301iABCE all contain the gRNA scaffold sequence under the control of the U6 promoter. All plasmids encode Kanamycin resistance (Kan^R). MTS = mitochondrial targeting sequence, NLS = nuclear localisation sequence.*

3.3 Expression of nuclear and mitochondrial Cas9 in mammalian cell culture

3.3.1 Verification of COX8A MTS function

To verify the ability of the COX8A MTS to mitochondrially target a protein of interest, the COX8A MTS from pEX-MTS was cloned in to the multiple cloning site of pEGFP-N1 to produce pMTS-EGFP. HeLa cells transiently transfected[vii] with pEGFP-N1 and pMTS-EGFP showed cytosolic and mitochondrial GFP localisations, respectively, Figure 3-6, confirming that under our experimental conditions the COX8A MTS, expressed under the CMV promoter can localise proteins to the mitochondria.

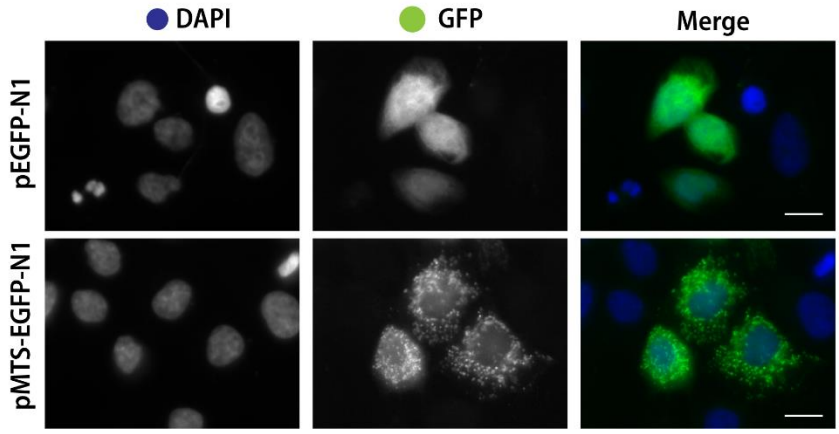

Figure 3-6 HeLa cells transfected with pEGFP-N1 and pMTS-EFGP *display cytosolic and mitochondrial GFP localisations, respectively DAPI (blue) 5ms; GFP (green), 250 ms Scale bar: 10 µm*

3.3.2 Transfection of NLS-Cas9 (pD1301i) and MTS-Cas9 (pD1301iABC)

pD1301i and pD1301iABC were transiently transfected into HeLa and RPE-1 mammalian cell lines. Figure 3-7A shows widefield microscopy images of RPE-1 cells transfected with pD1301i and pD1301iABC. The TAV CHYSEL sequence between Cas9 and GFP means GFP fluorescence will not necessarily correlate with Cas9 localisation, instead GFP can be used as a marker of successful transfection. NLS-Cas9 and MTS-Cas9 localisation should differ as reported by anti-Cas9 antibodies. Figure 3-7A shows cells transfected with pD1301i (NLS-Cas9), pD1301iABC (MTS-Cas9) and phCas9$_{D10A}$ (A commercial NLS-Cas9$_{D10A}$). There is no observable difference between NLS-Cas9 and MTS-Cas9. There does appear to be some cell-to-cell variation within each condition, but these variations do not correlate between anti-Cas9 and GFP. Moreover, the GFP signal is low, and there is a high background signal with the anti-Cas9 antibody staining.

[vii] Unless stated otherwise, all transient transfections in this section were performed with Lipofectamine 2000 as detailed in section 2.6.3.1.

Figure 3-7B shows immunoblotting for anti-Cas9 and anti-GFP of whole-cell proteins extracted from HeLa and RPE-1 cells. An antibody against tubulin is used as a protein loading control. GFP is expressed in RPE-1 cells transfected with pEGFP-N1 and pMTS-EGFP, but there is no specific signal from the anti-Cas9 or anti-GFP antibody in any of the cells transfected with a range of CRISPR plasmids.

phCas9$_{D10A}$ and phCas9$_{WT}$ are plasmids which have been successfully used by the Stephens lab (Bristol University) to generate CRISPR knock-out cell lines. They should be expected to be expressed well enough in cells when observed by immunoblotting and show a nuclear localisation in fluorescence microscopy – however neither were detected, Figure 3-7, though anti-Cas9 antibody staining did seem to be slightly correlated with raised GFP signal in some cells.

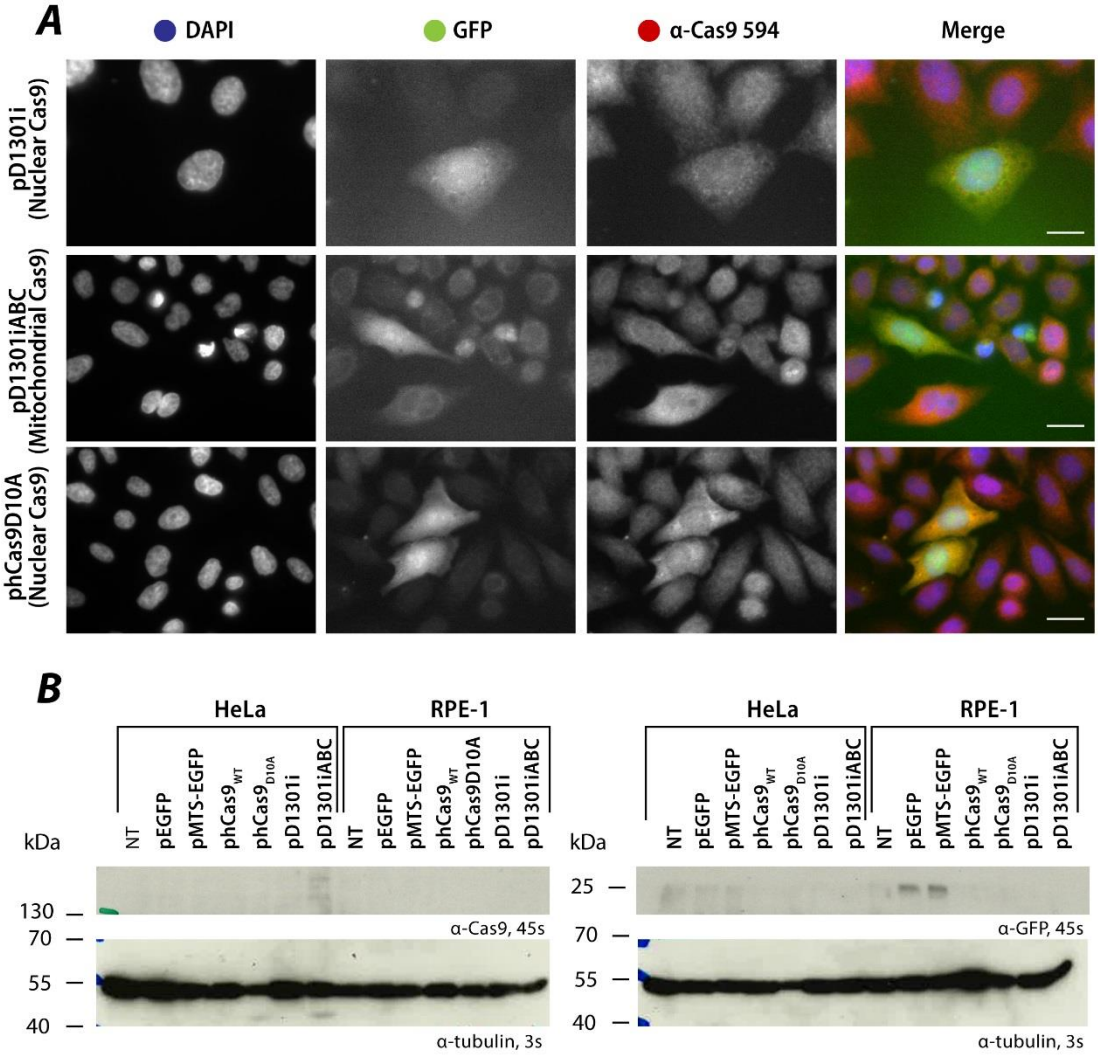

Figure 3-7 Cas9 cellular expression ***A*** *Fluorescence microscopy of RPE-1 cells transfected with pD1301i (NLS-Cas9), pD1301iABC (MTS-Cas9) and phCas9$_{D10A}$; scale bar 10 µm* ***B*** *Immunoblotting HeLa and RPE-1 cells transiently transfected with pEGFP, pMTS-EGFP, phCas9$_{WT}$, phCas9$_{D10A}$, pD1301i (NLS-Cas9) and pD1301iABC (MTS-Cas9).*

Following the poor expression of pD1301iABC (MTS-Cas9), RPE-1 cells were co-transfected with pD1301iABC and pDsRedMito, which expresses mitochondrial-targeted RFP under a CMV promoter. Cells taking up plasmid DNA should take up an equal mix of pDsRedMito and pD1301iABC, so RFP-positive cells should also be expressing pD1310iABC. Given both MTS-Cas9 and RFP are expressed under the CMV promoter, they should also be transcribed at comparable levels.

Figure 3-8 shows RPE-1 cells co-transfected with pD1301iABC and pDsRedMito. Although some cells showed RFP-positive cell mitochondrial networks (marked #), there was not any corresponding increase in GFP signal in these cells. Instead, the four cells marked # and * displayed similar GFP signal levels, despite having differing pDsRedMito expressions (# has high and * low pDsRedMito). This implies that the signal through the green channel could background, rather than a result of GFP expression from pD1301iABC – that is to say pD1301iABC is likely not being expressed in these cells.

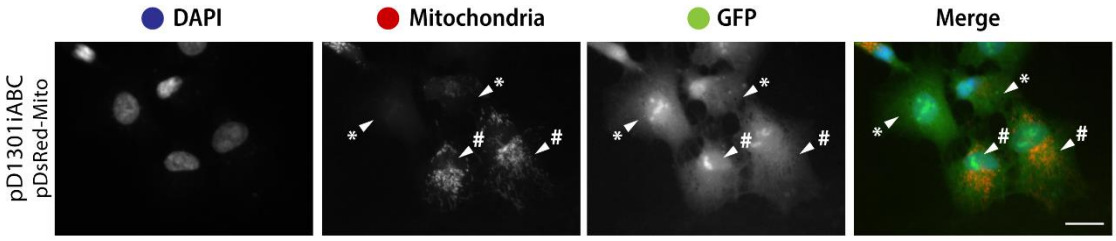

Figure 3-8 Co-transfection of pD1301iABC (MTS-Cas9) with pDsRed-Mito ; Scale bar 10 µm

3.3.3 Fluorescence Activated Cell Sorting (FACS)

Assuming a low level of transfection efficiency, we reasoned that successfully transfected cells could be separated and expanded from a small population by Fluorescence Activated Cell Sorting (FACS). FACS was used to separate a population of pD1301iABC and pD1301i expressing RPE-1 and HeLa cells from non-transfected cells, Figure 3-9. A population of non-transfected parent cells (*top panels*) were used to gate the cells such that GFP-negative cells could be sorted from GFP-positive cells. The density plots below show the GFP fluorescence (y-axis) against incorporation of propidium iodide (PI) (x-axis), a cell viability dye. Living cells do not incorporate PI (purple box), whereas dead cells do (pink box).

For HeLa cells, 0.76% of cells were GFP positive when transfected with pD1301iABC, Figure 3-9 *middle left* and 2.24% when transfected with pD1301i, *bottom left*. In both cases, there was a decreased viability on transfection in comparison to non-transfected cells.

According to the same gating parameters, RPE-1 cells transfected with pD1301iABC were 21.75% positive for pD1301iABC, Figure 3-9 *middle right*. It is important to consider that some of this signal might not be due to GFP expression and instead cell autofluorescence. In

general, larger and more granular cells have more autofluorescence, as do cells undergoing apoptosis; In particular, RPE cells accumulate lipofuscin with age, which is autofluorescent[178]. The large shift in PI incorporation, as well as the gross change in fluorescence at 530/40 nm implies that these cells had undergone a large change in viability or morphology with respect to the non-transfected cells.

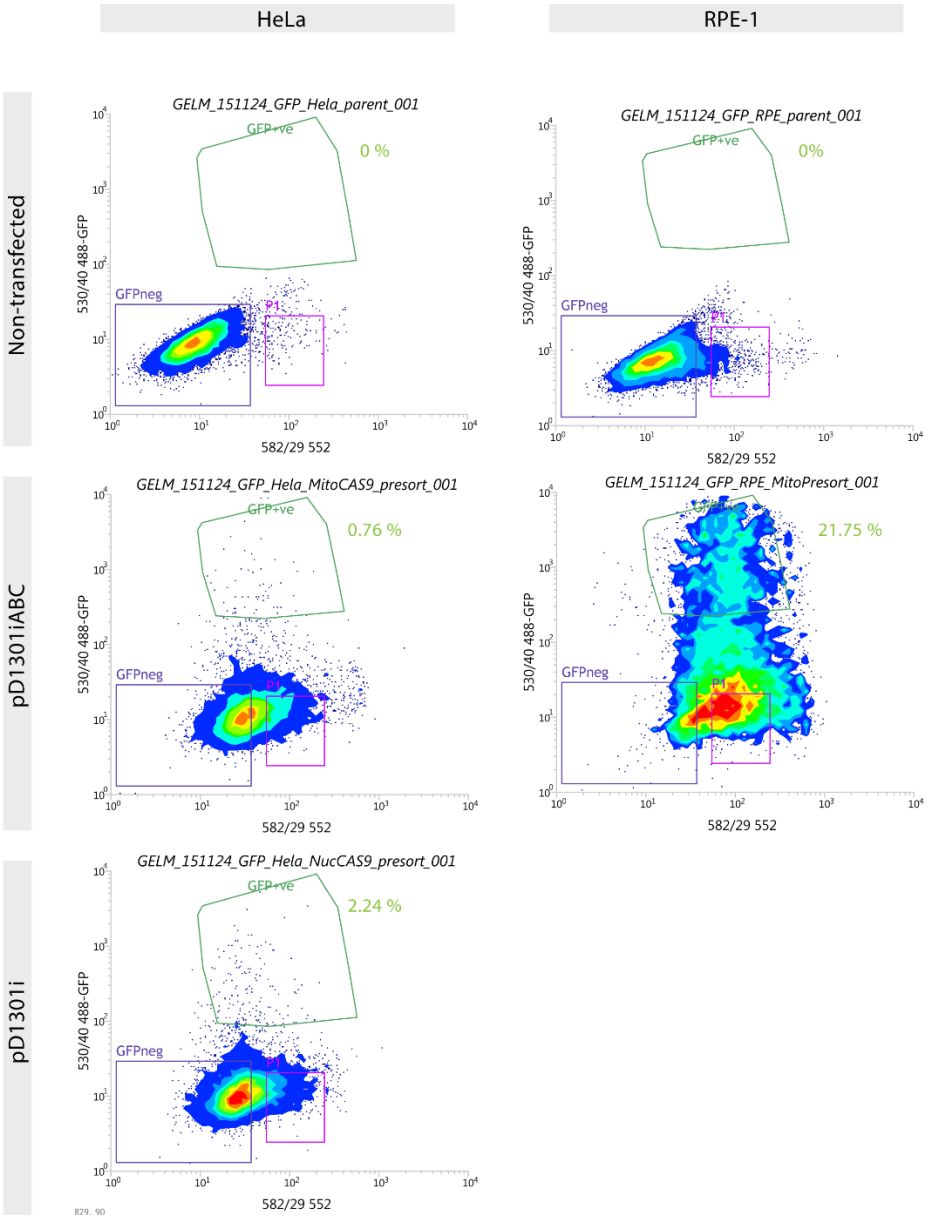

Figure 3-9 FACS of HeLa and RPE-1 cells transfected with pD1301i (NLS-Cas9) and pD1301iABC (MTS-Cas9)
All panels show y-axis: GFP fluorescence ($\lambda_{excitation}$ 488 nm; Filters: 530/40) x-axis: PI incorporation ($\lambda_{excitation}$ 552 nm; Filters: 582/29) Colour scale is representative of number of cells (Blue -> Red) top panels parent, non-transfected HeLa and RPE-1 cells middle panels HeLa and RPE-1 cells transfected with pD1301iABC (MTS-Cas9) bottom left HeLa cells transfected with pD1301i

3.4 Conclusions and further work targeting CRISPR nucleases to mitochondria

Prior to embarking on this project, the mitochondrial targeting of Cas9 was expected to be straightforward, particularly given the wide range of proteins which have been successfully targeted to mitochondria detailed in section 1.3.4. However, using a plasmid DNA approach for cellular expression of nuclear targeted and mitochondrial COX8A-targeted *Spy*Cas9 demonstrated that delivery of Cas9 is instead a critical step. Not only was a very low transfection efficiency seen in mammalian cells transfected with pD1301iABC and pD1301i, (just 0.76 and 2.24% respectively in HeLa cells) but expressing COX8A-Cas9 seems to lead to decreased cell viability as measured by PI uptake, a result which was particularly severe in RPE-1 cells, Figure 3-9. These two conclusions drawn from the FACS data help explain why immunofluorescence and immunoblotting experiments were largely unsuccessful in Figure 3-7 and Figure 3-8.

In early 2017, a BBSRC funded grant was awarded from the Bristol BrisSynBio centre and Dr Zuriñe Anton and Dr Holly Ford joined the MitoCRISPR project as postdoctoral researchers. Whereas the focus of this thesis became the modifications of gRNAs for MitoCRISPR, Zuriñe Anton has continued the work started in this chapter. Using pD1301iABCE, some MTS-Cas9-GFP signal can be seen in mitochondria 19h post-transfection in RPE-1 cells, Figure 3-10A. However, the signal is weak, and some cells still have nuclear and cytosolic GFP signal. NLS-Cas9-GFP (pD1301iE) is mostly localised to the nucleus, but also with some cytosolic signal.

Following longer expression periods (up to 48h), Figure 3-10A, there appeared to be an impact on mitochondrial health following MTS-Cas9-GFP expression, as the GFP signal became more cytosolic, and mitochondrial antibody staining (as seen by anti-TOM20 antibody staining) was noticeably fainter. In contrast, mitochondria in the NLS-Cas9-GFP expressing cells appeared healthier. The impact of MTS-Cas9-GFP expression on mitochondrial health is supported by live imaging of transiently transfected cells stained with Mitotracker Red, Figure 3-10B. In early stages of transfection and in cells expressing low levels of MTS-Cas9-GFP (white dashed line), mitochondrial networks appear healthier than in later stages and in cells expressing high levels of MTS-Cas9-GFP (orange dashed line). This is indicated by mitochondria becoming fragmented and by a potential absence of mitochondrial membrane potential, as indicated by low Mitotracker staining. Together these results confirm the indicated findings in Figure 3-9 that *Spy*Cas9 is likely disruptive to cellular homeostasis.

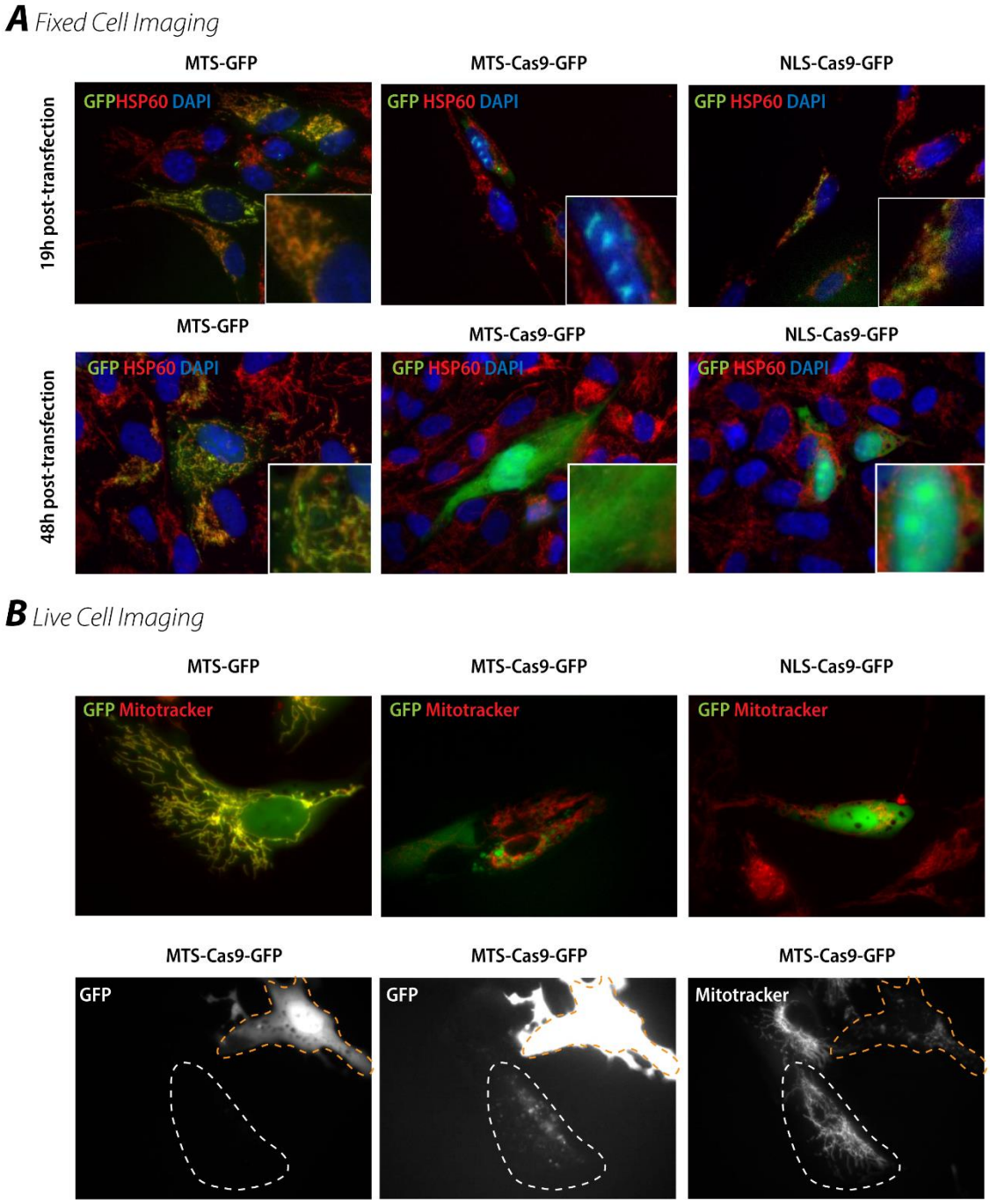

Figure 3-10 A Fixed Cell imaging *RPE-1 cells transfected with pMTS-GFP, pD1301iE (NLS-Cas9-GFP) and pD1301iABCE (MTS-Cas9-GFP). Cells are healthier 19h post-transfection than 48h post-transfection* ***B*** *Live Cell Imaging RPE-1 cells transfected with pMTS-GFP, pD1301iE (NLS-Cas9-GFP) and pD1301iABCE (MTS-Cas9-GFP). Data collected by Zuriñe Anton.*

A range of alternative CRISPR nucleases were cloned for mammalian cell expression, including *Sa*Cas9, *As*Cas12a, and *Lb*Cas12a. In each case, mammalian codon-optimised sequences were used. Additionally, alternative MTSs were tested in addition to COX8a, including Su9 and Atg4D, both introduced in section 1.3.4. The mitochondrial targeting efficiency, as observed with immunoblotting and fluorescence microscopy, was greatest using *Lb*Cas12a transiently transfected in RPE-1 cells. MTS-*Lb*Cas12a-GFP transfected cells

looked much healthier than MTS-Cas9-GFP cells, and all the tested MTSs show mitochondrial localisation by fluorescence microscopy. Su9-*Lb*Cas12a-GFP signal was the most efficient when measured by immunoblotting, while COX8A-*Lb*Cas12a-GFP cells also showed some cytosolic signal, Figure 3-11.

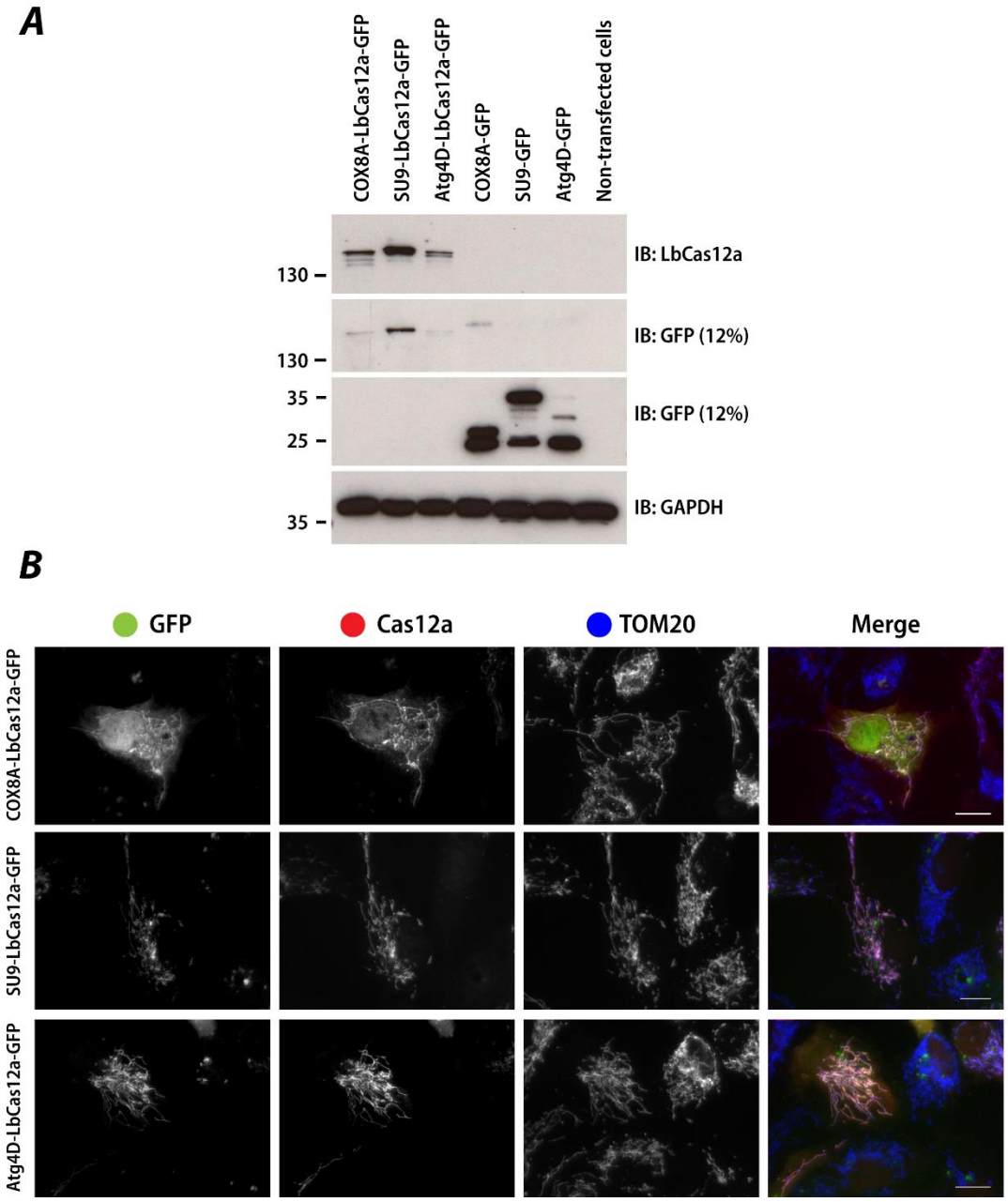

Figure 3-11 Cellular Expression of LbCas12a-GFP top *Immunoblotting and* ***bottom*** *fluorescence microscopy of RPE-1 cells transfected with LbCas12a-GFP, mitochondrially targeted with a range of MTSs, including those from Atg4D, SU9 and COX8A. Scale bars 10 µm. Data collected by Zuriñe Anton.*

There are a number of reasons why *Spy*Cas9 transfection and localisation is much poorer in comparison to *LbCas12a and Sa*Cas9. One could be the reduced size of *Sa*Cas9 (*Sa*Cas9 is 130 kDa/1053 aa, in comparison to *Spy*Cas9 being 160 kDa/1368 aa), however this is unlikely to be the sole factor - *Lb*Cas12a is not so much smaller. The relative charges and

amino acid bias of the proteins are likely to also play a role, as will the availability and identity of N-termini resulting in *Lb*Cas12a variants being trafficked and/or imported into the mitochondria more efficiently. In addition to factors favouring import, some unpublished reports suggest that Cas9 variants naturally have internal NLS-like sequences (Szczelkun, personal communication) which may disfavour mitochondrial import.

4 Modifying *Spy*Cas9 gRNAs for MitoCRISPR

4.1 Functionalising gRNAs for MitoCRISPR

Several groups have successfully equipped the gRNA structure with functional RNA motifs. Modifications of the gRNA in this way can localise accessory functionalities including fluorescence, transcriptional activation and repression to the CRISPR RNP and targeted DNA locus[108,156,179–181]. Although these 'accessorised' gRNAs have been shown to still function broadly, little work has been done to understand the impacts of gRNA modification on CRISPR RNP complex formation and function. In this chapter, a library of modified gRNAs for MitoCRISPR are designed which incorporate RNA motifs into several distinct locations in the gRNA. Single molecule and ensemble biochemical techniques are used to understand the impacts of these modifications on gRNA loading by Cas9, subsequent R-loop formation and endonuclease activity.

There are many distinct functionalities which might be advantageous to equip a MitoCRISPR gRNA with: structures which aid efficient cell uptake and mitochondrial localisation; fluorescence to allow gRNAs to be followed in the intracellular environment. Furthermore, by modulating interactions with mitochondrial proteins of interest one could better understand mitochondrial biology and dynamics or use interactions with mtDNA to understand mitochondrial nucleoid organisation, genetics and the DNA damage response. Of these functionalities, mitochondrial localisation is the most important for establishing MitoCRISPR, and as such the addition and characterisation of mitochondrial targeting structures to the gRNA form the focus of this chapter.

4.2 Designing a library of gRNAs for MitoCRISPR

The RNA structures described in section 1.5.2.2 have already proven therapeutic potential in disease cell lines and could provide a vector for mitochondrial delivery of gRNAs for MitoCRISPR. There have been several papers which add RNA modifications to gRNAs, however there has been no in-depth study of their impact on Cas9 RNP formation, intermolecular domain motions and target DNA cleavage. A library of gRNAs for MitoCRISPR which incorporated some of the mitochondrial targeting elements above was designed and transcribed with a view to firstly interrogate the impact of gRNA structural modifications in different sites, and secondly target them to mitochondria, which is studied in Chapter 6. This chapter firstly describes the design of a gRNA library for MitoCRISPR, and secondly interrogates the impact of bulky modifications to the gRNA structure on: gRNA loading with a FRET-based assay; R-loop formation using a magnetic tweezer set-up; endonuclease activity with a biochemical cleavage assay.

4.2.1 gRNA structure

The structures of *Apo*[182], RNA-bound[183] and RNA/DNA-bound *Spy*Cas9[184] have been solved. The 2.5 Å crystal structure, shown in Figure 4-1A, is of *Spy*Cas9 in complex with the minimised 98 nt single gRNA targeting a 23 nt DNA. A 20 nt spacer sequence at the 5′ end of the gRNA binds the target DNA strand through Watson-Crick base pairing. A second highly folded region of the gRNA is responsible for binding Cas9 through contacts with several regions of self-complementarity: the lower and upper stems, the nexus and hairpin regions, Figure 4-1B. The crystal structure reveals extensive contacts between the negatively-charged gRNA and the positively-charged surfaces of Cas9: Cas9 folds around the RNA/DNA duplex and the lower stem-bulge-upper stem region in two lobes, the recognition (REC) and nuclease (NUC) lobes; much of the hairpin regions of the gRNA contact a positively charged region on the Cas9 outer surface.

Studying Cas9 crystal structure alone does not reveal many likely candidate sites for modification, as much of the gRNA structure is in contact with either target DNA or the inner surfaces of the protein. Indeed, the gRNA forms most of the interactions between the REC and NUC lobes of Cas9 which do not form extensive protein-protein interactions themselves. One exception to this is the upper stem of the gRNA, which has already shown to be tolerant of modification, being truncated relative to the naturally occurring crRNA/tracrRNA duplex[89].

In addition to solving the RNA/DNA-bound *Spy*Cas9 crystal structure[184], Nishimasu *et al* also studied the impact of mutated gRNAs on CRISPR-induced indels. Removing structures with extensive Cas9-contacts, such as the bulge and nexus, completely abolished Cas9 function. Mutations were tolerated in other regions of the gRNA, particularly those which are not directly in contact with Cas9 such as the first of the 3′ hairpin structures. Briner *et al* [185] more extensively characterised the functional modules of the gRNA required for directing specificity. Agreeing that the bulge and nexus are the most important structures for Cas9 binding, this study also highlights the possibility of modifying the 5′ and 3′ termini, upper stem and hairpin 1 of the gRNA structure. Both of these studies are summarised as a theorised ‘heatmap’ of modification tolerance, Figure 4-2D.

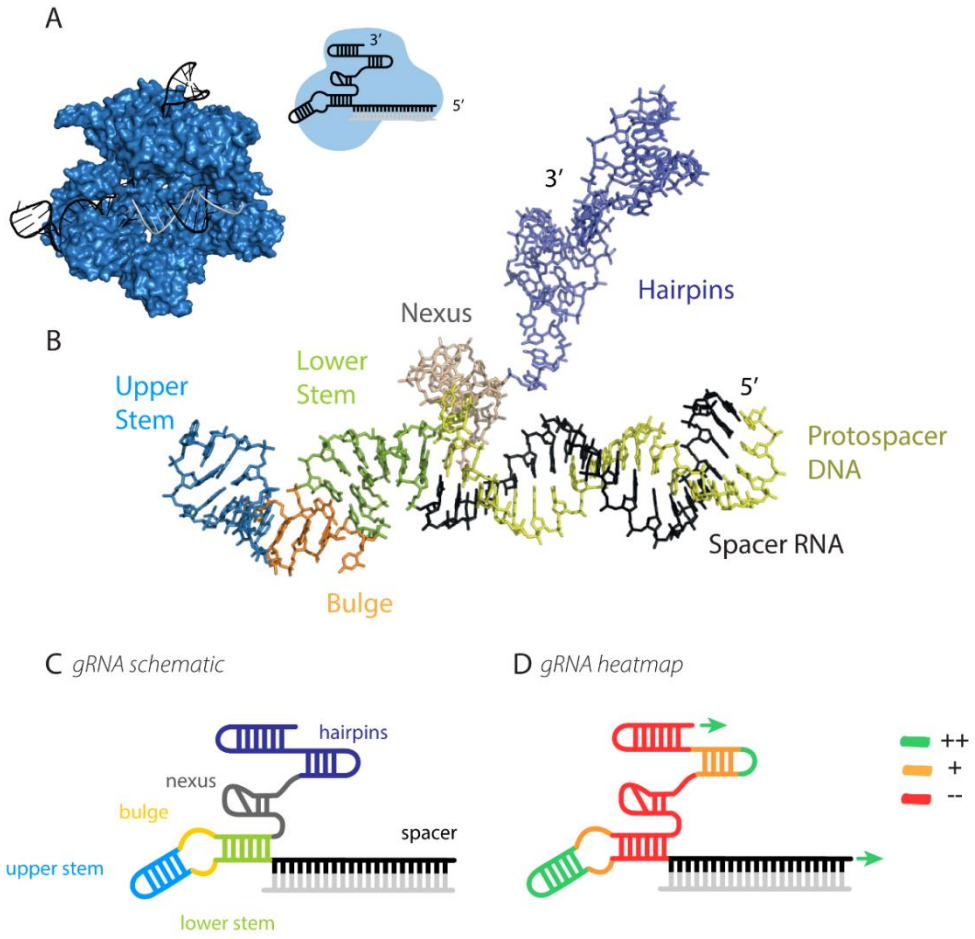

Figure 4-1 SpyCas9 gRNA structure ***A*** *The structure of SpyCas9 (blue) in complex with gRNA (black) and target DNA (grey) and simplified schematic (inset). PDB ID: 4008* [184]*.* ***B*** *gRNA structure from A with structural features labelled: spacer (black); lower stem (green); bulge (orange); upper stem (blue); nexus (beige); hairpins (purple).* ***C*** *gRNA schematic with colouring consistent with B.* ***D*** *gRNA heatmap, based on Briner et al*[185] *shows gRNA regions which tolerate (green), might tolerate (orange) and do not tolerate (red) modification.*

4.2.2 MitoCRISPR gRNA library

Based on the evidence in the previous section, a library of gRNAs was designed which incorporated mitochondrial targeting (RP, MRP, F1D1, tRK1) and fluorescent aptamers (Baby Spinach (BS), Bunch of Baby Spinach (BoBS)) into four locations in the gRNA structure: the 5′ end, 3′ end, upper stem (US) and hairpin 1 (H), Figure 4-2.

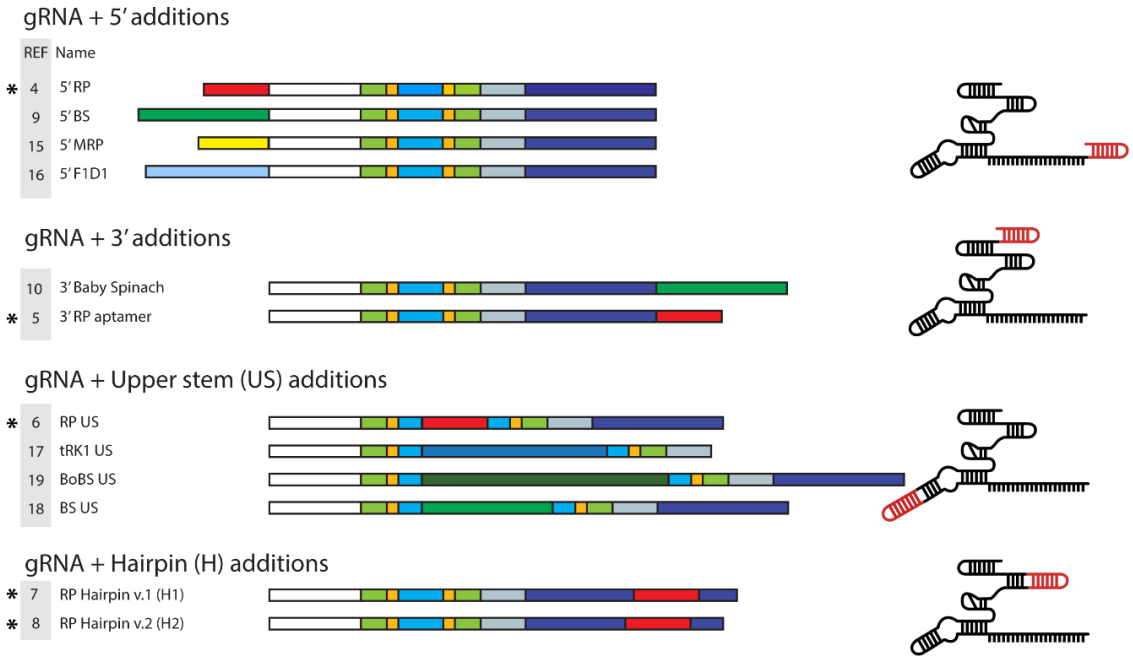

Figure 4-2 gRNA library *schematics of modified gRNA Library with generalised imagined fold, right. See Appendix A4 for complete sequences, colouring is consistent with Figure 4-1.* ******* *denotes the 'minimal' library.*

The RP, MRP, F1D1 aptamers and the full tRK1 structure were incorporated into the gRNA structure for mitochondrial targeting. RP, as the smallest aptamer, was added most extensively, and the RP-incorporating library (i.e. with the RP hairpin at the 5′, 3′, US and H1/H2 - RNAs 4,5,6,7 & 8, as marked with an asterisk (*) in Figure 4-2) is considered the 'minimal' set of gRNAs.

Fluorescent RNA aptamers based on those developed by the Jaffreys' lab[186,187] were also incorporated into the gRNA structure. Baby Spinach (BS) is a 51 nucleotide G-quadruplex containing aptamer which becomes fluorescent when in complex with the small molecule DFHBI-1T. Bunch of Baby Spinaches (BoBS) is a 129 nt aptamer, containing three copies of the Spinach aptamer in tandem resulting in greater fluorescence[181].

4.2.3 MitoCRISPR gRNA library *in vitro* transcription (IVT)

Using the gRNA template sequence from pD1301, modifications were made to introduce the coding sequences for mitochondrial targeting and fluorescent aptamers through inverse PCR and NEBuilder® HiFi assembly. DNA templates, once verified by sequencing, were amplified by PCR with primers to introduce the T7 promoter sequence at the 5′ of the PCR product, Figure 4-3A. This dsDNA product was purified by size exclusion spin-column chromatography, verified by agarose gel electrophoresis (Figure 4-3B), quantified using a spectrophotometer, and used as the substrates for *in vitro* transcription (IVT). RNAs were synthesised by IVT to give the modified gRNA library, Figure 4-2. The IVT products were DNase treated to remove the DNA template, purified by RNA size exclusion spin-column chromatography and verified by spectrophotometer and denaturing urea-PAGE, Figure 4-3C.

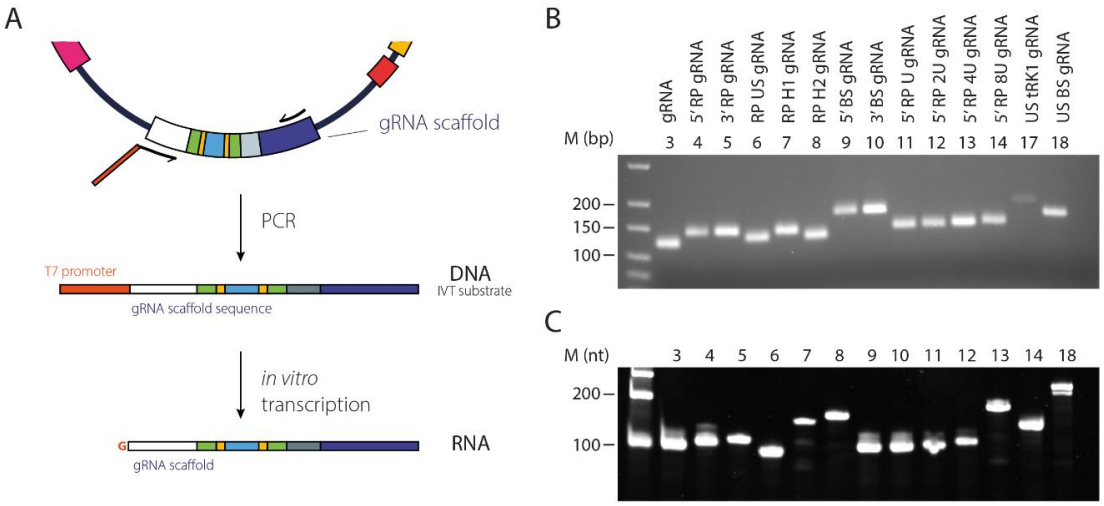

Figure 4-3 gRNA library IVT ***A*** *gRNA sequences are stored in plasmids. gRNAs are transcribed by IVT from templates which are dsDNA PCR products amplified form plasmids with primers which introduce the T7 promoter upstream of the gRNA sequence.* ***B*** *Example PCRs to be used for IVT templates (1.5% (w/v) agarose gel)* ***C*** *Example gRNAs separated on denaturing urea 10% (w/v) PAGE (For B and C, gRNA names and reference numbers are given); M = marker*

4.3 Effect of gRNA modification on Cas9 gRNA loading - $Cas9_{hinge}$ FRET

Cas9 loading of gRNAs was followed using a Förster resonance energy transfer (FRET)-based assay developed by Sternberg et al[91,188]. In FRET, a protein is labelled with two fluorophores with overlapping emission and excitation spectra. The labelled residues are chosen on protein domains which move within 1-10 nm of one-another. For the $Cas9_{hinge}$ mutant used in this assay, REC domain motions are followed as residues in the REC and RuvC domains move relative to one another upon loading of gRNAs. On excitation of the 'donor' fluorophore (here Cy3), the fluorophore's emitted spectra will excite the 'acceptor' fluorophore (here Cy5), if they are close enough to allow non-radiative dipole-dipole coupling (within approximately 10 nm). The extent to which the acceptor fluorophore is excited is a function of the distance between the two fluorophores.

$Cas9_{hinge}$ is a mutant in which the natural cysteines are mutated to serine, and positions E945 and D435 are mutated to cysteine for fluorophore labelling. $Cas9_{hinge}$ was purified and labelled with maleimide-Cy3 and -Cy5 (for protein purification and labelling see Materials and Methods and Appendix A4). In the *Apo* (gRNA unbound) state, the labelled residues are close to one another (21 Å), resulting in a high Cy5 acceptor fluorescence. As a gRNA is loaded into the Cas9 structure, the labelled residues are moved approximately 60 Å apart from one another (83 Å), resulting in a corresponding decrease in acceptor fluorescence relative to donor fluorescence (decrease in Cy5, increase in Cy3), Figure 4-4A. This relative change scales with increasing molar ratio of gRNA to Cas9, Figure 4-4B. The ratio between the Cy5 peak as excited by Cy3 fluorescence relative to direct excitation with 630nm light, $ratio_A$, Figure 4-4C&D, can be used as a proxy readout for energy transfer[188]. In the *Apo* state, where there is high donor-acceptor energy transfer, $ratio_A$ is high. Conversely, when donor-acceptor energy transfer is low, i.e. with a well bound gRNA, $ratio_A$ is low.

Using the $Cas9_{hinge}$ construct, the gRNA library gives similar relative acceptor fluorescence changes, of approximately 0.1, which is comparable to an unmodified gRNA (G, blue), as shown in Figure 4-5. We can therefore conclude that gRNA modifications appear to be well tolerated and do not have a significant impact on the Cas9 structure with respect to REC lobe positioning during gRNA loading.

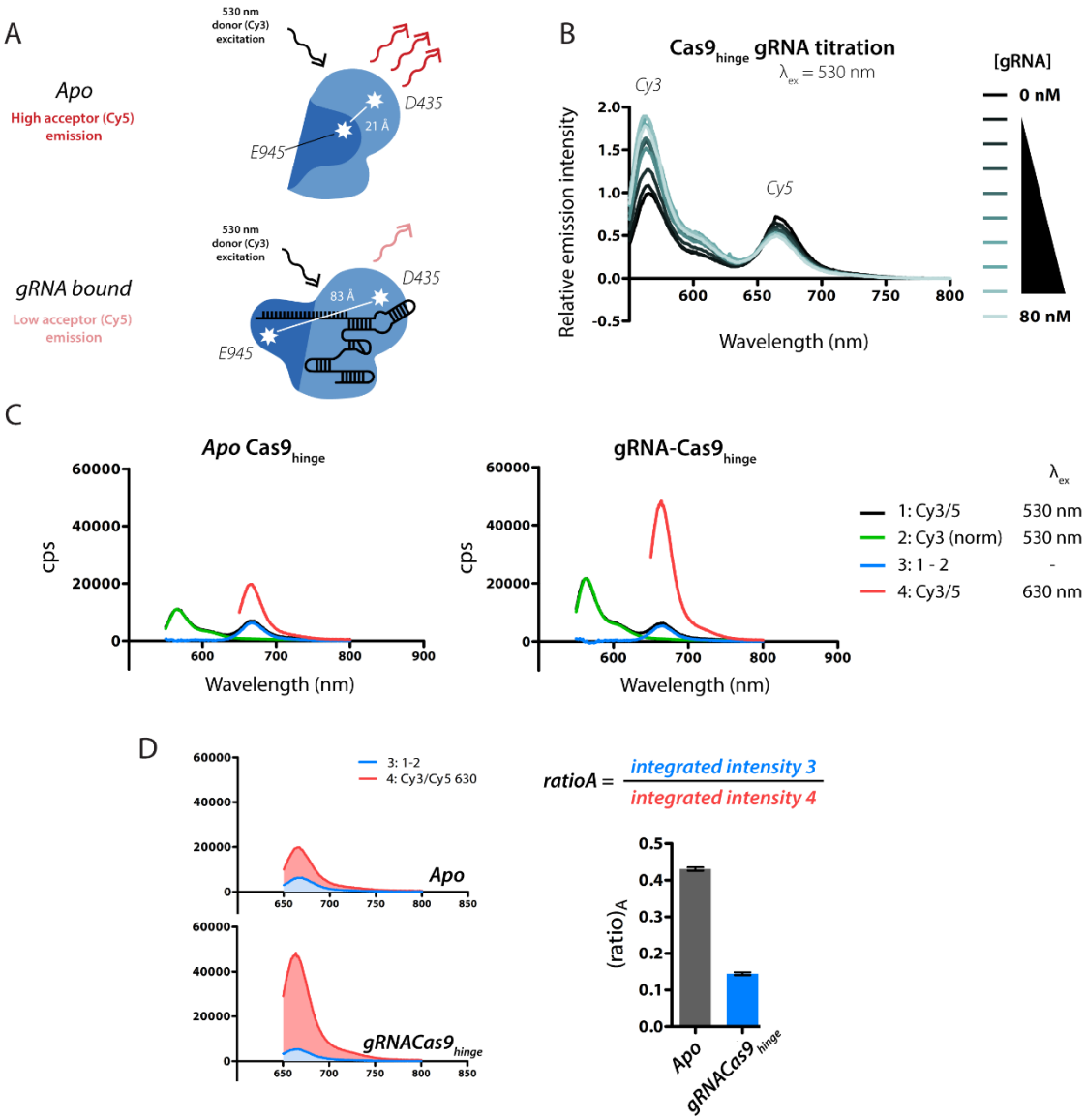

Figure 4-4 Cas9$_{hinge}$ FRET ***A*** *Cas9$_{hinge}$ is labelled with Cy3 and Cy5 at positions 435 and 945. In the Apo state, there is high acceptor fluorescence which decreases upon gRNA binding as fluorophores are moved apart* ***B*** *Donor (Cy3) fluorescence rises and acceptor (Cy5) fluorescence falls with increasing [gRNA] when the donor fluorophore is excited with 530 nm light,* ***C/D*** *Ratio$_A$ can be calculated by dividing the integrated intensity 3 (The difference between Cas9hinge-Cy3/5 and Cas9hinge-Cy3 excited at 530 nm, between 650 and 800 nm) by the integrated intensity 4 (Cas9hinge-Cy3/5 directly excited at 630 nm between 650 and 800 nm) Exmaple traces are shown for Apo and gRNA bound states* ***D*** *Ratio$_A$ for Apo and gRNA bound states from traces in C (N=3 ± SD)*

gRNA	ratio$_A$ ± SD
Apo	0.430 ± 0.008
3' RP	0.138 ± 0.009
RP US	0.132 ± 0.029
RP H1	0.113 ± 0.007
RP H2	0.104 ± 0.012
5' RP	0.154 ± 0.004
5' BS	0.166 ± 0.011
US BS	0.162 ± 0.022

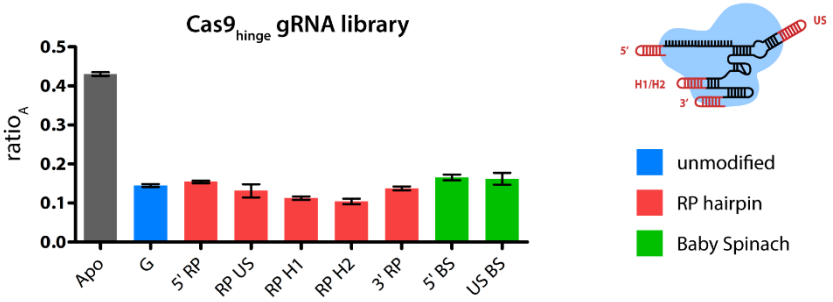

Figure 4-5 Modified gRNAs are loaded normally by Cas9$_{hinge}$ *Comparative ratio$_A$ (N=3 ± SD) for loading library of modified gRNAs. For example traces see Appendix A4-IV.*

4.4 The effect of gRNA modification on R-loop formation

Following gRNA loading, the Cas9 RNP searches the DNA for PAM sequences, binds, and forms a DNA/RNA hybrid (R-loop) at the target sequence by opening up the DNA double helix. One way to follow R-loop formation is with a magnetic tweezers-based assay, as previously described by this lab[92]. In the magnetic tweezers set-up, a linear DNA strand is tethered between a surface and a magnetic bead, Figure 4-6.

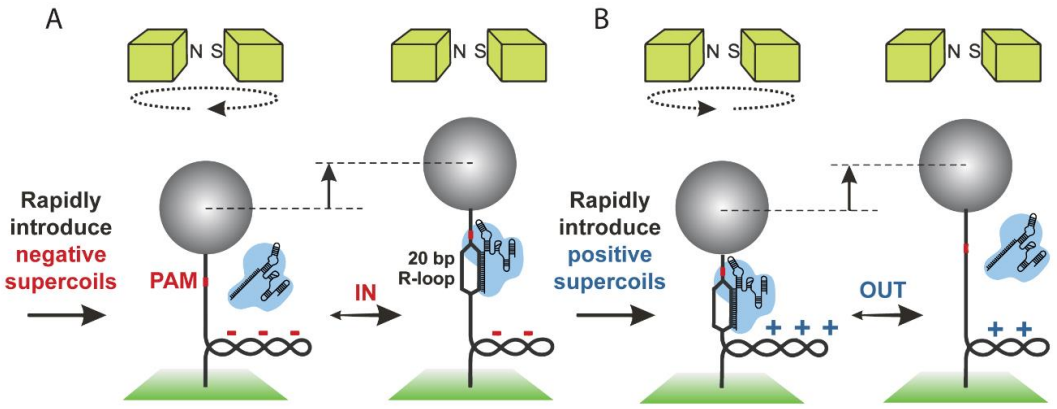

Figure 4-6 Magnetic Tweezers set-up

A magnet holds the bead so that it can be rotated, introducing DNA supercoiling. Proteins interacting with the tethered DNA can also result in changes to DNA supercoiling, which is translated to changes in the observed bead height. Bead height is followed by diffraction rings observed using video-microscopy, from which we can infer the z-height. The following experiments were carried out by Mark Szczelkun.

The assay is started as Cas9/gRNA complex is flowed into the flow cell where the tethered DNA is held negatively supercoiled at constant force (0.312 pN). The DNA is underwound, and this encourages R-loop formation. As the R-loop is formed, the opening bubble is translated into a decrease in negative supercoiling and observed as a raise in magnetic bead height, Figure 4-6A. Cas9 does not 'turnover', and so R-loops will not spontaneously fall off. To encourage complex dissociation, the supercoiling is reversed (but with the force kept constant) so that the DNA is now overwound. As the R-loop dissociates, the positive supercoiling decreases and there is a corresponding raise in bead height, Figure 4-6B.

Figure 4-7 shows magnetic tweezer traces for gRNAs with the RP hairpin in the 5′, 3′, upper stem and hairpin positions. The black line (right axis) displays the number of magnet rotations. At -6 rotations, DNA is negatively supercoiled and encourages R-loop formation, denoted by an increase in bead height (red arrows). Following R-loop formation, the magnet rotations are reversed to +4, positively supercoiling the DNA and encouraging R-loop dissociation (raise in bead height, blue arrows).

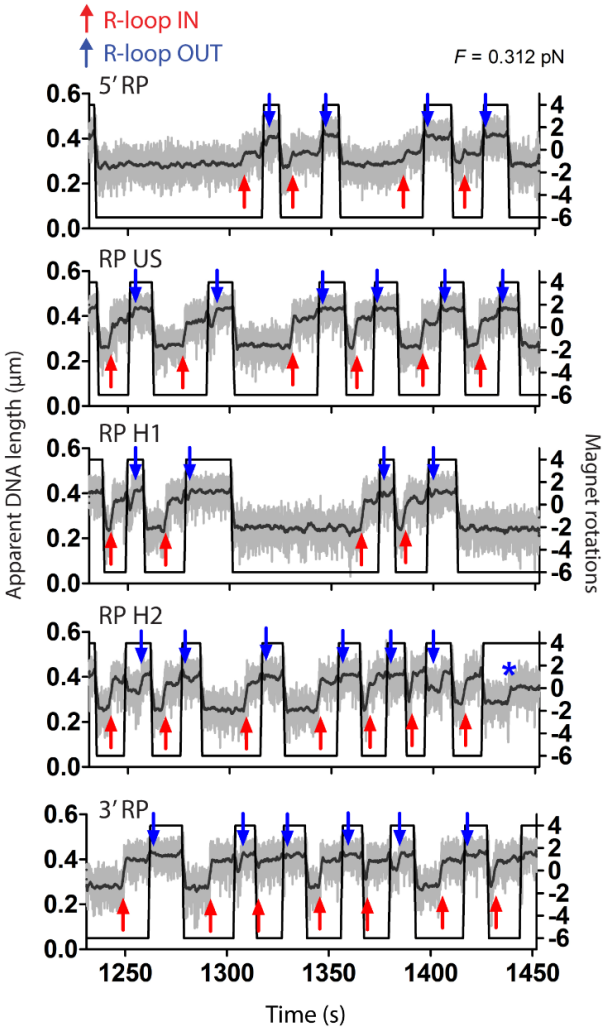

Figure 4-7 Magnetic Tweezers example data for modified gRNAs. *Grey = raw position data at 60 Hz, the black line = 1 s median filter. Arrows represent in (red) or out (blue) events. The Asterix (RP H2) denotes formation of a smaller R-loop; data collected by Mark Szczelkun.*

Following R-loop formation and dissociation in this way allows several distinct observations to be made including rate of R-loop formation and dissociation. The relative changes in bead height can also be correlated to the relative size of R-loop. Each of the modified gRNAs (minimal library) were observed in the magnetic tweezers assay to assess R-loop size and rates of association and dissociation. gRNAs with modifications at the 3′ end, upper stem, and hairpins are well tolerated, and form R-loops of comparative size to the unmodified gRNA, approximately the length of the spacer/protospacer RNA/DNA duplex, Figure 4-8. In contrast, a 20 nt hairpin addition to the 5′ end is not well tolerated, forming only a partial R-loop on target DNA of less than 10 nt, not surpassing the seed region. It might be hypothesised that this partial R-loop is formed due to the bulky 20 nt structure impeding RNA threading through the two strands of the DNA double helix. This would predict that the 5′ hairpin will have a significant impact on the rate of DNA cleavage.

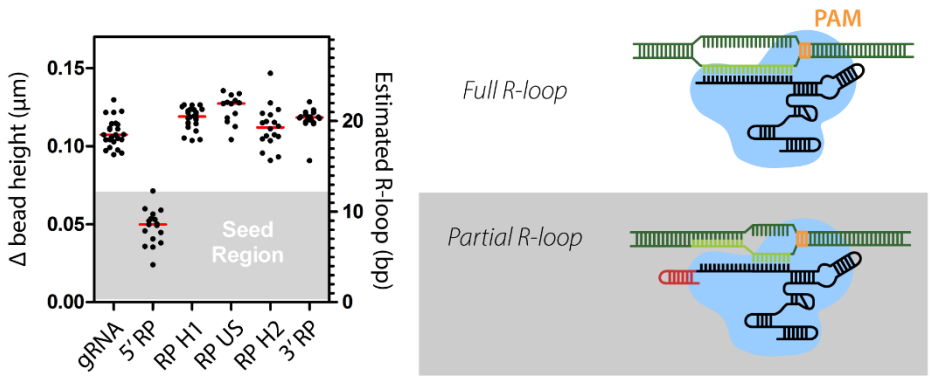

Figure 4-8 5′ modified gRNAs form partial R-loops ***left*** *R-loop size (relative changes in bead height) for modified gRNAs; data collected by Mark Szczelkun* ***right*** *partial R-loop schematic*

4.5 Effect of gRNA modifications on Cas9 activity - library cleavage data

To investigate further the impact of gRNA modifications, *in vitro* cleavage assays were performed on a supercoiled plasmid substrate to assess relative endonuclease activity. The substrate (pSP1) is a 2,726bp supercoiled tritium-labelled plasmid which contains a naturally-occurring protospacer sequence, derived from the first spacer (SP1) of the *S.thermophilus* CRISPR 3 array. Relative cleavage by modified gRNAs can be assessed by quantifying supercoiled, linear and open circle DNA by scintillation counting, Figure 4-9. A negative control plasmid (pUC19, 2686bp supercoiled) is not cleaved. Cleavage assay data for gRNAs with RP hairpins in each of the modified sites (except the 5′ end) are shown in Figure 4-10.

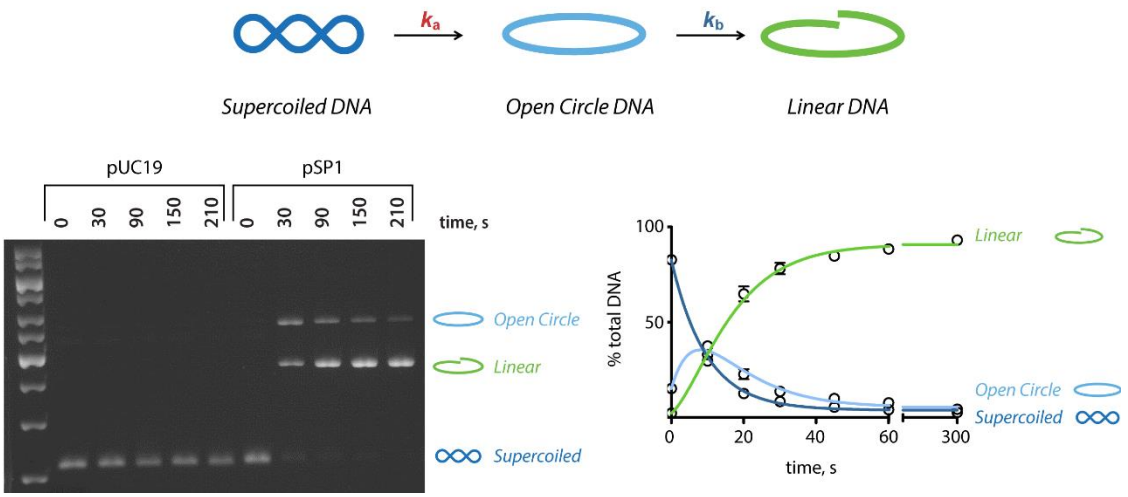

Figure 4-9 Supercoiled plasmid cleavage assay ***top*** *The first strand of supercoiled DNA is cleaved to give an open circle (nicked) DNA plasmid, followed by second strand cleavage resulting in linear DNA. These three forms of DNA can be separated by agarose gel electrophoresis (bottom left). Tritiated-DNA bands are cut out from agarose gel and quantified by scintillation counting (bottom right).*

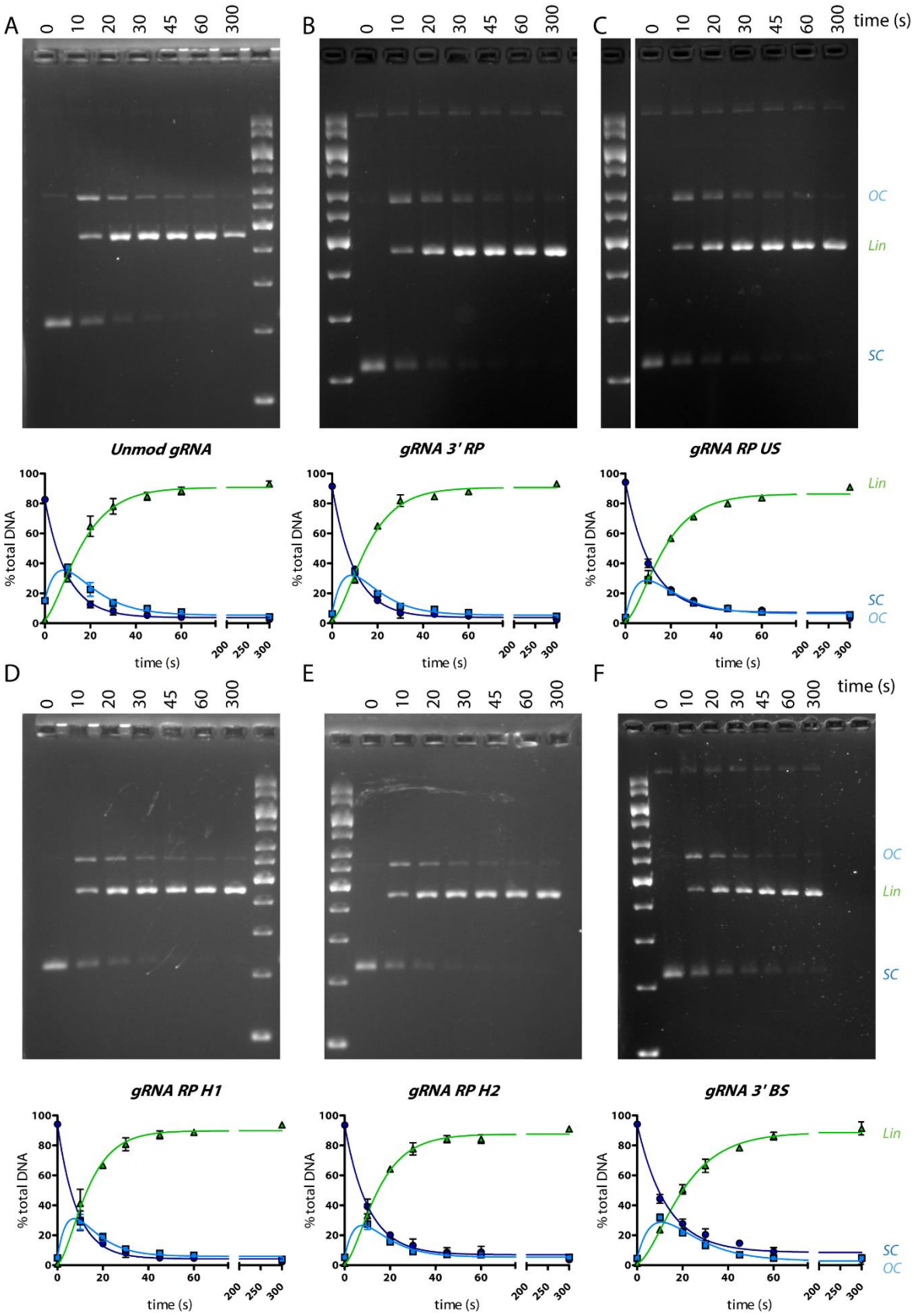

Figure 4-10 Scintillation data and example agarose gels from pSP1 cleavage assays. ***A*** *Unmodified gRNA* ***B*** *gRNA 3′ RP* ***C*** *gRNA with upper stem (US) RP* ***D*** *gRNA with RP in hairpin v1 (H1)* ***E*** *gRNA with RP in hairpin v2 (H2)* ***F*** *gRNA with 3′ Baby Spinach (BS)*

Following the time-dependent changes in DNA concentration in Berkeley Madonna enables simultaneous calculation of the rates of first and second strand cleavage (section 2.8.4), which can be compared for the library of modified gRNAs, Figure 4-11. As might be expected from the R-loop formation data, modified gRNAs which form full-length R-loops (namely 3′, upper stem and hairpin additions) cleave the first and second strands of supercoiled DNA at rates comparative to an unmodified gRNA. There are slight variations in k_a, the rate of first strand cleavage which are within experimental error. There seems to be more systematic yet minor increase in k_b, the rate of second strand cleavage, with upper stem and hairpin modifications. It might be hypothesised that this is due to the extra structure holding the Cas9/gRNA complex together more stably (the upper stem additions mimic the naturally occurring longer upper stem of the cr:tracrRNA) but more work on Cas9/gRNA complex formation would be needed to substantiate this.

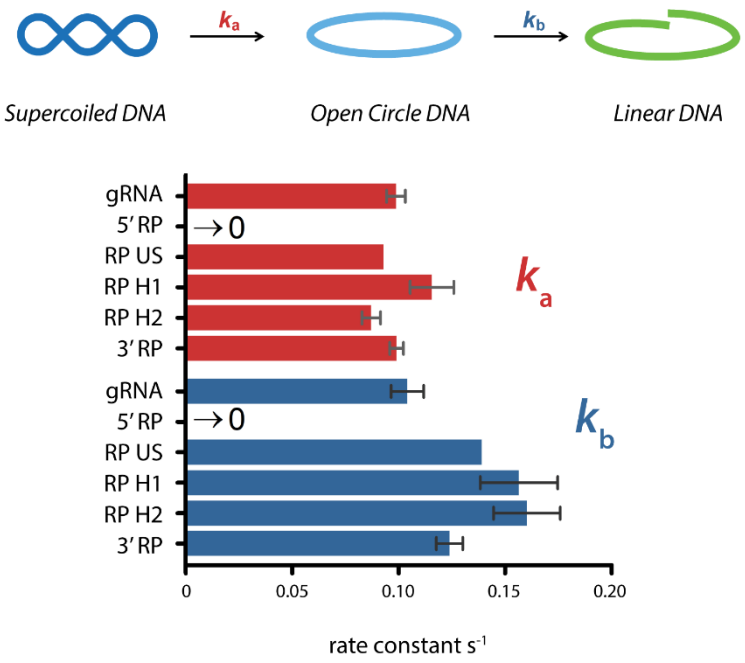

Figure 4-11 pSP1 cleavage assays with modified gRNAs *k_a, red is the rate of first strand cleavage, or appearance of open circle DNA; k_b is the rate of second strand cleavage, or appearance of linear DNA from open circle DNA; table of data including rates for k_{ini} in Appendix A4*

In agreement with the magnetic tweezers data, the partial R-loop formed by 5′ additions almost completely prevent RNP endonuclease activity, with k_a and k_b below measurable rates. Indeed, even after 16 hours there is minimal cleavage with these gRNAs, Figure 4-12.

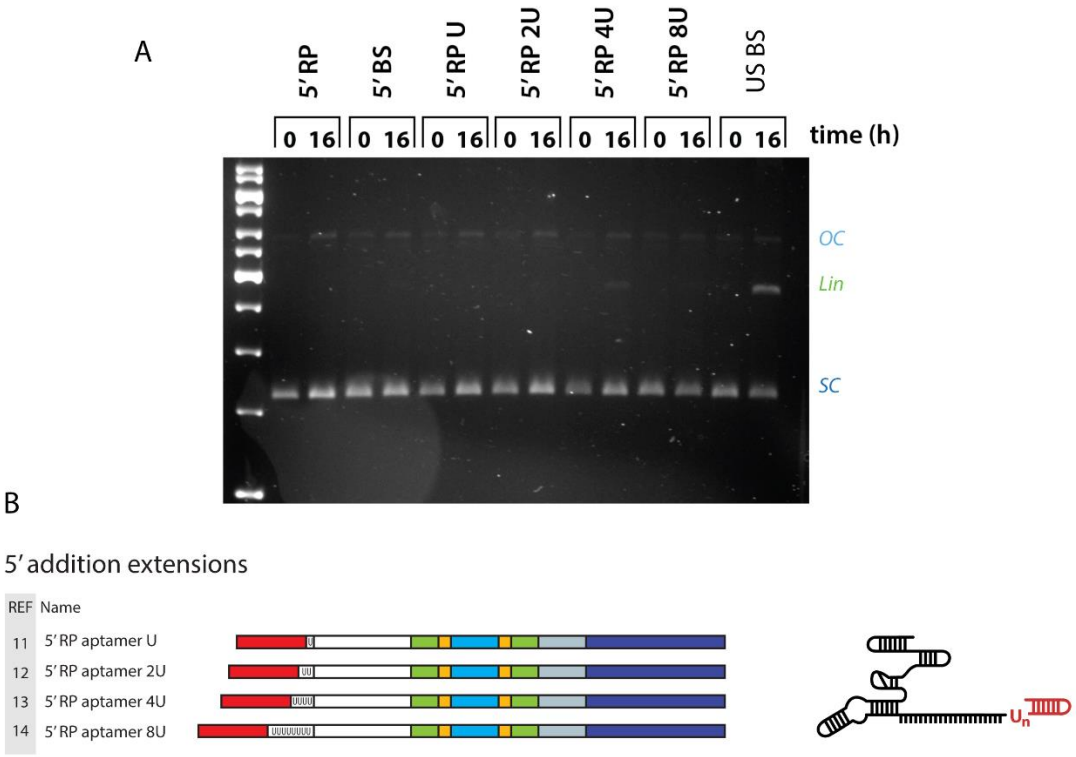

Figure 4-12 5′ Additions severely hinder Cas9 endonuclease activity A *16 hour cleavage assays with 5′ modified gRNAs show minimal cleavage of pSP1* ***B*** *gRNAs with additional uracils between RP and the gRNA spacer have minimal impact on cleavage activity*

After observing the minimal cleavage with the RP hairpin on the gRNA 5′ terminus, we wondered whether moving the RP modification away from the gRNA spacer would ameliorate cleavage. To this end, a set of gRNAs were designed with a variable number of uracil nucleotides (1, 2, 4 or 8) between the RP hairpin and the spacer, Figure 4-12B. Although there was a small increase in cleavage, gRNAs with 8U and 4U have a slightly higher percentage Linear DNA, this is largely negligible. Another gRNA with minimal observed cleavage was with gRNA USBS, with the fluorescent Baby Spinach sequence in the upper stem, Figure 4-12A. This is intriguing given the US BS gRNA appeared to be loaded normally by $Cas9_{hinge}$, Figure 4-5, and smaller modifications to the upper stem (RP US gRNA) had no significant impact on Cas9 endonuclease activity, Figure 4-11.

4.6 Effect of gRNA modification on HNH domain movement - $Cas9_{HNH}$ FRET

Crystal structures of Cas9 show the HNH cleavage domain to be positioned at least 30 Å away from the cleavage site[184], randomly sampling closer cleavage-competent states. In this way, the conformational state of the HNH nuclease domain controls the cleavage activity of the RNA/DNA/Cas9 RNP. In the same study as detailed in section 4.3, Sternberg et al designed a FRET construct to follow HNH endonuclease domain motion. $dCas9_{HNH}$ is a mutant

in which the natural cysteines are mutated to serine, and positions S355 and S867 are mutated to cysteine to be labelled with Cy3 and Cy5. The nuclease null dCas9 mutant is used to follow HNH domain motion to sample a cleavage competent state without resulting in DSB formation, Figure 4-13.

In the *Apo* state, Cy3 and Cy5 are held apart (59 Å), resulting in low acceptor fluorescence. When the HNH domain of a $dCas9_{HNH}$/RNA/DNA complex moves into a cleavage competent state, the Cy3 and Cy5 fluorophores are moved close together (21 Å), resulting in high acceptor fluorescence, Figure 4-13A. As with $Cas9_{hinge}$, the complete traces when excited at 530 nm (Cy3) can be observed, or alternatively the $ratio_A$ can be determined as a proxy for FRET.

Given that the decreased cleavage activity with 5′ modified gRNAs is mostly likely due to the reduced R-loop size observed by magnetic tweezers, one would expect that this would correlate to a decreased sampling of cleavage active conformations, as shown with $dCas9_{HNH}$.

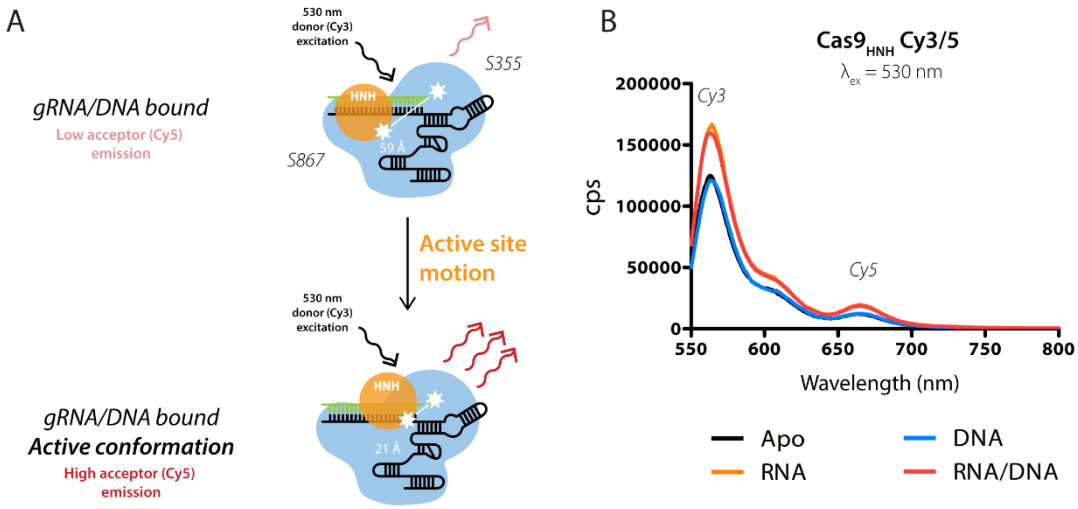

Figure 4-13 $Cas9_{HNH}$ FRET *A $dCas9_{HNH}$ samples active conformations where the fluorophore-labelled HNH domain is brought into close proximity with the REC lobe. B under our experimental conditions, we do not see an increase in acceptor fluorescence (Cy5) when DNA and RNA are present.*

Unfortunately, although $dCas9_{HNH}$ was expressed and purified twice, there was not an observed change in donor fluorescence on binding target DNA, a 55 bp dsDNA fragment, Figure 4-13B. Although a change in fluorescence is seen between the *Apo* state (black trace) and the gRNA bound state (orange trace), there is no change when DNA is also introduced into the cuvette (red trace). This implies that the HNH domain is not sampling cleavage competent states under our experimental conditions, although this is something which we

know to be true as we do see endonuclease activity in the plasmid cleavage assay with these gRNAs.

4.7 Conclusions

Chapter 4 showed that it is possible to design and *in vitro* transcribe a library of gRNAs with modifications at five distinct sites – namely the 5′ and 3′ ends, the upper stem (US) and two locations in the hairpins (H1, H2). gRNAs with modifications at all of these sites are loaded normally by Cas9, as shown by a FRET-based assay with $Cas9_{hinge}$. gRNAs with modifications at the 3′ end, upper stem and hairpins will form R-loops and cleave a supercoiled plasmid substrate with comparative rate to an unmodified gRNA. One gRNA with upper stem modification, US BS, displayed decreased endonuclease activity. This is surprising given the US RP gRNA displays endonuclease activity similar to the unmodified gRNA. A possible explanation for this is that the US BS gRNA does not fold correctly, however this gRNA was established to be loaded functionally by $Cas9_{hinge}$.

gRNAs with 5′ modifications only form partial R-loops which significantly hinders their endonuclease activity; 5′ RP gRNAs have cleavage rates approaching 0 s^{-1}. During DNA target binding, Cas9 first recognises the PAM, and searches nearby DNA for sequences complimentary to the gRNA[91]. At a correct target, a growing R-loop forms, requiring DNA unwinding and gRNA threading around the DNA helix to form the growing RNA/DNA heteroduplex. The bulky 5′ modification most likely impacts R-loop formation by hindering this gRNA threading through the separated DNA strands.

Although gRNAs with 5′ modifications do not result in cleavage competent complexes, the tweezers assay demonstrates that they do still bind DNA. Section 1.4.5 detailed the many uses for nuclease-null dCas9 mutants, raising the potential of using this slower rate as a feature rather than a disadvantage. For example, switching available gRNA from unmodified to one with a 5′ addition could switch a stably expressed Cas9 into a dCas9.

5 The generality of the effect of 5′ modifications

5.1 The effect of 5′ Gs on Cas9 gRNAs

Experiments in chapter 4 showed that *Spy* gRNAs do not tolerate modifications at the 5′ end, where they have a severe impact on R-loop formation and endonuclease activity. This chapter continues to question the generality of this effect, in particular: what is the impact of smaller modifications at the 5′ end of the gRNA? (which is addressed in section 5.1); and do our conclusions about *Spy*Cas9 gRNAs hold true for *Lb*Cas12a crRNAs? (section 5.2).

5.1.1 T7 polymerase requires a G in the (+1) position

T7 bacteriophage RNA polymerase is commonly used in the laboratory for *in vitro* transcription of RNAs, giving high yields of high-fidelity RNA. The T7 promoter has been minimised for *in vitro* use; whereas naturally occurring initiation sequences have up to 3 guanines in the +1, 2 and 3 positions, the minimal requirement for initiation is one guanine in the +1 position[189] which results in a guanine in the 5′ position on transcribed RNA. T7 polymerase has been used throughout this thesis for gRNA IVT. Given that the target DNA in pSP1 does not have a cytosine at the 3′ (PAM distal) end, all of the gRNAs in this thesis have therefore had a single nucleotide mismatch in this position, leading to an overhang of one guanine nucleotide, similar to the illustration in Figure 5-1, bottom right.

We suspect there will be research groups transcribing gRNAs with up to 3 guanine nucleotides on the 5′ end, this being the maximum number that might be introduced by IVT using T7. Equally, common eukaryotic promoters also have initiation requirements; gRNAs expressed in mammalian cells under the U6 promoter require a G or A in the (+1) position for high expression. Consequently, we suspect 5′ mismatched nucleotides are a common occurrence on gRNAs.

Given our observations regarding 5′ modifications in Chapter 4, we sought to investigate the impact of one, two and three 5′ guanine overhangs on gRNA loading, R-loop formation and endonuclease activity.

5.1.2 gRNAs with 5′ guanines

DNA templates were designed which introduced extra guanines at the +2 and +3 T7 promoter positions, 5′ of the 20 nt spacer, Figure 5-1, and gRNAs were *in vitro* transcribed to introduce 1, 2 or 3 guanines at the 5′ end.

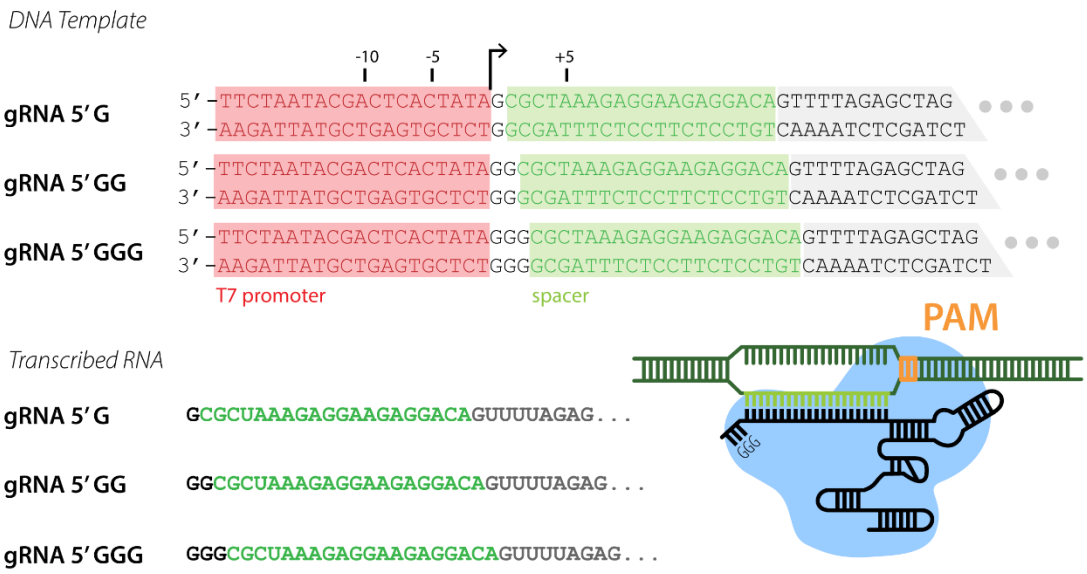

Figure 5-1 GGG gRNAs *The template for gRNA 5′GGG IVT is a dsDNA PCR product containing the minimised T7 promoter (red) and the gRNA spacer (green) and scaffold sequence (grey). IVT begins at the +1 position with a G. In this case, Gs have also been included in the +2 and +3 positions to result in a one, two and three-nucleotide overhang.*

5.1.3 gRNAs with 5′ guanines are loaded normally by Cas9

As in section 4.3, $Cas9_{hinge}$ was used to follow gRNA loading by Cas9, here assessing the impact of 5′ guanine nucleotide overhangs. Based on previous observations that modifications to the gRNA 5′, including the 51 nt BS, are loaded normally by $Cas9_{hinge}$ (Figure 4-5) we would not expect a loading effect. In line with this, Figure 5-2 shows that there is no significant impact between one to three 5′ guanines on gRNA loading by $Cas9_{hinge}$.

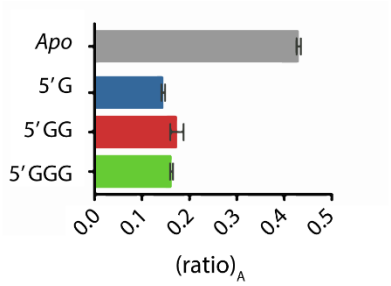

Figure 5-2 Impact of 5′ guanines on gRNA loading by $Cas9_{hinge}$ *Comparative $ratio_A$ (N = 3 ± SD) for loading 5′ G (blue)/GG(red)/GGG(green) gRNAs relative to Apo Cas9 (grey).*

5.1.4 5′ guanines impact R-loop dissociation

To test the effect of the 5′ modifications on the next step in the process, R-loop formation, the magnetic tweezers assay detailed in section 4.4 was employed. Figure 5-3A shows characteristic bead traces for each of the gRNAs. Using the bead height as a representation of the R-loop formation, there was no significant difference in the size of R-loop formed with gRNAs with one to three 5′ guanines.

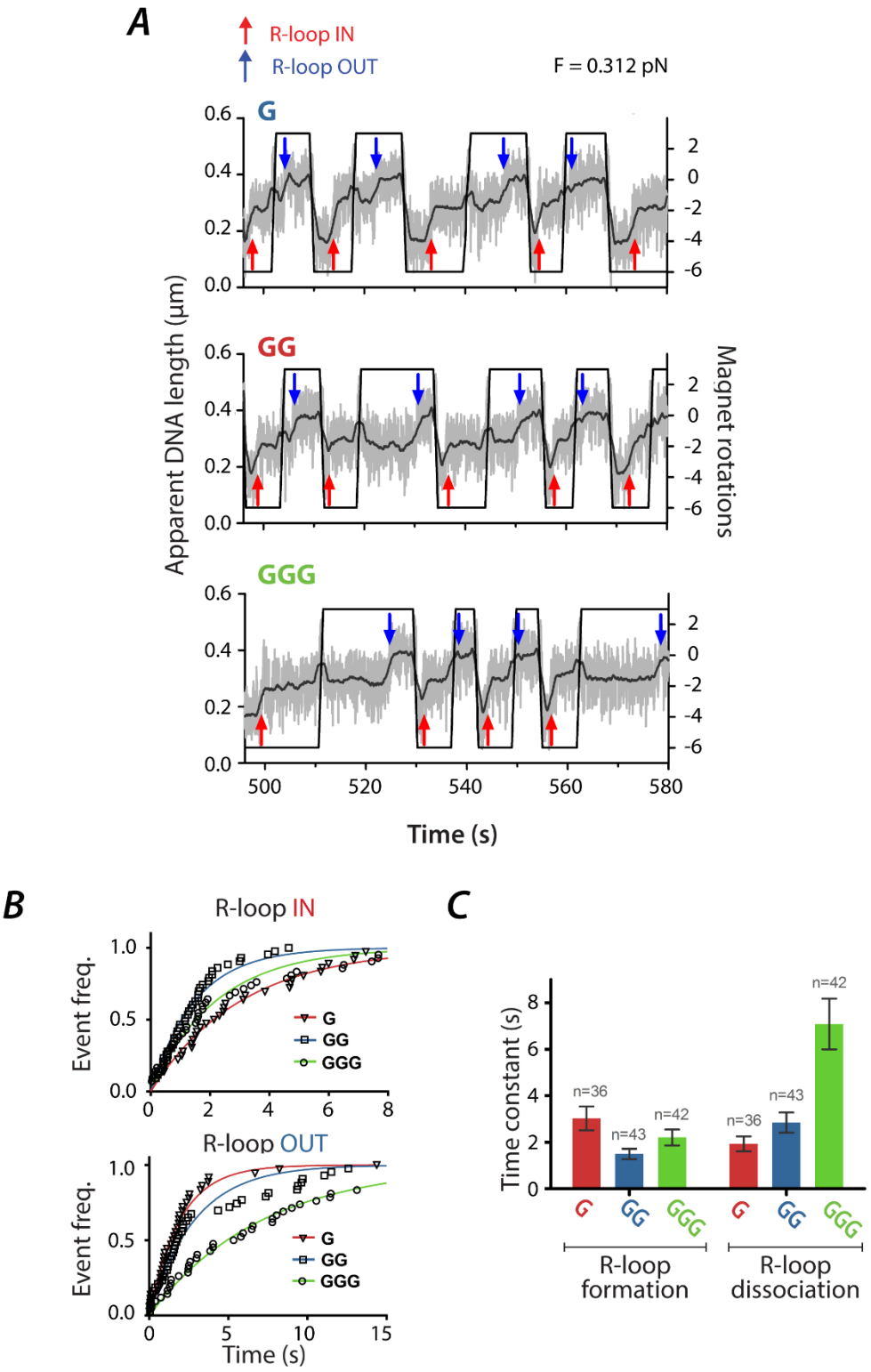

Figure 5-3 Impact of 5′ guanines on R-loop formation and dissociation *A G/GG/GGG gRNAs typical traces in magnetic tweezers - measurements carried out by Mark Szczelkun. Grey is the raw position data at 60 Hz, the black line a 1 s median filter. Arrows represent in (red) or out (blue) events.* ***B*** *Cumulative frequency plots of R-loop formation (IN)/dissociation (OUT) events, fitted to an exponential distribution, allowing calculation of the time constant, plotted in* ***C****. Error bars were calculated from the average values divided by the square root of the number of points (n values) in the bin.*

Figure 5-3B shows cumulative frequency event lifetime plots for in and out events, measured as the time between the stop of each magnet rotation and the midpoint of the subsequent

R-loop formation or dissociation event. The events are fitted to an exponential distribution to calculate the time constant, plotted in Figure 5-3C. The association kinetics reveal complex formation rate to be independent of the number of 5′ guanines on the gRNAs. However, gRNAs with three 5′ guanines (GGG) have a larger time constant for R-loop dissociation in comparison to one or two guanines, implying that the R-loop formed by a gRNA with three 5′ guanines is approximately 2-fold longer-lived than that with one or two.

5.1.5 5′ guanines have a stepwise effect on endonuclease activity

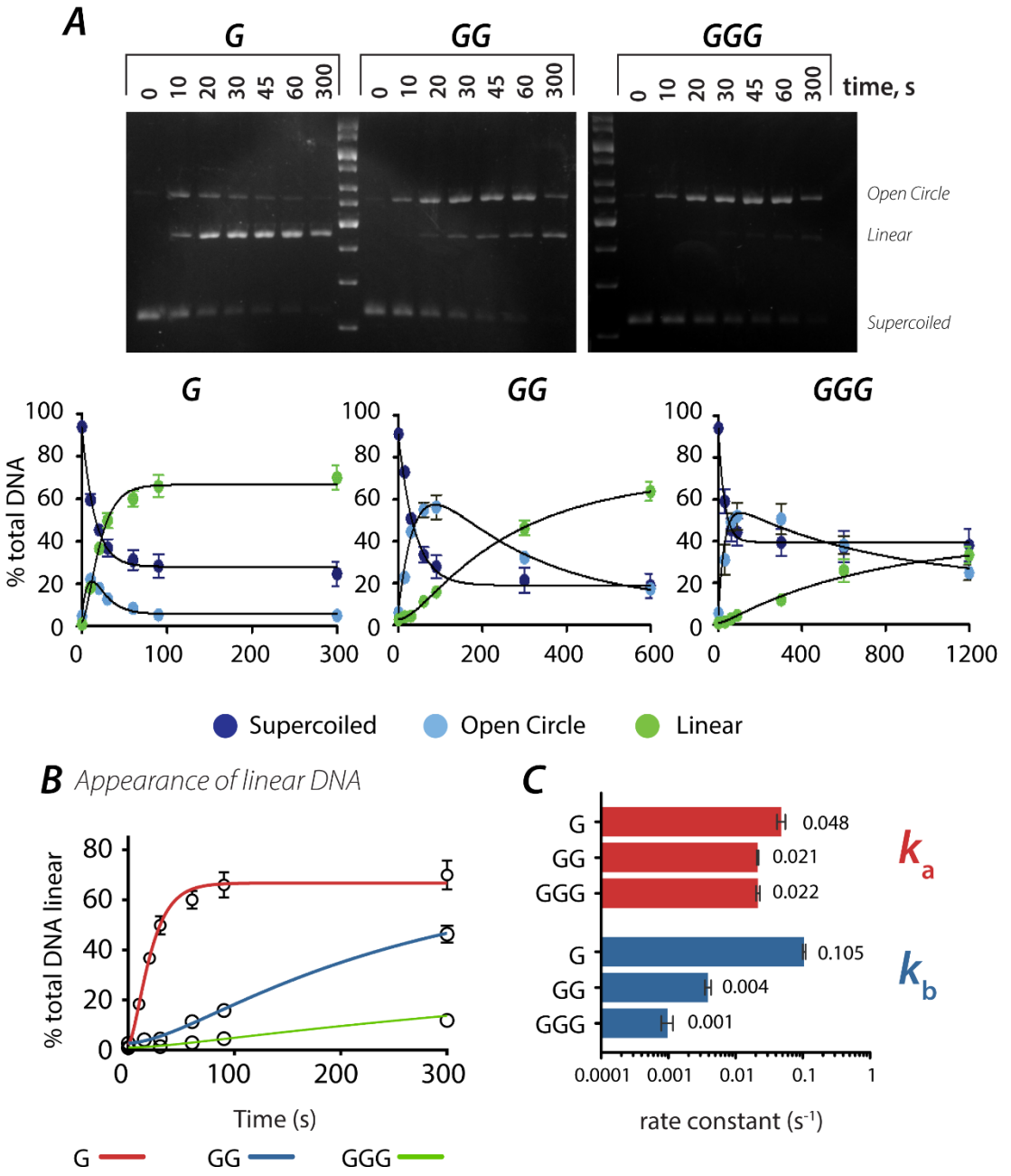

Figure 5-4 5′ guanines impact Cas9 second strand endonuclease activity A *Example pSP1 cleavage assay gels and corresponding Berkeley Madonna fitted data for each gRNA n=3 ± SE* ***B*** *Appearance of linear DNA from A n=3 ± SE* ***C*** *rates of first (k_a) and second (k_b) strand cleavage*

The same supercoiled plasmid cleavage assay as in 4.5 was used to assess *in vitro* Cas9 endonuclease activity with the three gRNAs, Figure 5-4. Figure 5-4A shows that increasing the number of overhanging guanines results in a stepwise decrease in RNP endonuclease activity. This effect is visible on the agarose gels themselves but is most clearly demonstrated by the appearance of linear DNA, Figure 5-4B; gRNAs with two and three guanines show a much lower percentage linear DNA at the same timepoints in comparison to gRNAs with one 5′ guanine. Fitting the data in Berkeley Madonna allows calculation of the rates of first (k_a) and second (k_b) strand cleavage Figure 5-4C. k_a is seen to be relatively consistent with all three gRNAs, whereas k_b shows an almost 10-fold decrease in rate with each addition of a guanine residue.

5.1.5.1 The IVT protocol does not impact gRNA endonuclease activity

The library of gRNAs used in Chapter 4 were synthesised by HiScribe™ T7 High Yield RNA synthesis whereas the G/GG/GGG gRNAs in Chapter 5.1 were generated by EnGen® sgRNA Synthesis, a one-tube method for gRNA transcription. The HiScribe™ IVT protocol requires an overnight incubation at 37°C with a dsDNA template, whereas the EnGen® method requires only a 30-minute reaction, where the user provides a ssDNA oligo with the T7 promoter, spacer sequence and an overlap region, Figure 5-5. Given the significant impact of 5′ Gs on endonuclease activity, we tested whether changes to the synthesis and processing of gRNAs also had an impact on RNP endonuclease activity.

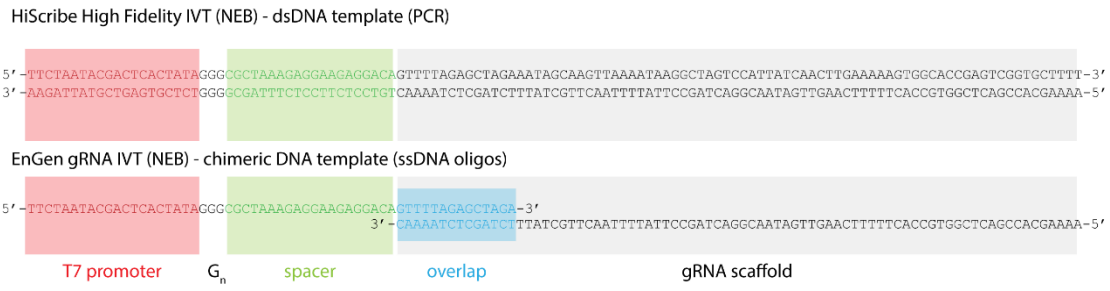

Figure 5-5 IVT templates *For HiScribe (top), the dsDNA PCR template is user provided whereas for EnGen (bottom) the ssDNA oligo encoding the T7 and spacer sequence is user provided whereas the scaffold primer is supplied by the IVT kit.*

The impact of 5′ guanines on EnGen gRNAs in a supercoiled plasmid cleavage assay, Figure 5-6, can be compared to analogous data with HiScribe gRNAs, Figure 5-4. The overall trend, i.e. the stepwise decrease in endonuclease activity, Figure 5-6A & B, is analogous to Figure 5-4 above. Figure 5-6C shows the rates of first and second strand cleavage k_a and k_b respectively, to be very similar.

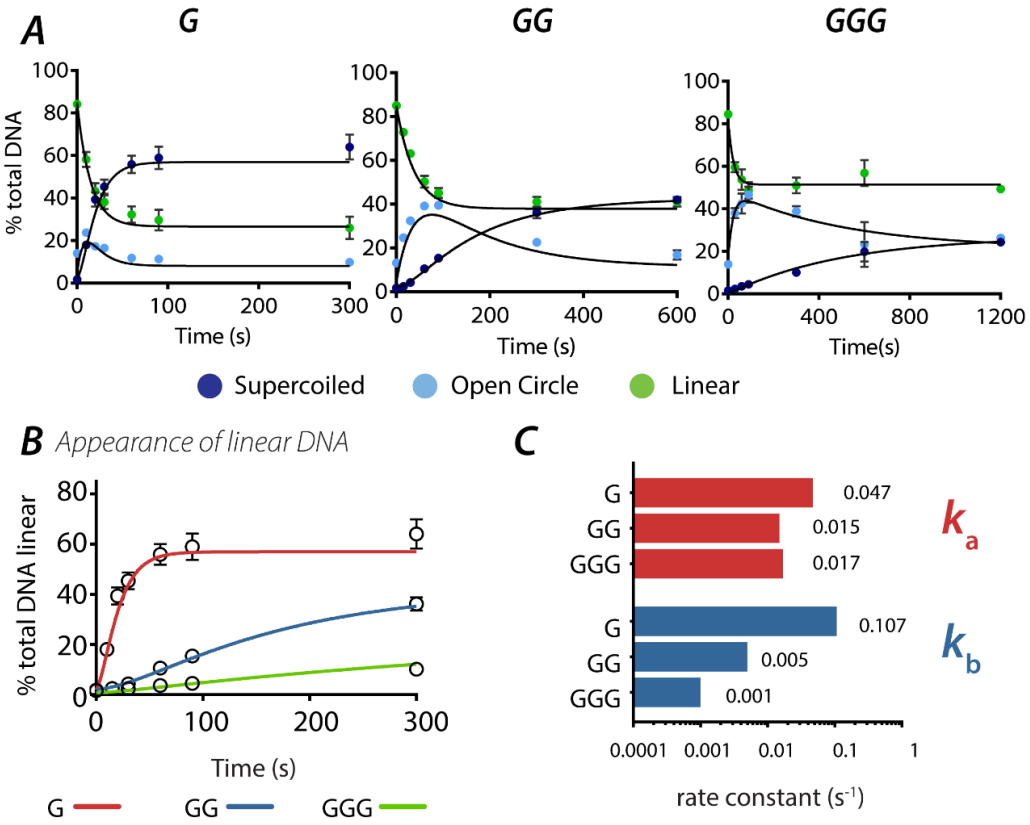

Figure 5-6 Impact of 5′ guanines on endonuclease activity: EnGen IVT A *Example pSP1 cleavage assay Berkeley Madonna fitted data for each gRNA n=3 ± SE* ***B*** *Appearance of linear DNA from A n=3 ± SE C rates of first (k_a) and second (k_b) strand cleavage*

5.1.6 Conclusions

In Chapter 4, a combination of single molecule and ensemble biochemical techniques ascertained the impact of a 5′ 20 nucleotide aptamer on Cas9 RNP formation. Although gRNAs were loaded normally by Cas9, addition of a medium sized aptamer to the 5′ end lead to gRNAs forming only partial R-loops on target DNA, which in turn impacted their endonuclease activity on supercoiled DNA substrates. The work in chapter 5.1 sought to investigate the impact of smaller additions to the 5′ end of the gRNA. This is particularly pertinent as gRNAs are often *in vitro* transcribed by the T7 polymerase which can leave up to 3 guanines at the 5′ end.

Addition of one, two or three unpaired 5′ guanines alters endonuclease activity significantly in a stepwise fashion, Figure 5-4. The observed decrease is not the result of gRNA loading as all gRNAs are loaded similarly when observed with a FRET-based assay, Figure 5-2. The decrease also cannot be explained by R-loop formation rates. R-loops are formed with similar time constants implying that RNP complex initiation and PAM-binding proceed as normal. An alternative proposal would be that the R-loop complex is unstable and collapses before the second strand cleavage can occur. The observed second strand cleavage rate would then be the result of multiple consecutive R-loop formation-cleavage events. However, gRNAs with an

overhang of three 5′ guanines have longer residency time on DNA in comparison to one or two 5′ guanines, suggesting that the R-loop complex may be *more* stable. Based on the data, it is not possible to determine why this more stable state results in slower cleavage. It is suggested that conformational transitions of the HNH domain regulate DNA cleavage[190]. On this basis, one speculation could be that the stable R-loop state represents an off-pathway state where one nuclease domain can engage (for first strand cleavage), but the other in a less productive orientation (for second strand cleavage). A sophisticated method to test this would be to use FRET measurements of each nuclease domain.

A simple test that could have been carried out here would have been to determine which strand was being nicked. The order of strand cleavage has not been explicitly shown as the rates of cleavage are similar; the three guanine gRNA could therefore provide information about this and this could be further validated by using the nicking mutants.

The results in this chapter are of value to any lab which use *in* vitro T7 RNA polymerase transcription to produce gRNAs. Although efficiency is reduced, substrates with a single 5′ guanine should be favoured. The single guanine overhangs produced by eukaryotic promoters (e.g. U6) are not an issue since the rates are equivalent to the crRNA-tracrRNA which has no overhang. The Kim lab reported that the impact of an unpaired 5′ nucleotide is particularly severe with Cas9 mutants engineered to minimise off-target effects such as eCas91.1[191] and Cas9-HF1[192]. To counter this, they designed a gRNA which incorporated a hammerhead ribozyme domain which removed the mismatched guanine prior to RNP formation and CRISPR activity[193]. Furthermore, the price of commercial RNA synthesis using phosphoramidites has decreased significantly in recent years, largely driven by research in the CRISPR field, meaning that unmatched 5′ guanines, and a corresponding sacrifice to cleavage activity, are now perhaps less of a problem than they used to be.

5.2 The impact of modifying Cas12a crRNAs for MitoCRISPR

5.2.1 Modified Cas12a crRNAs

Cas12a is a type V CRISPR endonuclease which naturally produces staggered nicks on DNA. Although most of the work in this thesis focusses on assessing the impact of modifications to Cas9 gRNAs on RNP activity and mitochondrial targeting, work by other members of the group, summarised in section 3.4, has shown Cas12a to be more efficiently expressed in mitochondria. *Lb*Cas12a is directed to target sequences on DNA by a single 44 nt crRNA. Given the conclusions in Chapter 4 on the effect of 5′ modifications on gRNAs, the experiments in this chapter sought to understand whether there were similar effects with 5 and 3′ cRNA modifications. To this end, a small library of crRNAs was designed incorporating 4 nt or 20 nt modifications to the 5′ and 3′ termini, Figure 5-7.

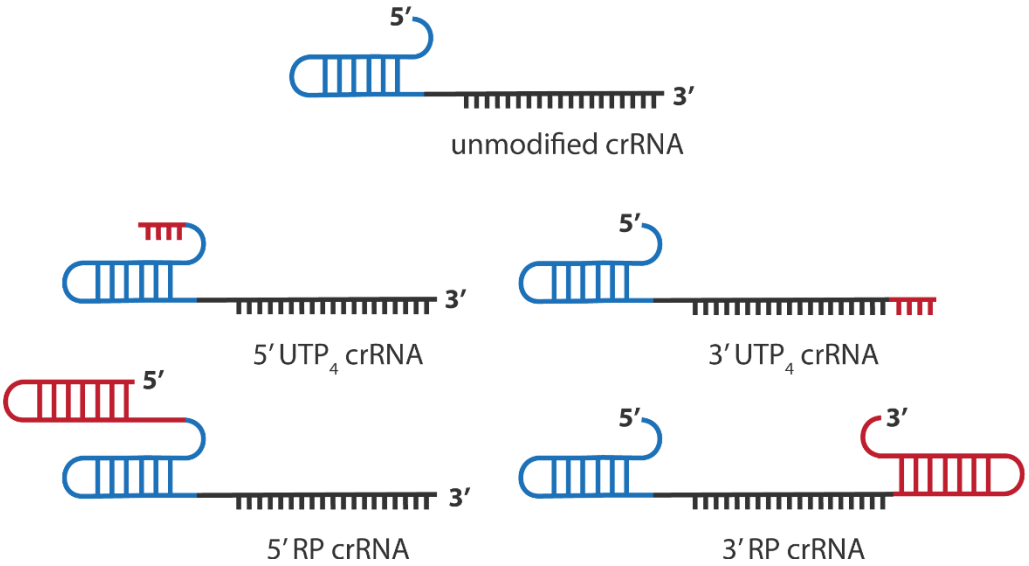

Figure 5-7 Modified Cas12a crRNAs *4 nt and 20 nt modifications (red) were made to the 5′ and 3′ termini of Cas12a crRNAs. For full sequences, see Appendix A5.*

5.2.2 Cas12a cleavage activity with modified crRNAs

Modified crRNAs were used in supercoiled plasmid cleavage assays, similar to section 4.5, to determine whether there was an impact on Cas12a endonuclease function.

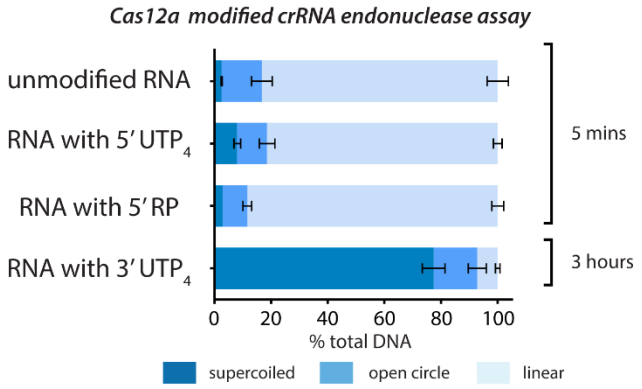

Figure 5-8 Cas12a modified crRNA cleavage assays *Cas12a RNPs were formed with crRNAs (unmodified or with 4 nt or 20 nt modifications) and endonuclease activity was measures in a cleavage assay against a supercoiled plasmid substrate, pSP1. n=3±SE.*

Following a single 5-minute timepoint, Cas12a in complex with an unmodified crRNA can be seen to cleave a supercoiled plasmid (pSP1) to 80% linear. Additions of 4 and 20 nts are tolerated at the 5′ end; after 5 minutes, 78% and 81% total DNA is linearised. In contrast, modifications are not tolerated at the 3′ end; after 3 hours, only 7% supercoiled DNA substrate has been linearised.

5.2.3 Cas12a crRNA processing

In addition to endonuclease activity, Cas12a processes RNA transcripts containing several pre-crRNA sequences into individual crRNAs. The requirements for crRNA processing are both sequence and structure dependent. In the type IV systems (such as *Spy*Cas9) Cas1-Cas2 proteins are required for RNA processing.

The above modified crRNAs do not have any of the requirements for crRNA processing as reported in the literature[194]. However, crRNA processing does occur upstream of a hairpin structure of similar length to the RP hairpin. Given that crRNA processing would result in an unmodified crRNA, and therefore no change in cleavage activity, modified crRNAs were checked for processing by Cas12a.

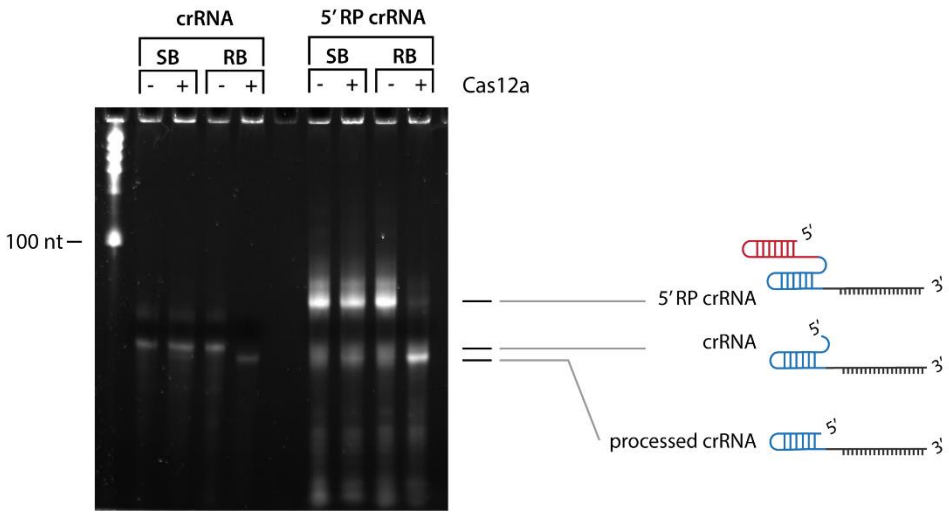

Figure 5-9 processing of crRNAs by Cas12a *2μM crRNA and 5′RP crRNA were incubated ± 10 μM Cas12a in 1XRB or 1XSB at 37 °C for 1 hour. Samples were then separated by urea-PAGE and stained with SYBR-Gold.*

crRNAs with and without 5′RP hairpins were incubated with or without Cas12a in 1 X SB (cleavage assay sample buffer) and 1 X RB (cleavage assay reaction buffer) for 1 hour at 37 °C, the standard RNP complex assembly conditions. Following this, RNAs were separated by denaturing urea-PAGE. Figure 5-9 shows that crRNAs both with and without the 5′ RP aptamer are processed in a magnesium dependent manner. Unmodified crRNAs undergo a small shift in size, perhaps due to the removal of only a couple of nucleotides. As with the *Spy*Cas9 gRNAs, *Lb*Cas12a crRNAs also have an additional 5′ guanine, so it is likely that this extra nucleotide is what is being processed here. 5′RP crRNAs incubated with Cas12a in 1XRB are processed to the same size as unmodified crRNAs, presumably the result of the RP hairpin being removed. We cannot explicitly state whether the observed cleavage in figure 5-8 is the result of a processed RNA or not.

5.2.4 Conclusions

The structural components of Cas12a crRNAs and Cas9 gRNAs occur on the opposite ends of their DNA-targeting spacer sequences, Figure 1-6, page 20. Section 5.1 showed that additions of 2 or 3 nucleotides to the gRNA 5′ impact Cas9 endonuclease activity significantly. Similarly, 4 nt modifications at the 3′ end of Cas12a crRNAs severely impact cleavage. Given the directionality of the R-loop in Cas9 and Cas12a complexes respectively, this suggests there is a common mechanism between crRNA and gRNA DNA target site binding which is hindered by small nucleotide overhangs at the PAM distal end, i.e. the end of the RNA that is furthest from the point of initiation of R-loop formation. Since the completion of R-loop formation presumably requires the unbound distal end of the RNA to thread through the unwinding DNA, bulky additions to the 5′ end (Cas9) or 3′ end (Cas12a) might inhibit the processes. An alternative way to test this would be to add non-nucleotide chemical moieties

with different sizes to the distal ends of the RNAs, and to observe the effects on the size of the R-loop formed.

The processing of 5′ modifications, and the unavailability of the crRNA 3′ end for modification might make crRNA targeting to the mitochondria with RNA aptamers difficult. However, there a number of opportunities which could be further explored. Firstly, extensions of the crRNA stem loop structure, analogous to the gRNA US position, were not explored here and might provide opportunity for modification. Secondly, several residues in Cas12a can be mutated to decrease RNA processing without impacting DNA cleavage[194], and future work could involve investigating the impact of 5′ crRNA modifications on these enzymes.

Alternatively, the RNA processing of Cas12a might be advantageous for a mitochondrial CRISPR system. If Cas12 were stably expressed so that it was only active within the mitochondrial matrix, mitochondrial targeting aptamers could be cleaved from crRNAs once they had been delivered into the matrix. This would also provide a mechanism for measuring RNA import, as processed RNAs would only be present in the mitochondrial matrix. To ensure no off-target activity on nDNA, this would rely on Cas12a expression or function exclusively within mitochondria.

6 Directing *Spy*Cas9 gRNAs for mitochondrial import

6.1 Methods for assessing mitochondrial import

As with much of the wider study of physiologically relevant RNAs, methods for determining *in vivo* subcellular RNA localisation are much less advanced than those for the study of proteins. Without one standardised technique to follow mitochondrial RNA import, the following chapter summarises several techniques which together can be used to determine whether our library of RNAs, as described in Chapter 4, can be imported into mitochondria.

Chapter 6 uses techniques to assess RNA import into both whole cells and isolated mitochondria, Figure 6-1. In whole cells, gRNAs are transfected into mammalian cells grown in culture and their subcellular localisation is either followed by a fluorescent tag, or cells are fractionated and probed for the presence of gRNAs by Northern blotting. Given the end goal of this project is to be able to engineer mitochondrial genomes in whole cells and organisms, assaying gRNA import into whole cells is most relevant to the end tool.

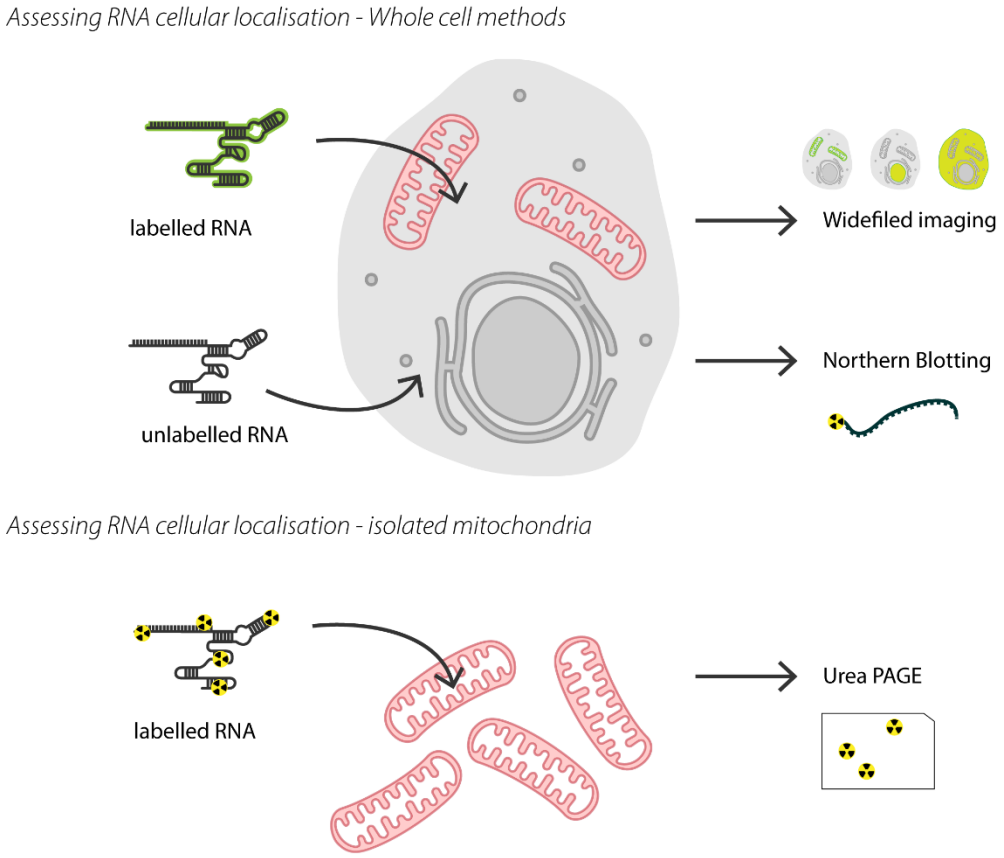

Figure 6-1 Whole cell and isolated mitochondrial assays for mitochondrial RNA import *can be used to follow RNA localisation within cells. Fluorescently labelled RNAs can be observed with widefield imaging in whole cells, and unlabelled RNA localisation can be followed by fractionating cells and using a Northern blotting technique. Radiolabelled RNA can be used in an assay to follow import into isolated mitochondria.*

However, there are several complexities which come with assaying cellular localisation of RNAs in whole cells and so gRNA import is also assayed *in vitro*. Radiolabelling RNAs allow their import into isolated mitochondria to be followed, an analogous protocol is standard for assessing mitochondrial protein import. Isolated mitochondria are a useful model for measuring import and have several advantages over whole cell assays. Firstly, isolated mitochondrial assays are much quicker, not requiring the several days for growing and transfecting cells. Secondly, isolated mitochondria allow the import of radiolabelled RNAs, which is problematic in mammalian cell culture given the safety precautions when using sources of ionising radiation. Radioisotopes provide a sensitive method of labelling RNAs and are less intrusive than fluorophore-labelled nucleotides. This method also allows the potential for different interventions such as blocking electron transport to be easily tested.

6.2 Whole cell methods - direct RNA transfection

6.2.1 Northern blotting

Northern blotting, summarised in Figure 6-2, is an indirect method of determining subcellular RNA localisation with radiolabelled DNA probes complimentary to the RNA of interest.

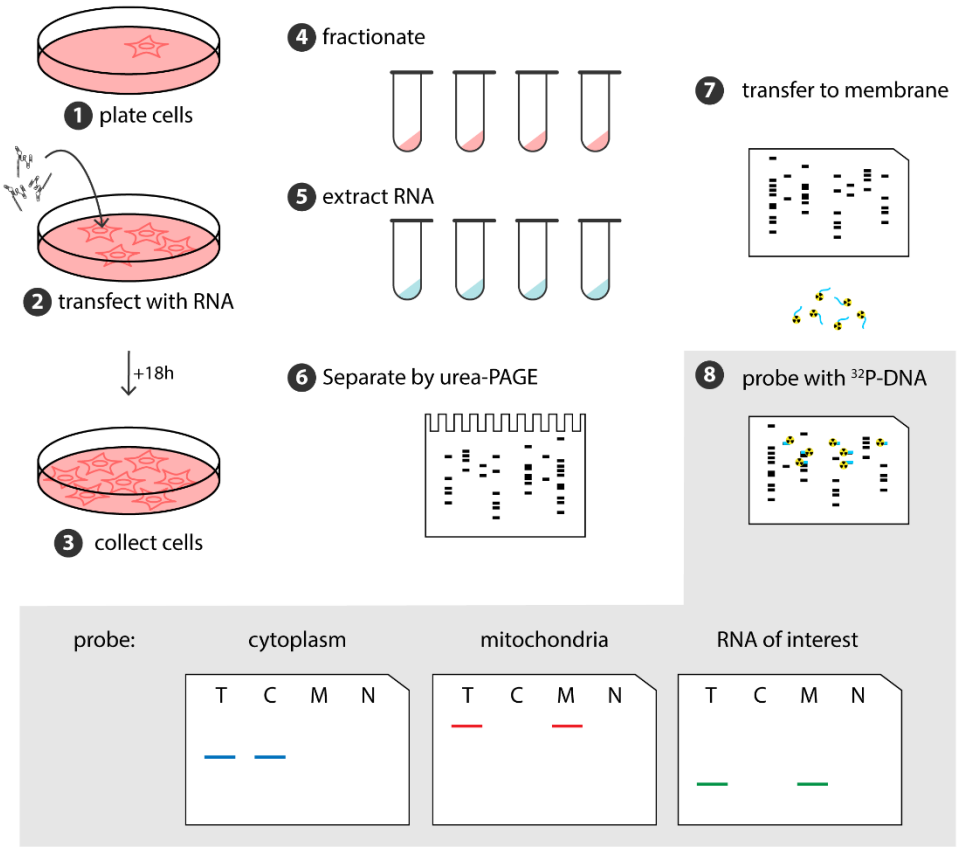

Figure 6-2 Northern blotting protocol *Cells are plated in a 10 cm dish and transfected with RNA when 70-80% confluent. After 18 hours, cells are harvested, homogenised and fractionated. RNA is extracted from fractions and separated by urea-PAGE. Separated RNAs are transferred to nitrocellulose membrane and probed with ^{32}P-DNA.*

HeLa cells, transfected with an RNA of interest (steps 1-3), are manually homogenised and then fractionated into cytoplasm, mitochondrial and nuclear fractions via differential centrifugation (step 4). RNA is extracted from each fraction (step 5) which is separated by denaturing urea-PAGE (step 6). Total separated RNA is transferred to a membrane (step 7) and RNAs of interest are probed for with radiolabelled DNA probes (step 8). Control RNAs against each fraction confirm fractionation has been successful. Here, a probe against a cytoplasmic RNA ($tRNA_{Lys}$) and a mitochondrial RNA ($tRNA_{Leu}$) confirm each fraction to be enriched in their characteristic RNAs. Probes designed against the transfected RNA of interest identify which fraction the RNA has been extracted with. The sequences of the probes used in this chapter is given in Table 17.

Kolesnikova *et al*[122] designed small synthetic RNAs based on the yeast $tRNA_{Lys}$ (tRK1) with a range of reported *in vitro* mitochondrial targeting efficiencies. The most and least efficiently imported RNAs, F1D1 (FD) and AD1 (AD), respectively (Figure 6-3A), were used in protocol optimisation. Of note is that the AD RNA runs as two bands on the urea-PAGE.

HeLa cells were transfected with AD and FD, and a time-course experiment was performed to determine the optimal time to harvest cells post-transfection, Figure 6-3C. Cell lysates at each timepoint were probed with the tRK1 probe (targeting AD and FD, Figure 6-3B), indicating that 18 hours post transfection gave the best signal for both AD and FD RNAs. After 18 hours, the transfected RNAs appear degraded by the cells. Although the same amount of RNA was transfected into the cells, the AD signal was much lower than that for FD, presumably because the AD RNA ran as two bands on the urea-PAGE, diluting the signal.

In Figure 6-3D, HeLa cells transfected with either AD or FD RNA were fractionated into cytoplasmic, mitochondrial and nuclear fractions 18h post-transfection. RNA was extracted from each fraction, separated by urea-PAGE and probed for cytoplasmic $tRNA_{Lys}$ mitochondrial $tRNA_{Leu}$ and tRK1, Figure 6-3D. The cytoplasmic probe ($tRNA_{Lys}$) and mitochondrial probe ($tRNA_{Leu}$) show that the mitochondrial and cytoplasmic fractions are enriched for their respective RNAs, as expected. However, it appears that the fractionation was not completely effective: the mitochondrial probe produces signal in the cytoplasmic fraction, and vice versa for the cytoplasmic probe. There are also very strong signals from the mitochondrial and cytoplasmic probes in the nuclear fraction. This can indicate contamination of the nuclear fraction with cytoplasmic/mitochondrial components.

The tRK1 probe signal shows the F1D1 aptamer to be present in the mitochondrial fraction, but also in the nuclear fraction, as seen with the mitochondrial $tRNA_{Leu}$ probe. The tRK1 probe shows that the majority of the AD RNA appears to be present in the nucleus. Unfortunately, Kolesnikova *et al*[122] did not show nuclear fractions in any of their Northern blotting

experiments or the cellular localisation of the AD1 RNA (they just show its absence in mitochondria). Consequently, it is not possible to compare this result.

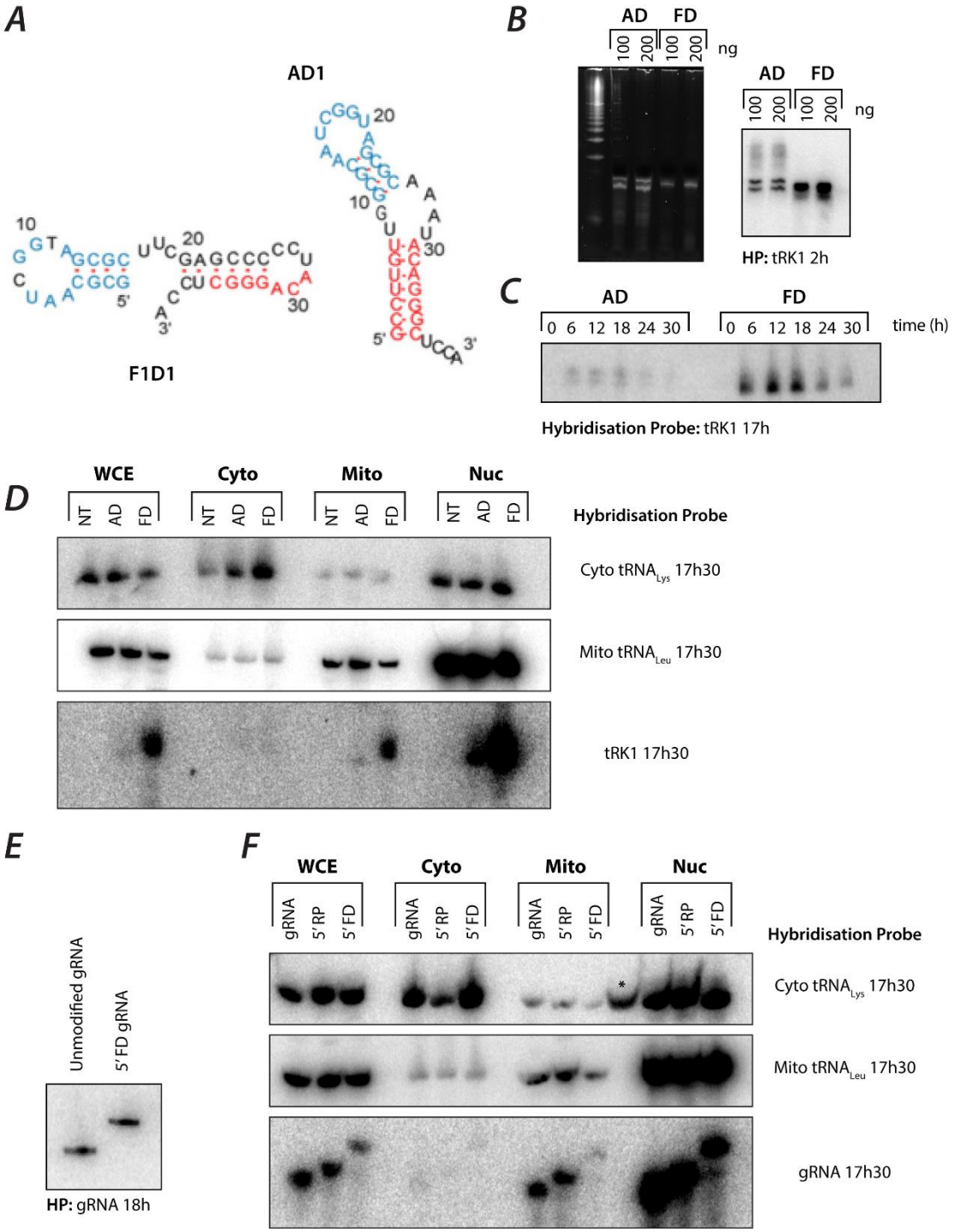

Figure 6-3 Northern blotting HeLa cells for AD and FD *A AD and FD RNAs from [122] B 100 and 200 ng AD and FD separated by urea-PAGE (left) was transferred to nitrocellulose membrane and probed against tRK1 probe (right) C transfection time course for AD and FD RNA D Northern blotting for AD/FD, E 50 ng RNA gRNA and 5′FD gRNA separated by urea-PAGE transferred to nitrocellulose membrane and probed against gRNA probe F Northern blotting for gRNA, gRNA 5′ RP and gRNA 5′ FD; WCE = whole cell extract; Cyto = Cytoplasm; Mito = Mitochondria; Nuc = Nuclear; HP = Hybridisation probe. Bands in lane marked* ***** *on Cyto-probed membrane are over-spill from adjacent gRNA Nuclear lane.*

Using the same protocol, cells were transfected with unmodified gRNA, gRNA with 5′RP and gRNA with 5′ FD, Figure 6-3F. The hybridisation signal is determined by the probe binding the hairpin region of the gRNA. Strong signals for all three gRNAs were produced in the nuclear fraction and, to a slightly lesser extent, the mitochondrial fraction. In contrast, the 5′ FD gRNA produced the least strong signal in the mitochondrial fraction, a result which is confirmed by a second northern blot, Appendix A6-I.

6.2.2 Fluorescent RNAs

Given the high level of sample processing required for the Northern blotting protocol, we sought to directly image RNA localisation in whole cells to complement the results in 6.2.1. The ability to use fluorescent-protein conjugated constructs has become an indispensable tool in cell biology, enabling visualisation of cellular protein distribution. In contrast, it has been difficult to pinpoint subcellular RNA distribution in the same way. There are several methods for labelling RNAs for imaging in cell culture which could be useful reporters of gRNA distribution, including: fluorescent RNA aptamers such as 'Baby Spinach' that can be appended to the gRNA structure (introduced in Chapter 4); and, Alexa™ fluorophore-coupled NTPs that can directly label RNAs when incorporated via IVT.

6.2.2.1 Alexa™-coupled NTPs

The water soluble Alexa™ fluorophore-labelled nucleotides enable direct labelling of RNA and DNA without addition of bulky structures. Here, Alexa™ 488-5-UTP, Figure 6-4A, was incorporated randomly along the length of transcribed RNAs. The Alexa™ fluorophore is separated from the UTP nucleotide by a 5-atom linker to reduce interactions between the RNA and fluorophore. The gRNA, 5′ RP gRNA, 5′ FD gRNA, AD RNA and FD RNA were successfully *in vitro* transcribed with Alexa™ 488-5-UTP, Figure 6-4B, C. The RNAs run at their expected sizes, though AD and FD RNAs produced less discrete bands.

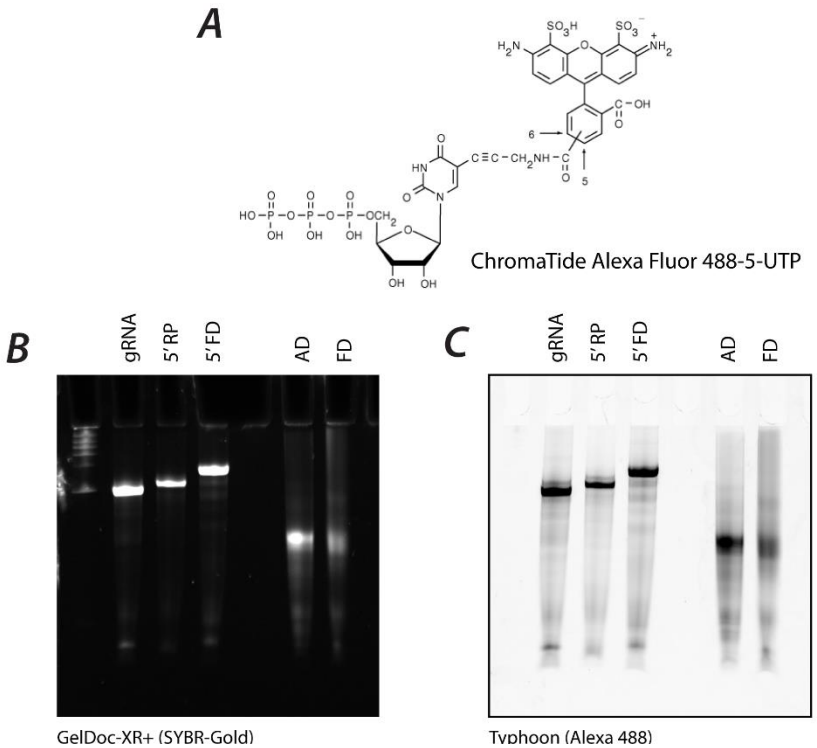

Figure 6-4 ChromaTide Alexa™ Fluor 488-5-UTP incorporation by IVT ***A*** *ChromaTide Alexa™ Fluor 488-5-UTP structure* ***B*** *488-5-UTP incorporated RNAs separated by urea PAGE, stained with SYBR-Gold* ***C*** *488-5-UTP incorporated RNAs separated by urea PAGE,488 fluorescence measured by Typhoon Scanner*

6.2.2.2 Imaging fluorescent RNAs in mammalian cell culture

Transfecting fluorescently-labelled RNAs into HeLa cells allows cellular localisation to be observed in intact whole cells[195]. Alexa™ 488-5-UTP-labelled AD and FD RNA were transfected into HeLa cells by PEI transfection[viii].

AD RNA (AD-488), Figure 6-5A, was observed in discrete, punctate structures, visible throughout the cytosol. AD-488 structures are present mostly in a perinuclear distribution and rarely found in the nucleus or at the cell periphery. To assess mitochondrial localisation, the mitochondria were stained with anti-Tom20, a central component of the TOM (translocase of outer membrane) receptor complex. The enlarged (200 x 200 px) image shows that Alexa™-488 and Tom20 signals almost seem to be mutually exclusive, suggesting that there is not any colocalization as would be expected. A fluorescence profile, taken along a 150 px line, show a collection of peaks in Alexa™-488 between 75 and 100 px are directly between mitochondrial structures.

[viii] Several transfection methods including lipofectamine, PEI, calcium chloride and electroporation were compared by an undergraduate summer student in the lab, Margaret Smith, data not shown.

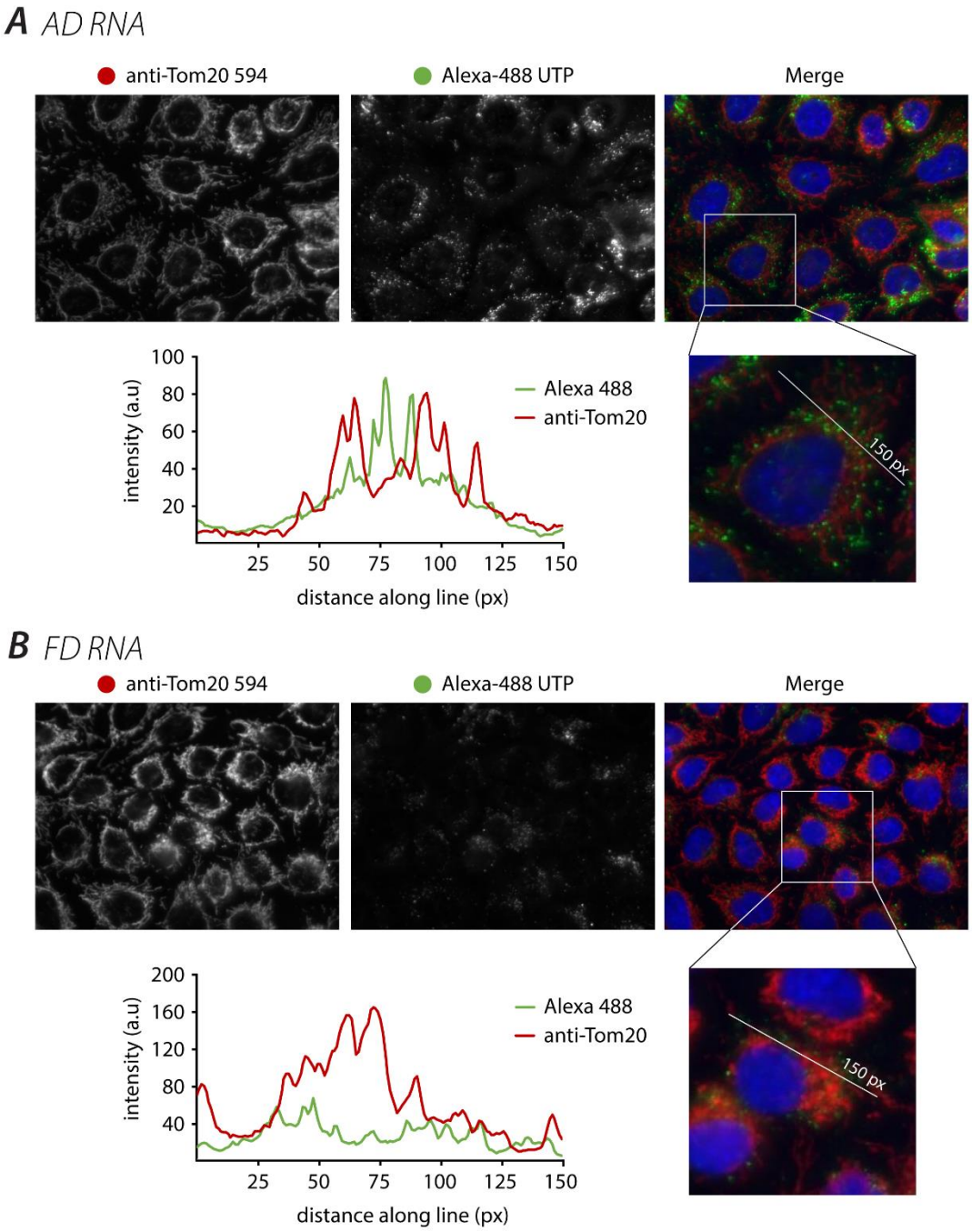

Figure 6-5 Alexa™-488 UTP labelled AD and FD RNAs *in both cases, AD (**A**) and FD (**B**) RNA is transfected into HeLa cells by PEI transfection. Cells are stained with DAPI and anti-TOM20 (2° anti-Mouse 647). DAPI: 30 ms; FITC: 500 ms; Cy 5: 2000 ms. Line profiles are taken along a representative 150 px line through the perinuclear region*

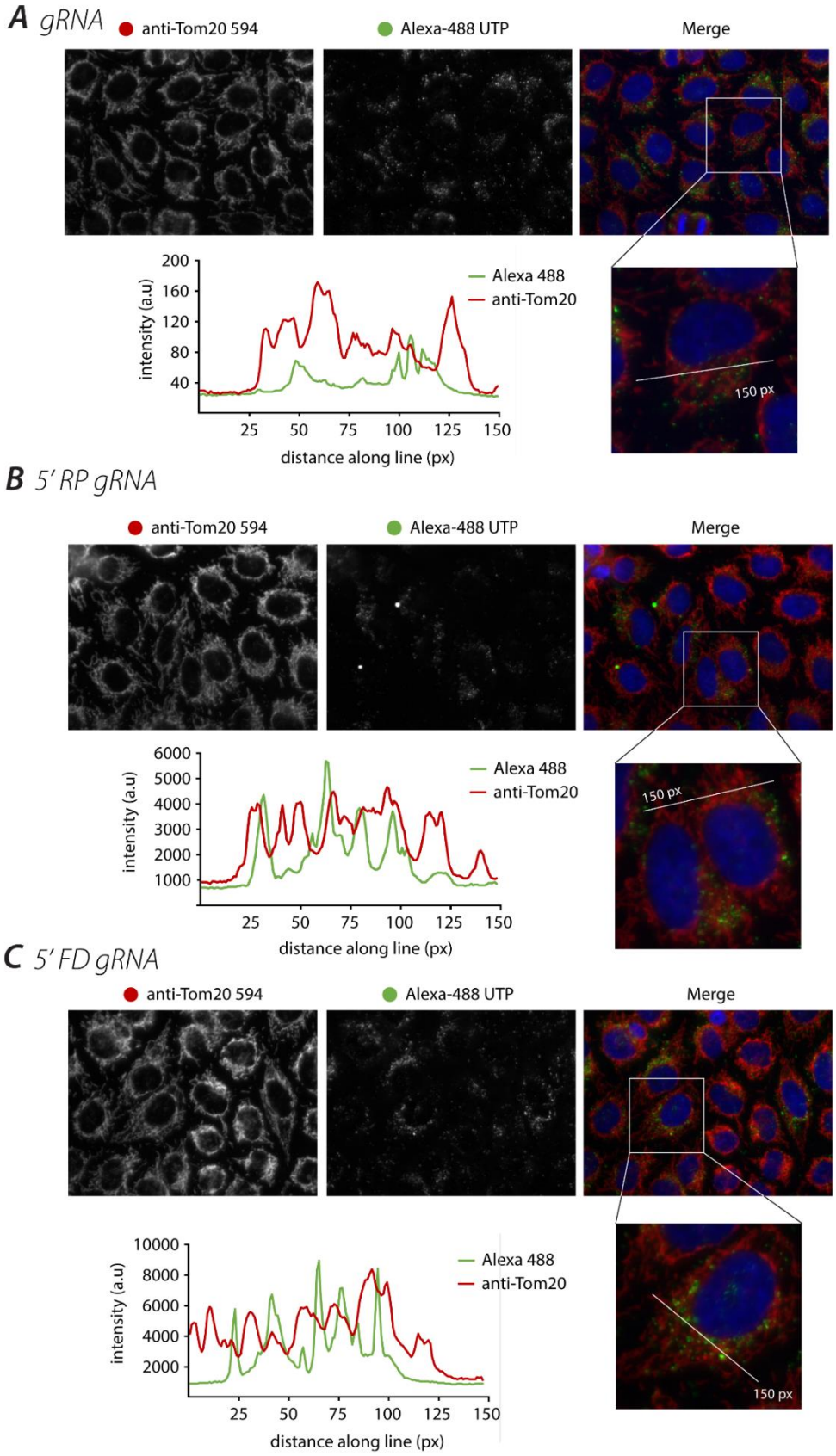

Figure 6-6 Alexa™-488-UTP incorpterated gRNA, 5′ RP gRNA and 5′FD gRNA in HeLa cells *RNA is transfected into HeLa cells by PEI transfection. Cells are stained with DAPI and anti-TOM20 (2° anti-Mouse 647). DAPI: 30 ms; FITC: 500 ms; Cy 5: 2000 ms. Line profiles are taken along a representative 150 px line through the perinuclear region*

Alexa™-488 UTP-labelled FD RNA (FD-488), Figure 6-5B, also appears located in perinuclear regions, though its distribution is not identical to AD-488. FD-488 contains some punctate structures, but overall is more diffuse throughout the cytosol. FD-488 does not seem to be explicitly mitochondrially localised. Although there are some regions of colocalisation, there is very little continuous overlap in the Tom20 and FD-488 signals. The more punctate FD-488 structures, as with AD-488, are never colocalised to mitochondria, but some of the more diffuse signal could be interpreted as being mitochondrially localised.

Alexa™ 488-5-UTP-labelled gRNAs (gRNA-488, 5′RPgRNA-488, 5′FDgRNA-488) were also transfected into HeLa cells by PEI transfection, Figure 6-6. All three gRNAs displayed similar localisations to one another – punctate and perinuclear in distribution, rarely colocalising with the nucleus or the cell periphery. The 488-labelled gRNAs show similarities to both the AD and FD-488 RNAs: Like AD-488, the most defined structures are explicitly found in locations distinct to the mitochondria – some of the most intense peaks in the line scans correlate with dips in mitochondrial signal - whereas some of the more diffuse regions could be interpreted as being mitochondrially associated.

Overall, these results give an uncertain impression of transfected RNA localisation within the cell; it is unclear whether RNAs are mitochondrially localised, or just mitochondrial adjacent and in another cellular compartment. At times, the images directly contradict findings from northern blotting analysis; the enrichment of RNAs in the nucleus for example. Further work is required to determine whether they might be in an endocytic or lysosomal compartment. RNAs are not being degraded by autophagy, as they show no colocalisation with LC3, a marker of autophagosomes, Appendix A6-II.

6.2.2.3 Fluorescent RNA aptamers

Baby Spinach (BS) is a 51 nucleotide G-quadruplex-based aptamer which fluoresces when in complex with the small molecule chromophore DFHBi-1T, Figure 6-7A[196]. The Spinach-DFHBi-1T conjugate fluoresces when excited at 460 nm, which can be conveniently imaged using a blue-light transilluminator (Figure 6-7C) or quantified in a spectrophotometer (Figure 6-7B). The emission spectra from 5′ and 3′ BS gRNAs in complex with DFHBi-1T were measured by fluorescence spectrophotometry (λ_{ex} = 460 nm). Assembling and immediately measuring the 5′ BS gRNA in complex with Cas9 and DFHBi-1T showed a six-fold increase in in fluorescence in comparison to gRNA/Cas9 RNP alone. Preassembly of the Cas9/5′ BS gRNA RNP for 1 hour at 37°C before adding the chromophore produced a fourteen-fold increase, Figure 6-7D. The 3′ BS gRNA/Cas9 showed only a small increase in fluorescence upon incubation with DFHBi1T. One explanation is that the BS aptamer is not folding correctly, perhaps a result of

its proximity to the Cas9 or 3′ gRNA hairpins, Figure 6-7E. Alternatively, there could be a quenching effect, perhaps a result of misfolding due to proximity to Cas9.

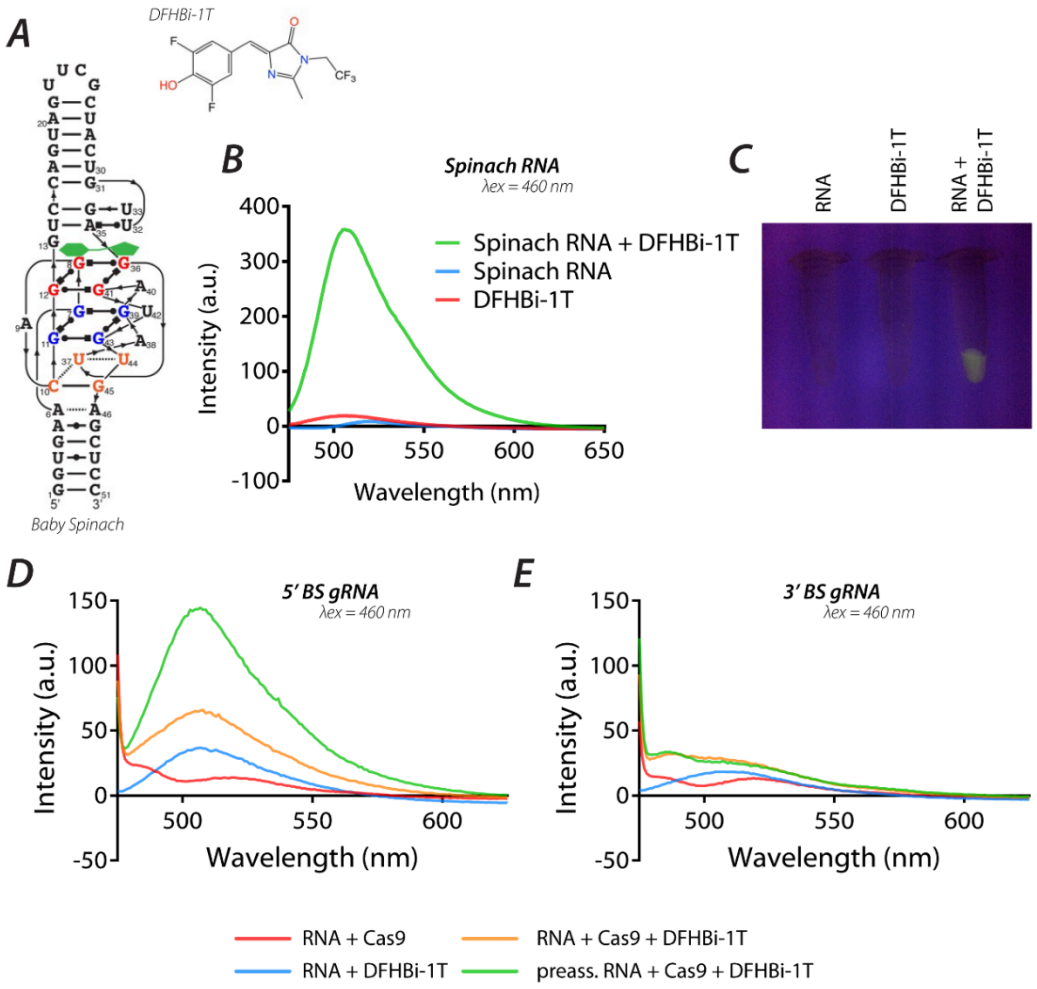

Figure 6-7 Baby Spinach gRNA fluorescence ***A*** *Baby Spinach theorised structure and DFHBi-1T (both from [197])* ***B*** *Spinach RNA ± DFHBi-1T fluorescence (λ_{ex} = 560 nm)* ***C*** *Spinach RNA ± DFHBi-1T fluorescence, DarkReader transilluminator* ***D*** *and* ***E*** *5′ and 3′ BS gRNA fluorescence ± Cas9 and DFHBi-1T (λ_{ex} = 560 nm)*

Although the BS aptamer allows imaging of 5′ labelled gRNAs, its incompatibility with 3′ labelling and the impossibility of producing an 'unmodified' gRNA (as can be followed with Alexa™ or northern blotting for example) are limitations to its application in this study. Due to these reasons, as well as time constraints, the BS aptamer has not yet been used to study gRNA localisation in cell culture by this research group. Nevertheless, it's characterisation here makes it a potential tool for use in future work.

6.3 Studying import in isolated mitochondria

Whole-cell methods for assessing whether RNA aptamers are capable of localising gRNAs to the mitochondria were inconclusive. To clarify whether our *in vitro* transcribed gRNAs can be imported into mitochondria, assays were also performed with isolated mitochondria.

6.3.1 Isolation of mitochondria from tissue culture cells

Common sources of mammalian mitochondria for import assays include bovine heart and rat liver. Without an appropriate tissue source, isolation of mammalian mitochondria was first attempted from cells grown in tissue culture, using a similar homogenisation and centrifugation method as for northern blotting, section 6.2.1.

A proton gradient and membrane potential are integral to mitochondrial structure and protein import. Given some RNAs have been suggested to be imported via the TOM/TIM machinery (section 1.5.2.1) it might be hypothesised that a proton gradient be a requirement for other RNA import pathways too. Accordingly, an assay for RNA mitochondrial import would ideally include coupled mitochondria.

Respiration capacity of isolated mitochondria was assessed as a readout of mitochondrial viability. This was carried out in different variations with a classical O_2 electrode, the Oroboros Oxygraph O2k (Oroboros Instruments), and the Xf^e Extracellular Flux Analyser (Seahorse Bioscientific). Substrates and inhibitors of the complexes of the electron transport chain were added to the mitochondria, but analyses with both machines showed the isolated RPE-1 cell mitochondria to be largely uncoupled and unsuitable for use in RNA import assays, Figure 6-8. This could be either due to damage during the isolation technique or due to the diminished respiratory capacity of cells grown in culture conditions.

The trace from the mitochondrial respiration assay carried out with the Oxygraph-2k O_2 electrode is given in Figure 6-8A. The initial substrates added to the isolated mitochondria were glutamate and malate, both substrates of complex I, converted to NADH in the mitochondrial matrix. The rate of O_2 consumption with glutamate and malate seen here is lower than would be expected for this concentration of mitochondria. This might be explained by the low concentration of mitochondria in the oxygraph chamber but could more likely be due to the poor functioning of the isolated mitochondria. Upon addition of ADP, an increase in respiration would imply the reliance on proton motive force for ATP generation, and the magnitude of this increase directly correlates to how coupled - i.e. how intact - the isolated mitochondria are[198]. The lack of any such increase in respiration upon addition of ADP implies that the isolated mitochondria are likely uncoupled or damaged. This conclusion is supported by the subsequent substrate and inhibitor additions: cytochrome *c*, which should feed

electrons into complex IV, showed no increase in O_2 uptake; while rotenone and antimycin A, inhibitors of complex I and III respectively led to an overall plateau of mitochondrial activity.

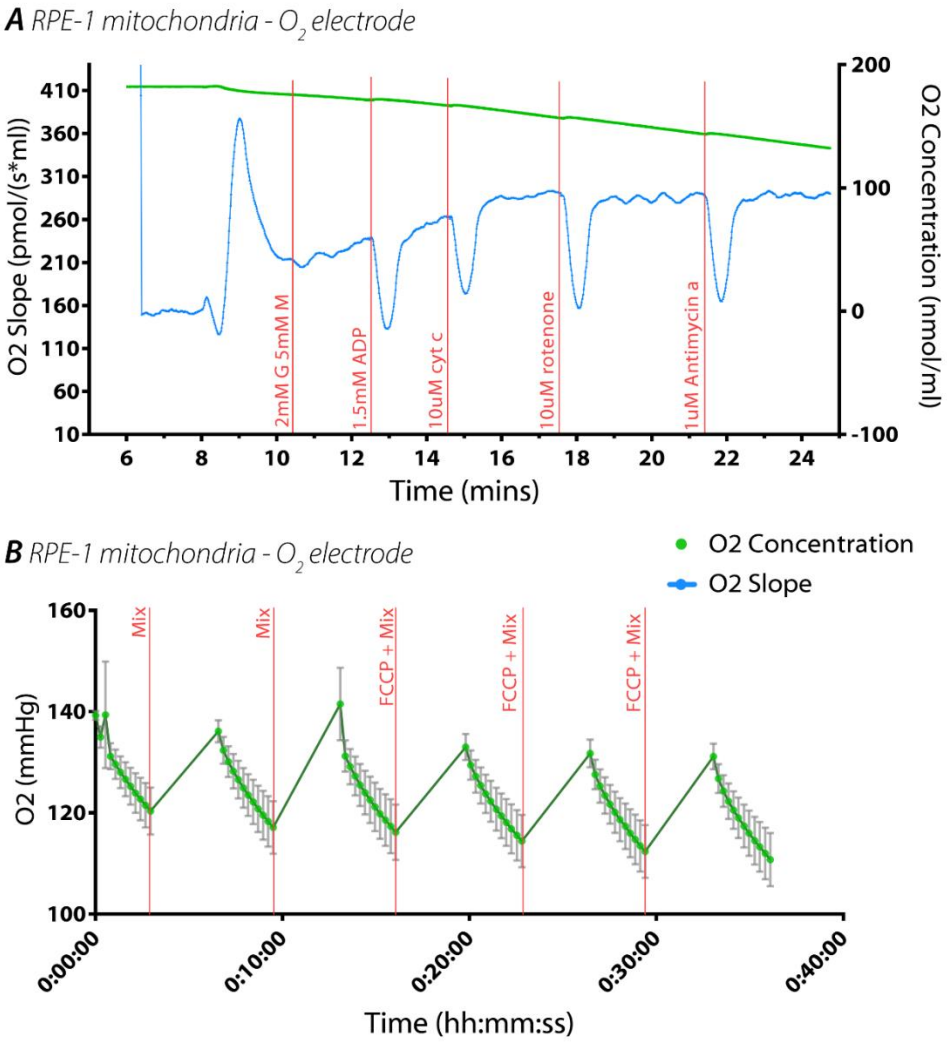

Figure 6-8 Isolated mammalian RPE-1 mitochondria ***A*** *O_2 electrode measurements of RPE-1 mitochondrial respiration. Trace is for 30µg mitochondrial protein loaded into the O_2 chamber; dips after each addition are due to mixing of substrate in the oxygen electrode chamber. G: Glutamate, M: Malate, cyt c: cytochrome c.* ***B*** *Seahorse measurements of RPE-1 mitochondrial respiration - Each point average of 3 datapoints from three independent wells; OCR= Oxygen consumption rate*

Figure 6-8B shows the O_2 consumption trace for isolated mitochondria respiration as measured with the XF^{e}96 Analyser. The small-scale nature of the XF Analyser is better suited for small sample volumes compared with the traditional O_2 electrode. The uncoupling agent carbonyl cyanide-*4*-(trifluoromethoxy)phenylhydrazone (FCCP) acts to dissipate the proton gradient across the mitochondrial membranes and is used to reveal maximal respiration rate. Upon addition of FCCP to the seahorse chamber, no change was seen in isolated mitochondria O_2 consumption. This provides further evidence that the mitochondria are largely uncoupled, either due to damage during the isolation technique or due to their little respiratory capacity.

To assess whether it was the damage to the cells or the cells' respiratory capacity themselves, RPE-1 cells permeabilised with digitonin were measured for oxygen consumption with the Oxygraph oxygen electrode (data not shown). This revealed no enhanced respiration compared to isolated mitochondria, suggesting that the failure of isolated mitochondria to respire could be a result of reduced dependence on mitochondrial function in the tissue culture environment where substrates are readily provided. In hindsight, growing cells in galactose containing media might have helped to push the cells to be more dependent on OXPHOS for cellular energy production. However, given it was also difficult to get a high concentration of mitochondrial protein, this was not revisited.

Another common source of mitochondria for import assays are yeast, *Saccharomyces cerevisiae*. Yeast can be readily grown in large quantities and maintain their OXPHOS and membrane potential following freeze-thawing, a key advantage over mammalian mitochondria isolated from tissues. An established protocol from the Collinson lab (University of Bristol) for isolation of yeast mitochondria was used here.

6.3.2 Isolation of yeast mitochondria

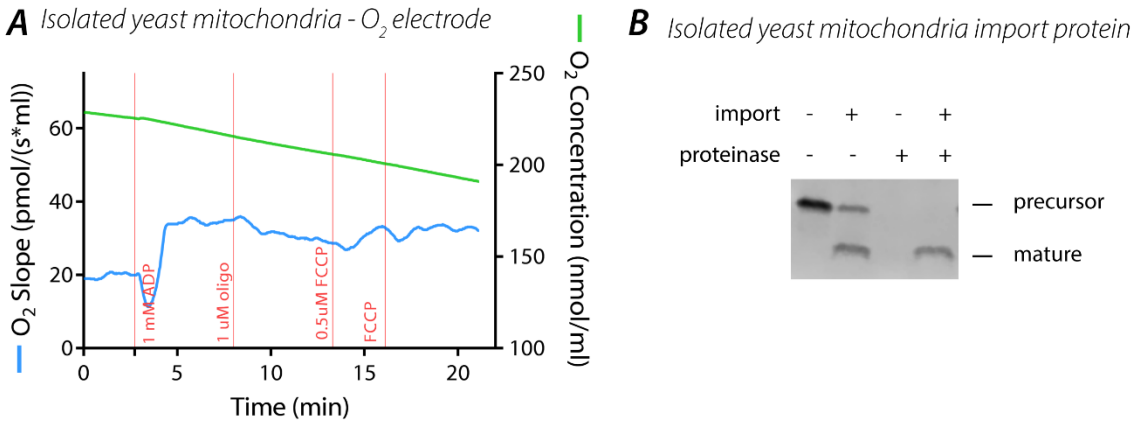

Figure 6-9 Isolated Yeast mitochondria **A** O2 electrode measurements of isolated yeast mitochondrial respiration. Trace is for 500µg mitochondrial protein loaded into the O2 chamber; at t=0, mitochondria are given 1 mM NADH, oligo = oligomycin ***B*** *Data collected by Dr Holly Ford. Isolated yeast mitochondria import cytb2-DHFR precursor protein and cleave it to its mature form; ± import = ± VOA mix.*

Mitochondrial respiration capacity of isolated yeast mitochondria was assessed with the Oroboros Oxygraph O2k, Figure 6-9A. At the start of the measurement, isolated mitochondria are in a buffer containing NADH, the substrate for complex I. The increase in respiration upon addition of ADP, a direct substrate for ATP synthase, shows that there is some proton motive force dependent ATP generation, unlike with the RPE-1 isolated mitochondria above. Oligomycin is an ATP synthase inhibitor and should drop O_2 consumption, which is does slightly. However, healthy, coupled mitochondria should show a large increase in O2 consumption on addition of FCCP, which establishes maximal respiratory capacity. This is not

seen here, and respiration only returns to a rate similar to before oligomycin treatment. Overall, these isolated mitochondria do not respire as efficiently as might be expected. However, this preparation of yeast mitochondria are capable of importing preproteins, Figure 6-9B, which are processed into their mature form (MTS cleaved) in the mitochondrial matrix by MMP. Application of *VOA*, which abolishes membrane potential and proton motive force (-import) also abolishes import. Seen together this implies that, although compromised, yeast mitochondria (or at least a sub-population) are sufficiently intact and functional for assessing mitochondrial protein import – for this reason they were used in subsequent assays.

6.3.3 Radiolabelled RNA import

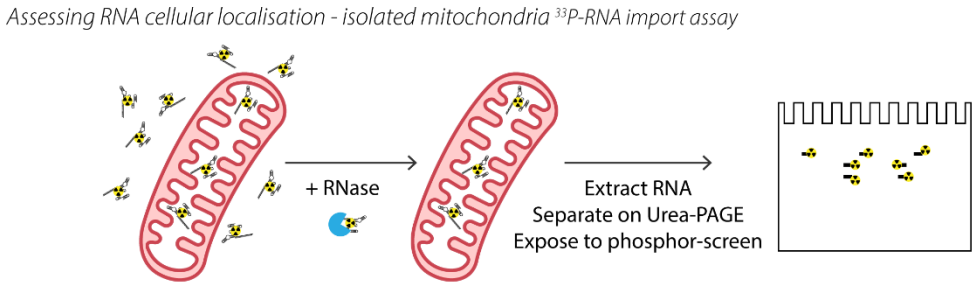

Figure 6-10 Assessing RNA import in isolated mitochondria *RNA import can be measured by directly importing radiolabelled RNAs*

Radiolabelled RNAs provide a sensitive method for following RNA import into isolated mitochondria. RNAs were *in vitro* transcribed with ^{33}P-UTP in the reaction mixture, Figure 6-11B. gRNAs and gRNAs with a 5′FD, the two most efficiently transcribed RNAs, were incubated with mitochondria with or without functioning import machinery (±VOA). Following a 10 minute incubation at 25 °C, mitochondria were treated with RNase to degrade non-imported RNA. An RNase test was performed (Figure 6-11D, right) to ensure that the RNase treatment was sufficient to degrade total loaded RNA. In Figure 6-11C, whole import assay samples were directly separated on urea-PAGE whereas in Figure 6-11D, RNA was first extracted from the yeast import mix by TRIzol extraction. TRIzol extraction of RNAs lead to a much cleaner image with more discrete bands when exposed to a phosphor screen.

Figure 6-11D shows both gRNAs and 5′FD gRNAs are protected by mitochondria: RNase treatment does not degrade all RNA in the sample. The gRNA protection by mitochondria is independent of VOA treatment, implying that if RNA import has been achieved it has been achieved independently of membrane potential. The protected gRNA bands appear to migrate more slowly than corresponding bands before treatment; this contrasts with the FD gRNA which appears as a single faint band of the same size. One possibility is that the gRNA is not fully imported, and the RNase can partially digest the polynucleotide. However, it should be noted that this assay does not explicitly demonstrate import, but rather demonstrates

protection. For the protein import assays, evidence of delivery to the matrix is ascertained by a change in the protein size as the MTS is proteolytically removed. There is no equivalent aptamer processing activity.

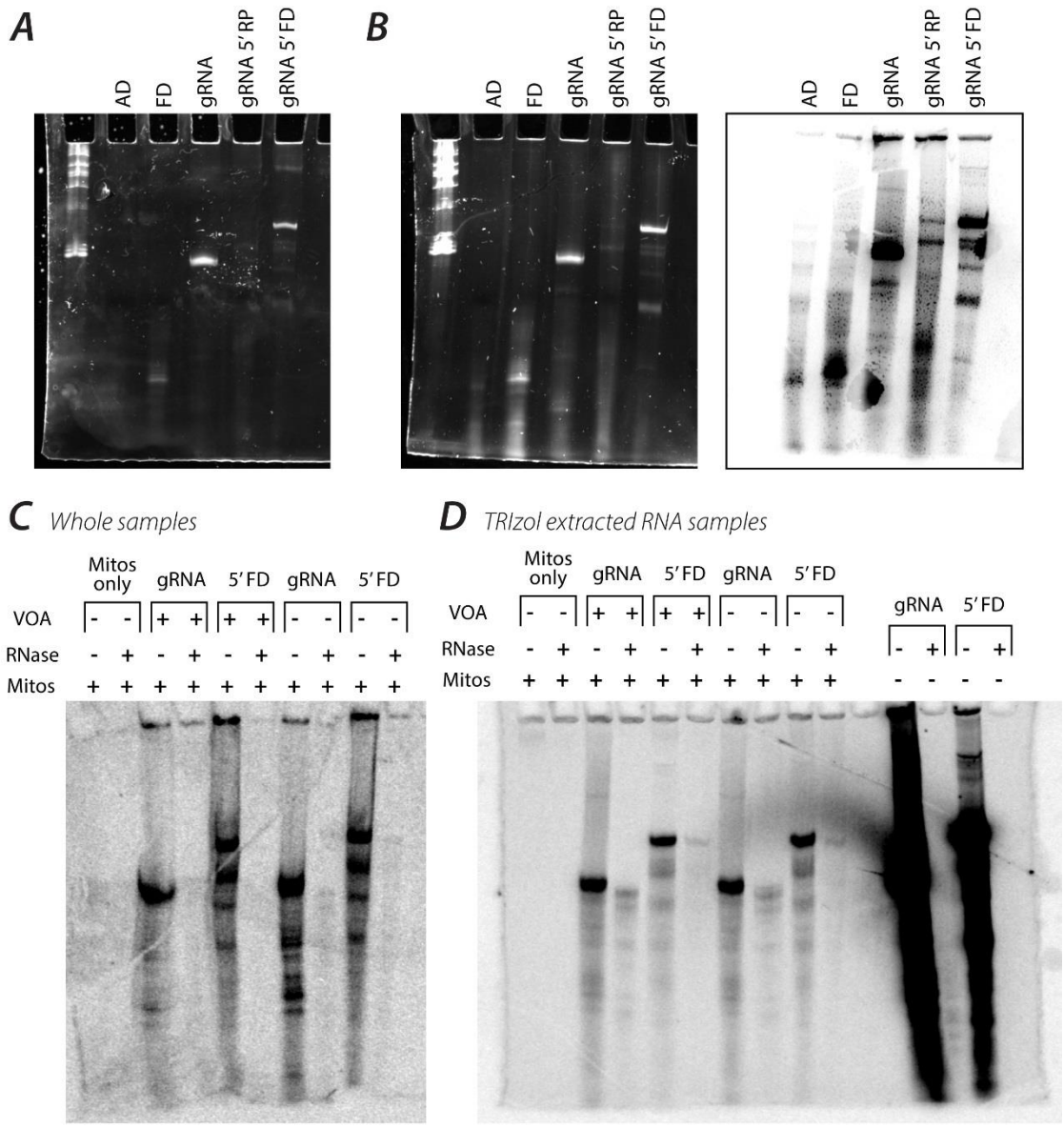

Figure 6-11 Radiolabelled import of RNA into isolated yeast mitochondria ***A*** *cold IVT and* ***B*** *hot IVT incorporating ^{33}P UTP, 250 ng RNA loaded per lane.* ***C and D*** *For RNA import assay, 25 µg mitochondria were incubated with 8 pmol ^{33}P UTP-RNA for 10 minutes at 25°C. Unimported RNA was degraded with RNase and VOA dissipates membrane potential;* ***C*** *whole import sample on urea-PAGE,* ***D*** *TRIzol extracted RNA on urea-PAGE. Following separation, gels were fixed, dried and exposed to a phosphor screen.*

6.4 Conclusions

In Chapter 6, three assays were used to assess gRNA import in both whole cells and isolated mitochondria. A Northern blotting protocol, Figure 6-3, was used to determine which mammalian cell fractions transfected gRNAs were enriched in. The results showed gRNAs with and without 5′ targeting aptamers to be mitochondrially localised, a result which is supported by assays following radiolabelled RNA import into isolated yeast mitochondria, Figure 6-11. gRNAs with and without 5′ targeting aptamers are protected from RNase degradation when incubated with yeast mitochondria. Imaging fluorescently labelled RNAs with and without targeting aptamers showed gRNAs to be perinuclear in distribution, but not necessarily mitochondrial – Alexa™ 488-UTP labelled gRNAs do not confidently colocalise with mitochondria, and at times seem to be explicitly distinct, Figure 6-6. Further to this, each of the protocols have several shortcomings which further complicate the findings. Each assay is commented upon further below:

6.4.1 Northern blotting

Although a significant period was spent optimising the Northern blotting protocol, cellular fractionation is not perfect, and fractions display a significant amount of overlap. Most significantly, the nuclear fraction is positive for both the mitochondrial and cytoplasmic probes. This can partially be explained as an artefact of the fractionation protocol: the nuclear fraction is the product of the first centrifugation step, and so any cells which have not been lysed will also be contained within this fraction. Indeed, the Alexa™ 488-UTP labelled gRNAs do not indicate a significant nuclear localisation and so most of this signal can be presumed to be from whole cells, rather than a genuine nuclear localisation. It cannot be dismissed however that in the case of a mitochondrial CRISPR system it would be important to be able to prevent off-target action in the nucleus.

6.4.2 Fluorescently labelled gRNAs

Alexa™ 488-UTP can be efficiently incorporated into gRNAs for their cellular imaging. However, the cellular localisation of the FD RNA, chosen as a positive marker of the mitochondrial compartment, does not confidently colocalise to mitochondrial protein. A potential impact could be on mitochondrial folding and hairpin formation: given that altering the 3-dimensional structure of RNAs has the potential to impact RNA import into the mitochondria, it is important to ensure that their incorporation has not impacted their normal fold and function. If incorporation of dyes does impact on gRNA folding, other possibilities for fluorescent UTP incorporation which might be less invasive could be explored such as end-labelling. Although Alexa™ dyes are commonly used in cellular imaging, it is also worth asking whether the dye itself might preclude normal import through some other mechanism.

The Baby Spinach fluorescent aptamer can function when appended to the 5′ end of gRNAs, however it's incompatibility with the 3′ end, meant we did not pursue it further for cellular imaging.

6.4.3 Radiolabelled RNA import into isolated yeast mitochondria

Although attempts were made to isolate mammalian mitochondria, only yeast mitochondria were viable for performing import assays. Yeast import assays with ^{33}P labelled gRNAs and 5′FD gRNA showed gRNAs to be protected from RNase treatment in a manner which is independent of membrane potential. It is important to remember that there might be some inconsistencies between yeast and mammalian mitochondrial import pathways. Furthermore, isolated mitochondria are not in the usual cytosolic context, meaning there might be missing cytosolic factors, such as PNPase (section 1.5.2.1.4), which aid import.

Together, these results suggest that even unmodified gRNAs could be mitochondrially localised. Though none of the assays prove this definitively, there is mounting evidence that gRNAs can import without any modification, particularly given the recent data from Loutre et al[156] showing import, though not function, of gRNAs independent of mitochondrial targeting motifs. This also lends credence to the 2014 Jo et al paper[160]. Reports of directed import of exogenous RNA, summarised in section 1.5.2.2, rely on addition of structured RNAs, typically made up of one or more hairpin structures. Since similar structures are found in gRNAs, it is possible that these are acting as intrinsic import aptamers, in a similar manner to intrinsic MTSs found internally in some proteins such as Atg4D[61]. However, RNA import is a controversial area[125] and as noted above, the import assays as carried out do not provide explicit proof of matrix delivery.

7 The public perception of genome editing

7.1 Summary

There has been widespread agreement on the importance of communication with the public around genome editing[199]. Although many technological advances have the potential to shape ourselves and our society, no other tool holds quite the explicit power of editing DNA. Members of wider society, particularly those who might be impacted by advances in genome editing technologies, should have a level of scientific literacy which is sufficient to enable informed consent (in the case of medical interventions, for example) and informed debate around potential applications of genome editing technologies. As academics I believe it is important to see ourselves as part of society, rather than separate from it. Given our high level of understanding of the current and future possibilities of genome editing, we have a unique opportunity to contribute to the ongoing discourse surrounding scientific development, and to facilitate scientifically-grounded dialogue between publics, policymakers and the research community.

Towards these aims, I undertook an art-based project that was funded by BrisSynBio and which was carried out during a 3-month internship, the 'Professional Internship for PhD students' (PIPs), which is a compulsory component of the South West Biosciences Doctoral Training Programme. This project directly drew on my experiences of using CRISPR in the lab.

Created in collaboration with three Bristol-based artists, *SynBioExpo* was a week-long art exhibition which started a dialogue between Bristol-based publics and researchers surrounding genome editing. *SynBioExpo* allowed a space for members of the public to explore the current and future potential of genome editing, and to have an open and honest discussion with researchers currently working in the field. This chapter starts by contextualising *SynBioExpo* and describing the exhibition. As a researcher, SynBioExpo offered an opportunity to gauge the public perception of genome editing. The second part of this chapter evaluates the impact of *SynBioExpo*: the ways in which publics interacted with the exhibition; the impact on the scientists and artists involved; and whether the exhibition itself, and science-art more broadly, was an effective medium to start this dialogue in Bristol.

7.2 Context: the need for public engagement in genome editing

CRISPR has revolutionised biological research with clear possibilities of transfer to the clinic. The perceived power of the genome editing tool is such that some of the most influential names in the field, including Jennifer Doudna and George Church, called for a moratorium on research in 2015[200]. The group called for a pause in research whilst a consensus was found between research and governmental organisations over the scientific, medical, legal and ethical implications of CRISPR applications. The importance of engaging society in the genome editing field is highlighted by the public rejection of genetically modified organisms

(GMOs) in the 1980s and 1990s. 25 years on from the first commercialised GMO crop (the Flavr Savr tomato[201]) rejection of GMO crops across Europe has had major societal, scientific and economic implications[202] meanwhile they are being profitably farmed across North and South America and China, without any measurable safety problems. The shadow that GM casts over the CRISPR debate highlights the importance of how we choose to frame conversations with the public, and how researchers can respectfully adapt and respond to public concerns.

New technologies often follow a similar pattern with regards to their acceptance by the public[203,204]. When technologies are very new, they are commonly accepted, but with growing media coverage, a feeling of unease rises and there is a phase of public resistance. With time, technologies evolve and the understandings and expectations of the public change. Fears fall, and the new technologies are gradually re-accepted and finally assimilated into day-to-day life, and culture. However, it is not always this straightforward. The initial resistance phase can sometimes turn into a 'technopanic', with intense public backlash – as was the case with GMOs. As cultural and ethical baselines change even these adapt. In the case of GMOs, although there are still many people who are anti-GMO, this is a much smaller percentage of the population in comparison to the 1990s[205].

Given the potential power of CRISPR-based technologies, to completely halt genome editing research in the UK would be a huge disadvantage not only scientifically and economically, but also in not being able to realise a whole host of advantages. That being said, it is important that technological advancements are mindful of the power they create, especially when involving ethically sensitive topics such as germline genome editing.

With fast-paced technological development, it is extremely difficult for regulatory measures to be sufficient to completely control technological applications. The Presidential Commission for the Study of Bioethical Issues' report on Synthetic Biology stated that "creating a culture of responsibility in the synthetic biology community could do more to promote responsible stewardship in synthetic biology than any other single strategy"[206]. This fits with the growing expectation of institutions to take a responsible approach to their research and innovation; Research bodies are increasingly actively considering the wider context and impacts of research and being transparent with the public with regards to their research[207]. This is not to say that the onus should fall wholly onto the individual researcher – a job role which seems to be constantly expanding. But it *is* to say that individual researchers, as gatekeepers of this knowledge, should realise the potential impact they could have on the wellbeing of their own present and future societies. Knowledge sharing, driving excitement for world-class science, and encouraging best practice and ethical research practices in their direct research environment can all be powerful actions within the context of RRI.

A Wisconsin study[208] found that a higher level of knowledge about genome editing (measured by participants who got more than 60% in a test) corresponded with greater acceptance of it (76% of the participants). Similar studies have also found that there is an appetite for learning about genome editing, but it is the responsibilities of experts and governments to ensure that there is information available.

This is particularly pertinent as TALEN-based therapies are already being applied in human patients - a 2014 study was the first to administer TALEN edited cells to human patients with HIV[209] - and CRISPR-based therapies are on the horizon. Although disease amelioration in somatic cells is one of the most widely accepted applications of genome engineering, being agreed on by 64% of people in one study[208], impacted individuals have the right to access clear and open information. Such groups affected by advancements in the treatment of these diseases include patients and their families and carers; fertility patients, who are required for donation of supernumerary embryos to be used in research; and the medical professionals in contact with both groups. As the applications of CRISPR technologies broaden, an ever-increasing percentage of the population will be in contact with these them. Ideally, public literacy surrounding emerging technologies should develop alongside technological advances so that a common language and understanding has been developed well in advance of decision making[210].

7.2.1 Context: BrisSynBio

BrisSynBio is a multidisciplinary £13M Research Council-funded Synthetic Biology Research Centre based at the University of Bristol. BrisSynBio are actively engaged in ethics and responsible research and innovation (RRI) and public engagement in Synthetic Biology, and as part of this provided £1,450 for the development of *SynBioExpo*. *SynBioExpo* was a new project which built on no previous art-science projects by BrisSynBio. It can be seen as a proof-of-concept to determine whether art-science collaborations and an exhibition format is an effective way of encouraging community dialogue around genome editing that could be more widely employed.

7.2.2 Context: Art-Science Collaborations

Following a swell in popularity in the early 2000s[211], art-science collaborations have been becoming increasingly popular as a tool for public engagement. Although art itself does not equate to public engagement, art can provide an alternative 'language' through which to speak about ideas and welcome a different audience, and one that may be more acceptable to some people who, for one reason or another, are "science averse". For the scientists involved, the collaborative process with artists is often found to be mutually enriching, encouraging them to reimagine and revaluate their work and its societal context. Equally, it

offers artists access to a world usually locked away in universities and research labs. The exhibition format allows a narrative journey, and a move away from traditional scientific settings and stereotypes; some groups can therefore find it easier to interact with a scientific topic which they may usually be intimidated by, or not have access to.

7.3 SynBioExpo Aims

SynBioExpo was a collaboration between three University of Bristol researchers and three local Bristol artists which culminated in a week-long exhibition. The overall aim of *SynBioExpo* was:

To curate an art exhibition which facilitated discussion between members of the public and researchers about genome editing technologies.

SynBioExpo aspired to achieve the following public engagement aims:

1. To increase awareness of genome editing technologies, for example CRISPR.
2. To share examples of research projects in Bristol which use genome editing.
3. To enable visitors to interact with researchers who use genome editing.
4. To encourage visitors to question their own opinions on the future applications of genome editing.

And the following aims for us as the organisers:

5. To help understand the public perception of genome editing.
6. To assess whether science-art collaboration is a suitable format for starting an open discussion and debate surrounding genome editing.

7.4 *SynBioExpo* Exhibition Overview

SynBioExpo was held in SPACE gallery, an exhibition space in Old Market, central Bristol. SPACE is co-owned by The Island and ArtSpace LiveSpace, two local community-run charities. Figure 7-1 shows the floorplan of the 3.8 x 6.2 m gallery space, which was split into three sections for *SynBioExpo*:

1. **What is CRISPR?** An introduction to genome editing tools
2. **CRISPR in Bristol** Three Bristol-based research projects which use CRISPR
3. **The Future** An invitation for visitors to imagine the future of CRISPR

Although visitors could visit the pieces in any order, and they were left to explore the exhibition alone, the narrative worked best if visitors travelled through them in order, moving clockwise around the space starting at the door, Figure 7-1 *bottom left*.

Figure 7-1 SynBioExpo *left Floorplan of SPACE gallery, as seen from above. Right top photograph of visitors in the exhibition space*[ix] *right bottom photograph of Arts West Side (SPACE gallery) on the opening night from the outside*[x]

[ix] Unless stated otherwise, all photographs in this chapter thanks to Joe Brown

[x] Photo thanks to Alistair Scott

7.4.1 What is CRISPR

The first section of *SynBioExpo* "What is CRISPR" served as an introduction to the exhibition. A floor-length banner "Symphony" by Theo Wood, a multimedia artist from Bristol. Shown in Figure 7-2 (left), "Symphony" displayed printed words which Theo Wood chose out of the artist-scientist exhibition development meetings. Theo Wood also developed a performance of the words displayed in the piece. "What is CRISPR" also included an introduction of the space consisting of a piece of writing containing information about genome editing tools, Figure 7-2 (right).

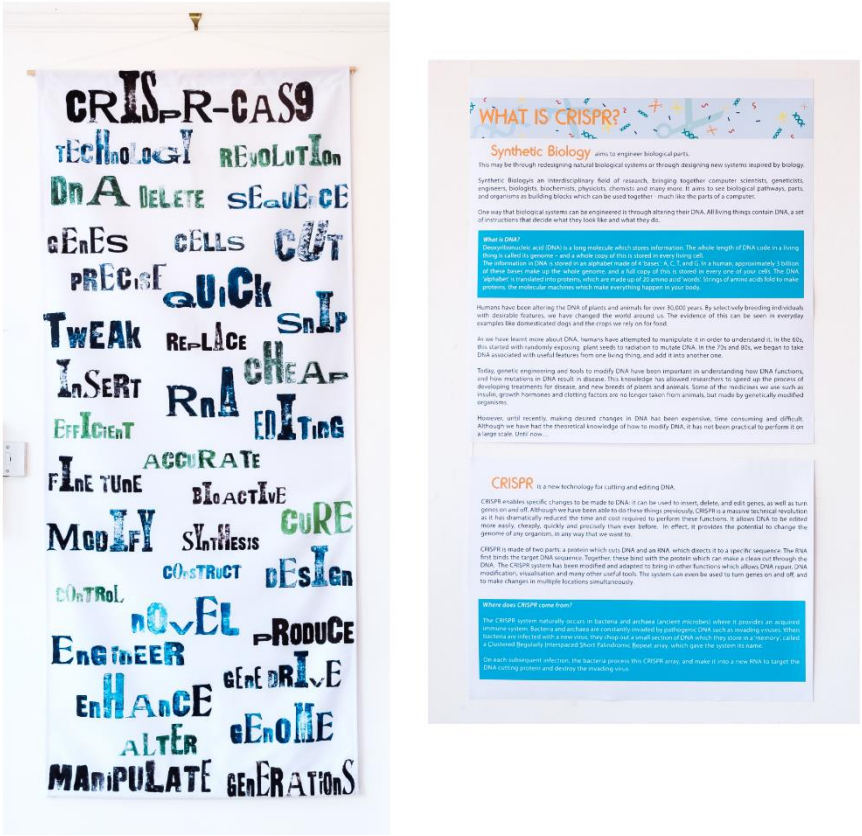

Figure 7-2 What is CRISPR? *Left "Symphony" - Theo Wood and right exhibition introduction*

7.4.2 CRISPR in Bristol

The second section of *SynBioExpo* "CRISPR in Bristol" focused on three University of Bristol research projects which utilise CRISPR. This section of the exhibition aimed to show the importance of genome editing tools to cutting-edge research projects which are currently ongoing; each project was represented in the exhibition with a short summary and two illustrations shown in Figure 7-3, one by Claudia Stocker and one by Imogen Coulter, both illustrators. The projects in this section of the exhibition aimed to highlight the importance of showing a broad range of research which were still in their infancy, some which are closer to basic research, and some which are more explicitly synthetic biology.

The first highlighted project was the work of Joe Hawksworth, a BrisSynBio funded PhD student in the Toye group working to use CRISPR to produce engineered red blood cells. Engineered blood may serve numerous purposes: to mimic disease states for research; to develop a universally accepted blood type; to improve the lifespan or storage properties of cultured blood; for therapeutic purposes such as long-lasting drug delivery vehicles.

The second project was the work of Amber Knapp-Wilson, a University of Bristol funded PhD student in the Kuwabara lab. Amber is using CRISPR to study mitochondrial protein import in the nematode *Caenorhabditis elegans.* Though *C.elegans* is one of the most extensively studied organisms genetic engineering of the worm has traditionally been difficult. The development of CRISPR tools for *C.elegans* has had a significant impact on the use of this model organism. We thought it important to reflect the significant impact of this basic science application of genome engineering technologies to show the impact having CRISPR as a standard laboratory tool. The MitoCRISPR project presented in the earlier chapters formed the third highlighted project in SynBioExpo.

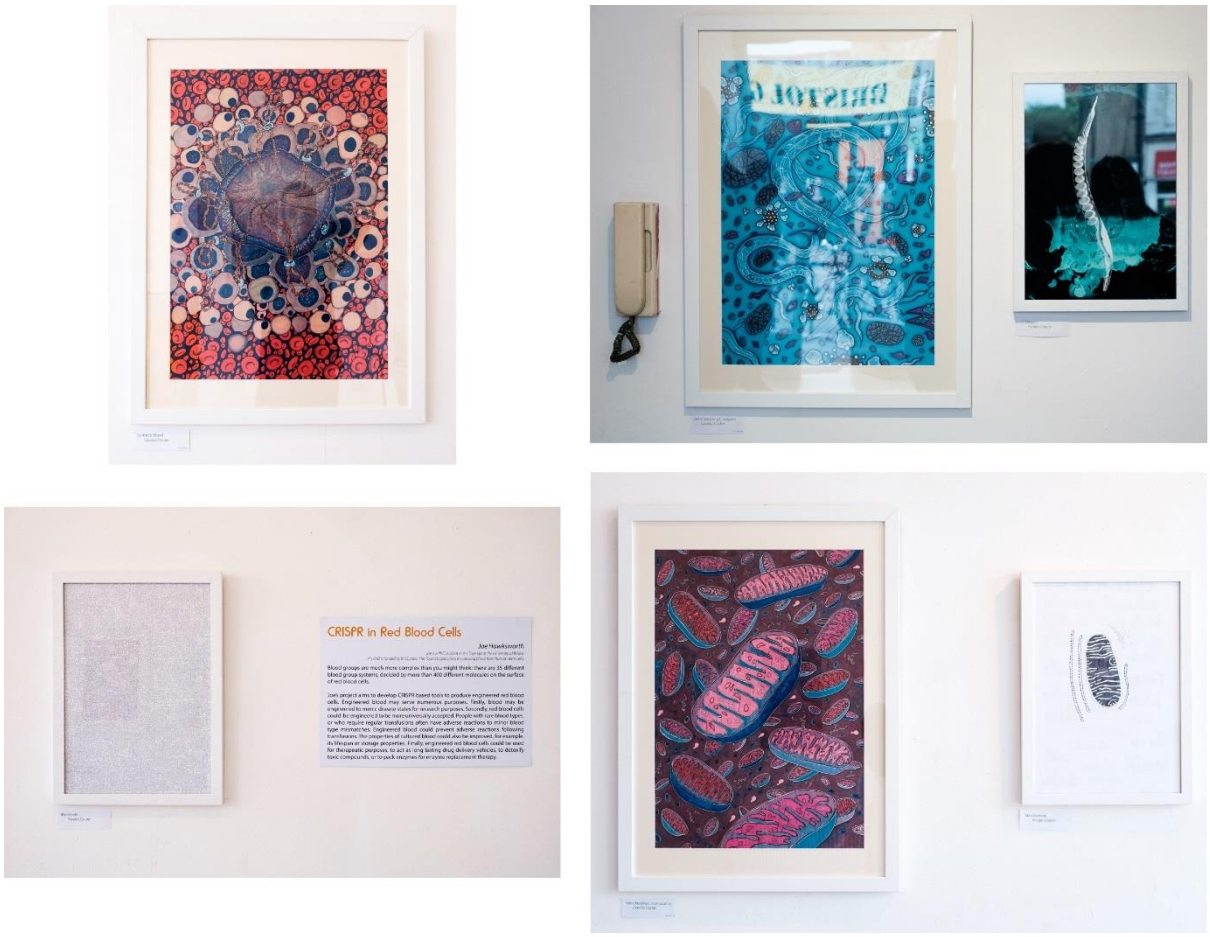

Figure 7-3 CRISPR in Bristol *left top Synthetic Blood – Claudia Stocker; left bottom Blood cells – Imogen Coulter; Right top Deconstructing C.Elegans – Claudia Stocker, C.Elegans – Imogen Coulter; right bottom Mitochondrial Chromosomes – Claudia Stocker, Mitochondria – Imogen Coulter*

7.4.3 CRISPR in the future

The third section of the exhibition prompted visitors to consider the future reimagined with CRISPR technologies. There were three pieces in this section, each encouraging increasing visitor engagement. “The future, bold and new” by Theo Wood featured under-lit brown bottles with flags, each holding an imagined future headline from different times down an imagined timeline of genome engineering. One of the headlines was accompanied by a small ceramic micropig, Figure 7-4.

“Dilemmas”, also developed by Theo Wood, consisted of a set of cards, each with a different bioethical ‘dilemma’ on them, describing an application of genome engineering. After reading the scenario, readers were encouraged to vote on how comfortable they felt with the application by taking a counter and placing it into a box. Counters were colour coded on a traffic light system: Green for ok, amber for maybe and red for no. All the voting counters went into the same wooden box. Responses were not recorded. Instead, the action of the exercise was to prompt visitors to decide, have an internal (and perhaps external) dialogue. A full list of “dilemmas” is provided in Appendix A7-II.

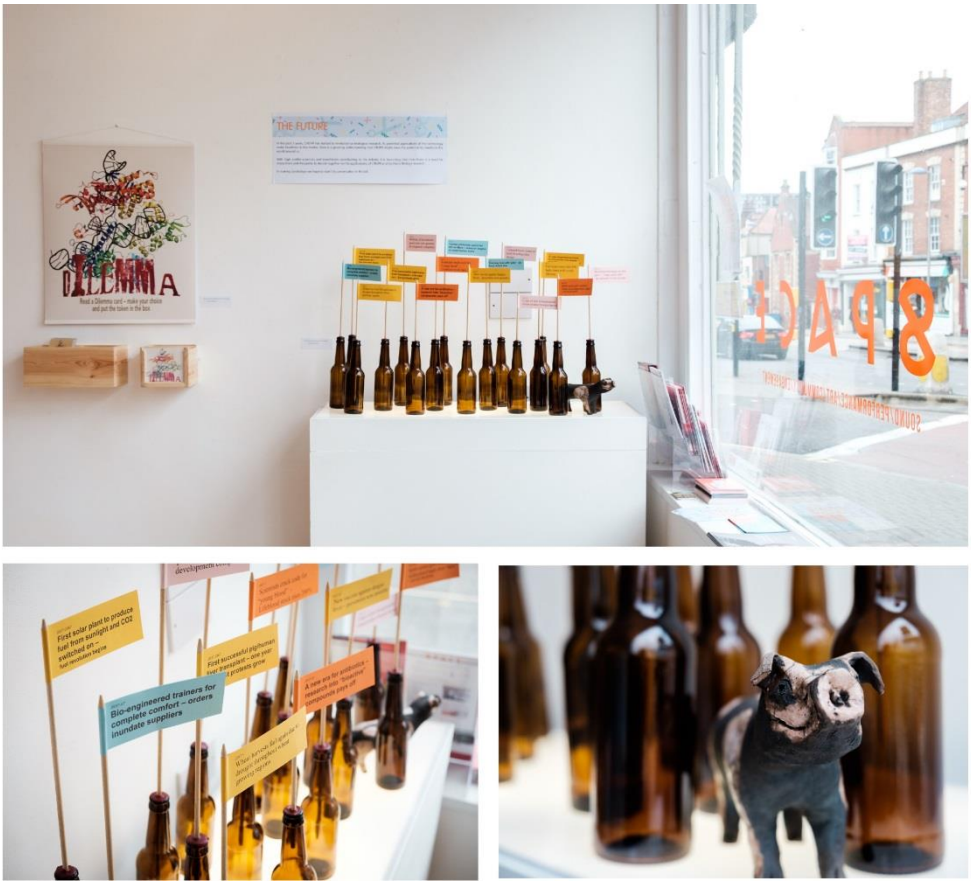

Figure 7-4 The Future

The future section also included a discussion podium, Figure 7-9. Three questions were posed to visitors, written around a podium in the centre of the exhibition space. Visitors were invited to respond to the questions, and other visitors' comments, by taking a post-it note and sticking it on the podium. The podiums were particularly useful given many visitors came to the exhibition alone. Reading and responding to the other comments allowed a dialogue to emerge between visitors who were temporally separated.

Figure 7-5 SynBioExpo

7.4.3.1 Invigilator/Scientist

Throughout the time that the exhibition was open, there was always an invigilator in the space. This was usually myself, but at times I was accompanied by the scientists or artists.

Some visitors were asked whether they would answer a few questions on their experiences of *SynBioExpo*, and were given the option to either fill in a questionnaire on an iPad, or to have their verbal answers transcribed. The 8 individuals all chose the latter, and the results from this are summarised in Figure 7-8 and discussed later in this chapter.

7.5 Evaluating SynBioExpo

Art itself does not equate to public engagement. In order to understand the public perception of genome editing, and to assess whether the engagement aims (section 7.3) were met, visitors to SynBioExpo were invited to participate in a number of evaluation processes, including discussion podiums (Figure 7-9), an evaluation graph (Figure 7-6) and evaluation questionnaire (Figure 7-8). Attendance records were also kept.

To evaluate the impact of *SynBioExpo* on the artists and scientists: the University Centre for Public Engagement ran a focus group with the involved artists and scientists following the exhibition to study art-science collaborations

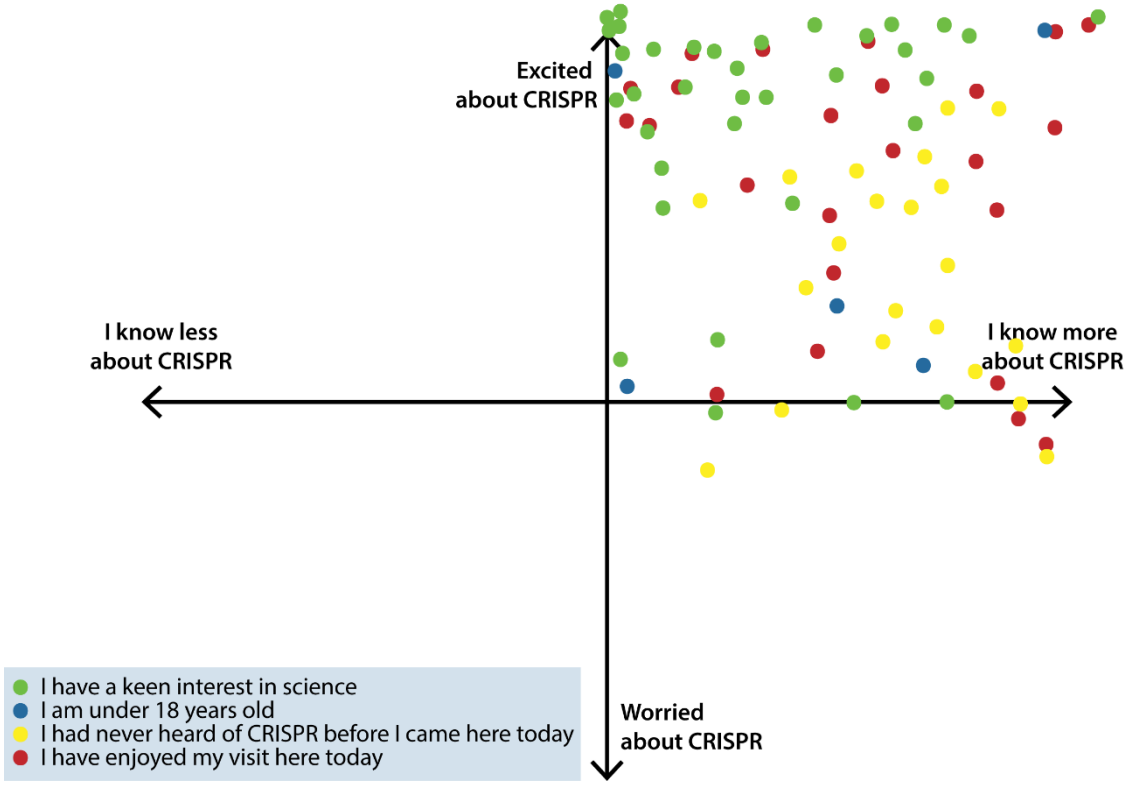

Figure 7-6 Evaluation graph, *contributed to by 85 visitors. 34 green stickers - I have a keen interest in science (40%); 5 blue stickers – I am under 18 years old (6%); 21 yellow stickers – I have never heard of CRISPR before today (25%); 25 red stickers – I have enjoyed my visit here today (29%)*

7.5.1 Visitor attendance and makeup

Over the week of the 24th April 2017, over 170 visitors came to *SynBioExpo*, Figure 7-7. Approximately 75 people came to the exhibition opening evening, most of whom knew either the scientists or researchers involved.

Although this is not insignificant, much could be done to improve attendance in similar events in the future; several questionnaire participants mentioned that they thought the exhibition

would have wider appeal and should have attracted a larger audience; one visitor said in ther evaluation "Do you have any plans for this to be shown again after this? It really is fantastic!". A gallery space in a more central location and altering the run of the exhibition to include more weekend days would have been advantageous: the busiest day, excluding the opening night, was Saturday. Given the proximity to the Easter holidays, timing is also a consideration. Advertising was though leafleting (local cafés and community noticeboards), local radio, and social media, but paid advertisements (for example on social media) might have broadened the reach.

SynBioExpo - Visitor Numbers

	Tues 25th April	Weds 26th April	Thurs 27th April	Fri 28th April	Sat 29th April
10 AM - 12 PM	7	2	2	1	7
12 PM - 2 PM	1	7	5	4	10
2 pm - 4 PM	1	2	2	4	7
4 PM - 6 PM	0	8	2	7	20
Total	**9**	**19**	**11**	**16**	**44**

Mon 24th Opening Evening: ~75 visitors
Tues 25th - Sat 29th: 99 visitors
Total attendance: ~174 visitors

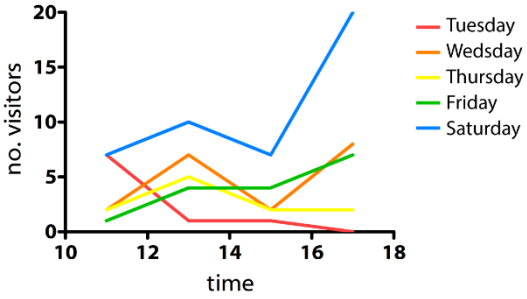

Figure 7-7 SynBioExpo visitor attendance numbers

7.5.2 Evaluating the impact of *SynBioExpo* on the public

In this section, each of the engagement aims from section 7.3 will be discussed in turn.

1. **To increase awareness of genome editing technologies, for example CRISPR**

SynBioExpo was largely successful at achieving an increased awareness of genome editing technologies in its visitors. 25% of the visitors who placed a sticker on the evaluation graph (21/85 individuals) said they had never heard of CRISPR before their visit, Figure 7-6. All the 8 questionnaire participants said they knew more about CRISPR on leaving, and 5 out of 8 said they knew “a lot” more, Figure 7-8. The take-home messages for visitors were broader than just relating to genome editing, however. In response to the question “Can you tell us something you didn’t know before”, every respondent was able to give an answer. Some responses were project specific such as “I didn’t know there were that many blood groups”, and others drew on themes form the exhibition as a whole: “the potential [of CRISPR] is huge, covering all areas”.

2. **To share examples of research projects in Bristol which use genome editing.**

SynBioExpo had a deliberate focus on University of Bristol research projects using genome editing tools. When asked “Can you tell us one thing you have discovered today that you didn't

know before?" one participant replied, "That it's all going on in Bristol - I didn't realise it was such a hub for science and that this was all going on here".

When asked "Can you tell us one thing you have discovered today that you didn't know before?" more than half of the participants gave examples which was linked to the Bristol research projects such as "mitochondrial editing", "the red blood cell research".

3. **To allow publics to interact with researchers who use genome editing**

When asked "What is the most powerful image you are left with after your visit today?" one participant said "it's great to meet the people involved"

Figure 7-8 Evaluation Questionnaire Summary

4. **To encourage visitors to question their own opinions on the future applications of genome editing.**

Through interactive elements such as “Dilemmas” and the question podiums, *SynBioExpo* aimed to prompt visitors into forming new and questioning existing opinions about genome editing. There was no consensus between respondents to the evaluation questionnaire over whether *SynBioExpo* had changed their attitudes towards Synthetic Biology and genome editing. Some who had changed their opinion had become more positive, whereas some had become more concerned. Figure 7-8 displays some selected quotations from the questionnaire.

7.5.3 The public perception of genome editing

SynBioExpo gave an interesting insight into the public perception of genome editing, through evaluation responses, direct conversations or interactions with the exhibits and other visitors.

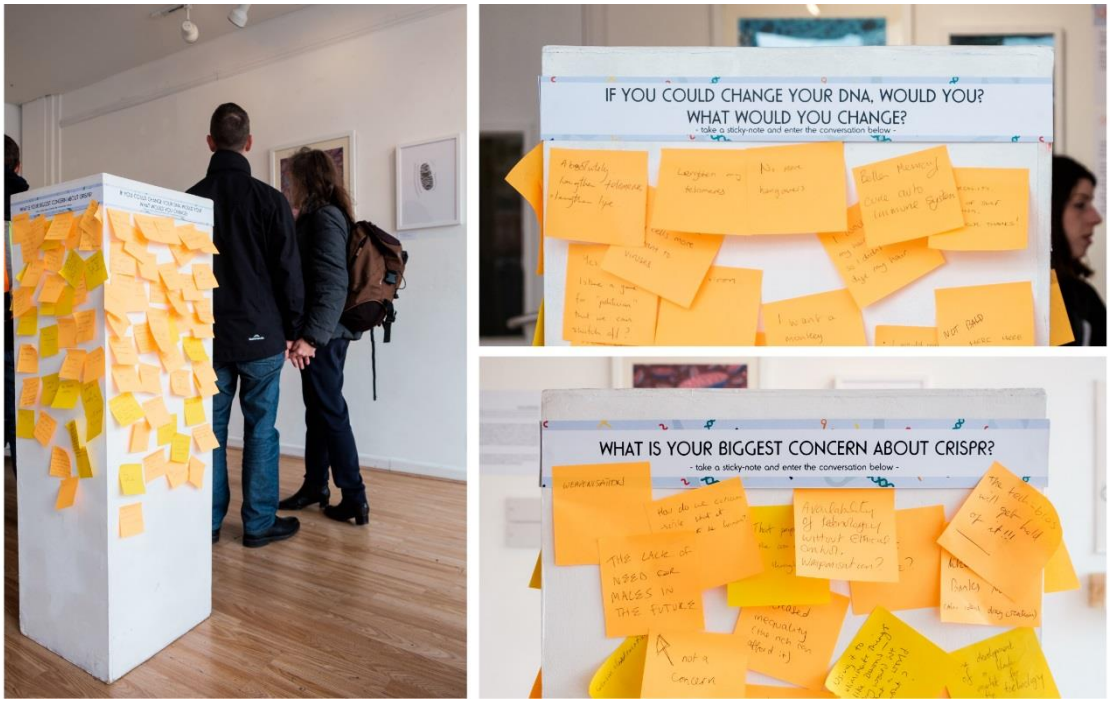

Figure 7-9 Discussion Podiums

Responses on the discussion podiums were a source of insight into the public’s hopes and fears. Most of the responses to the question “What is your biggest concern about CRISPR?” focused on a general lack of safety (“Is it safe?”; “Is it good?”) and misuse of genome editing tools (“weaponization”). Lack of regulation also featured heavily (“in the wrong hands what happens?”) although a small number of individuals were concerned with over-regulation (“people will stop the use of CRISPR through fear”) and the media response to technological advances (“'False facts' being propagated in the media”). Economically-themed concerns

were common (“Corporate misuse of dangerous technologies”; “tailoring humans to create what capitalism wants”; “misuse/abuse for profit”), with the potential for genome editing to worsen social inequality being a common fear. These ranged from issues which are already common place (“medical treatments or other advantages only available to the rich”) through to potential longer-term impacts (“creating a bigger rich/poor divide”; “two tier society of normal/enhanced humans”). A number of philosophical concerns were also aired (“how do we circumscribe what it means to be human”; “not being ‘human’ eventually).

In contrast, “What would you most like to see CRISPR used for?” and “If you could change your DNA, would you? What would you change?” were much more positive. The 38 responses to “What would you most like to see CRISPR used for?” were roughly evenly split between applications in health (“Disease eradication”; cure of inherited disease”), society (“creating a more equal society”, “reduction of poverty and suffering”) and agriculture (“food security”; “reduced pesticide use”), though these responses can all be broadly summarised as the general “Improving quality of life”. Interestingly of the 55 responses to “If you could change your DNA, would you? What would you change?” only 4 responses were explicitly negative (“no”; “not for me personally”) though about 10 responses were joke comments.

The evaluation graph shows us that those with a keen interest in science were, overall, more excited about CRISPR than those who had never heard of CRISPR before their visit, whereas those not from a science background were warier of genome editing. This is in line with previous studies mentioned in section 7.2 which find a correlation between knowledge and acceptance of a topic.

7.5.4 On using art to start discussion about genome editing

Overall, the response to whether an art exhibition was a good medium to introduce a scientific topic was positive. In the public evaluation questionnaire, 7 out of 8 respondents said that they enjoyed the format. The sentiment that the art brought something enjoyable was also brought up by a scientist in the focus group in the months following the exhibition, saying “I just think it's quite good for public engagement to generally inspire people in a sort of creative, fun way”.

There was a general feeling that using visual images made it “very easy to break down the language barrier you might have”, in the words of one of the artists. “I think it's really good because a lot of science work can be really abstract…It's hard to picture” said one if the scientists, so it can help to “try and bridge that gap”. And this was sentiment was echoed by a visitor in the evaluation questionnaire who said the “powerful images help[ed] contextualise the scientific information”. Through providing “a different way of looking at it [the science]” the art certainly seemed to help visitors engage in the science, and perhaps

brought in a new audience, one visitor making the comment that “I wouldn’t have come if it was just a science exhibition”.

7.5.5 Evaluating the impact of SynBioExpo on the artists involved

The artist/scientist focus group gave some interesting insights into the artists’ experiences of the process, and how it has impacted on them personally, their understanding and working practices. It was clear that the project overall was enjoyable for the artists, but moreover it allowed them greater understanding and knowledge of the field. One artist said “[it was] a really interesting project to work on” and another “[it] force[ed] me to do things I'd never done before… [I was] learning from it. So that's why I enjoyed doing it.” SynBioExpo set out to improve the science literacy of the public, and it appeared that this was seen with the artists too; “it was an opportunity to find out more… which was exciting, [it is] a very exciting topic” said one. Another is still actively researching the genome editing field “I did do a lot of research about what's out there … and I continue to do it.” – indeed she still periodically sends emails around the group with science stories of interest.

When asked what the most valuable part of the process was, one artist answered the “opportunity to work with actual scientists”. “I actually do like doing an art and science collaboration rather than just art interested in science” one artist said. Another commented that “collaboration … enhances what you're making” – a sentiment which is thematic of the whole exhibition, as well as the individual pieces. In response to the question “Would you like to be involved in public engagement in the future?” there was an unanimously positive response – “I'd definitely be up for doing more” one keenly exclaimed.

7.5.6 Evaluating the impact of SynBioExpo on the scientists involved

The role of the scientists, excluding myself, was primarily in the development phase of *SynBioExpo* rather than delivery. This was partially due to time concerns, but also other motivations, such as a lack of confidence in, or desire to take part in public engagement. In the focus group, one individual said that “I did the classic scientist thing of not wanting to get involved with the public… this is the way for me to be involved in public engagement without having to talk to any members of the public”. Unfortunately, this might have led to some feelings of a lack of control over the end product; one scientist remarked “the outcome was amazing… but I didn't feel like it was very much down to me”.

Although claiming, for example, that “art is quite far out of my comfort zone”, the two researchers said that they found the process useful (“a really valuable experience”). Both said it allowed them to articulate their own research in different ways; one saying it helped them in “knowing how to communicate [your] research and how to talk to people on a level they can understand”. When asked whether the process helped them in preparation for

talking to the public, the other responded that “it definitely helped me”. Moreover, *SynBioExpo* seemed to shape the scientists’ views of what public engagement could be, how it could be different from their pre-existing ideas, for example: “the thing that's changed for me, is just how to imagine future engagement projects”; and, “I feel like it's given me ideas on how to communicate … a bit more appreciation that it doesn't always have to be the same interpretation that you had imagined”. Overall, it appeared that it was valuable for the scientists to have an insight into the thoughts of the public; “it's very interesting to see how people respond to [the exhibition]”.

When talking about whether being involved in the exhibition had changed the way they approach their work in the lab, it seems that changes have not been directly related to the scientists’ research, although they did spend time “thinking about the bigger picture of the actual applications of my work”. One scientist also said it impacted their teaching work alongside their PhD, saying it made them “change how I would write the tutorials to try and put it into a more visually engaging way”. One PhD student highlighted a perceived lack of confidence, saying that “I don't think it has changed the way I work, but I think it's definitely got the potential to - maybe it's partly because we're PhD students”.

7.5.7 Comment on efficacy of the evaluation methods

Broadly speaking, the evaluation methods for *SynBioExpo* were fit for purpose, with sufficient information collected to answer whether the engagement aims were met. However, a greater depth of information might have been able to be collected if the evaluation questionnaire had been collected by dictaphone as inputting the responses in to the iPad was awkward.

An effort was made to have the discussion podiums and evaluation graph situated as far away from the invigilator’s desk as possible but given the small exhibition space there still might have been some impact on responses. The presence of the invigilator whilst all the evaluation questionnaires were filled out should also be taken into consideration.

7.6 Conclusions and Recommendations

SynBioExpo set out to “curate an art exhibition which facilitated discussion between members of the public and researchers about genome editing technologies”. The evaluation in section 7.5 showed this to be largely successful: an exhibition of work was developed and delivered which not only increased awareness of genome editing research but made a space for public discussion and debate surrounding how genome editing should, or shouldn’t, be implemented. Moreover, the context of an art exhibition seemed to work. The visual interpretation was enjoyed by visitors and facilitated them to engage with the research and gave the researchers involved a fresh perspective on their work.

Perhaps the greatest conclusion from the process of developing and delivering *SynBioExpo* was expressed by of one of the artists: “collaboration … enhances what you're making”. All of the individuals involved with the project were pivotal to its development, perhaps because it was a project where all involved were working mutually away from their comfort zones; “art is quite far out of my comfort zone” said one of the scientists in the focus group, a comment mirrored by an artist comment that “[it] force[ed] me to do things I'd never done before… [I was] learning from it. So that's why I enjoyed doing it”. As a result, the process can be said to have been beneficial to both the artists and scientists involved, as described in sections 7.5.5 and 7.5.6. Interestingly, the scientists did not necessarily need to deliver the exhibition to the public for it to be of benefit to them. The process of meeting with the artists and speaking about their research in-depth to non-specialists itself was enriching, and the publics’ views were captured on the discussion podium. However, from the point of view of the artists and public, interacting with researchers is one of the most valuable parts of the exercise, of which there is no substitute.

7.6.1 Reflections

The following section details a few reflections on the exhibition which are worth considering if similar projects are developed in the future.

Words

Whilst advances in CRISPR have greatly accelerated the pace of genome editing, it is important to recognise that related ethical conversations are simply continuations of those already happening, for example surrounding ZFNs, TALENs and the MRT fertility treatments introduced in Chapter 1. Although the tools are changing, there is a core theme in the bioethical debate that is more general and will certainly continue to happen following future technological advancements. In this way, it is important to consider the language we choose to use in public engagement exercises, ensuring that the terminology of the tools does not interfere with the underlying debate. If the aim of a public engagement exercise is to equip publics with a scientific literacy which will enable them to take part in debate, using the names of specific tools perhaps unnecessarily narrows the topic being discussed, especially as new advances are made. There is, of course, a balance to be struck - whilst society has a right to discuss science without oversimplification, technical terms can obstruct communication.

In the context of *SynBioExpo*, the term “CRISPR” was used a lot as it was the common technology used in the three research projects focussed on in the exhibition. Indeed, many general discussions about genome editing - in the exhibition space but also more widely in the media - have started to use “CRISPR” interchangeably with genome editing. To do this

limits not only the term CRISPR - as discussed in Chapter 1, the scope of CRISPR-based tools is so much more now - but also has the potential to restrict future conversations surrounding genome editing.

We did not take time whilst developing *SynBioExpo* to consider whether it was necessary to use the term CRISPR. In hindsight, using several terms (genome editing, genome engineering, CRISPR and more) might have been confusing to visitors. It was clear that the amount of writing in the introduction to the exhibition should have been reduced, as highlighted by two visitors in the evaluation questionnaire: "To be honest there is an awful lot of reading - all these long words I think ooh, god!"; "there is a lot of text but actually it's very easy to understand once you've started". Nonetheless, CRISPR is a snappy acronym that is undoubtably memorable to many and has become a shorthand for editing more generally.

"I don't want this to be a PR thing"

Throughout the process, the artists involved in *SynBioExpo* brought a refreshing perspective. One artist felt very strongly about the overall message of the exhibition: "I mean, I said very early on, 'I don't want this to be a PR thing'" they recap in the focus group. Through this comment, the artist was stressing their desire that through SynBioExpo we make a space where conversations with the public were a genuine, two-way exchange. They wanted public voices to be respected and reflected-on by researchers. This comment went on to very much shape the exhibition.

A very common concern among academics taking part in public engagement exercises is that they are going to be expected to defend science. They are wary of entering into tricky discussions in which they feel cornered and don't have a simple answer. Due to the innately controversial nature of genome editing, this is an understandable concern. In developing SynBioExpo, we intended to make a space where people could honestly explore together their opinions regarding how genome editing technologies are used, now and in the future. It was important that public engagement in genome editing did not simply become an advertising campaign, but instead be a place where scientists themselves questioned their own motives behind their research, thought of themselves as citizen and scientist.

Preaching to the converted

Science public engagement activities are often heavily attended by scientists. From the engagement graph, this can be seen to be true of *SynBioExpo* too. In holding *SynBioExpo* in an exhibition space, we hoped to appeal to a new audience which would not usually interact with a science event, and avoid any science hierarchy, stereotypes. However, one of the artists commented on the podiums that "I could see a lot of researchers had been and almost hijacked that column". The podium had several comments, which were clearly scientific 'in-

jokes', written on it, and this artist was concerned that these comments would mean that the discussion podium "didn't work in the way that it was perhaps intended". A deliberate choice was made not to censor the discussion podiums at all, but it is possible that these comments resulted in other visitors feeling that they could not comment openly without judgement.

7.7 Legacy

Much of the work developed and lessons learnt during *SynBioExpo* have been shared in new contexts since the *SynBioExpo* exhibition. The dilemma cards formed the basis of a workshop that I delivered at Hillfield's Project Night, a youth group for 11 - 18-year olds run by a local charity in North East Bristol. This pilot session was used as the basis of a successful application to the Biochemical Society Diversity in Science Fund. The pieces themselves were also reexhibited at "Synthetic? | Synthetic Biology meets art", an internal exhibition at BrisSynBio's annual conference.

In October 2017, the National Coordinating Centre for Public Engagement (NCCPE) arranged a Genome Engineering Public Engagement Synergy 'What Works' event at the Wellcome Trust, London. The event brought together a range of researchers, research councils, policy makers and public engagement professionals who are working in public engagement in genome engineering. I attended this event and hosted a sharing session about using art to engage with the public on genome engineering. The lessons learnt through the process were also summarised in an internal seminar that I presented as part of the Centre of Public Engagement's "Engagement Bites" seminar series, also in October 2017.

8 Discussion and Future Work

Tools for manipulating mitochondrial genomes have been in development since the 1990s with the first mtDNA targeting restriction endonucleases. Since then, technological advances have often been applied to understanding the basic biology of the mitochondria, and for development of potential therapeutics through clearing mutated populations of mtDNA. Whereas tools for the manipulation of nDNA are extensive, in particular benefitting from a wave of CRISPR-based tools in the last half decade, there is an unmet challenge in the development of the same breadth of tools for mtDNA. The work detailed in this thesis seeks to expand the tools available for the study of mtDNA by beginning the development of MitoCRISPR, a suite of tools for the manipulation of mitochondrial genomes.

Work in the early stages of this project highlighted that both achieving and assaying a *Spy*Cas9 based system targeting mtDNA will be complicated given the inefficient mitochondrial targeting of the nuclease. Following an expansion in the research group in the intervening years development of the MitoCRISPR system, most likely a Cas12a-based system, is ongoing.

Nevertheless, work detailed in this thesis has laid the foundations for how we might achieve the cellular implementation of MitoCRISPR. Through designing a library of gRNAs for MitoCRISPR, the work detailed in this thesis has interrogated the impact of gRNA structural modifications on gRNA/Cas9 complex formation and activity, the conclusions from which are of value to the CRISPR field more broadly. Additionally, although more work will need to be done in confirmation, we have evidence to suggest that unmodified and 5′ modified *Spy*Cas9 gRNAs are imported into the mitochondria, corroborating findings from other research groups[156,160].

8.1 Targeting CRISPR nucleases to mitochondria

Chapter 3 detailed the steps taken to clone a plasmid encoding mitochondrial targeted *Spy*Cas9 (COX8A-Cas9) under the CMV promoter. Unfortunately, transiently transfecting mammalian cells in culture with plasmid DNA lead to poor cellular expression of mitochondrial and nuclear localised Cas9 as measured by western blotting, immunofluorescence and FACS. Subsequent work by Dr Zuriñe Anton with the same construct showed that cells expressing *Spy*Cas9 suffer a deterioration in mitochondrial health, which is likely impacting cell viability and health overall. At present, the exact cause of this impact on mitochondrial health is unknown, though overexpression and mitochondrial import of a large protein is likely largely disruptive to mitochondrial biology. In contrast, *Lb*Cas12a has since been successfully mitochondrially expressed with three MTSs, the most successful of which being Su9-Cas12a. Dr Anton is currently undergoing work to characterise a stable cell line expressing Su9-Cas12a-GFP.

The difference in mitochondrial targeting efficiency between Cas9 and Cas12a is intriguing. MTS accessibility is important for protein import, and it may be that the peptide is presented suboptimally on Cas9. Exploring mitochondrial targeting of Cas9 with alternative MTSs or introducing a flexible linker between the MTS and Cas9 structure in conjunction with *in silico* modelling might ameliorate this. However, the observed transfection of nuclear targeted Cas9 was also inefficient which might reflect expression problems at the RNA or protein level, overcome to some extent with Cas12a. Amino acid bias or differences in overall peptide charge of imported proteins should also be considered, as favourable interactions with TOM/TIM will encourage mitochondrial import. If features favouring Cas12a import over Cas9 are understood there would be the potential to modify the Cas9 structure, optimising it for mitochondrial import. This is particularly attractive since there is now such a broad range of CRISPR tools which are optimised for the Cas9-based system. Furthermore, any general rules governing mitochondrial import could be screened for against the large number of CRISPR-Cas variants in the pangenome.

8.2 Modifying CRISPR RNAs for mitochondrial targeting

Chapter 4 designed and *in vitro* transcribed a library of gRNAs with mitochondrial targeting and functional structures. Through a series of ensemble and single molecule assays, we determined that *Spy*Cas9 gRNAs can be edited at several sites, namely the 3′ end, upper stem and hairpins with no impact on gRNA loading, R-loop formation or endonuclease activity. In contrast, even small modifications are not tolerated adjacent to the spacer at the 5′ end of the gRNA. gRNAs with a 20 nt hairpin on the 5′ end form small R-loops and consequently cannot cleave a supercoiled DNA substrate. Chapter 5.1 explored this effect further, finding that nucleotide mismatches at the 5′ end, such as from the natural T7 RNA polymerase, negatively impact endonuclease activity. Adding successive unmatched nucleotides in this position results in a stepwise reduction in endonuclease activity.

Initially, the finding that 5′ gRNA modifications negatively impact endonuclease activity seems a disadvantage. However, of consideration is the fact that nuclease null Cas9 mutants have had widespread application in the growing CRISPR toolbox (section 1.4.5). Reframed in this context, the findings of chapters 4 and 5 begin to characterise a system where an active Cas9 can be “turned-off” by switching the available gRNA. There may also be other benefits to these overhanging nucleotides: gRNAs with two mismatched 5′ guanines have been shown to show decreased off-target CRISPR activity[212]. It is likely that the decreased cleavage at both on-target and off-target sites has a common mechanism, perhaps the result of altered RNP structure or stability.

Following the work in Chapter 3, it appears increasingly likely that *Lb*Cas12a, rather than *Spy*Cas9, will be the CRISPR nuclease employed in a MitoCRISPR tool. Nevertheless, there is still benefit in understanding the impact of Cas9 gRNA structural modifications given the widespread application of gRNA structural and functional modifications in CRISPR/Cas9 tools targeting nDNA.

Unfortunately, the efficiency of Cas12a mitochondrial targeting was discovered too late in this project to study Cas12a crRNA modifications as rigorously as with *Spy*Cas9 gRNAs; Chapter 5.2 briefly investigated the impact on crRNA modifications on endonuclease activity. Similar to the gRNA, crRNA modifications adjacent to the spacer - the *Lb*Cas12a crRNA 3′ end - were not tolerated by Cas12a. Four unmatched nucleotides on the 3′ end had a great impact on Cas12a endonuclease activity. Initially, 5′ crRNA modifications seemed to be tolerated by Cas12a. However, this is likely due to the fact that our crRNA 5′ modifications were cleaved off by Cas12a, which possesses RNase activity for processing pre-crRNAs, leaving an unmodified crRNA.

This thesis was not able to explore whether Cas12a crRNAs are able to be mitochondrially targeted, though the smaller size of Cas12a crRNAs might be more favourable for mitochondrial import. Given that the 3′ end cannot be modified without compromising endonuclease activity and the 5′ end will be processed, upper stem modifications might be of interest. Alternatively, characterising and ensuring crRNA processing of targeting modifications once inside the mitochondria could also be advantageous. The MitoCRISPR research group is also currently pursuing methods for mitochondrial targeting of crRNAs which do not rely on RNA structures, as outlined below.

8.3 Directing CRISPR RNAs to the mitochondria

Much of this thesis focussed on the addition of RNA structures to *Spy*Cas9 gRNAs with the expectation that they would be required in order to deliver these RNAs to the mitochondrial matrix. Work described in Chapter 6 tested whether this was indeed the case through assays with whole cells and isolated yeast mitochondria. In contrast to our initial expectations, work described in Chapter 6 adds to a growing body of research surrounding the mitochondrial localisation of unmodified gRNAs, without the requirement for targeting modifications [125,156,160]. It remains to be seen whether gRNAs are reliably delivered to mitochondria with RNA aptamers, and whether they are able to deliver the broad functionality available for manipulation of nuclear DNA.

Isolated yeast mitochondria import assays suggest that radiolabelled gRNAs are imported independently of membrane potential. Import is also seen by Northern blotting for unlabelled RNAs in whole mammalian cells, though the fractionation protocol was too crude to exclude

mixing of fractions mixed. The importation of Alexa™-labelled RNAs was less clear, and even FD-488 RNA, a positive control, did not show distinct mitochondrial localisation. In each of these assays, the addition of a mitochondrial targeting hairpin, be that RP or FD, did not appear to alter gRNA cellular localisation. Overall, it is worth following up these experiments with other techniques to ascertain whether RNAs are mitochondrially localised; of particular importance is the generation of assays for following mitochondrial import with clear positive and negative controls.

Given the inconclusive nature of these studies using RNA structures, Dr Holly Ford is currently investigating alternative methods of targeting RNAs to the mitochondria including peptide-RNA chimeras. Peptide MTSs have been crosslinked to oligonucleotides for delivery to the mitochondria via the TOM/TIM protein import machinery[213–215]. Using 44 nt ssDNA as a prototype for *Lb*Cas12a crRNA, Dr Ford has conjugated a truncated COX8A MTS to the 5′ or 3′ end of a ssDNA and seen that the chimeras are imported into isolated yeast mitochondria. The chimeras are cleaved by the processing peptidase in the mitochondrial matrix and protected from subsequent treatment with proteinase. She is now moving on to develop peptide-RNA chimeras and measure their import by the same assay. As with the RNA aptamers, it will be necessary to ensure peptide modifications are not inhibitory to Cas12a complex formation and endonuclease activity, whether that be through Cas12a RNA processing or other means. The obvious limitation to a peptide-RNA fusion is that endogenous expression from a recombinant plasmid or virus would not be possible. Nevertheless, there could be advantages, such as the peptide being cleaved off by MPP after mitochondrial import, providing a method for measuring import, and the incorporation of other reporters or functionalities.

There are also several other methods which could be explored for the mitochondrial targeting of RNAs if unmodified gRNAs are not targeted to the mitochondria, or if mitochondrial localisation is to be enhanced. Non-specific RNA binding proteins such as DHFR have been shown to be able to deliver RNAs to mitochondria[216]. RNAs could also be delivered to mitochondria in vesicles such as with MITOporter, a liposome-based system for delivery of macromolecules in to the mitochondria. MITOporter liposomes have a diameter of approximately 200 nm and have been used to deliver RNA[217] and proteins[67] to the mitochondria. They could be efficacious for delivery of RNPs for mtDNA manipulation, which might have benefits over stable expression, or separate delivery of RNA and protein compionents, as discussed in Chapter 3. Similarly, dequalinium amphiphile nanoparticles, DQAsomes, self-assemble around DNA, and interact with cardiolipin in the mitochondrial membrane, and could be used for delivery of RNA[218–220].

8.4 The manipulation of mitochondrial genomes

Given the impact that tools for the efficient manipulation of mtDNA would have on the study of mtDNA and disease, it is not surprising that there have been several published efforts to develop MitoCRISPR tools by other research groups during the course of this PhD. Though there have been several studies published, summarised in 1.6, none have yet described a tool that is as efficient as the best ZFN and TALEN examples. The most successful iteration to date has achieved a depletion of mtDNA copy number[156], but CRISPR-mediated heteroplasmy purification has yet to be achieved. Based on our findings, we would suggest that the development of MitoCRISPR is a more complex task than was first anticipated.

Given the difficulties developing MitoCRISPR, other methods for mtDNA manipulation which have previously been demonstrated to work (such as TALENs), may be more suitable for further development. Although MitoCRISPR may not be available in the short term, or possibly never[125], development and refinement of alternative tools may drive mtDNA editing into wider use.

As research progresses and we are able to edit genomes more efficiently and at lower cost than ever before, there is a pressing need to address the bioethical implications of the tools we are developing. The successful use of heteroplasmy purification technologies in model organisms shows that mtDNA editing technologies are perhaps not far from the clinic, a fact which has real bioethical implications. The widespread public acceptance and licencing of MRT fertility treatments means that there is a precedent for mtDNA interventions to be accepted by the public. Nevertheless, it is important for researchers to be actively involved in discourse with the public surrounding the application of such technologies from the offset, in doing so facilitating the avoidance of a 'technopanic' of the scale seen with GMO crops.

To this end, Chapter 7 detailed an art-science public engagement exercise, through which we evidenced that simple projects can impact upon the public understanding of and attitude towards genome editing technologies. The evaluation of the *SynBioExpo* project lead us to a number of conclusions which might be of use to researchers conducting similar exercises. In particular, rather than a 'PR exercise' it is important that public engagement surrounding controversial issues such as genome editing are entered into expecting a 2-way exchange, where researchers respect and listen to the voices of the public. It is important that researchers be reflexive with respect to exploring their own role in society and research practices and are open to entering into discussion. Importantly, exercises should be developed to be mindful of the language they use, striking a balance between discussing science without over simplification whilst not obstructing important bioethical debate with detail.

Appendices

A1 Chapter 1

A2 Chapter 2

The following sequences were supplied by Eurofins Genomics as synthesised gene fragments in pEX plasmids, listed in Table 9. All sequences are given 5′ - 3′

pEX-A2-MTS and Spinach

ACATGTCCGTCCTGACGCCGCTGCTGCTGCGGGGCTTGACAGGCTCGGCCCGGCGGCTCCCAGTGCCGCG
CGCCAAGATCCATTCGTTGGGGGATCCACCGGTCGATGTAACTGAATGAAATGGTGAAGGACGGGTCCAG
TAGGCTGCTTCGGCAGCCTACTTGTTGAGTAGAGTGTGAGCTCCGTAACTAGTTACATC

pEX-A2-g#GM SP1gRNA 5′ Baby Spinach

GGTACCGGTGAAGGACGGGTCCAGTAGTTCGCTACTGTTGAGTAGAGTGTGAGCTCCCGCTAAAGAGGAA
GAGGACAGTTTTAGAGCTAGAAATAGCAAGTTAAAATAAGGCTAGTCCGTTATCAACTTGAAAAAGTGGC
ACCGAGTCGGTGCTTTTTTG

pEX-A2-g#GM SP1gRNA 3′ Baby Spinach

GGTACCCGCTAAAGAGGAAGAGGACAGTTTTAGAGCTAGAAATAGCAAGTTAAAATAAGGCTAGTCCGTT
ATCAACTTGAAAAAGTGGCACCGAGTCGGTGCGGTGAAGGACGGGTCCAGTAGTTCGCTACTGTTGAGTA
GAGTGTGAGCTCCTTTTTTGAATTC

pEX-A2-g#GM SP1gRNA 5′ RP

GGTACCTCTCCCTGAGCTTCAGGGAGCGCTAAAGAGGAAGAGGACAGTTTTAGAGCTAGAAATAGCAAGT
TAAAATAAGGCTAGTCCGTTATCAACTTGAAAAAGTGGCACCGAGTCGGTGCTTTTTTGAATTC

pEX-A2-g#GM SP1gRNA 3′ RP

GGTACCCGCTAAAGAGGAAGAGGACAGTTTTAGAGCTAGAAATAGCAAGTTAAAATAAGGCTAGTCCGTT
ATCAACTTGAAAAAGTGGCACCGAGTCGGTGCTCTCCCTGAGCTTCAGGGAGTTTTTTGAATTC

pEX-A2-g#GM SP1gRNA US RP

GGTACCCGCTAAAGAGGAAGAGGACAGTTTTAGAGCTCCCTGAGCTTCAGGGAGCAAGTTAAAATAAGGC
TAGTCCGTTATCAACTTGAAAAAGTGGCACCGAGTCGGTGCTTTTTTGAATTC

pEX-A2-g#GM SP1gRNA H RP_1

GGTACCCGCTAAAGAGGAAGAGGACAGTTTTAGAGCTAGAAATAGCAAGTTAAAATAAGGCTAGTCCGTT
ATCAACTTGACTCCCTGAGCTTCAGGGAGAAAAGTGGCACCGAGTCGGTGCTTTTTTGAATTC

pEX-A2-g#GM SP1gRNA H RP_2

GGTACCCGCTAAAGAGGAAGAGGACAGTTTTAGAGCTAGAAATAGCAAGTTAAAATAAGGCTAG
TCCGTTATCAACTCCCTGAGCTTCAGGGAGTGGCACCGAGTCGGTGCTTTTTTGAATTC

pEX-A2-BoBS & tRNA(K)

CTCGAGAAGGACGGGTCCGGACGCAAGGACGGGTCCGACCGAAAGGACGGGTCCAATGGTGGAA
ACACCATTGTTGAGTAGAGTGTGAGTCGGTCGTTGAGTAGAGTGTGAGGCGTCCGTTGAGTAGA
GTGTGAGGCTAGCGAGCCTTGTTGGCGCAATCGGTAGCGCGTATGACTCTTAATCATAAGGTTA
GGGGTTCGAGCCCCCTACAGGGCTCCCCGGG

A3 Chapter 3

A3-I Cloning pD1301

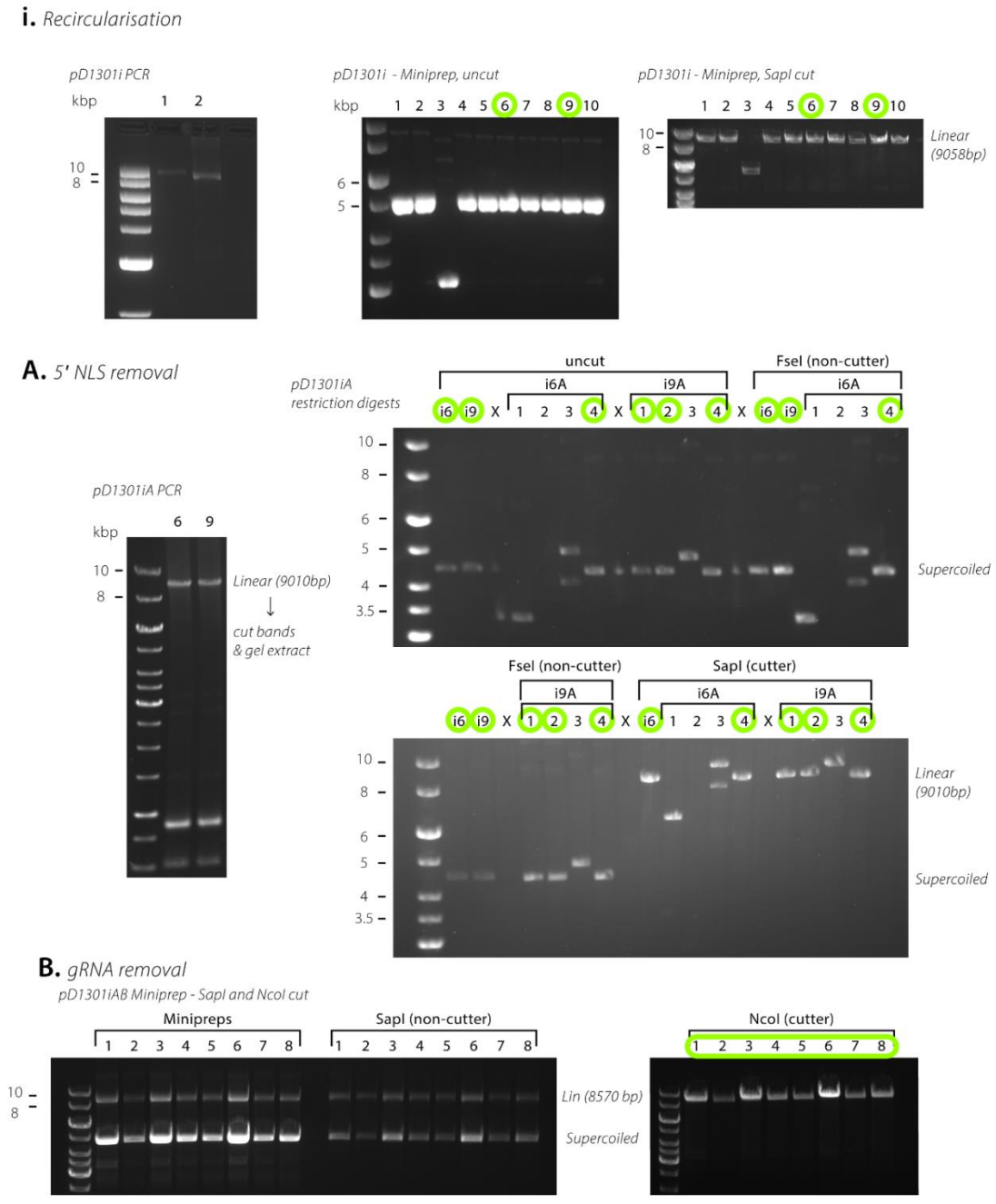

Figure A-1 pD1301 cloning **i** *left pD1301i PCR product centre pD1301i ligated and miniprepped right pD1301i linearised with SapI, showing introduction of sites by PCR. Two colonies pD1031i6 and pD1301i9 have the correct sequence (green circle)* ***A*** *left 5′ NLS removal by PCR gives 9010 bp product right pD1301iA is ligated and miniprepped. Removal of FseI site shows correct PCR amplification. Single cut with SapI shows correct size plasmid.* ***B*** *gRNA removal by PCR (not shown) gives a product of 8570 bp which Is ligated. Non-cutting with SapI confirms gRNA scaffold is removed, NcoI (single cutter) confirms correct length of product. All gels are 1% agarose. Green circle = correct clone.*

A3-II Cloning pD1301

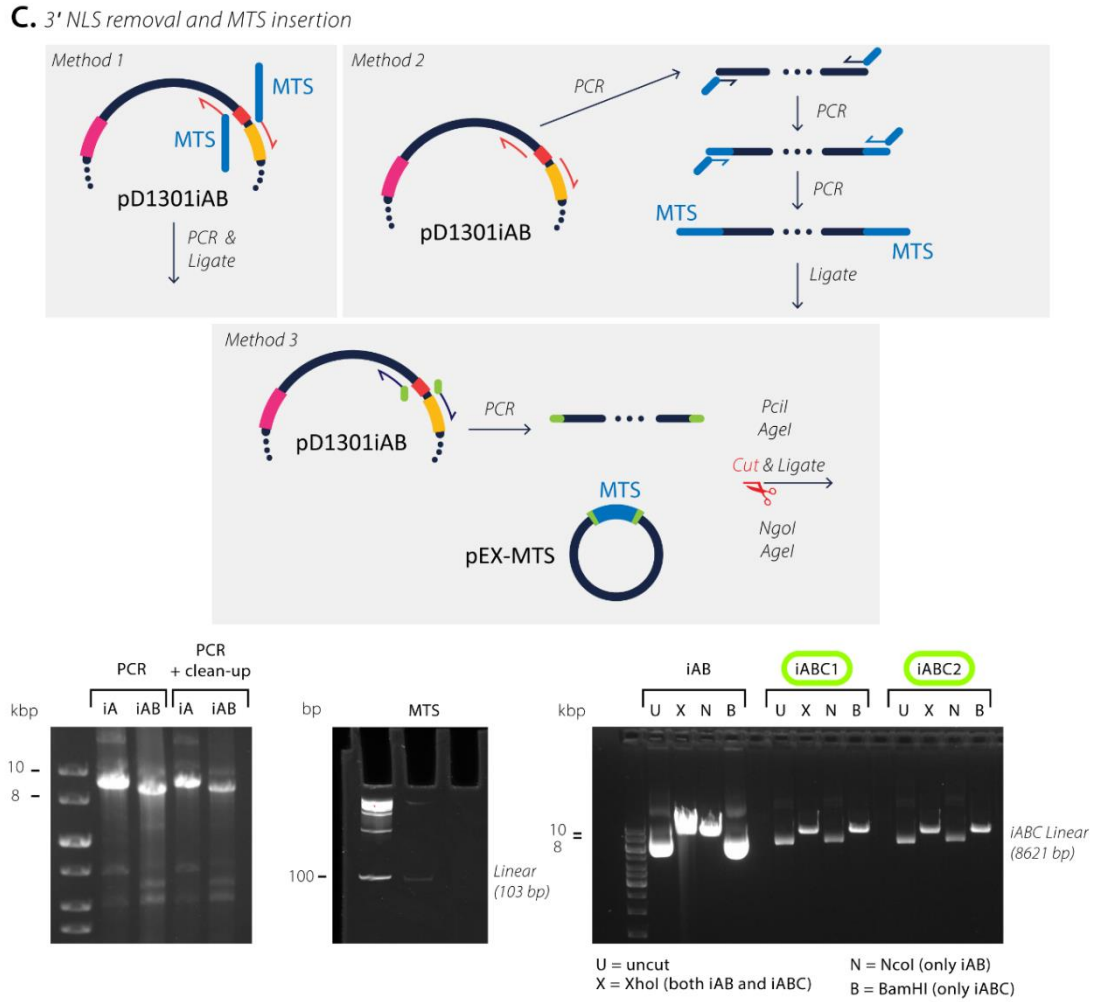

Figure A-2 pD1301 cloning C Method 1 *Introducing MTS through inverse PCR* ***Method 2*** *Introducing MTS through nesdted primer PCR* ***Method*** *3 Introducing MTS as insert cout out of another plasmid pEX-MTS.* ***bottom left*** *PCR of pD1301iA and pD1301iAB to make pD1301iAC and pD1301iABC* ***centre*** *F103 bp MTS fragment cut out of pEX-MTS, separated on 10% native PAGE* ***right*** *Restriction digests to determine correct insertion of MTS into pD1301iAB to give pD1301iABC. Green circle = correct clone.*

A3-III Genomic Cleavage Detection Assay

Many kits were developed during the course of this project which advertised decreased timescales and increased efficiency through RNP approaches to CRISPR workflows. Following a lack of progress with the plasmid transfection approach for studying Cas9 localisation, we decided to attempt an RNP approach. This also provided a tool with which to look at the work from Jo *et al*, introduced in section 1.6, which claimed to show depletion of mtDNA with a nuclear-targeted Cas9 and an unmodified gRNA [160]. Jo *et al* designed three mtDNA-targeted gRNAs targeting the mitochondrial COX1, COX2 and COX3 genes. Figure A-3 shows the GeneArt® Genomic Cleavage Detection Assay (Invitrogen) kit used to target a control nuclear gene (HPRT), provided with the kit, and the three mitochondrial genes COX1, COX2 and COX3. Very low cleavage was seen, with the kit's positive control (nuclear HPRT), and no cleavage was seen with COX1-3. For a brief description of the GCDA assay, see section 2.12.2.

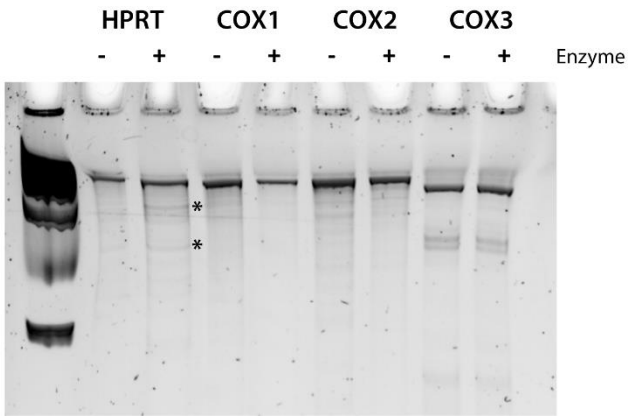

Figure A-3 Genomic Cleavage Detection Assay *HeLa cells were transfected with Cas9RNP targeting either the nuclear HPRT gene, or mitochondrial COX1/2/3 genes, using the GeneArt™ gRNA Synthesis and Precision™ Cas9 nuclease transfection protocol. A PCR was performed across the region of interest for use with the GCDA. The control HPRT reaction shows some cleavage (* bands) whereas there is no cleavage with COX1/2/3.*

A4 Chapter 4

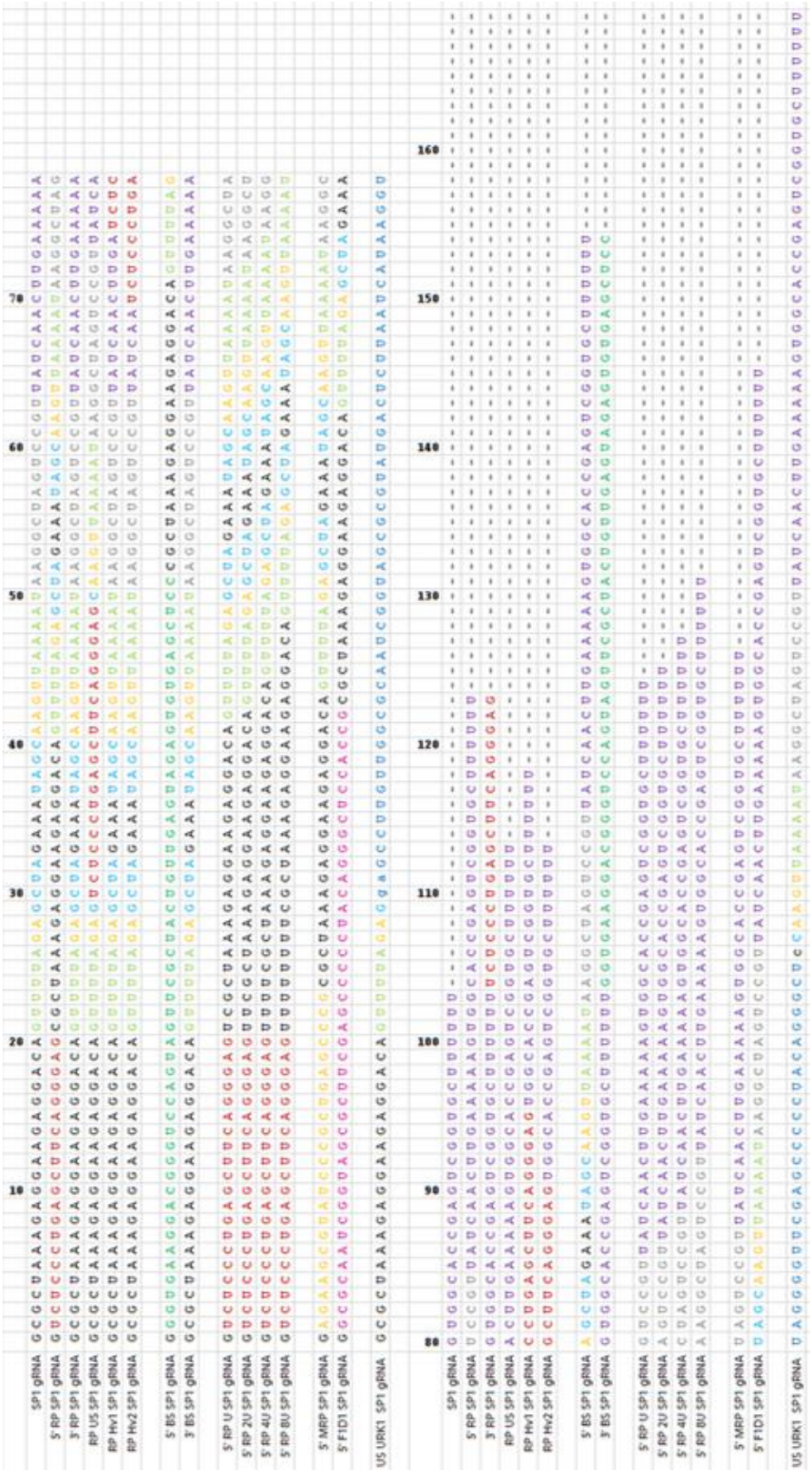

Figure A-4 Chapter 4 gRNA library sequences *colouring is consistent with Figure 4-1.*

A4-II Cas9$_{hinge}$ purification

5ml HisTrap HP
Column 1

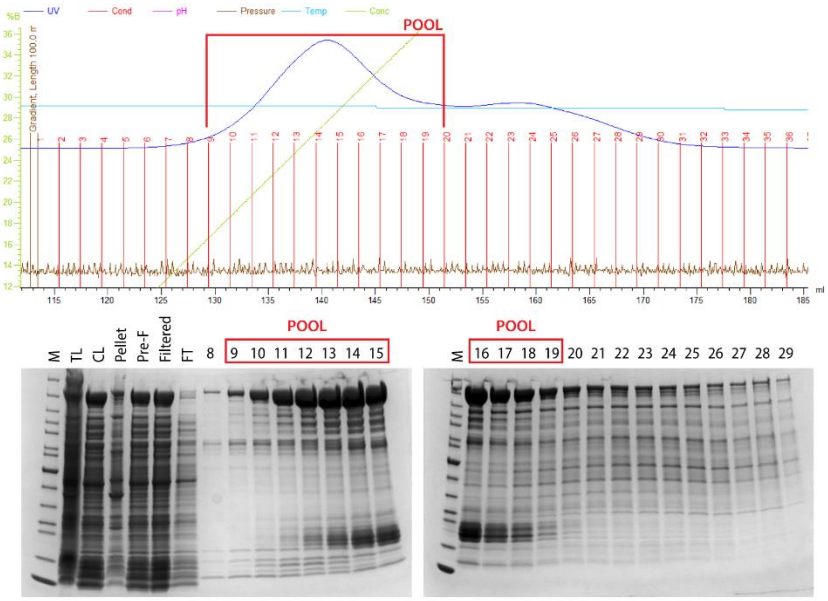

[Cas9$_{hinge}$ His1 pool] = 1.36mg/ml, 22ml (approx. 29.2 mg Cas9$_{hinge}$ total)

Overnight SUMO protease cleavage (30 mg SUMO protease in SnakeSkin dialysis tubing; dialysis against 2L *HisWash 2*; 4°C)

5ml HisTrap HP
Column 2

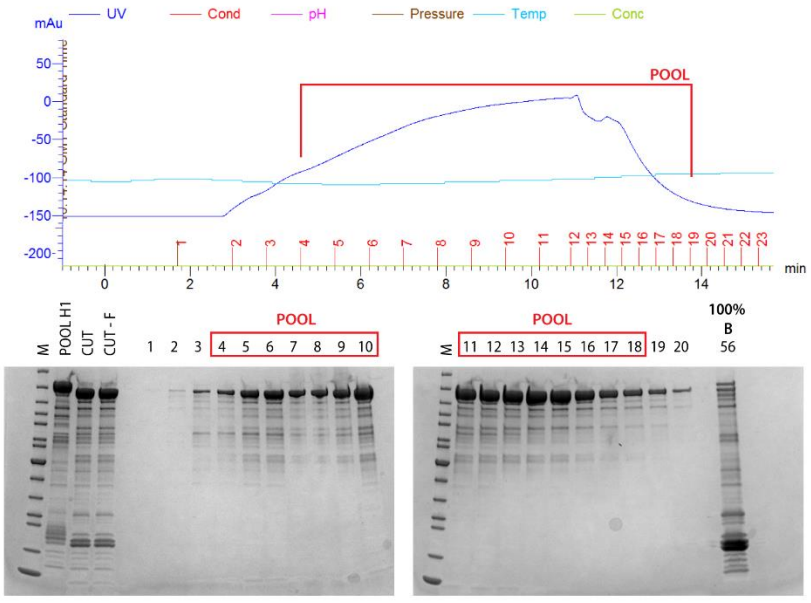

Concentrate Cas9$_{hinge}$ His2 pool

50k Amicon Centrifugal filter units;
buffer exchange into *GF buffer* for labelling

[Cas9hinge His2 pool] = 31.2 mg/ml, 197.47 µM

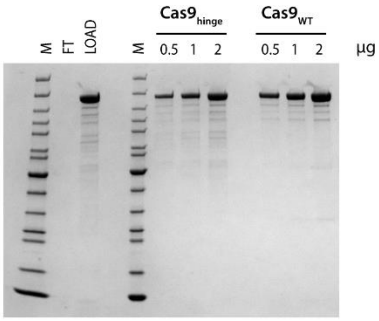

Figure A-5 Cas9$_{hinge}$ purification *See section 2.7.1 for details*

A4-III Cas9$_{hinge}$ labelling

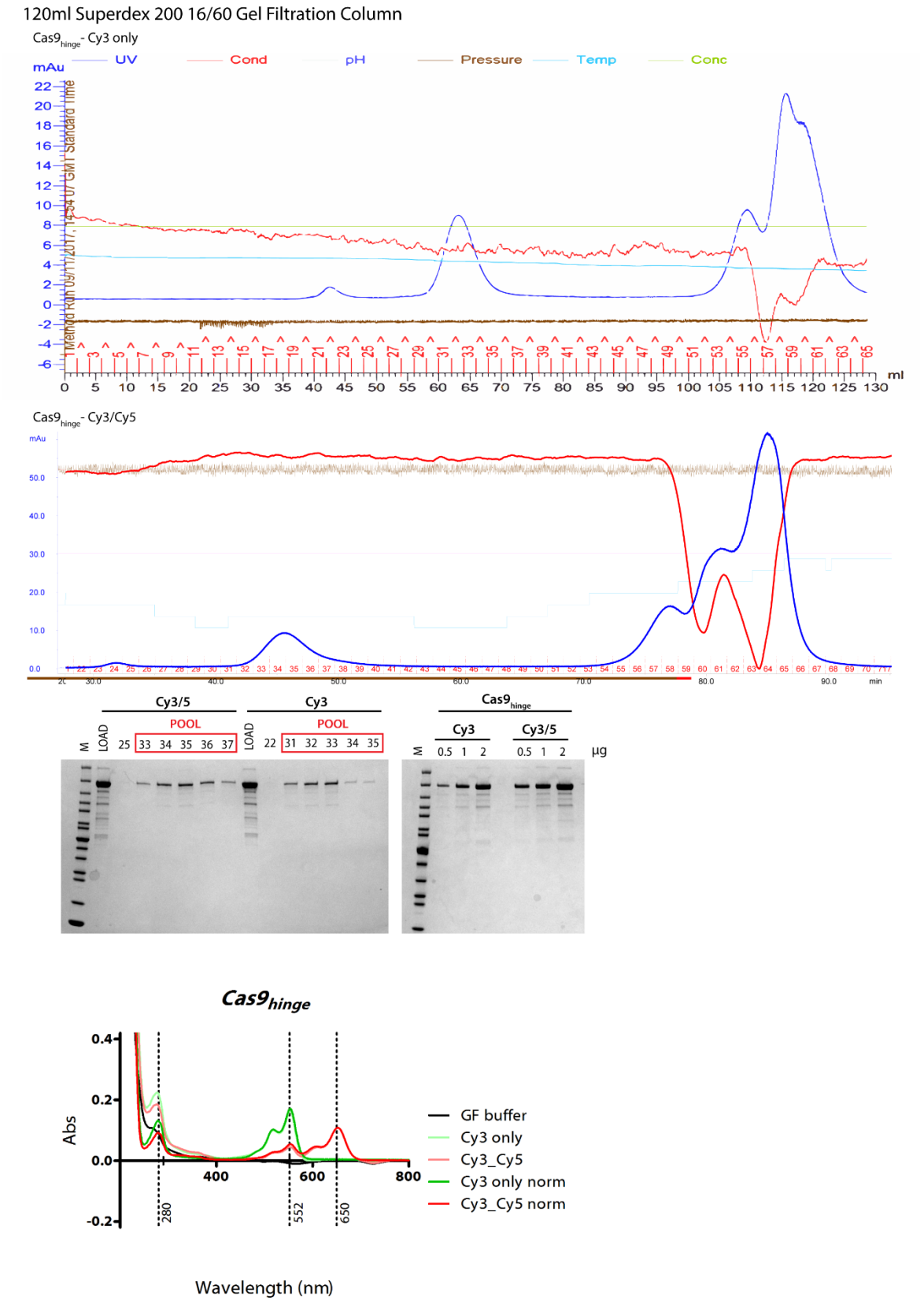

Figure A-6 Cas9$_{hinge}$ labelling *See section 2.7.1 for details*

A4-IV Cas9$_{hinge}$ traces

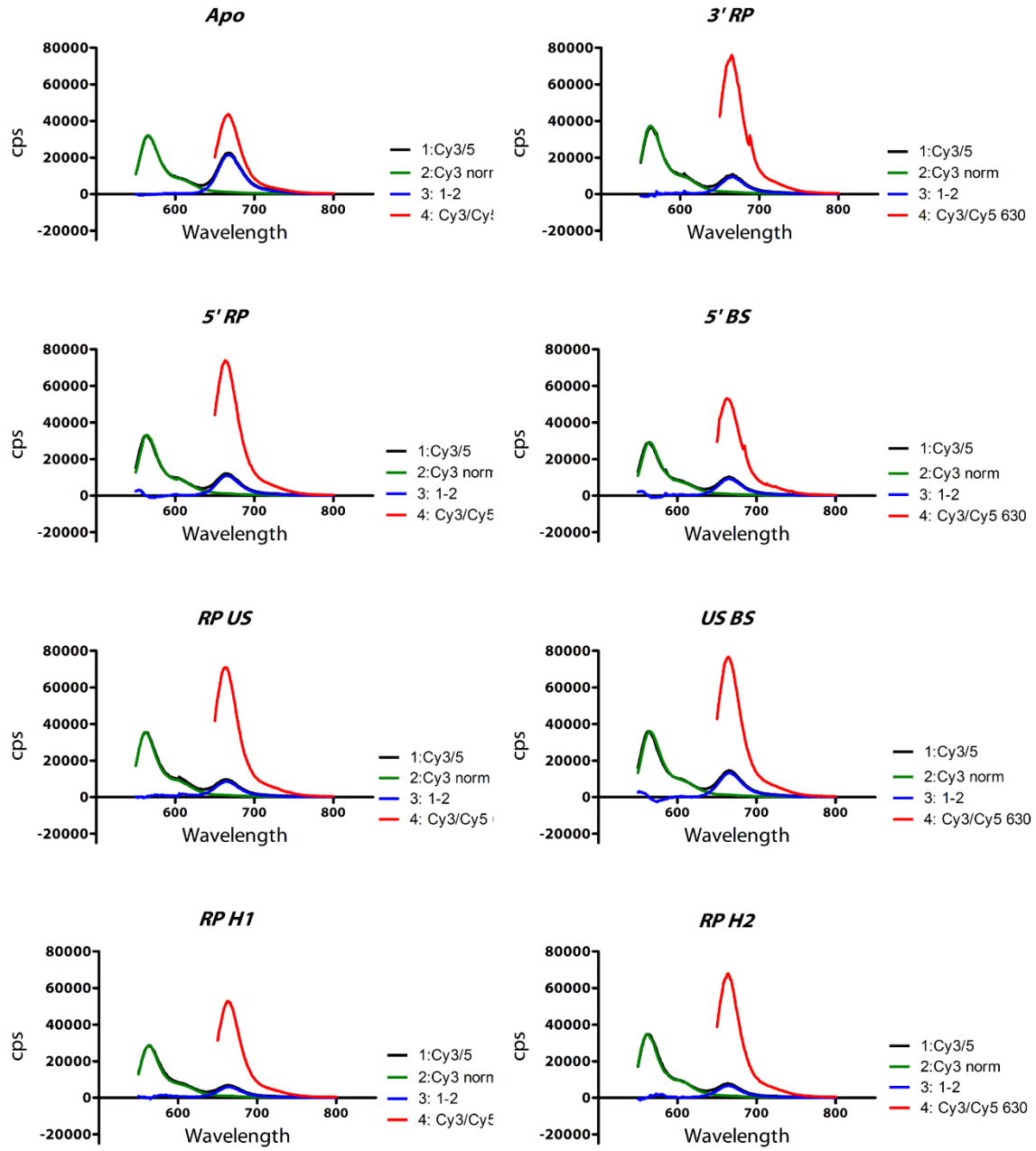

Figure A-7 Cas9$_{hinge}$ Example Fluorolog traces

A4-V Cas9$_{HNH}$ purification

5ml HisTrap HP
Column 1

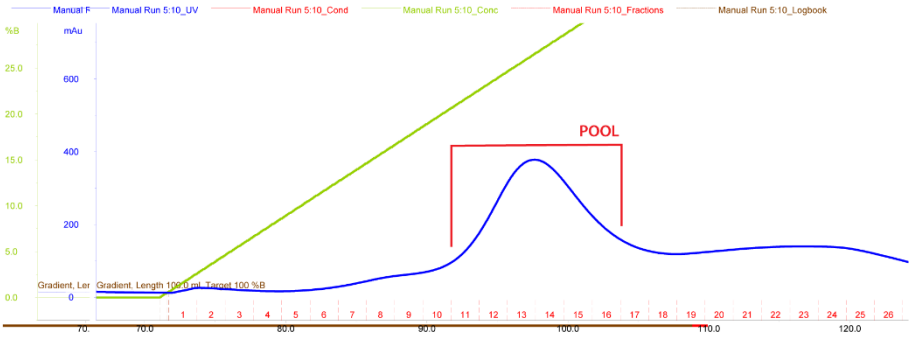

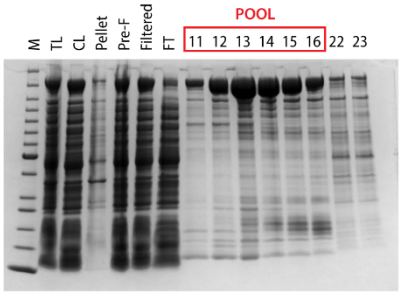

[dCas9$_{HNH}$ His1 pool] = 1.47mg/ml, 12ml (approx. 17.64 mg dCas9$_{HNH}$ total)

Overnight SUMO protease cleavage (20 mg SUMO protease in SnakeSkin dialysis tubing; dialysis against 2L *HisWash 2*; 4°C)

5ml HisTrap HP
Column 2

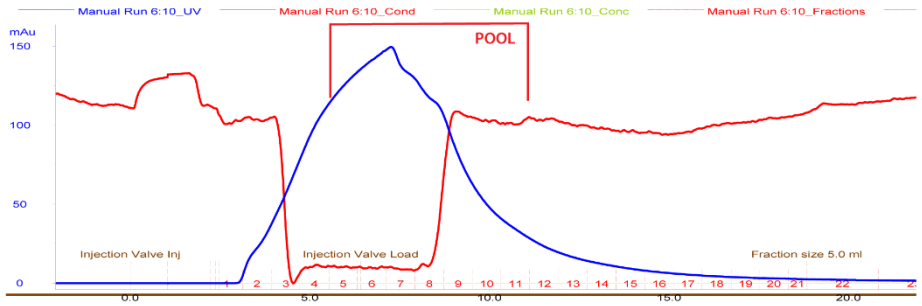

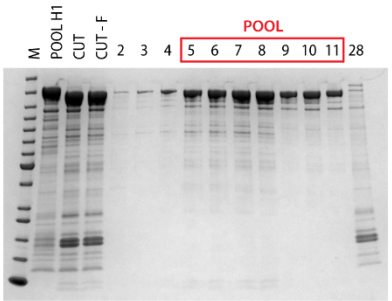

Concentrate dCas9$_{HNH}$ His2 pool

50k Amicon Centrifugal filter units;
buffer exchange into *GF buffer* for labelling

[dCas9$_{HNH}$ His2 pool] = 8.09 mg/ml, 51.27 µM

Figure A-8 dCas9$_{HNH}$ Purification *See section 2.7.1 for details*

A4-VI Cas9$_{HNH}$ labelling

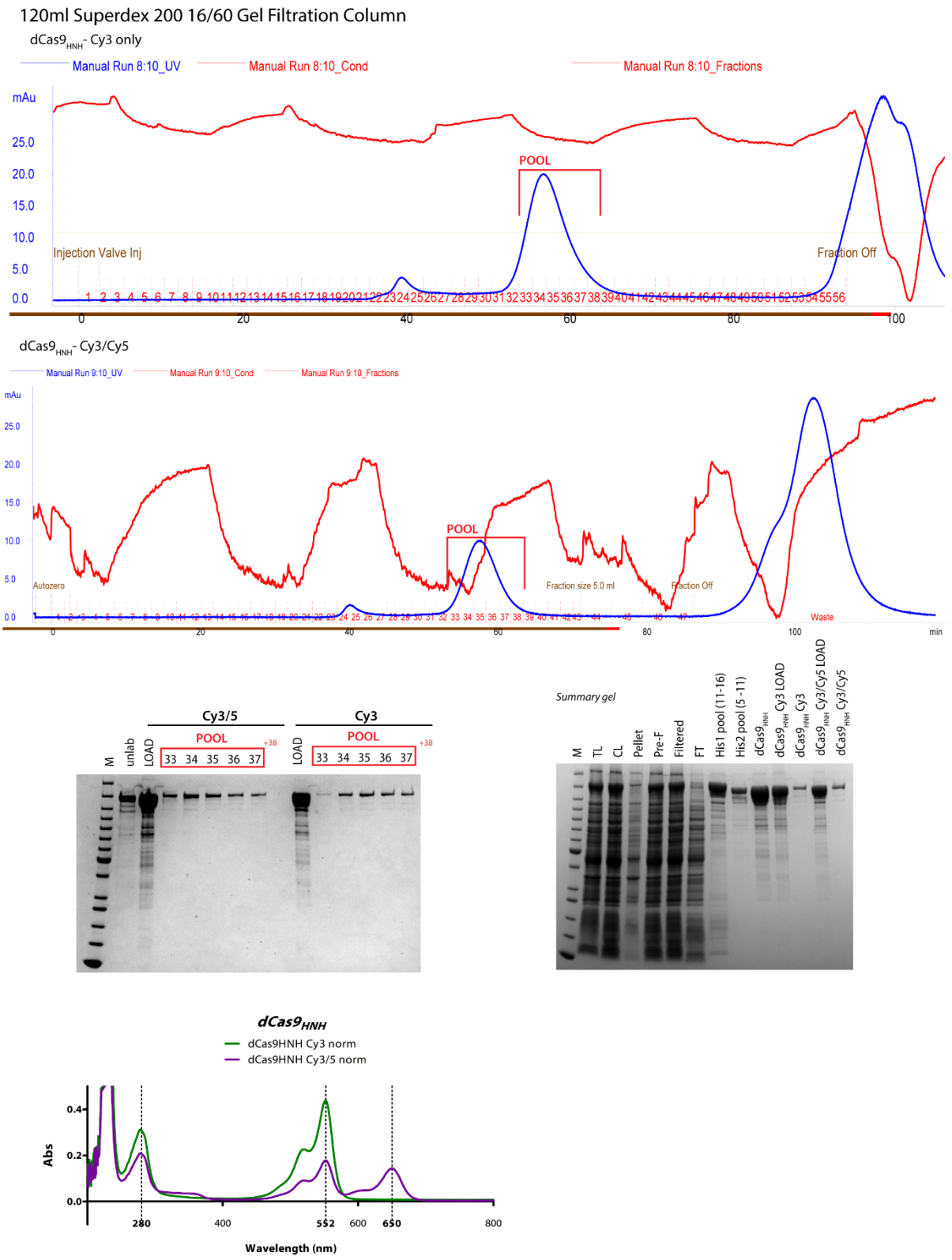

Figure A-9 dCas9$_{HNH}$ Labelling *See section 2.7.1 for details*

A4-VII k_a, k_b k_{ini} and k_{ini2}

Table 24 rates of first and second strand cleavage ± SEM Data from Figure 4-13

	ka	kb	kini	kini2
gRNA	0.099±0.004	0.104±0.007	0.005±0.001	0.006±0.0005
US	0.093	0.139	0.008	0.01
H1	0.116±0.010	0.157±0.018	0.006±0.004	0.011±0.001
H2	0.087±0.004	0.160±0.016	0.007±0.005	0.010±0.002
3'	0.099±0.003	0.124±0.006	0.005±0.001	0.008±0.001

A5 Chapter 5

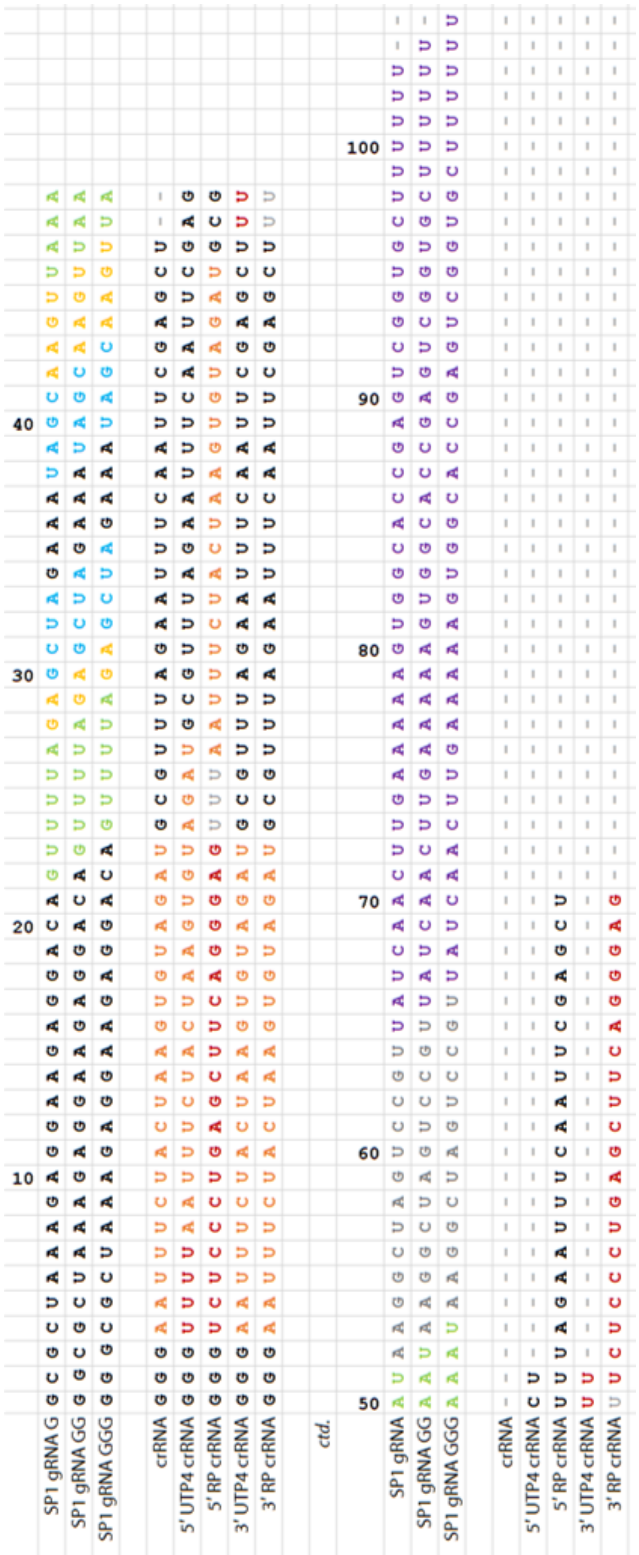

Figure A-10 Chapter 5 gRNA and crRNA sequences

A6 Chapter 6

A6-I gRNA Northern blotting

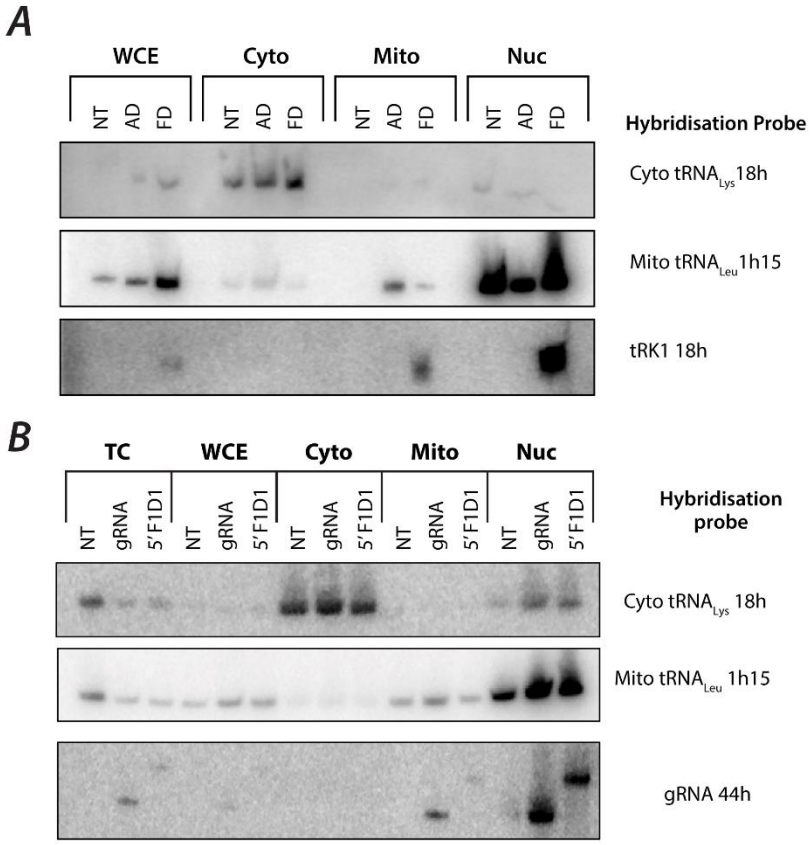

Figure A-11 gRNA Northern blotting A *Northern blotting for AD/FD* ***B*** *Northern blotting for gRNA, and gRNA 5′ FD; WCE = whole cell extract; Cyto = Cytoplasm; Mito = Mitochondria; Nuc = Nuclear;*

A6-II Fluorescent RNAs do not colocalise with LC3

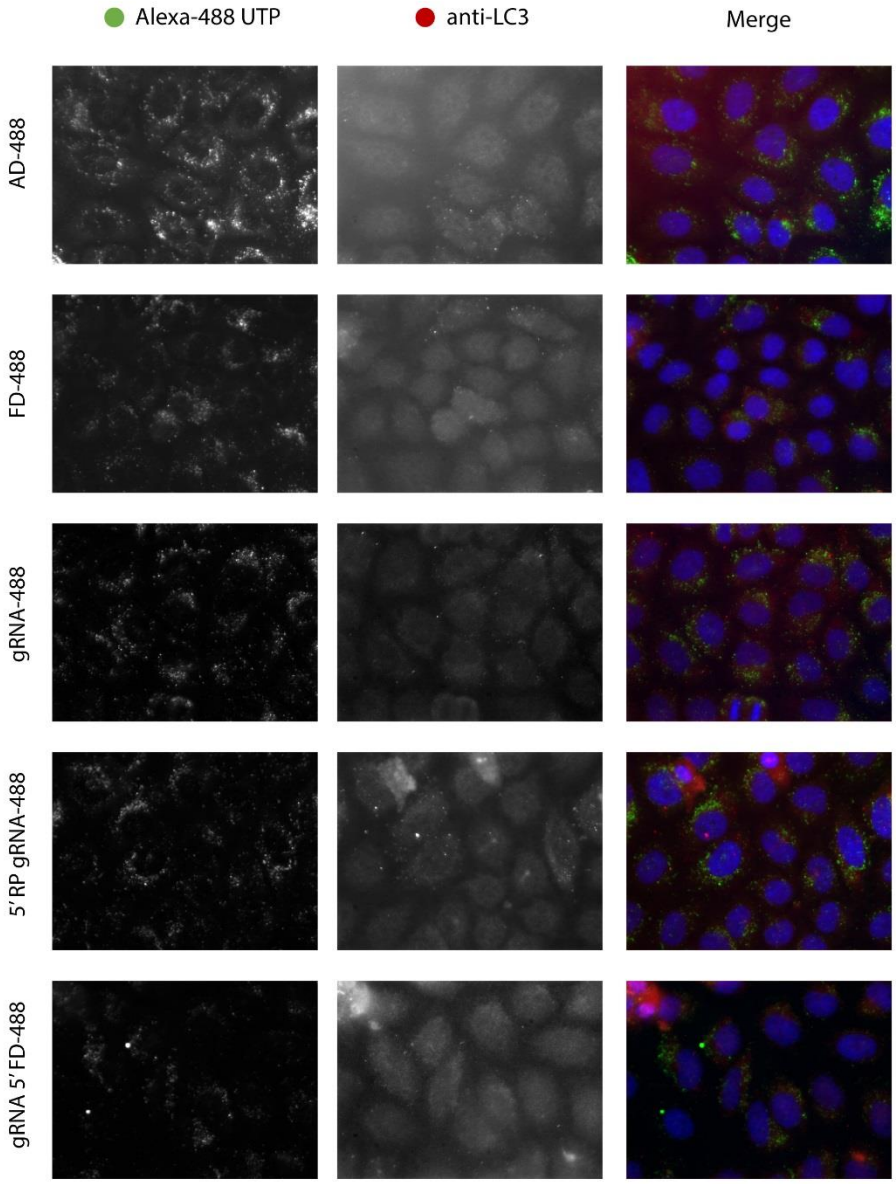

Figure A-12 Alexa™-labelled RNAs do not colocalise with LC3 *AD-488, FD-488, gRNA-488, 5′RP gRNA-488 and 5′ FD gRNA-488 are transfected into HeLa cells by PEI transfection. Cells are stained with DAPI and anti-LC3 (2° anti-Rabbit 594). DAPI: 30 ms; FITC: 500 ms;*

A7 Chapter 7

A7-I Artists/Scientists profiles

Theo Wood

Theo Wood is a multimedia artist from Bristol

> I was delighted on being invited to take part in this exhibition being an ardent science, sci- and future gazing fan. My ongoing project the Museum of Space Exploration is based on a future after the year 3000 – Synthetic Biology will be entrenched and more by then. For SynBioExpo my response has been to take a sideways look, consider the issues, and produce pieces of work that hopefully will provoke questions. Is this a good idea? Is this real or fake news?

Theo Wood – April 2017

Imogen Coulter

Imogen Coulter is an illustrator from Bristol

> It has been a great experience being involved in such a unique exhibition. Having always been interested in science and art it's been a great opportunity to actually work with the scientists first hand, looking and learning about each of their projects.

Imogen Coulter – April 2017

Claudia Stocker

Claudia Stocker is a graphic designer and illustrator from Bristol.

> Visualising cutting edge science is something I'm fairly comfortable with - my day job is running the science illustration and graphic design company Vivid Biology. This is why I was drawn more towards the current technical details of the research rather than the future potential of the technology. This exhibition did give me the chance to work at a larger scale than usual. Most of my work is constrained by how big my scanner is. It also let me catch up on what was going on in the field (I studied synthetic biology as part of my MSci, but that was back in 2012). I tried to make the works as visually distinct as possible, I'm always a little a bit paranoid that by being too scientifically rigorous they become somewhat formulaic. There's only so many ways you can draw DNA before it veers into territory where you're making statements that are factually wrong.

Claudia Stocker – April 2017

A7-II Dilemmas

1. With synthetic biology, it could be possible to produce vegan cow's milk, a liquid which has the same molecular identity as cow's milk, but without the need for an actual cow. This 'milk' could then be used to make vegan cheese—a cheese made from what is essentially real cow's milk, only with zero animal involvement. Would you be happy to eat this?
2. Research suggests that it will not be long before a strain of peanut (ground nut) will be available that will not create an allergic reaction (the gene causing this will
3. There is a worldwide shortage of organs suitable for transplantation. It has previously been suggested that animal organs could be transplanted into humans, but no trials to date have been entirely successful. There is a much higher incidence of organ rejection in these animal-to-human transplant cases. It could be possible to modify the genes *in the implanted animal organs* that cause negative reactions in the human recipients. This could mean fewer cases of organ rejection/failure and perhaps freedom from having to take immune-suppressive drugs forever. Should this research continue?
4. There is a worldwide shortage of organs suitable for transplantation. It has previously been suggested that animal organs could be transplanted into humans, but no trials to date have been entirely successful. There is a much higher incidence of organ rejection in these animal-to-human transplant cases.
5. It could be possible to modify the *human genes* that cause negative reactions to animal transplants in the immune system. This could mean fewer cases of organ rejection/failure and perhaps freedom from having to take immune-suppressive drugs forever. Should this research continue?
6. Mosquitoes have been genetically engineered so that they spread a lethal gene which cuts down populations of Zika carrying mosquitoes. Should they be released into the environment for testing?
7. CRISPR creates the potential to reintroduce extinct species. Mammoth like elephants could be bred by including certain mammoth genes into an elephant embryo. To allow this to continue, an artificial womb would have to be created. Do you think research of this type is a good idea?
8. A team of Chinese scientists have begun using genome-editing techniques on viable human embryos, creating embryos with genetic mutations. These cells are an exact model of embryonic disease which could be used in the development of new therapies to see if these could be corrected. The work is in early stages of development. Should this type of work continue – perhaps producing a cure for genetic disease?

9. ‘Genetically modified’ foods, as first released into the consumer market in the 90s, often involved the insertion of genes into crops which did not naturally occur in that species. In Europe, all food containing more than 0.9% GM products must be labelled. Do you think that consumer products which have been modified with CRISPR should be allowed to be sold without explicit labelling?
10. CRISPR can be used to genetically modify some single-celled organisms (like yeast) so that they produce polymers and precursors to biofuels. Biomanufacture like this could be used to help alleviate our dependence on edible and crude oils. Do you think this is a good idea?
11. CRISPR kits can now be bought commercially online for under £100, enabling anyone to become a “garage scientist” or “biohacker” and start tinkering with DNA from the comfort of their own home. Do you think these gene editing kits should be available commercially online?
12. In the egg industry, male chicks are often slaughtered as they have no use. CRISPR could be used to help identify male eggs before they hatch, so that they can be redirected into another industry (such as vaccine production). Do you think CRISPR should be used to reduce the need for farmers to cull animals in the food industry in this way?
13. Invasive species disrupt natural ecosystems worldwide, driving natural species extinct and threatening protected habitats. Where other methods of population control have failed, modifying a few members of the invasive species with CRISPR could be used to spread genes through the population and control numbers. Do you think research of this type is a good idea?
14. Many premium breeds of meat and dairy cattle have long horns. These can cause the animals to injure each other, particularly when they are packed into trailers for transport. As a result, the horns are often removed in a painful process. Using traditional methods of cross breeding to eliminate the horns in these premium cattle breeds has been unsuccessful as it produces low-quality offspring. CRISPR is being used to produce high quality cattle without horns. Do you think this technology should be used on animals in the food industry in this way?
15. As tools for modifying DNA are developed, the potential for private businesses to commercialize human genetic enhancement could become a reality – resulting in an industry of ‘genome plastic surgery’. Do you think businesses of this type should be allowed?
16. CRISPR provides the potential to develop cell based therapies – where cells can be taken out of a patient’s body, modified by CRISPR, and then replaced. An example

could be edited white blood cells which bolster the immune system of an HIV patient. Do you think edited cells should be used to treat human disease in this way?

17. CRISPR provides the potential to edit the DNA in human somatic cells - all the cells except the sperm or eggs. This means that a patient could have a genetic mutation corrected, but would not pass on any edited DNA to future generations. Do you think edited cells should be used to treat human disease in this way?
18. CRISPR provides the potential to edit the DNA in human cells – including the germ line cells, the sperm and the eggs. This means that a patient could have a genetic mutation corrected, and would pass on edited DNA to future generations. Do you think edited cells should be used to treat human disease in this way?
19. Many successful modern drugs are based on molecules from natural products such as plants. In some cases using the natural product directly can lead to the extinction of its source. Using CRISPR to synthetically produce these products will mean this will no longer need to happen. Is this a good idea for future development?
20. African swine fever is a virus which infects domestic pig herds and can have a detrimental impact on pig farmers. Some warthogs are naturally immune to African swine fever. Altering immune genes in domestic pigs to match more closely those of warthogs would confer resistance to the virus. If this is successful there would be a new breed of pig available as a food source and less disease in these pig herds. *Do* you think editing pig DNA to match more closely to warthogs should happen?
21. Medical tourism is the name given to patients travelling to other countries to seek medical or fertility treatments which aren't available in their own countries. The development of CRISPR technologies could lead to a new era of genetic tourism, where individuals travel abroad for unregulated procedures. Is genetic medical tourism ok?

References

1. Rich, P. R. & Maréchal, A. The mitochondrial respiratory chain. *Essays Biochem.* **47,** 1–23 (2010).

2. Rizzuto, R., De Stefani, D., Raffaello, A. & Mammucari, C. Mitochondria as sensors and regulators of calcium signalling. *Nat. Rev. Mol. Cell Biol.* **13,** 566–578 (2012).

3. Graef, M. & Nunnari, J. A role for mitochondria in autophagy regulation. *Autophagy* **7,** 1245–1246 (2011).

4. Wang, C. & Youle, R. J. The role of mitochondria in apoptosis*. *Annu. Rev. Genet.* **43,** 95–118 (2009).

5. Gray, M. W., Burger, G. & Lang, B. F. The origin and early evolution of mitochondria. *Genome Biol.* **2,** reviews1018.1 (2001).

6. Anderson, S. *et al.* Sequence and organization of the human mitochondrial genome. *Nature* **290,** 457–65 (1981).

7. Bereiter-Hahn, J. & Jendrach, M. Mitochondrial Dynamics. *Int. Rev. Cell Mol. Biol.* **284,** 1–65 (2010).

8. Liesa, M., Palacín, M. & Zorzano, A. Mitochondrial Dynamics in Mammalian Health and Disease. *Physiol. Rev.* **89,** 799–845 (2009).

9. Chan, D. C. Mitochondrial Fusion and Fission in Mammals. *Annu. Rev. Cell Dev. Biol.* **22,** 79–99 (2006).

10. O'Rourke, B. Mitochondrial Ion Channels. *Annu. Rev. Physiol.* **69,** 19–49 (2007).

11. Calvo, S. E. & Mootha, V. K. The mitochondrial proteome and human disease. *Annu. Rev. Genomics Hum. Genet.* **11,** 25–44 (2010).

12. Pagliarini, D. J. *et al.* A Mitochondrial Protein Compendium Elucidates Complex I Disease Biology. *Cell* **134,** 112–123 (2008).

13. Shoubridge, E. A. & Wai, T. in *Current topics in developmental biology* **77,** 87–111 (2007).

14. Taanman, J.-W. The mitochondrial genome: structure, transcription, translation and replication. *Biochim. Biophys. Acta - Bioenerg.* **1410,** 103–123 (1999).

15. Greber, B. J. & Ban, N. Structure and Function of the Mitochondrial Ribosome. *Annu. Rev. Biochem.* **85,** 103–132 (2016).

16. Alexeyev, M., Shokolenko, I., Wilson, G. & LeDoux, S. The maintenance of mitochondrial DNA integrity--critical analysis and update. *Cold Spring Harb. Perspect. Biol.* **5,** a012641 (2013).

17. Moretton, A. *et al.* Selective mitochondrial DNA degradation following double-strand breaks. *PLoS One* **12,** e0176795 (2017).

18. Peeva, V. *et al.* Linear mitochondrial DNA is rapidly degraded by components of the replication machinery. *Nat. Commun.* **9,** 1727 (2018).

19. DiMauro, S. & Schon, E. A. Mitochondrial Respiratory-Chain Diseases. *N. Engl. J. Med.* **348,** 2656–2668 (2003).

20. Altmann, R. Die Elementarorganismen und ihre Beziehungen zu den Zellen. *Veit* **145,** (1890).

21. Erickson, R. P. Leber's optic atrophy, a possible example of maternal inheritance. *Am. J. Hum. Genet.* **24,** 348–9 (1972).

22. Wallace, D. C. *et al.* Mitochondrial DNA mutation associated with Leber's hereditary optic neuropathy. *Science* **242,** 1427–30 (1988).

23. Clinvar. at <https://www.ncbi.nlm.nih.gov/clinvar/>

24. Gorman, G. S. *et al.* Prevalence of nuclear and mtDNA mutations related to adult mitochondrial disease. *Ann. Neurol.* (2015). doi:10.1002/ana.24362

25. Khan, N. A., Govindaraj, P., Meena, A. K. & Thangaraj, K. Mitochondrial disorders: challenges in diagnosis & treatment. *Indian J. Med. Res.* **141,** 13–26 (2015).

26. Rossignol, R. *et al.* Mitochondrial threshold effects. *Biochem. J.* **370,** 751–62 (2003).

27. Boulet, L., Karpati, G. & Shoubridge, E. A. Distribution and threshold expression of the tRNA(Lys) mutation in skeletal muscle of patients with myoclonic epilepsy and ragged-red fibers (MERRF). *Am. J. Hum. Genet.* **51,** 1187–200 (1992).

28. Sciacco, M., Bonilla, E., Schon, E. A., DiMauro, S. & Moraes, C. T. Distribution of wild-type and common deletion forms of mtDNA in normal and respiration-deficient muscle fibers from patients with mitochondrial myopathy. *Hum. Mol. Genet.* **3,** 13–9 (1994).

29. Hao, H., Bonilla, E., Manfredi, G., DiMauro, S. & Moraes, C. T. Segregation patterns of a novel mutation in the mitochondrial tRNA glutamic acid gene associated with myopathy and diabetes mellitus. *Am. J. Hum. Genet.* **56,** 1017–25 (1995).

30. Schon, E. A. Mitochondrial genetics and disease. *Trends Biochem. Sci.* **25,** 555–60 (2000).

31. Howell, N. *et al.* Mitochondrial gene segregation in mammals: is the bottleneck always narrow? *Hum. Genet.* **90,** 117–20

32. Chinnery, P. F., Howell, N., Lightowlers, R. N. & Turnbull, D. M. MELAS and MERRF. The relationship between maternal mutation load and the frequency of clinically affected offspring. *Brain* **121 (Pt 10),** 1889–94 (1998).

33. Grier, J., Hirano, M., Karaa, A., Shepard, E. & Thompson, J. L. P. Diagnostic odyssey of patients with mitochondrial disease. *Neurol. Genet.* **4,** e230 (2018).

34. Liang, C., Ahmad, K. & Sue, C. M. The broadening spectrum of mitochondrial disease: Shifts in the diagnostic paradigm. *Biochim. Biophys. Acta - Gen. Subj.* **1840,** 1360–1367 (2014).

35. Rahman, J. & Rahman, S. Mitochondrial medicine in the omics era. *Lancet (London, England)* **391,** 2560–2574 (2018).

36. Pfeffer, G. *et al.* New treatments for mitochondrial disease—no time to drop our standards. *Nat. Rev. Neurol.* **9,** 474–481 (2013).

37. Dyer, C. Law, ethics, and emotion: the Charlie Gard case. *BMJ* **358,** j3152 (2017).

38. Avula, S., Parikh, S., Demarest, S., Kurz, J. & Gropman, A. Treatment of mitochondrial disorders. *Curr. Treat. Options Neurol.* **16,** 292 (2014).

39. Chicani, C. F., Chu, E. R., Miller, G., Kelman, S. E. & Sadun, A. A. Comparing EPI-743 treatment in siblings with Leber's hereditary optic neuropathy mt14484 mutation. *Can. J. Ophthalmol.* **48,** e130-3 (2013).

40. Veyrat-Durebex, C. *et al.* How Can a Ketogenic Diet Improve Motor Function? *Front. Mol. Neurosci.* **11,** (2018).

41. Mahoney, D. J., Parise, G. & Tarnopolsky, M. A. Nutritional and exercise-based therapies in the treatment of mitochondrial disease. *Curr. Opin. Clin. Nutr. Metab.*

Care **5,** 619–29 (2002).

42. da Cruz, L. *et al.* Phase 1 clinical study of an embryonic stem cell–derived retinal pigment epithelium patch in age-related macular degeneration. *Nat. Biotechnol.* **36,** 328–337 (2018).

43. Zhou, R. & Caspi, R. R. Ocular immune privilege. *F1000 Biol. Rep.* **2,** (2010).

44. Brown, D. T. *et al.* Transmission of mitochondrial DNA disorders: possibilities for the future. *Lancet (London, England)* **368,** 87–9 (2006).

45. Bredenoord, A. *et al.* Preimplantation genetic diagnosis for mitochondrial DNA disorders: ethical guidance for clinical practice. *Eur. J. Hum. Genet.* **17,** 1550–9 (2009).

46. HEFA Press Release: UK's independent expert panel recommends cautious adoption of mitochondrial donation in treatment. (2017). at <https://www.hfea.gov.uk/about-us/news-and-press-releases/2016-news-and-press-releases/uks-independent-expert-panel-recommends-cautious-adoption-of-mitochondrial-donation-in-treatment/>

47. Check Hayden, E. Regulators weigh benefits of 'three-parent' fertilization. *Nature* **502,** 284–285 (2013).

48. Vogel, G. FDA Considers Trials of 'Three-Parent Embryos'. *Science (80-.).* **343,** 827–828 (2014).

49. Barritt, J. A., Willadsen, S., Brenner, C. & Cohen, J. Cytoplasmic transfer in assisted reproduction. *Hum. Reprod. Update* **7,** 428–435 (2001).

50. Poulton, J., Kennedy, S., Oakeshott, P. & St John, J. Nuclear transfer to prevent mitochondrial DNA diseases. *Lancet (London, England)* **368,** 841 (2006).

51. Yamada, M. *et al. Genetic Drift Can Compromise Mitochondrial Replacement by Nuclear Transfer in Human Oocytes*. *Cell Stem Cell* **18,** (2016).

52. Appleby, J. B. The ethical challenges of the clinical introduction of mitochondrial replacement techniques. *Med. Health Care. Philos.* (2015). doi:10.1007/s11019-015-9656-3

53. Palacios-González, C. Does egg donation for mitochondrial replacement techniques generate parental responsibilities? *J. Med. Ethics* medethics-2017-104400 (2017). doi:10.1136/medethics-2017-104400

54. Bolender, N., Sickmann, A., Wagner, R., Meisinger, C. & Pfanner, N. Multiple pathways for sorting mitochondrial precursor proteins. *EMBO Rep.* **9,** 42–9 (2008).

55. Omura, T. Mitochondria-targeting sequence, a multi-role sorting sequence recognized at all steps of protein import into mitochondria. *J. Biochem.* **123,** 1010–6 (1998).

56. Gakh, O., Cavadini, P. & Isaya, G. Mitochondrial processing peptidases. *Biochim. Biophys. Acta* **1592,** 63–77 (2002).

57. Wiedemann, N. & Pfanner, N. Mitochondrial Machineries for Protein Import and Assembly. *Annu. Rev. Biochem.* **86,** 685–714 (2017).

58. Verechshagina, N. A., Konstantinov, Y. M., Kamenski, P. A. & Mazunin, I. O. Import of Proteins and Nucleic Acids into Mitochondria. *Biochem.* **83,** 643–661 (2018).

59. Hartl, F. U., Pfanner, N., Nicholson, D. W. & Neupert, W. Mitochondrial protein import. *Biochim. Biophys. Acta* **988,** 1–45 (1989).

60. Westermann, B. & Neupert, W. Mitochondria-targeted green fluorescent proteins: convenient tools for the study of organelle biogenesis inSaccharomyces cerevisiae. *Yeast* **16,** 1421–1427 (2000).

61. Betin, V. M. S., MacVicar, T. D. B., Parsons, S. F., Anstee, D. J. & Lane, J. D. A cryptic mitochondrial targeting motif in Atg4D links caspase cleavage with mitochondrial import and oxidative stress. *Autophagy* **8,** 664–76 (2012).

62. Law, R. H., Farrell, L. B., Nero, D., Devenish, R. J. & Nagley, P. Studies on the import into mitochondria of yeast ATP synthase subunits 8 and 9 encoded by artificial nuclear genes. *FEBS Lett.* **236,** 501–5 (1988).

63. Manfredi, G. *et al.* Rescue of a deficiency in ATP synthesis by transfer of MTATP6, a mitochondrial DNA-encoded gene, to the nucleus. *Nat. Genet.* **30,** 394–399 (2002).

64. Pingoud, A., Wilson, G. G. & Wende, W. Type II restriction endonucleases--a historical perspective and more. *Nucleic Acids Res.* **42,** 7489–527 (2014).

65. Pingoud, A., Fuxreiter, M., Pingoud, V. & Wende, W. Type II restriction endonucleases: structure and mechanism. *Cell. Mol. Life Sci.* **62,** 685–707 (2005).

66. Srivastava, S. & Moraes, C. T. Manipulating mitochondrial DNA heteroplasmy by a mitochondrially targeted restriction endonuclease. *Hum. Mol. Genet.* **10,** 3093–9 (2001).

67. Tanaka, M. *et al.* Gene Therapy for Mitochondrial Disease by Delivering Restriction Endonuclease <i>Sma</i>I into Mitochondria. *J. Biomed. Sci.* **9,** 534–541 (2002).

68. Bayona-Bafaluy, M. P., Blits, B., Battersby, B. J., Shoubridge, E. A. & Moraes, C. T. Rapid directional shift of mitochondrial DNA heteroplasmy in animal tissues by a mitochondrially targeted restriction endonuclease. *Proc. Natl. Acad. Sci. U. S. A.* **102,** 14392–7 (2005).

69. Bacman, S. R., Williams, S. L., Garcia, S. & Moraes, C. T. Organ-specific shifts in mtDNA heteroplasmy following systemic delivery of a mitochondria-targeted restriction endonuclease. *Gene Ther.* **17,** 713–20 (2010).

70. Reddy, P. *et al.* Selective Elimination of Mitochondrial Mutations in the Germline by Genome Editing. *Cell* **161,** 459–469 (2015).

71. Bogdanove, A. J., Bohm, A., Miller, J. C., Morgan, R. D. & Stoddard, B. L. Engineering altered protein–DNA recognition specificity. *Nucleic Acids Res.* **46,** 4845–4871 (2018).

72. Kim, Y. G., Cha, J. & Chandrasegaran, S. Hybrid restriction enzymes: zinc finger fusions to Fok I cleavage domain. *Proc. Natl. Acad. Sci. U. S. A.* **93,** 1156–60 (1996).

73. Smith, J. *et al.* Requirements for double-strand cleavage by chimeric restriction enzymes with zinc finger DNA-recognition domains. *Nucleic Acids Res.* **28,** 3361–9 (2000).

74. Gaj, T., Gersbach, C. A. & Barbas, C. F. ZFN, TALEN, and CRISPR/Cas-based methods for genome engineering. *Trends in Biotechnology* **31,** (2013).

75. Minczuk, M., Papworth, M. A., Kolasinska, P., Murphy, M. P. & Klug, A. Sequence-specific modification of mitochondrial DNA using a chimeric zinc finger methylase. *PNAS* (2006).

76. Minczuk, M., Papworth, M. a, Miller, J. C., Murphy, M. P. & Klug, A. Development of a single-chain, quasi-dimeric zinc-finger nuclease for the selective degradation of

mutated human mitochondrial DNA. *Nucleic Acids Res.* **36,** 3926–38 (2008).

77. Gammage, P. A., Rorbach, J., Vincent, A. I., Rebar, E. J. & Minczuk, M. Mitochondrially targeted ZFNs for selective degradation of pathogenic mitochondrial genomes bearing large-scale deletions or point mutations. *EMBO Mol Med.* **6,** 458–466 (2014).

78. Romer, P. *et al.* Plant Pathogen Recognition Mediated by Promoter Activation of the Pepper Bs3 Resistance Gene. *Science (80-.).* **318,** 645–648 (2007).

79. Bacman, S. R., Williams, S. L., Pinto, M., Peralta, S. & Moraes, C. T. Specific elimination of mutant mitochondrial genomes in patient-derived cells by mitoTALENs. *Nat. Med.* **19,** 1111–3 (2013).

80. Hashimoto, M. *et al.* MitoTALEN: A general approach to reduce mutant mtDNA loads and restore oxidative phosphorylation function in mitochondrial diseases. *Mol. Ther.* (2015). doi:10.1038/mt.2015.126

81. Moraes, C. T., Bacman, S. R. & Williams, S. L. Manipulating mitochondrial genomes in the clinic: playing by different rules. *Trends Cell Biol.* **24,** 209–11 (2014).

82. Sternberg, S. H. & Doudna, J. A. Expanding the Biologist's Toolkit with CRISPR-Cas9. *Mol. Cell* **58,** 568–574 (2015).

83. Ishino, Y., Shinagawa, H., Makino, K., Amemura, M. & Nakata, A. Nucleotide sequence of the iap gene, responsible for alkaline phosphatase isozyme conversion in Escherichia coli, and identification of the gene product. *J. Bacteriol.* **169,** 5429–33 (1987).

84. Grissa, I., Vergnaud, G. & Pourcel, C. The CRISPRdb database and tools to display CRISPRs and to generate dictionaries of spacers and repeats. *BMC Bioinformatics* **8,** 172 (2007).

85. Makarova, K. S. *et al.* An updated evolutionary classification of CRISPR-Cas systems. *Nat. Rev. Microbiol.* **13,** (2015).

86. Koonin, E. V, Makarova, K. S. & Zhang, F. Diversity, classification and evolution of CRISPR-Cas systems. *Curr. Opin. Microbiol.* **37,** 67–78 (2017).

87. Shmakov, S. *et al.* Discovery and Functional Characterization of Diverse Class 2 CRISPR-Cas Systems. *Mol. Cell* **60,** 385–397 (2015).

88. Shmakov, S. *et al.* Diversity and evolution of class 2 CRISPR–Cas systems. *Nat. Rev. Microbiol.* **15,** 169–182 (2017).

89. Jinek, M. *et al.* A programmable dual-RNA-guided DNA endonuclease in adaptive bacterial immunity. *Science* **337,** 816–21 (2012).

90. Mojica, F. J. M., Díez-Villaseñor, C., García-Martínez, J. & Almendros, C. Short motif sequences determine the targets of the prokaryotic CRISPR defence system. *Microbiology* **155,** 733–740 (2009).

91. Sternberg, S. H., Redding, S., Jinek, M., Greene, E. C. & Doudna, J. A. DNA interrogation by the CRISPR RNA-guided endonuclease Cas9. *Nature* **507,** 62–7 (2014).

92. Szczelkun, M. D. *et al.* Direct observation of R-loop formation by single RNA-guided Cas9 and Cascade effector complexes. *Proc. Natl. Acad. Sci. U. S. A.* **111,** 9798–803 (2014).

93. Nishimasu, H. *et al.* Crystal structure of Cas9 in complex with guide RNA and target DNA. *Cell* **156,** 935–49 (2014).

94. Zetsche, B. *et al.* Cpf1 Is a Single RNA-Guided Endonuclease of a Class 2 CRISPR-Cas

System. *Cell* (2015). doi:10.1016/j.cell.2015.09.038

95. Dong, D. *et al.* The crystal structure of Cpf1 in complex with CRISPR RNA. *Nature* **532,** 522–526 (2016).

96. Yamano, T. *et al.* Crystal Structure of Cpf1 in Complex with Guide RNA and Target DNA. *Cell* **165,** 949–962 (2016).

97. Gao, P., Yang, H., Rajashankar, K. R., Huang, Z. & Patel, D. J. Type V CRISPR-Cas Cpf1 endonuclease employs a unique mechanism for crRNA-mediated target DNA recognition. *Cell Res.* **26,** 901–913 (2016).

98. Jiang, Y. *et al.* Multigene editing in the Escherichia coli genome via the CRISPR-Cas9 system. *Appl. Environ. Microbiol.* **81,** 2506–14 (2015).

99. Cong, L. *et al.* Multiplex genome engineering using CRISPR/Cas systems. *Science* **339,** 819–23 (2013).

100. Mali, P. *et al.* RNA-guided human genome engineering via Cas9. *Science (80-.).* **339,** (2013).

101. Mali, P., Esvelt, K. M. & Church, G. M. Cas9 as a versatile tool for engineering biology. *Nat. Methods* **10,** 957–63 (2013).

102. Hwang, W. Y. *et al.* Efficient genome editing in zebrafish using a CRISPR-Cas system. *Nat. Biotechnol.* **31,** 227–229 (2013).

103. Harms, D. W. *et al.* in *Current Protocols in Human Genetics* **83,** 15.7.1-15.7.27 (John Wiley & Sons, Inc., 2014).

104. Wang, L., Wu, J., Fang, W., Liu, G.-H. & Belmonte, J. C. I. Regenerative medicine: targeted genome editing in vivo. *Cell Res.* (2015). doi:10.1038/cr.2015.11

105. Ran, F. A. *et al.* Double nicking by RNA-guided CRISPR cas9 for enhanced genome editing specificity. *Cell* **154,** (2013).

106. Savic, N. *et al.* Covalent linkage of the DNA repair template to the CRISPR-Cas9 nuclease enhances homology-directed repair. *Elife* **7,** (2018).

107. Komor, A. C., Kim, Y. B., Packer, M. S., Zuris, J. A. & Liu, D. R. Programmable editing of a target base in genomic DNA without double-stranded DNA cleavage. *Nature* **61,** (2016).

108. Konermann, S. *et al.* Genome-scale transcriptional activation by an engineered CRISPR-Cas9 complex. *Nature* **517,** 583–588 (2014).

109. Deng, W., Shi, X., Tjian, R., Lionnet, T. & Singer, R. H. CASFISH: CRISPR/Cas9-mediated in situ labeling of genomic loci in fixed cells. *Proc. Natl. Acad. Sci. U. S. A.* **112,** 11870–11875 (2015).

110. Chen, B. & Huang, B. Imaging Genomic Elements in Living Cells Using CRISPR/Cas9. *Methods Enzymol.* **546C,** 337–354 (2014).

111. Malina, A. *et al.* Adapting CRISPR/Cas9 for Functional Genomics Screens. *Methods Enzymol.* **546C,** 193–213 (2014).

112. Rusk, N. CRISPR circuits. *Nat. Methods* **11,** 710–711 (2014).

113. Truong, D.-J. J. *et al.* Development of an intein-mediated split-Cas9 system for gene therapy. *Nucleic Acids Res.* gkv601- (2015). doi:10.1093/nar/gkv601

114. Schmelas, C. & Grimm, D. Split Cas9, not hairs - advancing the therapeutic index of CRISPR technology. *Biotechnol. J.* 1700432 (2018). doi:10.1002/biot.201700432

115. Polstein, L. R. & Gersbach, C. A. A light-inducible CRISPR-Cas9 system for control of endogenous gene activation. *Nat. Chem. Biol.* **11,** 198–200 (2015).

116. Zetsche, B., Volz, S. E. & Zhang, F. A split-Cas9 architecture for inducible genome editing and transcription modulation. *Nat. Biotechnol.* **advance on,** (2015).

117. Davis, K. M., Pattanayak, V., Thompson, D. B., Zuris, J. A. & Liu, D. R. Small molecule–triggered Cas9 protein with improved genome-editing specificity. *Nat. Chem. Biol.* **advance on,** (2015).

118. Mali, P. *et al.* RNA-guided human genome engineering via Cas9. *Science* **339,** (2013).

119. Konermann, S. *et al.* Genome-scale transcriptional activation by an engineered CRISPR-Cas9 complex. *Nature* **517,** 583–588 (2015).

120. Niazi, A. K. *et al.* Targeting nucleic acids into mitochondria: Progress and prospects. *Mitochondrion* **13,** 548–558 (2013).

121. Wang, G., Shimada, E., Nili, M., Koehler, C. M. & Teitell, M. A. Mitochondria-targeted RNA import. *Methods Mol. Biol.* **1264,** 107–16 (2015).

122. Kolesnikova, O. *et al.* Selection of RNA aptamers imported into yeast and human mitochondria. *RNA* **16,** 926–41 (2010).

123. Dovydenko, I. *et al.* Mitochondrial targeting of recombinant RNA. *Methods Mol. Biol.* **1265,** 209–25 (2015).

124. Kim, K. M., Noh, J. H., Abdelmohsen, K. & Gorospe, M. Mitochondrial noncoding RNA transport. *BMB Rep.* **50,** 164–174 (2017).

125. Gammage, P. A., Moraes, C. T. & Minczuk, M. Mitochondrial Genome Engineering: The Revolution May Not Be CRISPR-Ized. *Trends Genet.* **0,** (2017).

126. Osawa, S., Jukes, T. H., Watanabe, K. & Muto, A. Recent evidence for evolution of the genetic code. *Microbiol. Rev.* **56,** 229–64 (1992).

127. Sripada, L. *et al.* Systematic Analysis of Small RNAs Associated with Human Mitochondria by Deep Sequencing: Detailed Analysis of Mitochondrial Associated miRNA. *PLoS One* **7,** e44873 (2012).

128. Mercer, T. R. *et al.* The human mitochondrial transcriptome. *Cell* **146,** 645–58 (2011).

129. Campo, M. L., Peixoto, P. M. & Martínez-Caballero, S. Revisiting trends on mitochondrial mega-channels for the import of proteins and nucleic acids. *J. Bioenerg. Biomembr.* **49,** 75–99 (2017).

130. Alfonzo, J. D. & Söll, D. Mitochondrial tRNA import – the challenge to understand has just begun. *Biol. Chem.* **390,** 717–22 (2009).

131. Martin, R. P., Schneller, J. M., Stahl, A. J. & Dirheimer, G. Study of yeast mitochondrial tRNAs by two-dimensional polyacrylamide gel electrophoresis: characterization of isoaccepting species and search for imported cytoplasmic tRNAs. *Nucleic Acids Res.* **4,** 3497–510 (1977).

132. Hancock, K. & Hajduk, S. L. The mitochondrial tRNAs of Trypanosoma brucei are nuclear encoded. *J. Biol. Chem.* **265,** 19208–15 (1990).

133. Martin, R. P., Schneller, J. M., Stahl, A. J. C. & Dirheimer, G. Import of nuclear deoxyribonucleic acid coded lysine-accepting transfer ribonucleic acid (anticodon C-U-U) into yeast mitochondria. *Biochemistry* **18,** 4600–4605 (1979).

134. Entelis, N. *et al.* A glycolytic enzyme, enolase, is recruited as a cofactor of tRNA

targeting toward mitochondria in Saccharomyces cerevisiae. *Genes Dev.* **20,** 1609–20 (2006).

135. Kamenski, P. *et al.* tRNA mitochondrial import in yeast: Mapping of the import determinants in the carrier protein, the precursor of mitochondrial lysyl-tRNA synthetase. *Mitochondrion* **10,** 284–293 (2010).

136. Tarassov, I., Entelis, N. & Martin, R. P. An Intact Protein Translocating Machinery is Required for Mitochondrial Import of a Yeast Cytoplasmic tRNA. *J. Mol. Biol.* **245,** 315–323 (1995).

137. Thomas W. O'Brien. The General Occurrence of 55 S Ribosomes in Mammalian Liver Mitochondria. *J. Biol. Chem.* **246,** 3409–3417 (1971).

138. Smirnov, A. *et al.* Two distinct structural elements of 5S rRNA are needed for its import into human mitochondria. *RNA* 749–759 (2008). doi:10.1261/rna.952208.throughout

139. Smirnov, A. *et al.* Mitochondrial Enzyme Rhodanese Is Essential for 5 S Ribosomal RNA Import into Human Mitochondria. *J. Biol. Chem.* **285,** 30792–30803 (2010).

140. Magalhães, P. J., Andreu, A. L. & Schon, E. A. Evidence for the presence of 5S rRNA in mammalian mitochondria. *Mol. Biol. Cell* **9,** 2375–82 (1998).

141. Agrawal, R. K. & Sharma, M. R. Structural aspects of mitochondrial translational apparatus. *Curr. Opin. Struct. Biol.* **22,** 797–803 (2012).

142. Entelis, N. S., Kolesnikova, O. A., Dogan, S., Martin, R. P. & Tarassov, I. A. 5 S rRNA and tRNA import into human mitochondria. Comparison of in vitro requirements. *J. Biol. Chem.* **276,** 45642–53 (2001).

143. Lopez Sanchez, M. I. G. *et al.* RNA processing in human mitochondria. *Cell Cycle* **10,** 2904–2916 (2011).

144. Rossmanith, W. & Potuschak, T. Difference between mitochondrial RNase P and nuclear RNase P. *Mol. Cell. Biol.* **21,** 8236–7 (2001).

145. Puranam, R. S. & Attardi, G. The RNase P associated with HeLa cell mitochondria contains an essential RNA component identical in sequence to that of the nuclear RNase P. *Mol. Cell. Biol.* **21,** 548–61 (2001).

146. Holzmann, J. *et al.* RNase P without RNA: Identification and Functional Reconstitution of the Human Mitochondrial tRNA Processing Enzyme. *Cell* **135,** 462–474 (2008).

147. Wang, G., Shimada, E., Koehler, C. M. & Teitell, M. A. PNPASE and RNA trafficking into mitochondria. *Biochim. Biophys. Acta - Gene Regul. Mech.* **1819,** 998–1007 (2012).

148. Lee, D. Y. & Clayton, D. A. RNase mitochondrial RNA processing correctly cleaves a novel R loop at the mitochondrial DNA leading-strand origin of replication. *Genes Dev.* **11,** 582–92 (1997).

149. Lee, D. Y. & Clayton, D. A. Initiation of mitochondrial DNA replication by transcription and R-loop processing. *J. Biol. Chem.* **273,** 30614–21 (1998).

150. Wanrooij, P. H., Uhler, J. P., Simonsson, T., Falkenberg, M. & Gustafsson, C. M. G-quadruplex structures in RNA stimulate mitochondrial transcription termination and primer formation. *Proc. Natl. Acad. Sci. U. S. A.* **107,** 16072–7 (2010).

151. Wang, G., Shimada, E., Koehler, C. M. & Teitell, M. a. PNPASE and RNA trafficking into mitochondria. *Biochim. Biophys. Acta* **1819,** 998–1007 (2012).

152. Wang, G. *et al.* PNPASE regulates RNA import into mitochondria. *Cell* **142,** 456–67

(2010).

153. Entelis, N. *et al.* Import of nuclear encoded RNAs into yeast and human mitochondria: experimental approaches and possible biomedical applications. *Genet. Eng. (N. Y).* **24,** 191–213 (2002).

154. Gowher, A., Smirnov, A., Tarassov, I. & Entelis, N. Induced tRNA import into human mitochondria: implication of a host aminoacyl-tRNA-synthetase. *PLoS One* **8,** e66228 (2013).

155. Comte, C. *et al.* Mitochondrial targeting of recombinant RNAs modulates the level of a heteroplasmic mutation in human mitochondrial DNA associated with Kearns Sayre Syndrome. *Nucleic Acids Res.* **41,** 418–33 (2013).

156. Loutre, R., Heckel, A.-M., Smirnova, A., Entelis, N. & Tarassov, I. Can Mitochondrial DNA be CRISPRized: *Pro* and *Contra*. *IUBMB Life* (2018). doi:10.1002/iub.1919

157. Wang, G. *et al.* Correcting human mitochondrial mutations with targeted RNA import. *Proc. Natl. Acad. Sci. U. S. A.* **109,** 4840–5 (2012).

158. Bacman, S. R., Williams, S. L., Pinto, M. & Moraes, C. T. The Use of Mitochondria-Targeted Endonucleases to Manipulate mtDNA. *Methods Enzymol.* **547,** 373–97 (2014).

159. Doudna, J. A. & Charpentier, E. The new frontier of genome engineering with CRISPR-Cas9. *Science (80-.).* **346,** (2014).

160. Jo, A. *et al.* Efficient Mitochondrial Genome Editing by CRISPR/Cas9. *Biomed Res. Int.* **2015,** 305716 (2015).

161. Garrido-Maraver, J. *et al.* Screening of effective pharmacological treatments for MELAS syndrome using yeasts, fibroblasts and cybrid models of the disease. *Br. J. Pharmacol.* **167,** 1311–28 (2012).

162. O'Connell, M. R. *et al.* Programmable RNA recognition and cleavage by CRISPR/Cas9. *Nature* (2014). doi:10.1038/nature13769

163. Samuel H. Sternberg1, Benjamin LaFrance2 & Matias Kaplan3† & Jennifer A. Doudna. Conformational control of DNA target cleavage by CRISPR–Cas9. *Nature* **527,** (2015).

164. LaManna, C. M. & Barrangou, R. Enabling the Rise of a CRISPR World. *Cris. J.* **1,** 205–208 (2018).

165. Lino, C. A., Harper, J. C., Carney, J. P. & Timlin, J. A. Delivering CRISPR: a review of the challenges and approaches. *Drug Deliv.* **25,** 1234–1257 (2018).

166. Glass, Z., Lee, M., Li, Y. & Xu, Q. Engineering the Delivery System for CRISPR-Based Genome Editing. *Trends Biotechnol.* (2018). doi:10.1016/j.tibtech.2017.11.006

167. Wang, M. *et al.* Efficient delivery of genome-editing proteins using bioreducible lipid nanoparticles. *Proc. Natl. Acad. Sci.* **113,** 2868–2873 (2016).

168. Horii, T. *et al.* Generation of an ICF Syndrome Model by Efficient Genome Editing of Human Induced Pluripotent Stem Cells Using the CRISPR System. *Int. J. Mol. Sci.* **14,** 19774–19781 (2013).

169. Schmidt, F. & Grimm, D. CRISPR genome engineering and viral gene delivery: A case of mutual attraction. *Biotechnol. J.* **10,** n/a-n/a (2015).

170. Liang, X. *et al.* Rapid and highly efficient mammalian cell engineering via Cas9 protein transfection. *J. Biotechnol.* **208,** 44–53 (2015).

171. Seki, A. & Rutz, S. Optimized RNP transfection for highly efficient CRISPR/Cas9-mediated gene knockout in primary T cells. *J. Exp. Med.* **215,** 985–997 (2018).

172. Mir, A. *et al.* Heavily and Fully Modified RNAs Guide Efficient SpyCas9-Mediated Genome Editing. *bioRxiv* 290999 (2018). doi:10.1101/290999

173. Hendel, A. *et al.* Chemically modified guide RNAs enhance CRISPR-Cas genome editing in human primary cells. *Nat. Biotechnol.* **advance on,** (2015).

174. Yin, H. *et al.* Partial DNA-guided Cas9 enables genome editing with reduced off-target activity. *Nat. Chem. Biol.* **14,** 311–316 (2018).

175. Yin, H. *et al.* Therapeutic genome editing by combined viral and non-viral delivery of CRISPR system components in vivo. *Nat. Biotechnol.* **34,** 328–333 (2016).

176. de Felipe, P. Skipping the co-expression problem: the new 2A "CHYSEL" technology. *Genet. Vaccines Ther.* **2,** 13 (2004).

177. OligoCalc. at <http://biotools.nubic.northwestern.edu/OligoCalc.html>

178. Eldred, G. E., Miller, G. V, Stark, W. S. & Feeney-Burns, L. Lipofuscin: resolution of discrepant fluorescence data. *Science* **216,** 757–9 (1982).

179. Lee, K. *et al.* Synthetically modified guide RNA and donor DNA are a versatile platform for CRISPR-Cas9 engineering. *Elife* **6,** e25312 (2017).

180. Mali, P. *et al.* CAS9 transcriptional activators for target specificity screening and paired nickases for cooperative genome engineering. *Nat. Biotechnol.* **31,** 833–838 (2013).

181. Shechner, D. M., Hacisuleyman, E., Younger, S. T. & Rinn, J. L. Multiplexable, locus-specific targeting of long RNAs with CRISPR-Display. *Nat. Methods* **12,** 664–670 (2015).

182. Jinek, M. *et al.* Structures of Cas9 Endonucleases Reveal RNA-Mediated Conformational Activation. *Science (80-.).* **343,** (2014).

183. Jiang, F. *et al.* Structures of a CRISPR-Cas9 R-loop complex primed for DNA cleavage. *Science (80-.).* aad8282 (2016). doi:10.1126/science.aad8282

184. Hiroshi Nishimasu, F. Ann Ran, Patrick D. Hsu, Silvana Konermann, Soraya I. Shehata, Naoshi Dohmae, Ryuichiro Ishitani, F. Z. Crystal Structure of Cas9 in Complex with Guide RNA and Target DNA.

185. Briner, A. E. *et al.* Guide RNA functional modules direct Cas9 activity and orthogonality. *Mol. Cell* **56,** 333–339 (2014).

186. Warner, K. D. *et al.* Structural basis for activity of highly efficient RNA mimics of green fluorescent protein. *Nat. Struct. Mol. Biol.* **21,** 658–663 (2014).

187. Strack, R. L., Disney, M. D. & Jaffrey, S. R. A superfolding Spinach2 reveals the dynamic nature of trinucleotide repeat-containing RNA. *Nat. Methods* **10,** 1219–24 (2013).

188. Sternberg, S. H., LaFrance, B., Kaplan, M. & Doudna, J. A. Conformational control of DNA target cleavage by CRISPR–Cas9. *Nature* **527,** 110–113 (2015).

189. Milligan, J. F. & Uhlenbeck, O. C. [5] Synthesis of small RNAs using T7 RNA polymerase. *Methods Enzymol.* **180,** 51–62 (1989).

190. Chen, J. S. *et al.* Enhanced proofreading governs CRISPR–Cas9 targeting accuracy. *Nature* **550,** 407–410 (2017).

191. Slaymaker, I. M. *et al.* Rationally engineered Cas9 nucleases with improved specificity. *Science (80-.).* (2015). doi:10.1126/science.aad5227

192. Kleinstiver, B. P. *et al.* High-fidelity CRISPR–Cas9 nucleases with no detectable genome-wide off-target effects. *Nature* (2016). doi:10.1038/nature16526

193. Kim, S., Bae, T., Hwang, J. & Kim, J.-S. Rescue of high-specificity Cas9 variants using sgRNAs with matched 5' nucleotides. *Genome Biol.* **18,** 218 (2017).

194. Fonfara, I., Richter, H., Bratovič, M., Le Rhun, A. & Charpentier, E. The CRISPR-associated DNA-cleaving enzyme Cpf1 also processes precursor CRISPR RNA. *Nature* **532,** 517–521 (2016).

195. Blower, M. D., Feric, E., Weis, K. & Heald, R. Genome-wide analysis demonstrates conserved localization of messenger RNAs to mitotic microtubules. *J. Cell Biol.* **179,** 1365–73 (2007).

196. Paige, J. S., Wu, K. Y. & Jaffrey, S. R. RNA mimics of green fluorescent protein. *Science* **333,** 642–6 (2011).

197. Ouellet, J. RNA Fluorescence with Light-Up Aptamers. *Front. Chem.* **4,** 29 (2016).

198. Madeira, V. M. C. Overview of mitochondrial bioenergetics. *Methods Mol. Biol.* **810,** 1–6 (2012).

199. National Academies of Sciences, E. and M. *Human Genome Editing*. (National Academies Press, 2017). doi:10.17226/24623

200. Baltimore, D. *et al.* Biotechnology. A prudent path forward for genomic engineering and germline gene modification. *Science* **348,** 36–8 (2015).

201. Bruening, G. & Lyons, J. M. The case of the FLAVR SAVR tomato. *Calif. Agric.* **54,** 6–7 (2000).

202. Brookes, G. & Barfoot, P. Global income and production impacts of using GM crop technology 1996–2014. *GM Crops Food* **7,** 38–77 (2016).

203. Reimschisel, J. & Thierer, A. Might We Avoid a CRISPR Technopanic Altogether? – Plain Text. *Plain Text* (2017). at <https://readplaintext.com/might-we-avoid-a-crispr-technopanic-altogether-7b73ec434351>

204. Reimschisel, J. & Thierer, A. A Model Roadmap for Genome Education – Plain Text. *Plain Text* (2017). at <https://readplaintext.com/a-model-roadmap-for-genome-education-c5c0da942941>

205. Poortinga, W. & Pidgeon, N. F. *Public Perceptions of Genetically Modified Food and Crops, and the GM Nation? Public Debate on the Commercialisation of Agricultural Biotechnology in the UK (Understanding Risk Working Paper 04-01)*. (2004). at <https://www.researchgate.net/publication/237371655_Public_Perceptions_of_Genetically_Modified_Food_and_Crops_and_the_GM_Nation_Public_Debate_on_the_Commercialisation_of_Agricultural_Biotechnology_in_the_UK>

206. Presidential Commission for the Study of Bioethical Issues. *New Directions: The Ethics of Synthetic Biology and Emerging Technologies | Presidential Commission for the Study of Bioethical Issues*. (2010). at <https://bioethicsarchive.georgetown.edu/pcsbi/synthetic-biology-report.html>

207. Rip, A. The past and future of RRI. *Life Sci. Soc. Policy* **10,** 17 (2014).

208. Scheufele, D. A. *et al.* U.S. attitudes on human genome editing. *Science* **357,** 553–554 (2017).

209. Tebas, P. *et al.* Gene Editing of *CCR5* in Autologous CD4 T Cells of Persons Infected with HIV. *N. Engl. J. Med.* **370,** 901–910 (2014).

210. Starr, S. How to talk about genome editing. *Br. Med. Bull.* **126,** 5–12 (2018).

211. Webster, S. Art and science collaborations in the United Kingdom. *Nat. Rev. Immunol.* **5,** 965–969 (2005).

212. Cho, S. W. *et al.* Analysis of off-target effects of CRISPR/Cas-derived RNA-guided endonucleases and nickases. *Genome Res.* **24,** 132–41 (2014).

213. Vestweber, D. & Schatz, G. DNA-protein conjugates can enter mitochondria via the protein import pathway. *Nature* **338,** 170–2 (1989).

214. Flierl, A. *et al.* Targeted delivery of DNA to the mitochondrial compartment via import sequence-conjugated peptide nucleic acid. *Mol. Ther.* **7,** 550–557 (2003).

215. D'Souza, G. G. M., Boddapati, S. V. & Weissig, V. Mitochondrial leader sequence-plasmid DNA conjugates delivered into mammalian cells by DQAsomes co-localize with mitochondria. *Mitochondrion* **5,** 352–358 (2005).

216. Sieber, F., Placido, A., El Farouk-Ameqrane, S., Duchêne, A.-M. & Maréchal-Drouard, L. A protein shuttle system to target RNA into mitochondria. *Nucleic Acids Res.* **39,** e96 (2011).

217. Furukawa, R., Yamada, Y., Kawamura, E. & Harashima, H. Mitochondrial delivery of antisense RNA by MITO-Porter results in mitochondrial RNA knockdown, and has a functional impact on mitochondria. *Biomaterials* **57,** 107–115 (2015).

218. D'Souza, G. G. ., Rammohan, R., Cheng, S.-M., Torchilin, V. P. & Weissig, V. DQAsome-mediated delivery of plasmid DNA toward mitochondria in living cells. *J. Control. Release* **92,** 189–197 (2003).

219. Weissig, V., Boddapati, S. V., Cheng, S.-M. & D'souza, G. G. M. Liposomes and Liposome-like Vesicles for Drug and DNA Delivery to Mitochondria. *J. Liposome Res.* **16,** 249–264 (2006).

220. Boddapati, S. V., D'Souza, G. G. M. & Weissig, V. in *Methods in molecular biology (Clifton, N.J.)* **605,** 295–303 (2010).

221. Wang, T., Wei, J. J., Sabatini, D. M. & Lander, E. S. Genetic Screens in Human Cells Using the CRISPR-Cas9 System. *Science (80-.).* **343,** 80–84 (2014).

222. Ran, F. A. *et al.* Genome engineering using the CRISPR-Cas9 system. *Nat. Protoc.* **8,** 2281–2308 (2013).